GEOLOGICA ULTRAIECTINA

Mededelingen van de
Faculteit Aardwetenschappen,
Universiteit Utrecht

no. 186

Survival under stress:
benthic foraminiferal patterns and Cenozoic biotic crises

Tanja J. Kouwenhoven

GEOLOGICA ULTRAIECTINA

Mededelingen van de
Faculteit Aardwetenschappen
Universiteit Utrecht

No. 186

Survival under stress:

benthic foraminiferal patterns and Cenozoic biotic crises

ISBN 90-5744-044-X

Survival under stress:
benthic foraminiferal patterns and Cenozoic biotic crises

Overleven onder stress:
benthonische foraminiferen en Cenozoische biotische crises

(met een samenvatting in het Nederlands)

Proefschrift

ter verkrijging van de graad van doctor
aan de Universiteit Utrecht
op gezag van de Rector Magnificus Prof. Dr. H. O. Voorma
ingevolge het besluit van het College voor Promoties
in het openbaar te verdedigen
op maandag 31 januari 2000 des middags te 14.30 uur

door

Tanneke Johanna Kouwenhoven
geboren op 3 september 1956
te Amsterdam

Promotores:

Prof. Dr. G. J. van der Zwaan	Faculty of Earth Sciences Utrecht University Faculty of Biology Nijmegen University
Prof. Dr. J. E. Meulenkamp	Faculty of Earth Sciences Utrecht University

Members of the dissertation committee:

Dr. W. A. Berggren	Woods Hole Oceanographic Institute Massachusetts, USA
Prof. Dr. S. A. Iaccarino	Institute of Geology University of Parma, Italy
Prof. Dr. C. G. Langereis	Faculty of Earth Sciences Utrecht University
Prof. Dr. H. Visscher	Faculty of Biology Utrecht University
Prof. Dr. Th. E. Wong	Faculty of Earth Sciences Utrecht University

The research described in this thesis was carried out at the Faculty of Earth Sciences, Utrecht University, under the programme of the Netherlands Research School of Sedimentary Geology (NSG).

CONTENTS

Chapter 1

Introduction

General introduction and summary

Benthic foraminifera (Phylum Foraminifera) developed during the Cambrian as part of the marine ecosystem. Since then, they are present in almost all marine environments. Their widespread occurrence and their numerical abundance above the CCD ranks them among the most powerful tools to reconstruct biotic events affecting fossil environments.

Marine life developed before its terrestrial counterpart, and the preservation potential of marine fossils is higher. At an early stage this led to the recognition that marine fossils provide clues as to the relative geological time scale. Much research has been done on benthic foraminifera, starting in the 17th century, after invention of the microscope, with description and classification. In the past century, researchers acknowledged that benthic foraminifera were maybe not the most useful stratigraphic markers, in contrast with planktonic forms, but excellently recorded past events and changes in the marine environment. This knowledge has been put to use in the reconstruction of biotic crises affecting the marine environment. This research still continues.

A problem with the fossil record is, amongst others, that it is fragmentary: much is preserved, but more is lost due to degradation and diagenesis. This is equally true for benthic foraminifera. Ecological structures, for example, are hardly preserved and recognizable; for this we rely on the steadily growing knowledge pertaining to the living counterparts of the fossil foraminifera which we aim to study. These in turn, do not provide us with knowledge of the duration of environmental processes, and their effects on the development and evolution of benthic communities. Research on tempi of evolution and environmental change is dependent on fossil faunas and accurate dating. The latter is provided by combined techniques, including bio- and magnetostratigraphy. In the Mediterranean area, where sapropels developed since the middle Miocene as a result of astronomical forcing, cyclostratigraphy proves to be an excellent dating method.

Major biotic crises mark the beginning and end of important geologic periods and era. This is related to the fact that initially the (relative) timescale was established using major breaks in the faunal record. The start of the Cenozoic, approximately 65 million years ago, was defined on the basis of such a biotic crisis: the Cretaceous/Paleogene boundary event affected both the terrestrial and the marine realm in an extraordinary way. The fact that an asteroid impact occurred at this time is no longer debated, although is is still a matter of controversy whether the impact was really instrumental in the extinctions. To this end, the effect of this crisis and the scale on which it acted have been studied extensively.

The Cenozoic has seen more biotic crises, operating on a global as well as on a more regional scale. Six important phases of environmental change can be discerned, some more or less gradual, some characterised by (on a geological time scale) rapid and profound changes. Each of these events is recorded by benthic foraminiferal assemblages, the subject of this thesis.

During the Cenozoic, the paleogeographic evolution of the Mediterranean area profoundly influenced the development of its benthic foraminiferal faunas. From a broad equatorial corridor in the Paleocene, the old Tethys seaway narrowed in the course of the Cenozoic due to convergence of the Eurasian and African plates. The area was fragmented into subbasins between which the connections were lost, the semi-enclosed Mediterranean Sea being one of them.

Some 10 my after the Cretaceous/Paleogene boundary, the Paleocene/Eocene boundary event was characterised by its short duration (150 ky) and worldwide extinctions, amongst others of groups of benthic foraminifera. During the second part of the Eocene and the transition into the Oligocene, more gradual processes affected benthic communities, that nevertheless caused large and lasting changes in benthic foraminiferal faunas. On a more regional scale, the middle Miocene restriction of the Mediterranean-Pacific connection brought about changes in the paleoenvironment that were probably instrumental in the development of sapropelitic sediments, and of benthic foraminiferal faunas that were characterised by endemic forms. In the late Miocene the continuing restriction of the Mediterranean basin, caused by ongoing plate convergence and localised tectonics, led most probably to the onset of the Messinian salinity crisis, that resulted in deposition of massive evaporites.

Paleoecological analysis of Cenozoic benthic foraminifera from the Mediterranean area form the subject of this thesis. All samples were recovered in the Tethyan realm, more precisely, the area that evolved into the Mediterranean Sea during the Cenozoic. The subject of Chapter 2 is the recovery of the benthic ecosystem after the Cretaceous/Paleogene boundary event, and the subsequent development towards the Paleocene/Eocene boundary, as recorded in sediments of the El Kef section in Tunisia. This section was located at the southern Tethyan margin in Paleogene times. Both the Cretaceous/Paleogene and the Paleocene/Eocene boundary intervals constitute periods of stress in the biotic record. Both events occurred on a world-wide scale, but with different causes and expressions. Where an extra-terrestrial event was involved at the Cretaceous/ Paleogene boundary, global warming characterised the Paleocene/Eocene transition. Both events proceeded rapidly, probably on the time scale of changes caused by human interaction with the environment.

Between the Paleocene and the events discussed in Chapters 3 to 7, a time gap of more than 45 million years exists. In the meantime the configuration of the Tethyan/Mediterranean area had ondergone profound changes. Chapters 3-7 describe late Miocene events affecting the Mediterranean area, and culminating in the Messinian salinity crisis (MSC; 5.96–5.33 Ma). Much research has been done on the causes and development of the actual crisis, that resulted in massive evaporite deposits. The MSC had a localised expression, but the effects probably operated on a larger geographic scale, if only because of the amount of salt that was removed from the oceans. The MSC was probably caused by plate convergence and related tectonics, isolating the Mediterranean basin from the surrounding oceans. The late Miocene faunal development preceding and following the actual crisis has been the scope of research during the past decades, and by now the knowledge of processes acting in the late Miocene Mediterranean is growing. We studied late Miocene sections deposited at different water depths, some in more detail than others, and tried to reconstruct trends and events related to the onset of the salinity crisis.

Detailed reconstructions of relatively deep-water sites are the subject of Chapters 3 and 4. In Chapter 3, we describe the Monte del Casino section and make a comparison with selected data from the Metochia section. The Monte del Casino section (8.15–6.3 Ma; northern Italy) was deposited on top of foredeep sediments derived from Apennine mountain building. Thus, the sediments of the section record regional environmental effects as well as local uplift. These effects could be separated on the basis of benthic faunal response patterns. Indications were found for onset of the MSC as early as 7.16 Ma, i.e. more than a million years before actual evaporite deposition.

Chapter 4 decribes the Metochia section: a detailed reconstruction of a 3 my period (9.7–6.7 Ma) of benthic foraminiferal development in the eastern Mediterranean. The section is located on Gavdos, just south of Crete. As in Monte del Casino, local tectonics are a complicating factor: differential vertical movements affected the area. Nevertheless, we found indications for the onset of the MSC far before actual evaporite deposition, possibly even far before 7.16 Ma, as a consequence of vertical movements affecting the portals to the Atlantic Ocean.

Research on modern living benthic foraminifera resulted in better understanding of benthic ecosystems and their reactions to environmental disturbances. This knowledge is used in reconstructions of past environments. Recently a proxy was developed for bottom-water oxygenation, on the basis of microhabitat patterns of Recent benthic faunas from several oceanic settings. Chapter 5 describes a first attempt to validate the proxy in a fossil environment using a well-described Miocene sequence: the Monte del Casino section. An important question to be answered was, whether Recent microhabitat patterns can be used as analogues for fossil ones, and whether this results in realistic reconstructions. The results are promising, and at the same time offer the opportunity to sharply define problems related to these reconstructions.

In Chapter 6 we applied the oxygen proxy to six sections deposited at different paleodepths, and made a tentative reconstruction of late Miocene circulation in the eastern and central part of the Mediterranean. The aim was to test whether this effort would result in a logical circulation pattern that was in line with theories formulated earlier. Furthermore, a question was whether evaporite deposition could be considered as a logical consequence of circulation in, and constriction of the basin. Considering the fact that the present circulation of the Mediterranean is not fully known, such a reconstruction is bound to lack great detail. However, the first results appear to be in accordance with theoretical expectations.

In Chapter 7 a descriptive model of late Miocene benthic faunas and their development towards the MSC is presented. The model is based on information collected during the research for this thesis, in combination with data from the literature. Faunas from five Mediterranean sections and one site at the Atlantic border are discussed, and the faunas are compared. Differences in faunal development between central, eastern and extra- Mediterranean sites are discussed. Faunas from different environments are found to respond in different ways to the pre-Messinian environmental changes.

In Chapter 8 we bring the different periods in time together in the form of a synthesis, and compare the response of Paleocene and Miocene faunas to environmental changes. We conclude that a shift in the structure of benthic foraminiferal communities has occurred over a period of some 50 my. Gradual processes, operating in periods without major environmental crises, may have been just as important in this respect, or maybe more, than the major crises per se.

Finally, taxonomic notes on selected species are presented. For pictures of the Paleocene taxa the reader is referred to earlier publications, where these taxa are well documented. Plates are added of selected Miocene taxa. Some of these taxa are the subject of continuing taxonomic discussion, and this way we hope to clarify our taxonomic concepts, as these are relevant to the paleoenvironmental reconstructions that were based on the benthic faunas.

A principal conclusion of this thesis is, that benthic foraminifera are excellent recorders of paleoenvironments and paleoenvironmental change. Insight in their community structure, and changes in this through time, is still increasing and will add to their usefulness in the reconstruction of past environments. Moreover, we found that gradual processes affecting the paleoenvironment are as instrumental in the evolution of benthic communities as short-lived ecological crises.

Chapter 2

Paleocene Tethys:
El Kef (Tunisia)

Benthic foraminiferal assemblages between two major extinction events: the Paleocene El Kef section, Tunisia

Abstract

The development of benthic foraminiferal assemblages from the Paleocene outcrops of the El Haria Formation near El Kef, Tunisia is discussed qualitatively and quantitatively. The aim of the study is to reconstruct the paleoenvironmental evolution between the K/Pg boundary interval and the late Paleocene event, and to compare this evolution with results from other sites along the southern Tethyan margin. Eighty-four samples, covering virtually the entire Paleocene, provide a dataset that allows detailed qualitative and multivariate analysis. The benthic foraminiferal faunas indicate a complex pattern of environmental changes during the Paleocene, marked by the succession of different benthic associations. Following the K/Pg boundary event, community restoration was characterized by the gradual build-up of faunal diversity. Decreasing dominance and the entry of taxa common to normal marine, outer-neritic to upper bathyal environments indicate the completion of the ecosystem restoration in Zone P1b. A highly diverse benthic foraminiferal assemblage persisted throughout the remainder of the early Paleocene into the earliest late Paleocene.

At the P3a-P3b zonal transition relative sea-level lowering is evidenced by the sudden disappearance or decreasing abundance of deeper-water taxa (e.g. *Anomalinoides affinis*, *A. susanaensis*, *Gavelinella beccariiformis*). Neritic deposition continued into Zone P4, when trophic levels at the seafloor increased as indicated by the entry and increasing dominance of species such as *Anomalinoides* cf. *aegyptiacus*, *Bulimina midwayensis*, and *B. strobila*, which we consider to be sensitive to eutrophication. The combined effect of shallowing and the subsequent eutrophication led to the establishment of assemblages similar to late Paleocene benthic foraminiferal assemblages from Egyptian sections, some of which record the latest Paleocene extinction event. These assemblages were also interpreted to be indicative of a middle neritic, highly eutrophic environment. Enhanced vertical fluxes of organic matter at several localities along the southern Tethyan margin may have resulted from intensified upwelling. This eventually led to oxygen deficiency at the seafloor. It appears that oxygen-deficient, high-productivity shelves were a common feature of the southern Tethyan margin during the latest Paleocene.

T. J. Kouwenhoven, R. P. Speijer, C. W. M. van Oosterhout & G. J. van der Zwaan, Marine Micropaleontology, 29, 105-127 (1997).

1. Introduction

This paper reports on a qualitative and quantitative analysis of benthic foraminiferal faunas from the Paleocene outcrops of the El Haria Formation near El Kef, Tunisia. The paleobathymetrical evolution is reconstructed on the basis of material from eighty four samples, covering most of the Paleocene part of this section. Major faunal events mark both the K/ Pg boundary interval and the latest Paleocene. Here we examine the more gradual changes which occur between these events. The Paleocene bathymetrical evolution of the section near El Kef is discussed in the context of paleoenvironmental parameters, such as eutrophication and oxygenation of the seafloor. Also, we compare the patterns reconstructed for the El Kef section with other Paleocene sections along the southern Tethys margin.

Paleocene marly sequences in North Africa contain benthic foraminiferal faunas that have many elements in common with assemblages recovered from other localities world-wide. The similarity between Tunisian faunas and those from other sites has been pointed out by Berggren and Aubert (1975) and Aubert and Berggren (1976). In addition to common cosmopolitan species, North African faunas contain more endemic elements, not recovered outside the Tethyan realm (Salaj et al., 1976; Aubert and Berggren, 1976). In the past decades, much attention has been paid to the definition of paleobathymetrical and paleoenvironmental ranges for individual species and associations, in particular with the aim of reconstructing sea-level fluctuations (e.g. Berggren, 1974a,b; Berggren and Aubert, 1975; Aubert and Berggren, 1976; Luger, 1985; Saint-Marc and Berggren, 1988; Saint-Marc, 1993; Speijer, 1994; Speijer and Van der Zwaan, 1994; Speijer et al., 1996). By analogy with West-Atlantic faunas, Tethyan Midway-type faunas (MF) and Velasco-type faunas (VF) were recognized, considered to be characteristic for continental shelves, and continental slope/abyssal plain environments, respectively (Berggren and Aubert, 1975). Faunas from Tunisian locations were described and interpreted in a paleobathymetrical sense by Aubert and Berggren (1976), Saint-Marc and Berggren (1988) and Saint-Marc (1993). Similarly, a paleobathymetrical model was developed based on late Paleocene-early Eocene benthic foraminiferal faunas recovered from mud shelf environments in Egypt (Speijer and Van der Zwaan, 1994).

Knowledge of species sensitivity to environmental factors other than depth is much more limited. Thus far, several Paleocene benthic foraminiferal associations and species have been interpreted to indicate restricted environments at the sea floor, such as lowered oxygen levels and eutrophication (e.g. Bou Dagher, 1987; Olsson and Wise, 1987; Gibson et al., 1993; Speijer and Van der Zwaan, 1994, 1996; Speijer et al., 1996). A number of these observations are based on morphological resemblances with recent species, studied in their natural environments (a.o. Corliss and Chen, 1988; Van der Zwaan and Jorissen, 1991; Barmawidjaja et al., 1991; Sjoerdsma and Van der Zwaan, 1992; Sen Gupta and Machain-Castillo, 1993; Linke and Lutze, 1993). A relation between fauna and substrate has also been established (e.g. Berggren, 1974b). Paleobathymetric distribution patterns of benthic species may change dependent on

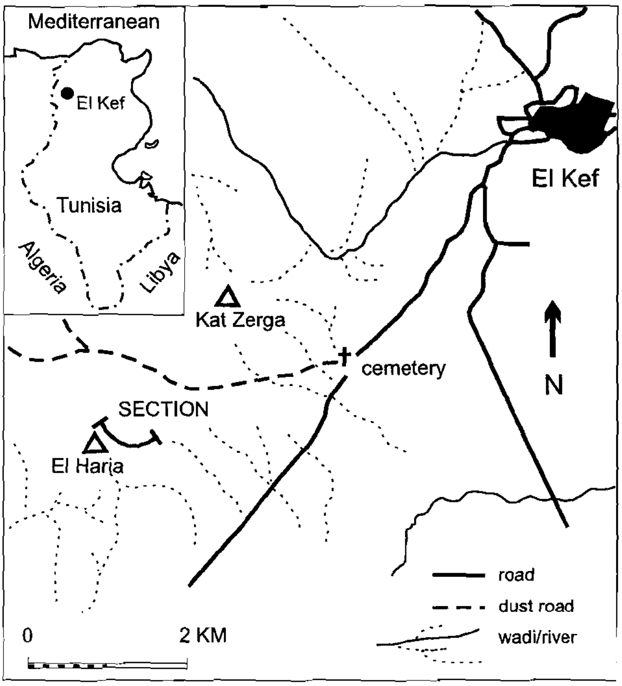

Figure 1. Location map of the El Kef area, with the sampled section (from Brinkhuis and Zachariasse, 1988).

a number of these environmental variables (e.g. Pflum and Frerichs, 1976; Sjoerdsma and van der Zwaan, 1992). Some evidence exists that during the Paleocene benthic foraminiferal distribution patterns were not fixed either: in relation to the latest Paleocene extinction event a neritic fauna temporarily colonized deeper environments, after the normally occurring deeper-water fauna had disappeared due to repeated oxygen deficiency (Speijer and Van der Zwaan, 1994). In this respect, the paleobathymetrical preferences of species and assemblages as established by previous research should be used with restraint.

The El Haria Formation as exposed near El Kef, Tunisia (Fig. 1) offers a reasonably continuous stratigraphic record of the Paleocene (Salaj et al., 1976; Salaj, 1980; Perch-Nielsen, 1981; Donze et al., 1982; Peypouquet et al., 1986). Paleoecological aspects of the Maastrichtian/Paleocene sequence near El Kef have been studied on the basis of benthic foraminiferal faunas (Salaj et al., 1976; Salaj, 1980, 1994; Keller, 1988, 1992; Saint-Marc, 1993; Speijer and Van der Zwaan, 1996), ostracode faunas (Donze et al., 1982; Peypouquet et al., 1986) and dinoflagellate cysts (Brinkhuis and Zachariasse, 1988). The Paleocene sequence is found to be a shallowing-upward one (Salaj et al., 1976; Salaj, 1980, 1994; Donze et al., 1982; Peypouquet et al., 1986; Saint-Marc, 1993), although no consensus exists as to the timing and extent of shallowing. The succession of ostracode faunas also indicates periods of decreased oxygenation of the seafloor due to oscillations of the oxygen minimum zone (Donze et al., 1982; Peypouquet et al., 1986). Eutrophication along the southern Tethys margin during the late Paleocene, possibly due to upwelling processes, was inferred by these authors.

2. Material and methods

The AFN-coded samples from the section near El Kef were collected in 1982 by A.J.T. Romein and J. Smit as members of the Cretaceous-Paleocene Working Group of the International Committee on Stratigraphy. In 1992 A. Nederbragt and J. Smit collected additional, SN-coded samples at the basal Paleocene part of the section. The samples were washed and divided into four size fractions (37-63 µm, 63-125 µm, 125-595 µm and >595 µm). An Otto microsplitter was used to obtain a representative aliquot, containing 200-300 benthic foraminiferal specimens in the 125-595 µm fraction. These specimens were identified, counted and permanently stored in Chapman slides. For this study, 84 samples were examined, covering the Paleocene part of the section (245 m). Samples SN221b-AFN600 (K/Pg + 1.2 cm - K/Pg + 10 m) were collected at centimetre to metre intervals. Samples AFN601-AFN641 (K/ Pg + 15 m - K/Pg + 245 m) were collected with a five m sample spacing.

Most benthic foraminifera were identified to species level. *Lenticulina* spp. and other nodosariids were identified to generic or higher order levels, as were poorly preserved specimens. Dominance is expressed as the percentage of the most abundant taxon in a sample. The initial dataset, containing 150 taxa, was used to determine Fisher-alpha diversity (cf. Murray, 1991). Subsequently, the dataset was condensed to 72 taxa and groups in order to perform a cluster analysis (unweighted pair group method) and a standardized principal component analysis. In order to suppress squeeze effects from abundant taxa, a BALANC routine was incorporated in the procedure (Drooger, 1982). For samples AFN601-AFN641 the foraminiferal numbers (i.e. number of specimens per gram of dry sediment) and the percentage of planktonics in the total foraminiferal assemblage were obtained from the 125-595 µm fraction of separately processed sample material. For the lowermost 10 m of the section (samples SN221b-AFN600) these parameters were derived from separately processed sample material which was washed over a 63 µm sieve, as the larger fraction contained too few planktonic foraminifera; the entire >63 µm fraction was used. The presence of some very large, environmentally or biostratigraphically diagnostic species (e.g. *Frondicularia phosphatica*) was checked in the >595 µm fraction. Nannoplankton smear slides were prepared in order to constraint the NP7/NP8 and the NP8/NP9 boundaries in our material.

Results from the lowermost 10 m of the section are described in detail in relation to latest Maastrichtian faunas and the K/Pg boundary extinction event by Speijer and Van der Zwaan (1996).

3. Lithology and biostratigraphy

The El Haria Formation near El Kef (Fig. 1) overlies the Campanian/ Maastrichtian Abiod Formation, and mainly consists of brown-grey, homogeneous marls. Most of the section is well exposed and accessible, although four 8-15 m thick intervals are not or only poorly exposed (Fig. 2). The K/ Pg boundary clay is a 1 m thick, rather distinct unit. A limestone bed at K/Pg+127 m, containing abundant *Frondicularia phosphatica*, is a marker bed in the middle of the section (cf. Salaj, 1986); in our view this unit represents a hardground (sample AFN 618A). Sedimentary laminations are preserved in the lowermost 3 m of the Paleocene section. The sediments contain pyrite and pyritized burrows up to K/Pg+120 m (sample AFN617), most frequently between K/Pg+3 m and K/Pg+9 m (samples AFN586-AFN598). Between K/Pg+165 m and K/Pg+185 m a more silty level occurs, containing bivalves. Glauconite is found in samples between K/Pg+145 m and K/Pg+210 m (samples AFN622-AFN634). Fish remains are found in several samples from the upper 100 m of the section. From a parallel section studied by Salaj (Salaj et al., 1976; Salaj, 1980) gypsum intercalations, possibly secondary, were reported in the upper Paleocene (*Globorotalia angulata* Zone of Salaj et al., 1976) and phosphatic deposits at the top of the Paleocene. The limestones above sample AFN641 (top of the studied section) belong to the Eocene Metlaoui Formation, overlying the El Haria Formation.

An integrated biozonation based on planktonic foraminifera and nannofossils is applied in this paper (Fig. 2). The planktonic foraminiferal biozonation adopts the criteria of Berggren and Miller (1988), recently revised in Berggren et al. (1995). Data are from Brinkhuis and Zachariasse (1988), and Brinkhuis et al. (1994). The calcareous nannofossil zonation adopts the criteria of Martini (1971), and Perch-Nielsen (1981), who studied material from a parallel section, and are combined with our own data for the upper Paleocene. All standard planktonic foraminiferal and nannofossil zones are represented in the section, although minor hiatuses can not be excluded. For some intervals the precise zonal boundaries could not be established due to the absence of zonal markers. Uncertainty exists on the nannofossil NP4-NP5 zonal transition and the thickness of NP5 (see Perch-Nielsen, 1981). The NP7-NP8 zonal boundary could not be established in our material. *Discoaster multiradiatus*, marker for the NP9 nannofossil zone, could only be ascertained in the top of the section (sample AFN638) although the NP8/NP9 boundary was expected at a lower point in the section (cf. Perch-Nielsen, 1981). The onset of the latest Paleocene extinction level may be recorded in the samples from the top of the studied section. This point in time coincides with a global drop in $\delta^{13}C$ values (e.g. Kennett and Stott, 1991).

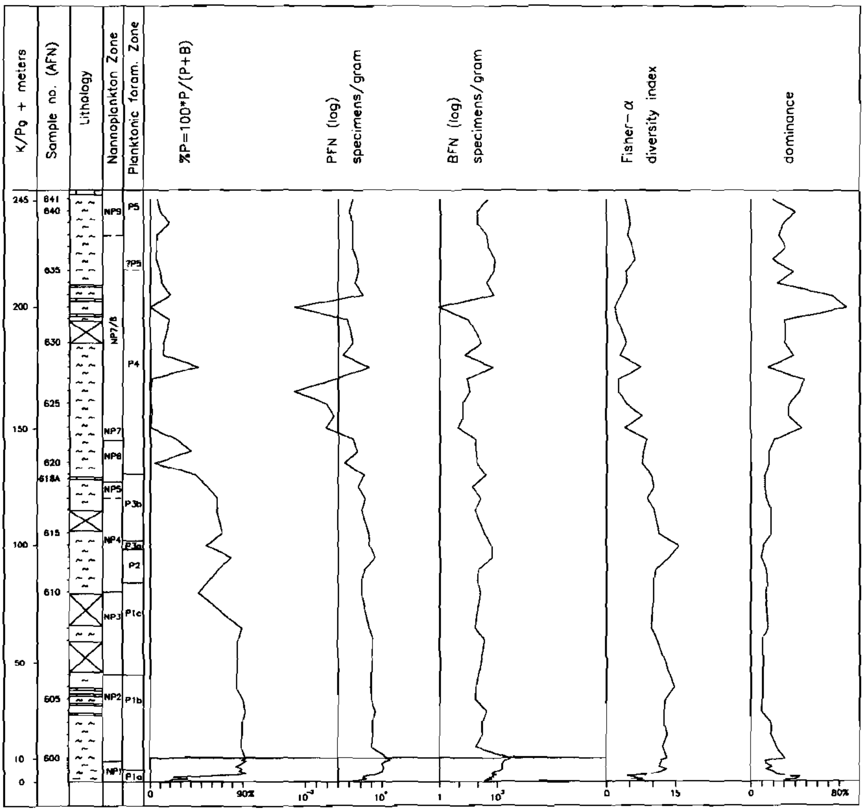

Figure 2. Lithology, biostratigraphy and sample positions in the El Kef section, with P/B ratios (expressed as %P = 100 * P(P+B)), planktonic and benthic foraminiferal numbers (PFN, resp. BFN: specimens per gram of sediment, log-scaled), diversity (Fisher-alpha index, cf. Murray, 1991), and dominance (relative frequency of the most abundant taxon in a sample). P/B ratios and FN were counted in the >63 μm fraction of the lowermost 10 m of the section (stippled area) and in the >125 μm fraction of the rest of the section.

4. Results

4.1. P/B ratios

P/B ratios are expressed as 100*P/(P+B), i.e. the percentages of planktonic foraminifera in the total foraminiferal assemblages (Fig. 2). P/B ratios can be used to estimate the paleobathymetric evolution at a site, provided that normal marine conditions prevailed at the time of deposition, and dissolution has not affected the sample material (e.g. Berger and Diester-Haass, 1988; Van der Zwaan et al., 1990).

These criteria are met in parts of the studied section. In the lowermost Paleocene, P/B ratios remain well below 50% P (see also Speijer and Van der Zwaan, 1996), and start to rise at K/Pg+3 m (Zone P1a), to reach levels of 85-95%P between K/Pg+3.5 m and K/Pg+65 m (Zone P1a-Zone P1c). Above the K/Pg+65 m level (upper Zone P1c, sample AFN609) the P/B ratios oscillate, and at the P3a-P3b zonal transition definitively fall to lower levels, maintained during the remainder of the Paleocene. No planktonic foraminifera were found in two samples from Zone P4 (samples AFN626 and AFN632), taken from intervals where preservation is poor and the material is decalcified. As preservation of faunas is less good in the top of Zone P1b, the base of Zone P1c, and parts of Zone P4, P/B ratios can not be used as paleodepth indicators for these parts of the section. However, preservation of faunas is quite good in upper Zone P1a - lower Zone P1b (P/B = 85-93% P) and in upper Zone P1c - lower Zone P4 (K/Pg+80 m - K/Pg+135 m). The latter part of the section records an overall drop in P/B ratios.

4.2. Foraminiferal numbers

Paleoproductivity trends have been assessed on the basis of foraminiferal accumulation rates ($N.cm^{-2}.ka^{-1}$) (e.g. Berger and Diester-Haass, 1988; Herguera and Berger, 1991; Speijer and Van der Zwaan, 1994). As time control in the section is too limited to provide us with reliable sedimentation rates, foraminiferal numbers (FN) were used instead (Fig. 2). FN have been counted in the >125 µm fraction of the samples, with the exception of the lowermost 10 m of the section, where the >63 µm fraction was used (stippled in Fig. 2). Thus, the foraminiferal numbers in the two parts of the section are not comparable but the trends can be used. Planktonic foraminiferal numbers (PFN) follow a pattern similar to the related P/B ratios, increasing in Zone P1b, reaching a maximum in Zone P1b – Zone P3a, and decreasing from Zone P3b onwards. Above Zone P1b, benthic foraminiferal numbers oscillate but reach a relative maximum in the upper Paleocene. Decalcification of sample material from parts of Zone P4 may cause an underestimation of the benthic foraminiferal numbers.

4.3. Diversity and dominance trends

Low-diversity assemblages, dominated by one or a few species, tend to occur in stressed environments, whereas a normal marine environment would be indicated by a relatively diverse association. In the latter case dominance, expressed as the percentage of the most abundant taxon, is usually found to be relatively low (e.g. Van der Zwaan and Jorissen, 1991; Sen-Gupta and Machain-Castillo, 1993). Diversity (Fisher-alpha index, cf. Murray, 1991; Fig. 2) is fairly low in the lowermost Paleocene (alpha = 5-8) and concurs with a relatively high dominance (30-45%; *Cibicidoides pseudoacutus*, Figs. 2, 3). An increasing diversity is apparent in the early Paleocene (P1b; alpha = 10-15), when at the same time dominance falls to 9-22%. Above Zone P3b diversity decreases and remains at lower levels during the remainder of the Paleocene (alpha = 2-10). Dominance reaches maximum levels in the upper P4 Zone. Dominant species include *Bulimina midwayensis* (up to 45%), *B. strobila* (72% in sample AFN633) and *Anomalinoides* cf. *aegyptiacus* (up to 25%).

4.4. Faunal succession

Benthic foraminiferal faunas recovered from upper Paleocene strata differ markedly from lower Paleocene faunas (Fig. 3). The assemblage present during the earliest Paleocene is progressively replaced by a new assemblage, the most marked shifts in faunal composition taking place in Zone P1b (enrichment) and following the P3a-P3b zonal transition (impoverishment). In the lowermost Paleocene a low-diversity assemblage is found, which is dominated by *Cibicidoides pseudoacutus* (up to 45%; Fig. 3). The relative abundance of *C. pseudoacutus*, together with the dominance, subsequently decreases, and the early Paleocene (upper Zone P1a, Zone P1b) is characterized by more than thirty species entering the record. A number of these species have also been found in Maastrichtian sediments at El Kef and temporarily disappear from the record in the K/Pg boundary interval; other species have not been observed in these Maastrichtian sediments (Speijer and Van der Zwaan, 1996). As only seven exits are counted above the K/Pg boundary interval, diversity increases to reach a maximum, and a stable association is maintained until the P3a-P3b zonal boundary. At the base of Zone P3b (sample AFN615) a number of species display decreasing abundances, or disappear from the record altogether (e.g. *Gavelinella beccariiformis*, *Pulsiphonina prima*) within a relatively short period of time. Entries during Zones P4 and P5 do not compensate for this loss of diversity, as species loss continues. In the course of Zone P4 the assemblage is again increasingly dominated by one or a few species, and diversity reaches a minimum. Siliceous agglutinants reach higher abundances.

A subdivision of faunal development into five main phases appears useful. A first phase comprises the lower P1a Zone. Faunal enrichment during the upper Zone P1a and part of Zone P1b characterizes a second phase, followed by a third phase in Zones P2 and P3a, in which a stable mid-Paleocene association is present. A fourth phase sets in at the P3a-P3b zonal boundary, when faunal impoverishment starts with the more or less simultaneous exit of a number of taxa. The subsequently decreasing diversity, and increasing dominance by among others buliminids towards the middle of Zone P4 delineates the onset of a fifth phase of faunal development.

4.5. Multivariate analysis

The dataset, originally containing 150 taxa (Appendix A), was condensed to 72 taxa and (supra-) generic categories. This condensed dataset (Fig. 3) was subjected to

---

Figure 3. Relative frequency data of the 72 most abundant taxa and groups, with lithology, biostratigraphy and position of samples in the section. Taxa are arranged according to entries.

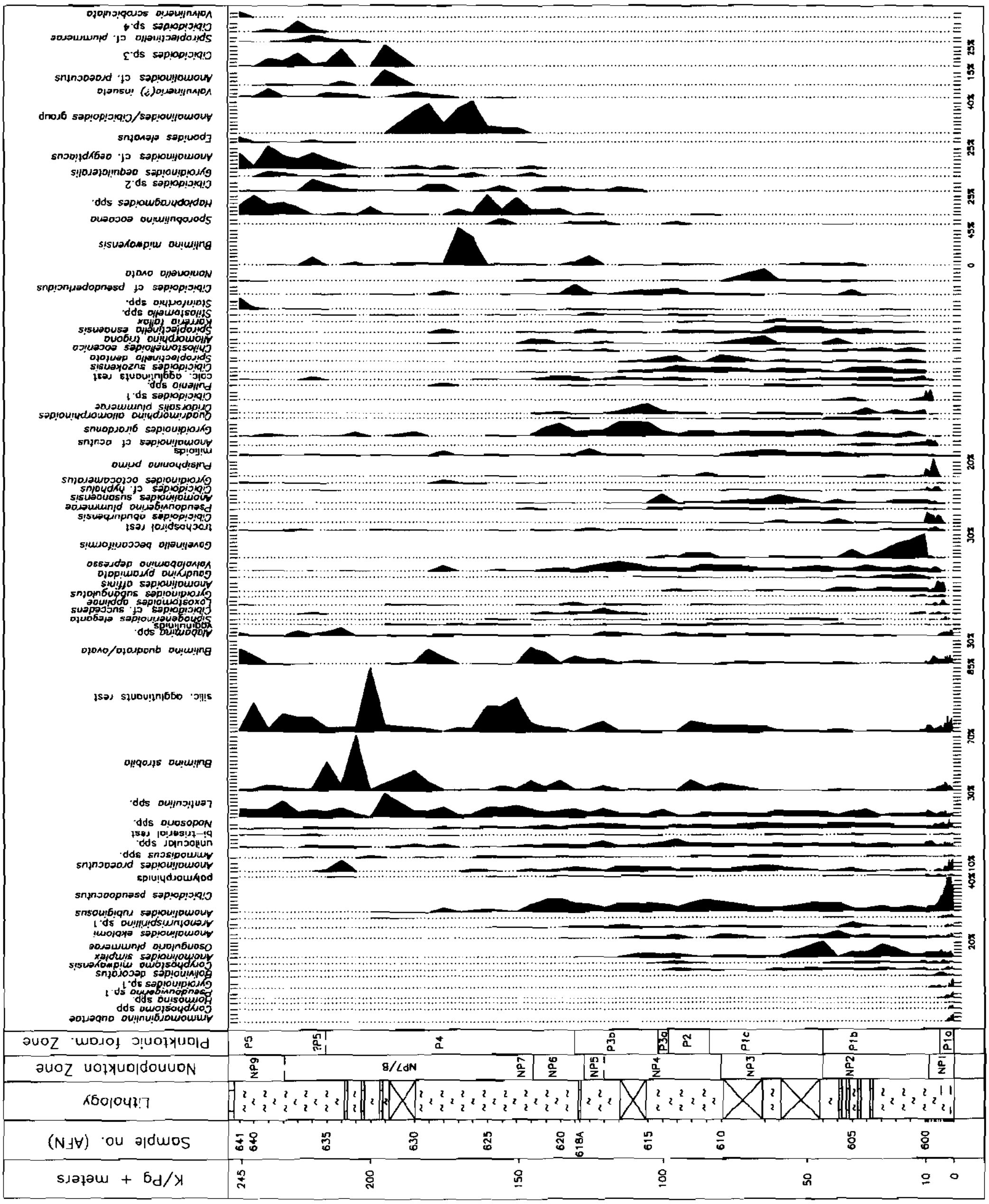
Valvulineria scrobiculata
Cibicidoides sp.4
Spiroplectinella cf. plummerae
Cibicidoides sp.3
Anomalinoides cf. praeacutus
Valvulineria(?) insueta
Anomalinoides/Cibicidoides group
Eponides elevatus
Anomalinoides cf. aegyptiacus
Gyroidinoides aequilateralis
Cibicidoides sp.2
Haplophragmoides spp.
Sporobulimina eocaena
Bulimina midwayensis
Nonionella ovata
Cibicidoides cf. pseudacutus
Stainforthia spp.
Stilostomella spp.
Allomorphina trigona
Chilostomelloides eocenica
Spiroplectinella dentata
Cibicidoides suzakensis
calc. agglutinants rest
Pullenia spp.
Cibicidoides sp.1
Quadrimorphina allomorphinoides
Gyroidinoides girardanus
Anomalinoides cf. acutus
miliolids
Pulsiphonina prima
Gyroidinoides octocameratus
Anomalinoides susanaensis
Pseudouvigerina plummerae
trochospiral rest
Gavelinella beccariiformis
Valvalabamina depressa
Gaudryina pyramidata
Anomalinoides affinis
Gyroidinoides subangulatus
Alabamina spp.
Bulimina quadrata/ovata
silic. agglutinants rest
Bulimina strobila
Lenticulina spp.
Nodosaria spp.
bi-triserial rest
unilocular spp.
Ammodiscus spp.
Anomalinoides praeacutus
polymorphinids
Cibicidoides pseudoacutus
Anomalinoides rubiginosus
Anomalinoides ekblomi
Osangularia plummerae
Anomalinoides simplex
Planktonic foram. Zone
P5
?P5
P4
P3b
P3a
P2
P1c
P1b
P1a
Nannoplankton Zone
NP9
NP7/8
NP7
NP6
NP5
NP4
NP3
NP2
NP1
Lithology
Sample no. (AFN)
641
640
635
630
625
620
618A
615
610
605
600
K/Pg + meters
245
200
150
100
50
10
0

an R-mode cluster analysis and a standardized principal component analysis. Plots of sample scores on the first and second principal component axes are shown in Figure 4a.

The first and second axes explain 22.4% of the variance (13.2% and 9.2%, respectively). Third and higher order axes explain less than 8% of the variance each, and are not considered. At first sight, scores on both axes show an overall trend that is comparable with faunal parameters (P/B ratios, PFN, diversity: Fig. 2). Differences between the axis patterns exist in particular in the lowermost Paleocene, and in Zone P3. The first axis is loaded positively by species occurring or displaying highest abundances in Zones P1b-P3b (e.g. *Valvalabamina depressa*, *Cibicidoides suzakensis*, *Spiroplectinella esnaensis*; Fig. 3). Species restricted to or reaching highest abundances in Zone P1a load most negatively on the first axis (e.g. *Cibicidoides pseudoacutus*; but also *Alabamina* spp.), whereas species proliferating in zones P4 and P5 load slightly negative (e.g. *Anomalinoides aegyptiacus*, *Valvulineria scrobiculata*). The second axis is loaded positively by species mainly occurring in zones P1a-P3a (e.g. *Anomalinoides simplex*, *Osangularia plummerae*, *Cibicidoides pseudoacutus*). Species loading this axis most negatively are those restricted to the top of Zone P4 and Zone P5 (e.g. *A. aegyptiacus*, *Valvulineria*(?) *insueta*, *Haplophragmoides* spp.) and species reaching highest abundances in this interval (e.g. *Bulimina midwayensis*, *Lenticulina* spp).

The bivariate plot of sample scores on the principal component axes (Fig. 4b) divides the faunas into three fields, with transitional phases in between, reflecting the faunal succession mentioned above. The main fields contain assemblages corresponding to the earliest Paleocene, the 'mid-Paleocene' and the late Paleocene. Samples from the basal Paleocene sediments (Zone P1a) occupy the upper left corner of the bivariate plot. Close clustering is due to close sample spacing, reducing intersample variability. Samples from Zones P1b-P3b occupy the upper right corner of the diagram. Samples from Zones P4 and P5 form the third, less coherent cloud in the lower middle of the diagram. Transitional phases are recorded by samples AFN585 - AFN591 (upper Zone P1a and lower Zone P1b: faunal enrichment) and AFN617 - AFN622 (Zone P3b and base of Zone P4: faunal impoverishment).

The R-mode cluster analysis results in the dendrogram shown in Figure 5. The fauna can be subdivided into five groups: four main clusters A - D, with cluster C consisting of two subclusters. Cluster A corresponds to the assemblage present in Zone P1a (Fig. 3). Cluster B mainly contains taxa entering the record in Zone P1b, most of which do not survive into the late Paleocene. Cluster C contains taxa proliferating during the period of maximum faunal diversity. However, most taxa present in subcluster C1 disappear or show strongly reduced frequencies at the P3a-P3b zonal transition (sample AFN615; e.g. *Gavelinella beccariiformis*, *Cibicidoides suzakensis;* Fig. 3). Taxa present in subcluster C2 show diminishing frequencies or disappear from the record at a later stage, starting in the lower P4 Zone (e.g. *Oridorsalis plummerae*). Cluster

---

Figure 4. (a). Sample score pattern on the first and second principal components. **(b).** Bivariate plot of sample scores on the first and second principal components. For explanation see text.

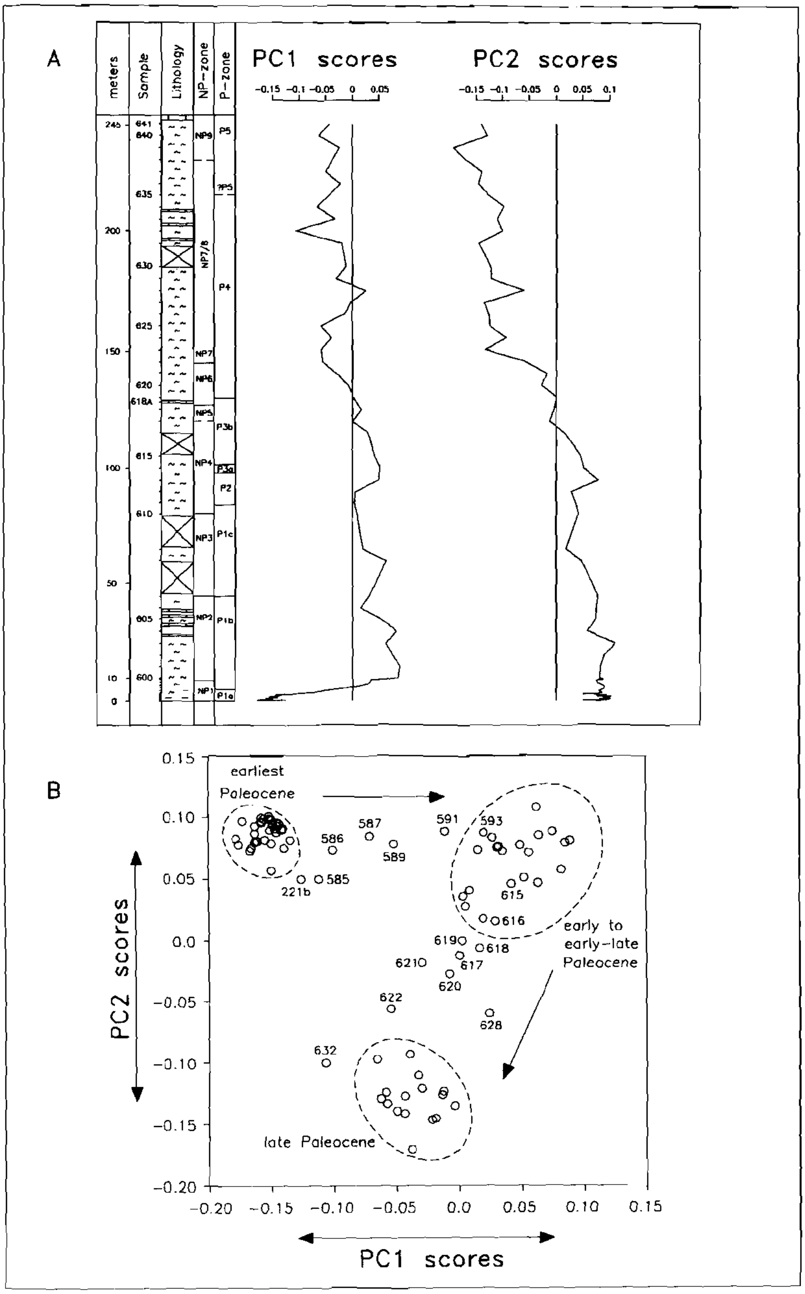
A
meters
Sample
Lithology
NP-zone
P-zone
PC1 scores
-0.15 -0.1 -0.05 0 0.05
PC2 scores
-0.15 -0.1 -0.05 0 0.05 0.1
245
200
150
100
50
10
0
641
640
635
630
625
620
618A
615
610
605
600
NP9
NP7/8
NP7
NP6
NP5
NP4
NP3
NP2
NP1
P5
?P5
P4
P3b
P3a
P2
P1c
P1b
P1a
B
earliest Paleocene
early to early-late Paleocene
late Paleocene
586
587
589
591
593
585
221b
615
616
618
619
617
620
621
622
628
632
PC2 scores
PC1 scores
0.15
0.10
0.05
0.0
-0.05
-0.10
-0.15
-0.20
-0.20
-0.15
-0.10
-0.05
0.0
0.05
0.10
0.15

D contains taxa appearing or showing highest abundances in the late Paleocene, following the faunal impoverishment that mainly characterizes Zone P3b, but continues into the lower P4 Zone. These clusters also roughly reflect the five phases of faunal development outlined above.

5. Discussion

The development of benthic foraminiferal communities in the Paleocene El Haria Formation near El Kef is characterized by progressive replacement of faunal associations. Changes in the paleoenvironment are indicated by the changing species abundance patterns and by paleoenvironmental parameters such as P/B ratios, foraminiferal numbers and diversity trends. Diversity, and P/B ratios with the associated planktonic foraminiferal numbers (PFN), increase during the early Paleocene and decrease after the P3a-P3b zonal transition. This trend more or less agrees with the pattern of sample scores on the first principal component axis. Benthic foraminiferal numbers show an overall tendency to rise to maximum values during the upper P4 Zone, a trend concurring with the sample score pattern on the second principal component axis.

5.1. Paleobathymetry

P/B ratios are a measure of paleodepth under certain restrictions (Adelseck and Berger, 1975; Van der Zwaan et al., 1990): indications of environmental stress at the time of deposition and (partial) dissolution of faunas prohibit the use of P/B ratios in this sense. Benthic foraminifera also provide an estimate of paleodepth, as several authors have related depositional depths to faunal associations and individual species, many of which are present in sediments from the southern Tethys margin (e.g. Kellough, 1965; Berggren, 1974a,b; Berggren and Aubert, 1975; Salaj et al., 1976; Aubert and Berggren, 1976; Salaj, 1980; Tjalsma and Lohmann, 1983; Luger, 1985; Bou Dagher, 1987; Saint-Marc and Berggren, 1988; Katz and Miller, 1991; Saint-Marc, 1993; Speijer and Van der Zwaan, 1994; Speijer, 1995: Speijer et al., 1996). Relevant data are summarized in Table I.

5.1.1. P/B ratios

P/B ratios are of limited use in parts of the section. In the lowermost 3 m indications exist for periods of oxygen stress at the seafloor, and the pelagic and benthic stocks had not yet fully recovered from the K/Pg boundary event (Brinkhuis and Zachariasse, 1988; Keller, 1992; Speijer and Van der Zwaan, 1996). Material from

Figure 5. Dendrogram resulting from cluster analysis. Cluster A corresponds to the earliest Paleocene assemblage. Cluster B contains early Paleocene taxa; most entries occur in Zone P1a. Cluster C contains early-late Paleocene taxa; most taxa in cluster C1 disappear at the P3a-P3b zonal transition. Cluster D corresponds to the late Paleocene assemblage.

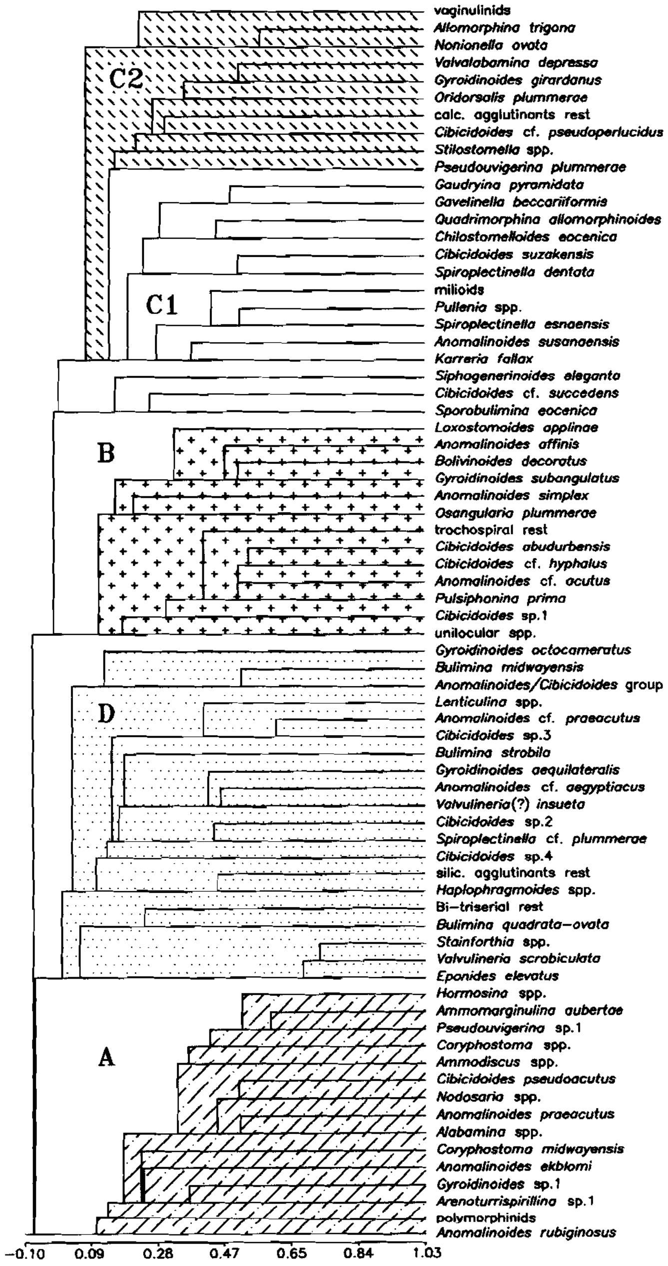
vaginulinids
Allomorphina trigona
Nonionella ovata
Valvalabamina depressa
Gyroidinoides girardanus
Oridorsalis plummerae
calc. agglutinants rest
Cibicidoides cf. pseudoperlucidus
Stilostomella spp.
Pseudouvigerina plummerae
Gaudryina pyramidata
Gavelinella beccariiformis
Quadrimorphina allomorphinoides
Chilostomelloides eocenica
Cibicidoides suzakensis
Spiroplectinella dentata
milioids
Pullenia spp.
Spiroplectinella esnaensis
Anomalinoides susanaensis
Karreria fallax
Siphogenerinoides eleganta
Cibicidoides cf. succedens
Sporobulimina eocenica
Loxostomoides applinae
Anomalinoides affinis
Bolivinoides decoratus
Gyroidinoides subangulatus
Anomalinoides simplex
Osangularia plummerae
trochospiral rest
Cibicidoides abudurbensis
Cibicidoides cf. hyphalus
Anomalinoides cf. acutus
Pulsiphonina prima
Cibicidoides sp.1
unilocular spp.
Gyroidinoides octocameratus
Bulimina midwayensis
Anomalinoides/Cibicidoides group
Lenticulina spp.
Anomalinoides cf. praeacutus
Cibicidoides sp.3
Bulimina strobila
Gyroidinoides aequilateralis
Anomalinoides cf. aegyptiacus
Valvulineria(?) insueta
Cibicidoides sp.2
Spiroplectinella cf. plummerae
Cibicidoides sp.4
silic. agglutinants rest
Haplophragmoides spp.
Bi-triserial rest
Bulimina quadrata-ovata
Stainforthia spp.
Valvulineria scrobiculata
Eponides elevatus
Hormosina spp.
Ammomarginulina aubertae
Pseudouvigerina sp.1
Coryphostoma spp.
Ammodiscus spp.
Cibicidoides pseudoacutus
Nodosaria spp.
Anomalinoides praeacutus
Alabamina spp.
Coryphostoma midwayensis
Anomalinoides ekblomi
Gyroidinoides sp.1
Arenoturrispirillina sp.1
polymorphinids
Anomalinoides rubiginosus
C2
C1
B
D
A
-0.10
0.09
0.28
0.47
0.65
0.84
1.03

the upper Zone P1b and lower Zone P1c shows signs of diagenetic alteration, and material from parts of Zone P4 is decalcified, also prohibiting paleodepth estimates. Fish remains, found in the upper 100 m of the section, point to incomplete decomposition of organic matter due to enhanced organic carbon supply and/or oxygen deficiency. Phosphate-rich sediments, deposited during the late Paleocene near El Kef (Salaj et al., 1976; Salaj, 1980; Peypouquet et al., 1986) and in other Tunisian sections (Aubert and Berggren, 1976) indicate eutrophication of the environment, which in turn may have led to a certain amount of oxygen deficiency. However, faunas from the top of Zone P1a, the greater part of Zone P1b and from the top of Zone P1c to the base of Zone P4 are reasonably well preserved and allow an estimation of paleobathymetrical trends on the basis of P/B ratios (Fig. 2). A shallowing from outer neritic/upper bathyal depths (upper Zone P1a to lower Zone P1c) to neritic depths (Zones P3b, P4) can be inferred. Short-term shallowing is visible at the P1c-P2 zonal transition, whereas the shallowing trend that starts at the P3a-P3b zonal transition appears to last throughout the upper Paleocene.

5.1.2. Depth-related species

Benthic foraminiferal data substantiate this interpretation and add detail to depth estimates. The relative abundance pattern of *Gavelinella beccariiformis*, regarded as an indicator of middle to upper bathyal environments (Salaj et al., 1976; Aubert and Berggren, 1976; Tjalsma and Lohmann, 1983; Katz and Miller, 1991; Saint-Marc, 1993; Speijer and Van der Zwaan, 1994), is in agreement with the trend of the P/B ratios in the interval between the top of Zone P1b and the P3a-P3b zonal transition (Figs. 2, 3). Furthermore, several other deeper-water species disappear or show decreasing abundances at the P3a-P3b transition (e.g. *Anomalinoides affinis*, *Osangularia plummerae*, *Coryphostoma midwayensis*, *Gyroidinoides subangulatus*), when *Frondicularia phosphatica*, an indicator species for shallow-water, phosphate-rich environments (Salaj et al., 1976), first enters the record in small numbers.

Many species appearing or showing increasing abundances during zones P4 and P5 were reported earlier from shallow depositional environments. *Frondicularia phosphatica* occurs in great numbers in a limestone bed in the top of Zone P3b, probably representing a hardground (see also Salaj, 1986). *Haplophragmoides* spp., mentioned by Berggren (1974a) as shallow-water species (20 m water depth) first appear at the top of Zone P2. *Haplophragmoides walteri* enters the record in Zone P3b; this species was found in shallow water (intertidal) environments (Kellough, 1965). *Anomalinoides* cf. *aegyptiacus*, *Valvulineria*(?) *insueta* and *V. scrobiculata*, appearing in Zone P4, were described from latest Paleocene neritic deposits in Egypt (Speijer and Van der Zwaan, 1994; Speijer et al., 1996). Bou Dagher (1987) ascribes peak occurrences of *Stainforthia* spp. to deposition in hyposaline, lagoonal environments. Shallowing, initiated at the P3a-P3b zonal transition, apparently led to deposition at middle to inner neritic depths during the late Paleocene. A short-term deepening appears to be recorded by all faunal parameters in sample AFN628 (K/Pg+175 m: Figs. 2, 3). Whether this is a real deepening pulse, is uncertain.

Table 1. Summary of paleobathymetrical preferences of selected, quantitatively important, species.

Species	Estimated paleobathymetry
Anomalinoides affinis	100m [2], MF [3], coastal to upper bathyal [8], outer neritic-upper bathyal [9]
Anomalinoides cf. aegyptiacus	middle neritic [9]
Anomalinoides praeacutus	MF (epicontinental) [5], bathyal [6], inner neritic-bathyal [8], wide bathymetrical range [9]
Anomalinoides rubiginosus	30-200 m [2], MF [3], inner neritic-bathyal [8], outer neritic-upper bathyal [9]
Anomalinoides susanaensis	mid-neritic to mid-bathyal [8]
Bulimina midwayensis	MF [4,5], inner neritic-bathyal [8], wide bathymetrical range [9]
Bulimina quadrata/ovata	MF [4,5], neritic [9]
Bulimina strobila	MF [5], wide bathymetrical range [9]
Frondicularia phosphatica	shallow, P-rich [5]
Cibicidoides pseudoacutus	bathyal [7], MF to bathyal [8], outer neritic-upper bathyal [9]
Gaudryina pyramidata	bathyal [6], inner neritic-bathyal [8]
Gavelinella beccariiformis	VF [4], epicontinental [5], bathyal [6,8], upper bathyal [9]
Gyroidinoides subangulatus	MF [3,4]
Gyroidinoides girardanus	neritic [9]
Haplophragmoides spp.	shallow (20m) [7], *H. walteri*: intertidal [1],
Lenticulina spp.	MF [4], mid-to inner neritic [8], wide bathymetrical range [9]
Neoeponides cf. *elevatus*	MF [5], middle neritic [9]
Oridorsalis plummerae	100m [2], MF [4,5], wide bathymetrical range [9]
Osangularia plummerae	MF [3,4], MF (epicontinental) [5], outer shelf-upper slope [8], outer neritic-upper bathyal [9]
Pullenia spp.	*P. americana*: VF [8], outer neritic-upper bathyal [9]
Pulsiphonina prima	20-100 m [2], MF [3,5], wide bathymetrical range [9]
Spiroplectinella dentata	VF [8]
Spiroplectinella esnaensis	VF [8], mainly outer neritic-upper bathyal [9]
Stainforthia spp.	neritic [9], lagoonal [10]
Tritaxia midwayensis	MF [3,4] , VF [8], outer neritic-upper bathyal [9]
Valvalabamina depressa	wide bathymetrical range [9]
Valvulineria(?) insueta	neritic [9]
Valvulineria scrobiculata	neritic [9]

MF = Midway-type fauna (characteristic of continental shelf); VF = Velasco-type fauna (continental slope/abyssal plain; Berggren and Aubert, 1975; Aubert and Berggren, 1976).

The following publicatons are referred to:

[1] Kellough, 1965; [2] Berggren, 1974a; [3] Berggren and Aubert, 1975; [4] Aubert and Berggren, 1976; [5] Salaj et al., 1976; [6] Tjalsma and Lohmann, 1983; [7] Katz and Miller, 1991; [8] Saint-Marc, 1993; [9] Speijer and Van der Zwaan, 1994; [10] Bou Dagher, 1987.

5.1.3. Summary of available data on paleobathymetry

Paleobathymetrical trends recorded in Paleocene outcrops near El Kef and in central Tunisia have been evaluated by several authors on the basis of microfaunas and sedimentary characteristics (Aubert and Berggren, 1976; Salaj et al., 1976; Salaj, 1980, 1986, 1994; Donze et al., 1982; Peypouquet et al., 1986; Saint-Marc and Berggren, 1988;

Saint-Marc, 1993). These authors agree upon shallowing in the course of the Paleocene, but not on the degree of shallowing, and the starting point in time. The latter disagreement may in some cases be due to differing biozonation schemes. In Figure 6 we summarize bathymetrical data discussed below together with the eustatic curve of Haq et al. (1987). Aubert and Berggren analyzed samples from eight outcrops in central Tunisia and reconstructed a deepening in part of these outcrops in Zones P2 and P3, and an overall shallowing during the Late Paleocene. Saint-Marc and Berggren (1988) applied statistical analyses to this sample set, and correlated shallowing at the P2-P3a zonal transition to the eustatic sea-level curve of Haq et al. (1987). Subsequently, deepening to outer neritic/upper bathyal depths was observed, followed by continuous shallowing to inner neritic and coastal depth, beginning in the upper P4 Zone. These data from central Tunisia were analyzed together with 14 samples from the El Kef section by Saint-Marc (1993). Primarily on the basis of benthic foraminiferal associations from the El Kef section, a trend was observed from upper bathyal (Zones P1a and P1b), via outer shelf (Zones P1c to P3b) to inner neritic, possibly coastal conditions (Zones P4 and P5). Salaj (1994) reported on small sponges and corals at the base of the Harian (=Montian s.l.; Zone P2). He inferred deposition on a local high, at a depth of 20-30 m for this interval, followed by a subsequent deepening to 50-150 m. In his view, a short interval of tectonic activity explains this shallowing event. Continuous shallowing, according to Salaj (1986), started just below, or at the base, of the *Planorotalia pseudomenardii* Zone (cf. Salaj, 1986: base of Zone P4), where a limestone bed with abundant *Frondicularia phosphatica* occurs. Comparing the morphologies of recent and fossil ostracode taxa, Donze et al. (1982) reconstructed a shallowing trend from upper bathyal depths to outer shelf environments, first registered in Zone P3b. Using the same material, Peypouquet et al. (1986) found a shallowing trend during their 'écozone 7', comprising Zone P3b and the base of Zone P4. Both papers mention five successive Paleocene ecozones, established on the basis of ostracode faunas and roughly corresponding to the five phases of benthic foraminiferal development reconstructed in this paper.

Sections from other localities on the southern Tethys margin provide additional data on paleobathymetrical trends (Fig. 6). In the Sirte Basin (Libya), shallowing was observed in Zones P3b-P4, based upon faunal changes and sedimentation patterns (Berggren, 1974b). In southern Egypt two transgressive phases were recorded, in Zone P1c and the lower P4 Zone, respectively, and a regression in Zones P3a and P3b. These observations were made in sediments from shallow-water deposits and their benthic foraminiferal faunas. Sea-level variations mentioned are minor, spanning coastal to middle neritic depths (Luger, 1985). Preliminary data from the Aweina section (Nile Valley, Egypt) indicate a short-term shallowing coinciding with the P3a-P3b zonal transition, followed by a return to earlier, outer neritic conditions. A temporary

Figure 6. Schematic representation of sea-level fluctuations as reconstructed by a number of authors for North-African Paleocene sections. Please note that we refer to the planktonic foraminiferal zonation adopted in this paper.

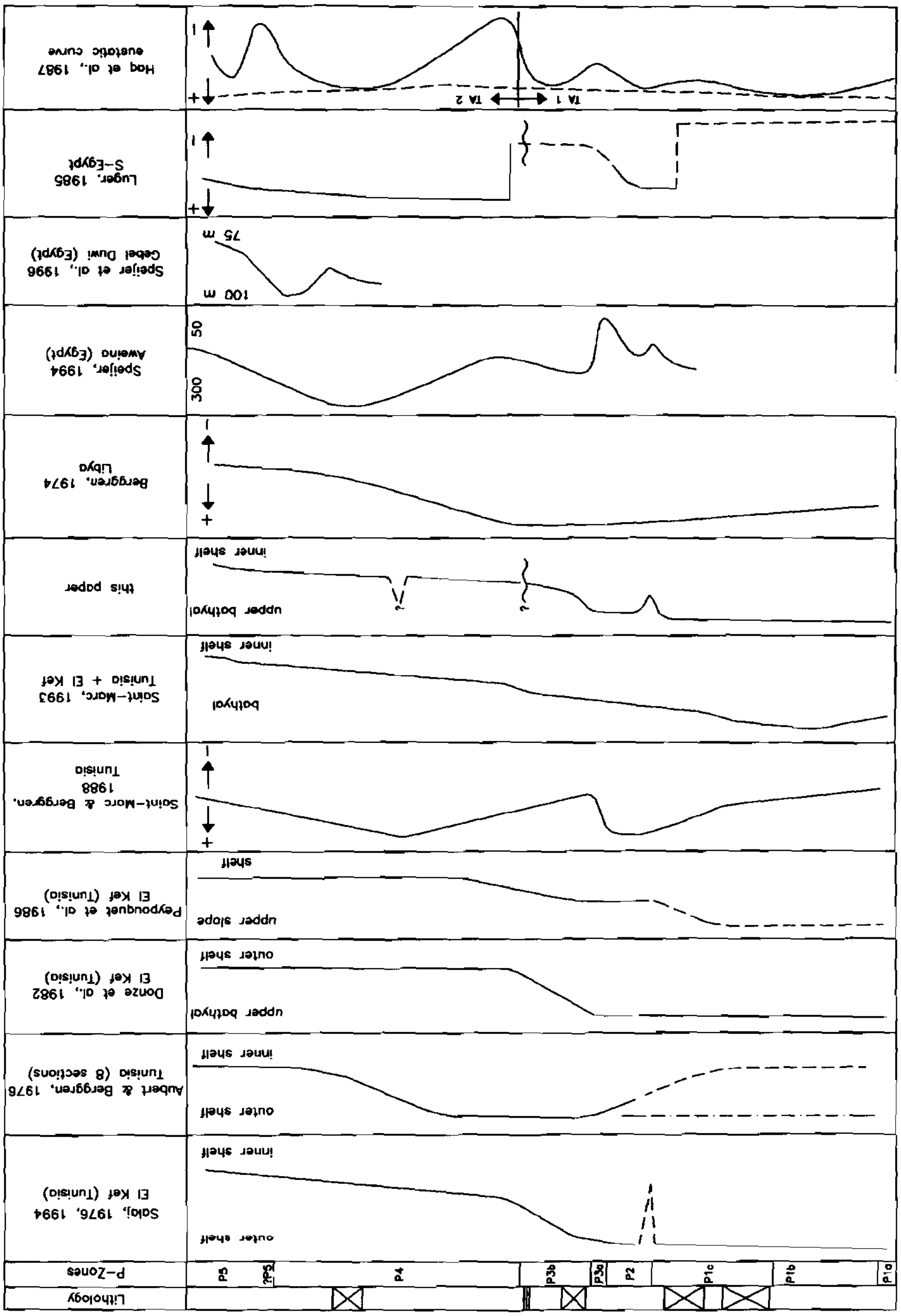
Lithology
P-Zones
P1a
P1b
P1c
P2
P3a
P3b
P4
?P5
P5
Salaj, 1976, 1994
El Kef (Tunisia)
outer shelf
inner shelf
Aubert & Berggren, 1976
Tunisia (8 sections)
outer shelf
inner shelf
Donze et al., 1982
El Kef (Tunisia)
upper bathyal
outer shelf
Peypouquet et al., 1986
El Kef (Tunisia)
upper slope
shelf
Saint-Marc & Berggren, 1988
Tunisia
+
-
Saint-Marc, 1993
Tunisia + El Kef
bathyal
inner shelf
this paper
upper bathyal
inner shelf
?
Berggren, 1974
Libya
+
-
Speijer, 1994
Aweina (Egypt)
300
50
Speijer et al., 1996
Gebel Duwi (Egypt)
100 m
75 m
Luger, 1985
S-Egypt
+
-
Haq et al., 1987
eustatic curve
TA 1
TA 2
+
-

deepening trend was established in the upper P4 Zone (Speijer, 1994; Speijer and Van der Zwaan, 1994). Upper Paleocene benthic faunas from Gebel Duwi (Red Sea, Egypt) indicate only minor sea-level fluctuations during the late Paleocene, when a transient deepening is recorded at the top of Zone P4 (Speijer et al., 1996).

Our present data from the El Kef section point to shallowing from outer neritic-upper bathyal to neritic depths, starting in Zone P3b, and continuing into Zones P4 and P5. A short-term shallowing is observed at the top of Zone P1, and possibly a short deepening spell in Zone P4. We therefore agree with most authors on an overall shallowing marking Zones P3b to P5 in Tunisia and Libya, although our results differ in details from those in other publications. Sea-level trends recorded in Egypt seem to differ from those observed in Tunisia and Libya. Our results do not agree with the eustatic sea-level curve proposed by Haq et al. (1987). This may in part be due to differences in biozonation schemes.

5.2. Trophic levels and oxygenation

Although sea level is not the only factor determining distribution of benthic foraminiferal species, effects of combinations of parameters are difficult to quantify. Several authors have assessed the behaviour of recent benthic foraminiferal faunas under extreme (food, oxygen) conditions. Results show that under oxygen stress, low-diversity assemblages tend to occur, characterized by strong dominance (e.g. Corliss and Chen, 1988; Van der Zwaan and Jorissen, 1991; Barmawidjaja et al., 1991; Sjoerdsma and Van der Zwaan, 1992; Sen-Gupta and Machain-Castillo, 1993; Linke and Lutze, 1993). In some cases, this oxygen stress is related to (periodically) enhanced supply of organic matter, depriving the environment of oxygen. Influence by river outflow, and consequently by organic carbon supply, on bathymetric distribution of benthic foraminifera was described by Pflum and Frerichs (1976). In relation to the latest Paleocene event, temporary migration of neritic taxa to an upper-middle bathyal site was noticed. Redeposition of sediments was considered highly unlikely; the site had apparently been vacated by the earlier occurring bathyal assemblage due to severe oxygen deficiency (Speijer and Van der Zwaan, 1994). Taxa that dominate associations during periods of environmental stress, or repopulate sites during short-lived periods of ameliorating conditions, are apparently favoured by a more opportunistic strategy. Their depth distribution is not fixed and they are able to survive under more or less severe dysoxia.

5.2.1. Trophic conditions

Paleoproductivity reconstructions on the basis of foraminiferal accumulation rates (PFAR, BFAR: $N.cm^{-2}.ky^{-1}$) are not feasible in our material. Stable carbon isotope data are only available for the earliest Paleocene (Keller and Lindinger, 1989), and point to low surface productivity, most probably affecting seafloor productivity indirectly. Evidence for low paleoproductivity levels during the earliest Paleocene was also mentioned by Keller (1988, 1992), and Speijer and Van der Zwaan (1996). Further paleoproductivity reconstructions rely on benthic foraminiferal numbers (BFN: Fig. 2), although an underestimation may be caused by dissolution, and dilution due to enhanced sediment supply. BFN from the lower 10 m of the section (63 µm fraction) indicate an increase in seafloor productivity in Zone P1a. BFN from the rest of the section (125 µm fraction) indicate that benthic productivity varied, but reached a relative maximum during the late Paleocene. Species, reported from eutrophic environments in Egypt (Speijer and Van der Zwaan, 1994; Speijer et al., 1996), enter the record or show increasing abundances in the El Kef section toward the end of the Paleocene: *Valvulineria scrobiculata*, *Anomalinoides* cf. *aegyptiacus*, *Stainforthia* spp. Decreasing diversity and increasing dominance in Zone P4 also indicate changes in the paleoenvironment. Peak abundances of buliminids already occurred in the middle of Zone P4. Moreover, *Frondicularia phosphatica* is regularly present in the coarse fractions of the sample material. Phosphate-rich sediments, deposited during the late Paleocene near El Kef (Salaj, 1976, 1980; Peypouquet et al., 1986), and at other localities in Tunisia (Aubert and Berggren, 1976) also suggest an increase of trophic levels.

5.2.2. Oxygenation

Oxygen deficiency is indicated by laminated sediments at the base of the Paleocene section (see also Speijer and Van der Zwaan, 1996). In upper Zone P1a and Zone P1b, amelioration of seafloor oxygenation is indicated by the entry of a number of species, common to a deeper water, open marine environment (e.g. *Gavelinella beccariiformis*, *Pulsiphonina prima*; Fig. 3, Table I). The appearance of small burrows in Zone P1a supports the view of an ameliorating environment. Towards the end of the Paleocene the benthic foraminiferal assemblages not only indicate high trophic levels, but also decreasing oxygen levels at the seafloor: the assemblage present in the upper Paleocene top sample of the El Kef section, AFN641, strongly resembles the uppermost Paleocene assemblages recorded in shallow, oxygen-deficient deposits in Egypt (Speijer and Van der Zwaan, 1994; Speijer et al., 1996). Seafloor oxygenation was emphasized by Donze et al. (1982) and Peypouquet et al. (1986) to be an important factor controlling ostracode distributions. These authors stressed the importance of water column stratification and the position of the oxygen minimum zone (OMZ), and found evidence for dysoxia and eutrophication due to upwelling during the late Paleocene.

Eutrophication of the environment due to increased upwelling during the latest Paleocene has been inferred for other sites along the southern Tethys margin (Speijer and Van der Zwaan, 1994; Speijer et al., 1996). If true, it is to be expected that paleobathymetrical estimates are affected by increased eutrophication, for instance by the 'delta effect' (Pflum and Frerichs, 1976). Although we infer sea-level fluctuations, with a prolonged shallowing starting around the P3a-P3b zonal transition, and continuing into the late Paleocene, we believe that eutrophic conditions and dysoxia cause a paleoenvironmental signal that may lead to overestimation of relative sea-level movements.

5.3. Multivariate analysis

Qualitative interpretations contained in the previous section are confirmed by the quantitative analysis. The first principal component axis (Fig. 4a) apparently represents paleo-oxygenation. Positive loadings are species occurring in Zones P1b-P3b, representing deeper-water well aerated environments. Negative loadings are species that occur in Zone P1a, the lowermost Paleocene, primarily representing an environment characterized by oxygen deficiency and low trophic levels (cf. Donze et al., 1982; Peypouquet et al., 1986; Keller, 1988, 1992; Keller and Lindinger, 1989; Speijer and Van der Zwaan, 1996). These species, like the positively loading taxa, were reported from outer neritic to upper bathyal depths (e.g. *Cibicidoides pseudoacutus*, *Osangularia plummerae*) or did not show clear depth preferences (*Anomalinoides praeacutus*, *Nodosaria* spp.; Tab.1). Paleobathymetrical indicator species show no clear pattern in loadings. Paleoproductivity does not significantly load the axis: species characteristic of eutrophic environments (e.g. *Anomalinoides* cf. *aegyptiacus*, *Valvulineria scrobiculata*) show only slightly negative loadings.

The sample score pattern on the second principal component appears to be related to benthic productivity. Positive loadings are species occurring in Zones P1a to P3a (*Anomalinoides simplex*, *Osangularia plummerae*; *Coryphostoma midwayensis*, *Cibicidoides pseudoacutus*), for which we concluded to low productivity conditions in the previous section. Species loading negatively occur in upper Zone P4 and Zone P5, which were characterized by higher trophic levels (e.g. *Anomalinoides aegyptiacus*, *Valvulineria*(?) *insueta*, *Gyroidinoides aequilateralis*, *Bulimina* spp.; also: *Haplophragmoides* spp., *Lenticulina* spp.). A number of these species are also considered to be characteristic of shallow deposits, indicating that paleodepth also loads the second axis.

In the bivariate plot of sample scores (Fig. 4b) samples from the basal Paleocene sediments (Zone P1a), representing low production and oxygenation levels at the seafloor, occupy the upper left corner. Samples from Zones P1b-P3b, the period of maximum diversity (Fig. 2), occupy the upper right corner of the diagram. Biconvex species characterize the associations in this interval; buliminids are relatively scarce (Fig. 3). Samples AFN585 - AFN591 (top of Zone P1a, base of Zone P1b) are positioned along a gradient on the first axis. In this interval oxygen levels ameliorated and some 30 species enter the record, causing an increase in diversity from alpha = 8.5 to alpha = 13 (Figs. 2, 3). Samples from Zones P4 and P5 represent increased trophic levels and a somewhat decreased seafloor oxygenation, and form the third sample cloud in the lower middle of the diagram. Samples AFN617 - AFN 622 (Zone P3b and lower Zone P4) are transitional along the second axis and correspond to a period of decreasing diversity (alpha = 10.5 to alpha = 3.9).

6. Conclusions

The Paleocene benthic foraminiferal record of the El Kef section reveals that major paleoenvironmental changes followed the biotic crisis at the K/Pg boundary. The most pronounced changes are the onset of shallowing during the early late Paleocene (P3a-P3b zonal transition) and increased eutrophication towards the late Paleocene. After the K/Pg boundary event and the subsequent period of lowered productivity and oxygenation normal paleoenvironmental conditions were gradually restored in Zones P1a and P1b. A more or less stable ecosystem then existed until the end of Zone P3a. The first signs of shallowing are recorded at the P1c-P2 zonal boundary, marked by a temporary lowering of the P/B ratios. At the P3a-P3b zonal transition shallowing is apparent from the rather sudden disappearance or decreasing abundance of deeper-water species. In Zone P4 this shallowing continued and increasing eutrophication occurred, as indicated by peak occurrences of buliminids and the entry of species characteristic of the latest Paleocene eutrophic environments.

The magnitude of relative sea-level movements is not easy to ascertain, due to interaction with the eutrophication signal. Shallowing from outer neritic-upper bathyal to middle-inner neritic depths is nevertheless likely. Sea-level fluctuations may not have been operating on a global scale, as correlation with the eustatic curve (Haq et al., 1987) is not convincing. On a regional scale, it appears that sea-level fluctuations in Egypt differ from those in Tunisia and Libya.

Combined shallowing and eutrophication led to the appearance of very characteristic late Paleocene assemblages in the El Kef section, that have also been recovered at other sites on the southern Tethys margin. Faunal development during the latest Paleocene at El Kef is comparable to faunal development in Egypt, recorded in connection with the latest Paleocene extinction event. It appears that eutrophic, oxygen-deficient mud shelves developed along the southern Tethys margin during the late Paleocene. These shelves were populated by benthic foraminiferal associations that differed considerably from those present before. Although these associations can be interpreted in a purely paleobathymetric context of rising and falling sea level, we emphasize the effect of trophic and oxygen levels on benthic foraminiferal depth distributions.

Acknowledgements

We wish to thank G. van 't Veld and G. Ittmann for processing the samples and G. Ittmann for making nannoplankton slides. T. van Hinte prepared the illustrations. We also thank W.A. Berggren, G. Keller and N. Ortiz for carefully reviewing the manuscript. RPS acknowledges financial support from the Swedish Institute and the Wenner-Gren Foundations.

Chapter 3

Miocene Mediterranean:
Monte del Casino (N-Italy)

Deep-water changes: The near-synchronous disappearance of a group of benthic foraminifera from the late Miocene Mediterranean

Abstract

Benthic foraminiferal and geochemical data from the Monte del Casino section in Northern Italy are employed to reconstruct the sequence of events preceding the late Miocene Mediterranean salinity crisis. We evaluate the effects of eustatic sea-level changes and tectonic events, affecting the Atlantic-Mediterranean connections. Changing benthic foraminiferal assemblages record changes in the deep-water environment, that can be explained by progressive isolation of the Mediterranean basin. The results of the analyses of stable oxygen- and carbon isotopes and redox-sensitive elements are in line with the benthic faunal trends. At 7.16 Ma, a first major step in isolation of the basin is indicated by the nearly simultaneous disappearance of a group of deeper-water benthic species usually found in middle to lower slope environments. At the same time, stable isotopes and redox-sensitive elements indicate cooling and decreasing bottom water oxygenation.

After 6.8 Ma gradual development of water-mass stratification, probably accompanied by increasing bottom-water salinity, is indicated by all proxies. The cyclic pattern of homogeneous and sapropelitic sediments in the section is related to astronomical parameters, and allows a detailed correlation with Mediterranean sections at considerable geographic distances. We compared the benthic foraminiferal faunas with those from the Metochia section (Gavdos, Greece), deposited at a similar water depth (~1000m), to find that the benthic foraminifera at both sites indicate a similar, synchronous paleoenvironmental development. All proxies indicate that the onset of the late Miocene Mediterranean salinity crisis dates back to the earliest Messinian. The development of the Mediterranean basin toward an evaporite trap is a result of interactions between a 400-ky eccentricity related climatic effect superimposed upon gateway dynamics at the Atlantic-Mediterranean connections. Benthic foraminifera accurately record the steps in increasing isolation of the Mediterranean basin.

T. J. Kouwenhoven, M.-S. Seidenkrantz & G. J. van der Zwaan, Palaeogeography, Palaeoclimatology, Palaeoecology, 152, 259-281.

1. Introduction

From the moment the extent of Messinian (late Miocene) evaporites in the deep Mediterranean basins became evident (DSDP Leg 13: Scientific Staff, 1970; Hsü et al., 1973), the Messinian 'salinity crisis' has been a subject of research and speculations. Evidence exists that although the end of the Messinian salinity crisis appears to have been rather abrupt, the onset was gradual. Throughout the Mediterranean, the pre-evaporite sediments display changing lithologies during the early Messinian, from predominantly marl/sapropel sequences to either diatomites (e.g. Sicily, Gavdos, NE Morocco, Algeria) or euxinic clays (e.g. northern Italy, Tyrrhenian Sea, eastern Mediterranean). Paleoenvironmental changes related to these lithological transitions are documented by faunal (a.o. Cita, 1976; Van der Zwaan, 1982; Glaçon et al., 1990; Benson and Rakic-El Bied, 1991; Benson et al., 1991; Sierro et al., 1993; Hodell et al., 1994; Calieri, 1996, 1997) and geochemical (stable isotope) parameters (a.o. Vergnaud-Grazzini, 1978, 1983; Vergnaud-Grazzini et al., 1977; McKenzie, 1979/1980; Van der Zwaan and Thomas, 1980; Van der Zwaan and Gudjonsson, 1986; Hodell et al., 1989, 1994; Kastens, 1992, Ferretti and Terzi, 1995). The increasing accuracy of time control (e.g. GPTS: Cande and Kent, 1992, 1995; APTS: Hilgen et al., 1995; Shackleton et al., 1995) improves the correlation of these phenomena throughout the Mediterranean.

Questions remain on paleoenvironmental and paleohydrographical conditions in the basin during the latest Miocene, and the sequence of events leading to the Messinian salinity crisis. Arguments for a tectonic cause for the closure of the Mediterranean basin have been mentioned in a.o. Weijermars (1988), Platt and Vissers (1989), and Krijgsman et al. (1999). In other publications it was argued that at the onset of the salinity crisis global sea level dropped (Ryan, 1973; Ryan et al., 1974; Vincent et al., 1980, 1985; Hsü et al., 1973; Van Couvering, 1976; Berggren and Haq, 1976; Adams et al., 1977; Berger and Vincent, 1986; Benson, 1991; Hodell et al., 1994). However, throughout the years it has proved to be difficult to correlate the start of such a glacio-eustatic sea-level lowering to the onset of the salinity crisis (Cita, 1979; Cita and Ryan, 1979; Hodell et al., 1986, 1994; Kastens, 1992). At several oceanic sites no shift in $\delta^{18}O$ values, supporting such a eustatic sea-level drop, was observed (Hodell and Kennett, 1986; Keigwin, 1987; Zhang and Scott, 1996). Papers on contemporaneous sections within the Mediterranean region are not conclusive in regard to this point.

Sonnenfeld (1984) argues that the accumulation of substantial amounts of evaporites can only be explained if the outflow from a basin with anti-estuarine circulation has been substantially obstructed for a considerable amount of time. Inflow of surface waters is mainly regulated by evaporitic loss, and the outflow is regulated by the cross-sectional area of the strait connecting the two basins, rather than the depth of the sill. Obstruction of the outflow will increase the residence time of the waters, and will lead to anoxic bottom waters and eventually to development of a brine.

Detailed records pertaining to the Mediterranean-Atlantic water exchange are scarce. Benson et al. (1991) and Krijgsman et al. (1999) present evidence for at least a partial closure of the Rifian Corridor during the earliest Messinian. The Betic Street (southern

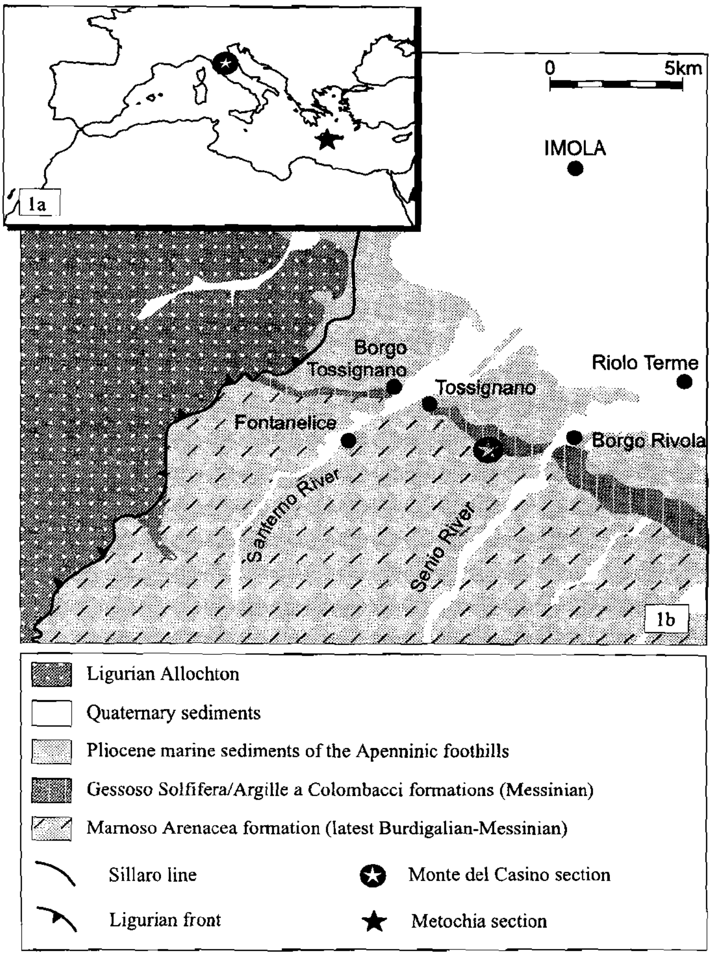

Figure 1. **(a)** Locations of the two sections discussed in the text: The Monte del Casino section in northern Italy and the Metochia section on Gavdos (south of Crete, Greece). **(b)** Detailed location of the Monte del Casino section. Modified from Van der Meulen et al. (1999).

Spain) was probably (but not conclusively: see Vai, 1997) the only other connection. Data summarised by Gebhardt (1994) suggest that the northern Betic Street, being the most effective connection between the Mediterranean and Atlantic since Oligocene times, started to shoal already during the early Tortonian, and that no significant water transfer occurred from late Tortonian times onward. In the more internal Betic Zone, evidence exists that the Fortuna Basin shoaled during the Tortonian/Messinian boundary interval (Müller and Hsü, 1987). In the Sorbas and Nijar Basins, however, marine sediments were deposited during part of the Messinian (Ott d'Estevou and Montenat, 1990; Van de Poel, 1992; Sierro et al., 1997).

The present paper aims at a detailed reconstruction of paleoenvironmental trends and events preceding the Messinian salinity crisis in the Monte del Casino section in northern Italy (Fig. 1). Sediments of the major part of this section were deposited at a paleodepth of approximately 1000 m. Benthic foraminiferal and geochemical data will be discussed, and compared with selected faunal data from the eastern Mediterranean Metochia section, located on Gavdos, near Crete (Seidenkrantz et al., subm.; Fig. 1a). Similar events at both sites are considered to have a causal relationship with the development of the proto-Mediterranean basin toward an evaporite trap.

2. Material and methods

2.1. Geological setting

The Monte del Casino section is part of the Euxinic Shale Formation (sensu Vai, 1997), that covers the Marnoso-arenacea Formation, a turbiditic wedge of Miocene age filling the Marnoso-arenacea Basin in the northern foothills of the Apennines. Extensive studies have been performed on the structural background and paleogeography of the Marnoso-arenacea Basin, and its position in the context of foreland basin migration (e.g. Ricci Lucchi, 1975, 1986; De Jager, 1979; Vai and Ricci Lucchi, 1977, and references therein). Foreland basin migration in the Apennines is generally directed to the northeast. Recently, Van der Meulen et al. (1998 and in press), testing the hypothesis of lateral migration of slab detachment formulated by Wortel and Spakman (1992), related a north-to-south (along-arc) component of depocentre migration to the detachment of subducted lithosphere underneath the Apenninic arc. In Van der Meulen et al. (in press) it is argued, that early Messinian uplift of the Romagnan Apennines is a regional phenomenon, related to dynamic equilibration after slab detachment in the deep subsurface.

The external (eastern) part of the Marnoso-arenacea turbiditic wedge is relatively undisturbed. On top of this wedge, open marine mudstones were deposited that offer sections suitable for high-resolution stratigraphy (Ricci Lucchi, 1986; see Krijgsman et al., 1997; Vai, 1997). In this region a number of early Messinian events have been recognized: a lithological transition from hemipelagic marls to euxinic clays, disappearance of megabenthos, enhanced preservation of organic matter, and deposition of Fe-sulfides (see a.o. Ricci Lucchi, 1975, 1986; Vai and Ricci Lucchi, 1977; Vai, 1989). The euxinic clays are overlain by the Calcare di Base limestones, the base of the evaporite series of the Gessoso-solfifera Formation (sensu Selli, 1960). As the Calcare di Base is considered to be - at least in this area - a stromatolitic, and thus shallow-water limestone unit, shallowing must have preceded evaporite deposition (Vai and Ricci Lucchi, 1977; Ricci Lucchi, 1986).

The Monte del Casino section is located between the Santerno and Senio valleys, near Riolo Terme (Fig. 1b). Hemipelagic mudstones and the transition to euxinic clays crop out in this section. The alternation of marls and sapropelitic beds is related to astronomical parameters (Vai et al., 1993; Vai, 1997; Krijgsman et al., 1997; Fig. 2) and thus, bed-to-bed correlations can be made with other sections in the Mediterranean.

2.2. Section and sampling

The major part of the Monte del Casino section consists of blue-grey, homogeneous hemipelagic marly clays, alternating with dark greenish-brown to black, laminated, sapropelitic sediments that smell of hydrocarbons. The latter are here referred to as 'sapropels'. Sedimentary cycles, each consisting of a sapropel and a homogeneous layer, are numbered C1 - C56 from bottom to top (Fig. 2). A greyish, non-laminated layer over- or underlies part of the sapropels or is developed instead of a sapropel. The Messinian cycles are thinner than those of the Tortonian. Moreover, in the Messinian part of the sequence nearly every insolation maximum correlates with a sapropel, contrary to the Tortonian part of the sequence. In the upper part of the section, the homogeneous layers of the sedimentary cycles are relatively thinner and the sapropels thicker. The colour of the homogeneous beds changes from blue-grey to dark greenish-brown, and the colour contrast between homogeneous sediments and sapropels is gradually lost in the uppermost twelve cycles sampled.

At the basis of the section, mainly below cycle C3, a large number of thin turbidites is intercalated. Biotite rich (ash-)layers occur in the late Tortonian part of the section (see also Vai et al., 1993; Krijgsman et al., 1997; Laurenzi et al., 1997). The top of the section is poorly exposed, disturbed by small faults and shear planes, and is separated from overlying evaporites of the Gessoso-solfifera series by a hiatus.

The samples used for this study were collected during field trips in 1995 and 1996. A composite section was created in order to avoid shear planes, that cause disturbances in the stratigraphy. In 1995 the samples were collected by coring; this sample set (cycles C15 - C42) was described by Krijgsman et al. (1997: magneto-, tephra- and biostratigraphy), and Calieri (1997: quantitative biostratigraphy). In 1996 additional hand samples were collected (cycles C1 - C14 and C43 - C56).

2.3. Numerical ages

The age model for the Monte del Casino section is based on papers by Hilgen et al. (1995), and Krijgsman et al. (1995, 1997). No coherent magnetostratigraphy was obtained for the section (see Krijgsman et al., 1997; Negri and Vigliotti, 1997). For cycles C15 - C42 the ages of Krijgsman et al. (1997), based mainly on biostratigraphy and cyclostratigraphy, were adopted. Cycles C1 - C14 and C43 - C56 were correlated to the 65^{0}N summer insolation curve of the astronomical solution La90 $_{1,1}$ (see Hilgen et al., 1995), by correlating sapropel midpoints to insolation maxima with a 3 ky time lag (Lourens et al., 1996; Reichart, 1997). Sample ages were calculated by assuming a constant sedimentation rate between sapropel midpoints and biostratigraphic datum levels. Numerical ages for cycles C1 and C2 are tentative and were calculated from sedimentation rates not exceeding 100 cm/ky, which may be underestimated in the given sedimentary environment. A miscorrelation of one or two cycles towards the top of the section can not be excluded, as biostratigraphic control is limited in this interval. However, we do not expect this to influence the main findings we present. The age model applied here places the Tortonian/Messinian boundary at 7.24 Ma, at the FCO of *Globorotalia conomiozea* group, conical morphotypes (Hilgen et al., 1995; Krijgsman et al., 1997). Based on the above considerations, the section as described in this paper represents the period between 8.144 - 6.304 Ma (Fig. 2).

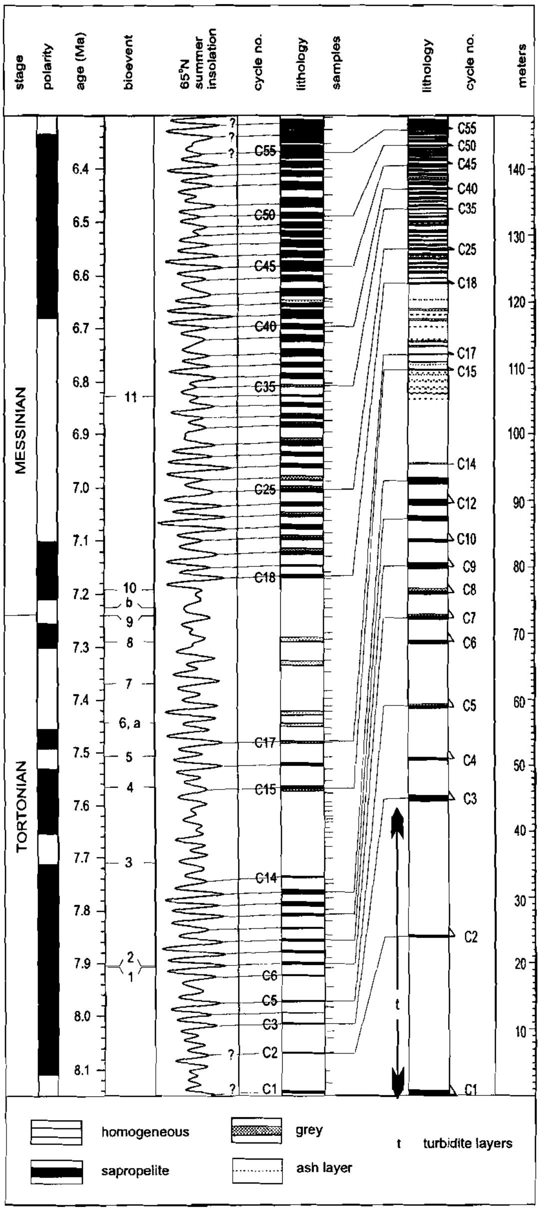

Figure 2. Lithostratigraphy and age model of the Monte del Casino section, giving the position of sapropels, grey bands, ash layers, and the samples counted for benthic foraminifera. Sedimentary cycles (1 cycle = sapropel + homogeneous marl) are numbered *C1-C56*. Bioevents as recorded in the section: Planktonic foraminifera: 1=FO *G. conomiozea* group; 2=lro *S. seminulina*; 3=hro *S. seminulina*; 4=d/s coiling shift of *G. scitula* group; 5=LCO *G. menardii* 4; 6=LO *C. parvulus*; 7=FO *G. menardii* 5; 8=influx *G. menardii* 4; 9=FRO *G. conomiozea* group, conical morphotypes; 10=influx *G. conomiozea*; 11=FO *G. nicolae*. Calcareous nannoplankton: a=FO *Amaurolithus* spp.; b=FCO *Amaurolithus* spp. Bioevents 4 to 11 and a + b from Krijgsman et al. (1997); 1 to 3 from F.J. Hilgen, pers. comm., 1998. Magnetic polarity based on Hilgen et al. (1995).

2.4. Sample treatment and faunal parameters

In this study we concentrate on the larger scale paleoenvironmental development through time. For this reason, the 95 samples we studied were selected from homogeneous sediments. In intervals with cyclic alternations of homogeneous and sapropelitic sediments, samples were preferentially chosen from the midpoints of the homogeneous layers; in intervals without sapropels care was taken to get a sufficient coverage of samples, i.e. at least one sample per ~20 ky (Fig. 2). The samples were dry weighed, disintegrated in water and washed over a set of 63 μm, 125 μm, and 595 μm sieves. Representative aliquots, containing 200-300 benthic foraminiferal specimens, were split using an Otto microsplitter. The picked specimens were mounted on permanent slides, identified, and counted.

Benthic faunal (simple) diversity and dominance are used as additional indications for normal marine versus restricted bottom water conditions. Dominance is expressed as the relative percentage of the most abundant benthic foraminiferal species in a sample. The percentage of planktonic foraminifera in the total foraminiferal fauna (P/B ratio) was estimated by counting 300-500 specimens from random squares on a picking tray, and is expressed as 100*P/(P+B). The P/B ratios were corrected for allochthonous and infaunal elements and were used to calculate paleobathymetry of the samples, following Van der Zwaan et al. (1990). Fluxes, used as a measure of productivity, were calculated from dry weights as PFAR and BFAR (planktonic and benthic foraminiferal accumulation rates, respectively) and expressed as numbers cm^{-2} ky^{-1}.

2.5. Statistical analysis

As an aid in defining benthic faunal assemblages, standard SPSS computer software was used to run statistical analyses on relative frequency data. The original data set contains 94 variables, consisting of species, and generic and suprageneric categories (Appendix). From the census data relative frequencies were calculated. For the purpose of a hierarchical cluster analysis (within-group, average linkage), allochthonous species, ill-defined remainder groups, and species occurring in frequencies below 5% were omitted. In order to avoid overrepresentation of species included in the analysis, no new closed sum was calculated. Hierarchical clustering (Pearson correlation) was performed on the remaining 37 variables. The same reduced data set was introduced into a factor analysis, with the purpose of describing the major trends in benthic faunal development. Unrotated factor scores of the first two axes are considered.

2.6. Geochemical analyses

Stable oxygen and carbon isotopes of planktonic and benthic foraminifera were analyzed. Preservation of the foraminiferal faunas was in general too poor to run analyses on monospecific samples. Instead, we randomly picked the best-preserved specimens, both planktonic and benthic, in an attempt to balance for species-related isotopic fractionation. Residues from the 125-595 μm fraction were dry-sieved over a 212 μm sieve in order to obtain larger (adult) specimens, as juveniles may carry a lighter isotopic signal. At least 30-50 planktonic and 15-20 benthic specimens were picked per sample. The specimens were roasted in vacuo, and subsequently treated with hydrophosphoric acid at 100 ^{0}C for 90 minutes. Measurements were carried out on a VG SIRA 24 mass spectrometer and are reported in the ∂-notation as permil deviations from the PDB standard. The differences between planktonic and benthic isotope signals, the $\Delta\partial^{18}O$ and $\Delta\partial^{13}C$, were calculated. Of these, especially the $\Delta\partial^{18}O$ gives an estimate the degree of stratification of water masses.

For the element analysis 5 gram of sediment was dried in a stove for 24 hours and then ground in an agate mortar. Of the resulting powder 0.125 gram was dissolved in an acid mixture of HF, $HClO_4$, and HNO_3. The dried residue was dissolved in 1M hydrochloric acid and analysed with a Perkin Elmer OPTIMA 3000 inductively coupled plasma atomic emission spectrometer (ICP-AES). The concentrations of the redox-sensitive elements manganese and vanadium were normalised to the aluminium content of the sediment in order to compensate for terrestrial input. The element ratios Mn/Al and V/Al are used to estimate the oxygenation state of the sediments at the time of deposition.

3. Results

3.1. Faunal and statistical analysis

The relative frequency data (Fig. 3) show a change in benthic faunal composition through time. Two major faunal assemblages can be discerned, with a transition occurring between 7.16 and 6.8 Ma. These assemblages conform to the main groups I and II in the dendrogram (Fig. 4), and can be further subdivided into discrete sub-assemblages: clusters 1 to 4 and 5 + 6 respectively (Figs. 4, 5). A minor shift in species composition occurs around 7.6 Ma, between species of clusters 1 and 3 (Figs. 4, 5), and corresponds to a temporary decrease in the faunal diversity (Fig. 6). In the first sample above the sapropel of cycle C18, at 7.16 Ma, a number of species have disappeared. Within cluster 1 (Fig. 4), the species marked with an asterisk are the species that left the record during deposition of the sapropel of cycle C18: *Cibicides wuellerstorfi, Cibicidoides italicus, Siphonina reticulata,* and *Uvigerina proboscidea*, and somewhat later *C. bradyi*. Subsequently, a completely different, low-diversity assemblage is established towards the top of the section. The decrease in benthic faunal diversity occurs in two major steps at 7.16 and 6.8 Ma, and is mirrored by increasing dominance (Fig. 6). Maximum abundances of species groups represented by clusters 2 to 6 follow each other through time.

Figure 3. Relative frequency data for a number of species, that were imported into statistical analysis.

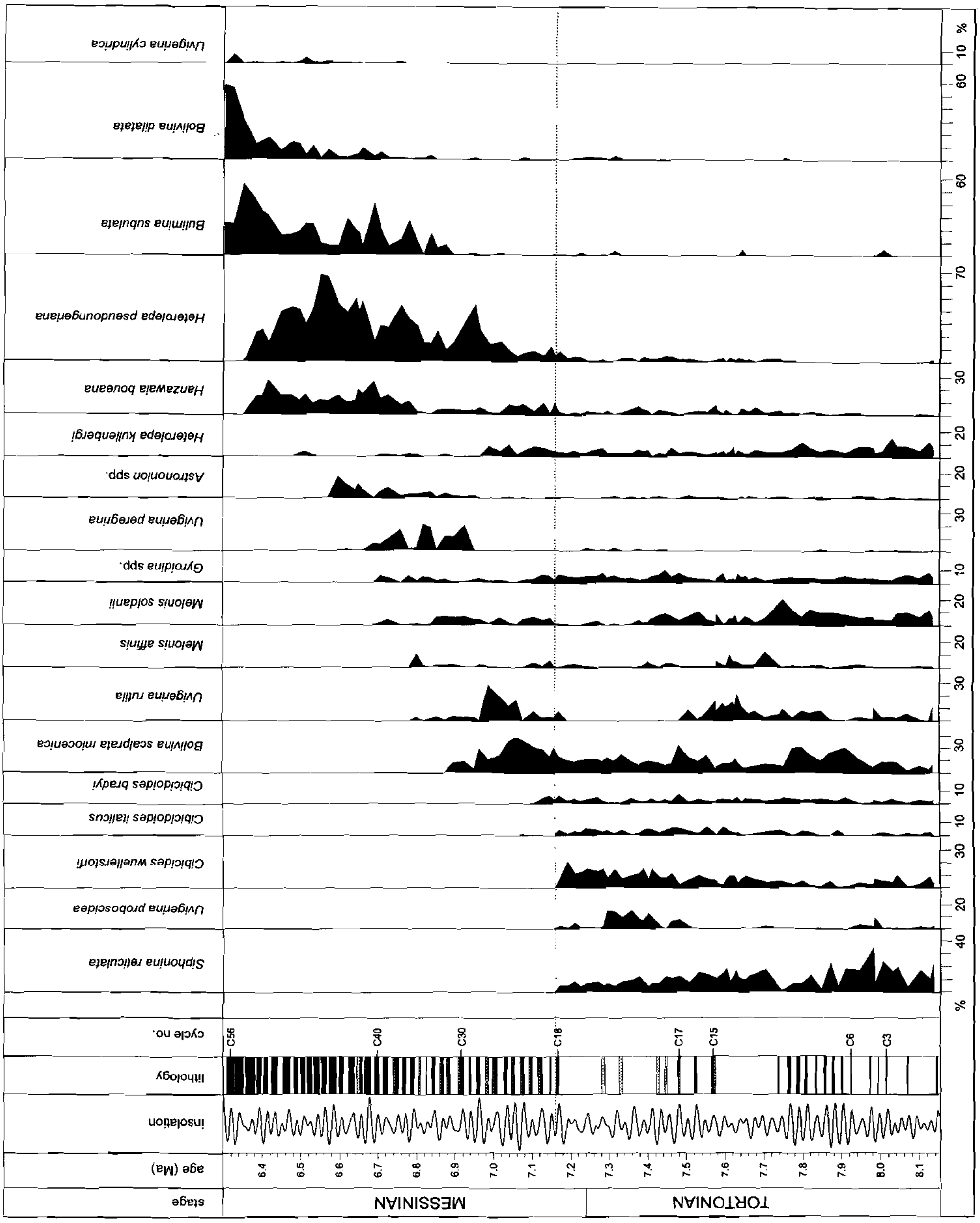
stage
MESSINIAN
TORTONIAN
age (Ma)
6.4
6.5
6.6
6.7
6.8
6.9
7.0
7.1
7.2
7.3
7.4
7.5
7.6
7.7
7.8
7.9
8.0
8.1
insolation
lithology
cycle no.
C56
C40
C30
C18
C17
C15
C6
C3
%
Siphonina reticulata
40
Uvigerina proboscidea
20
Cibicides wuellerstorfi
30
Cibicidoides italicus
10
Cibicidoides bradyi
10
Bolivina scalprata miocenica
30
Uvigerina rutila
30
Melonis affinis
20
Melonis soldanii
20
Gyroidina spp.
10
Uvigerina peregrina
30
Astrononion spp.
20
Heterolepa kullenbergi
20
Hanzawaia boueana
30
Heterolepa pseudungeriana
70
Bulimina subulata
60
Bolivina dilatata
60
Uvigerina cylindrica
10
%

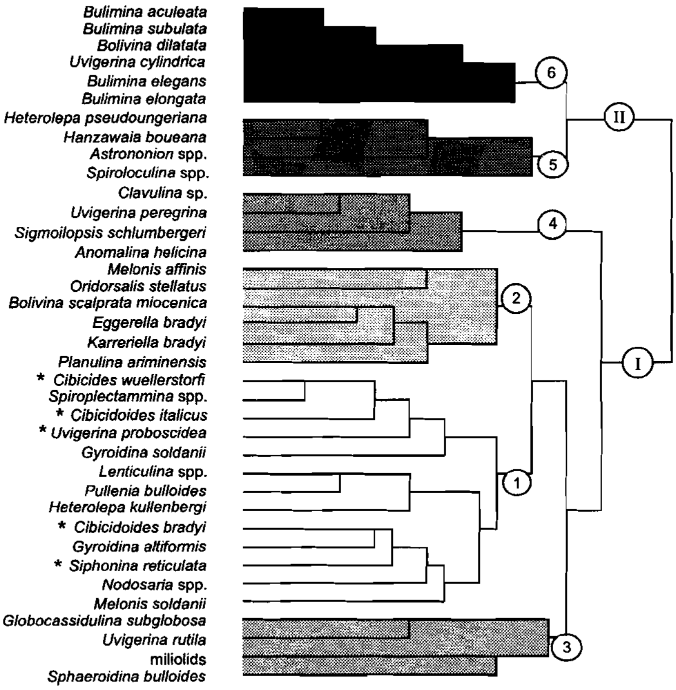

Figure 4. Dendrogram resulting from hierarchical clustering (Pearson correlation). Clustering divided the benthic foraminiferal faunas into two main groups and six clusters. Cluster I contains the group of species that disappears at 7.17 Ma: *Siphonina reticulata, Cibicides wuellerstorfi, Cibicidoides bradyi, C. italicus,* and *Uvigerina proboscidea*, marked with an asterisk.

Around 6.7 Ma, the P/B ratio falls, and subsequently, at 6.65 Ma, the benthic flux increases. Fluctuations in the planktonic flux are less conspicuous, except for a sudden drop at 7.6 Ma.

The first and second factor resulting from the principal component analysis are considered, and explain 24% and 8% of the variance respectively (Figs. 6 and 7; Table 1). Factor 1 scores start shifting from positive to negative values at ~7.16 Ma, and represent an overall dominating trend. Factor 2 scores have maximum values in the period between 7.16 and 6.8 Ma, and apparently represent a transitional interval.

3.2. Geochemical analyses

Curves of bulk planktonic and benthic oxygen and carbon stable isotopes are given in Figure 7. No monospecific record of sufficient quality could be generated, and although we picked the best preserved specimens, diagenetic overprint cannot be excluded altogether. Diagenetic modification can lead to lighter isotope values

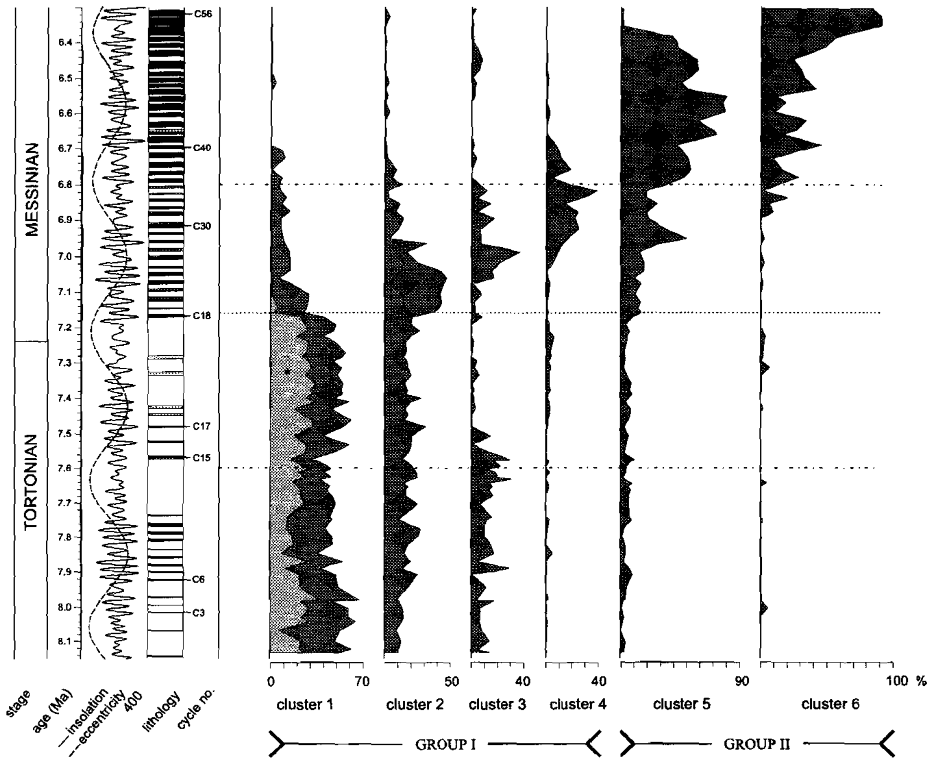

Figure 5. The six clusters of the dendrogram plotted against age, lithology and the 65^0 northern latitude summer insolation curve. Light shading in cluster I represents the species that disappear at 7.17 Ma (Fig. 4: marked with an asterisk).

(e.g. meteoric water); however, the effects of re-equilibration with pore waters should be acting on both isotope species. This often leads to both light ∂^{18}O and ∂^{13}C in Messinian sequences (Van der Zwaan and Gudjonsson, 1986), whereas we observe a trend towards heavy ∂^{18}O values during the Messinian, suggesting that diagenetic overprint could be minor.

Before ~7.16 Ma the oxygen and carbon isotopes are strongly correlated; after ~7.16 Ma the trends in oxygen and carbon isotopic values are diverging. Both the oxygen and the carbon isotopes shift towards lighter values at 7.6 Ma. The trend towards heavier values around 7.16 Ma is temporary for both isotope species. After 7.1 Ma the oxygen isotopes show an overall, continuing trend towards heavier values. The carbon isotopes shift to markedly lighter values between ~7.16 and ~6.8 Ma, and after 6.8 Ma show large shifts that cannot be explained by poor preservation of sample material. Towards the top of the section the carbon isotopes shift back to heavier values.

The $\Delta\partial$'s of especially the oxygen isotopes are used as an estimate of water mass stratification (see for instance Vergnaud-Grazzini, 1983). The Δ of ∂^{18}O reaches

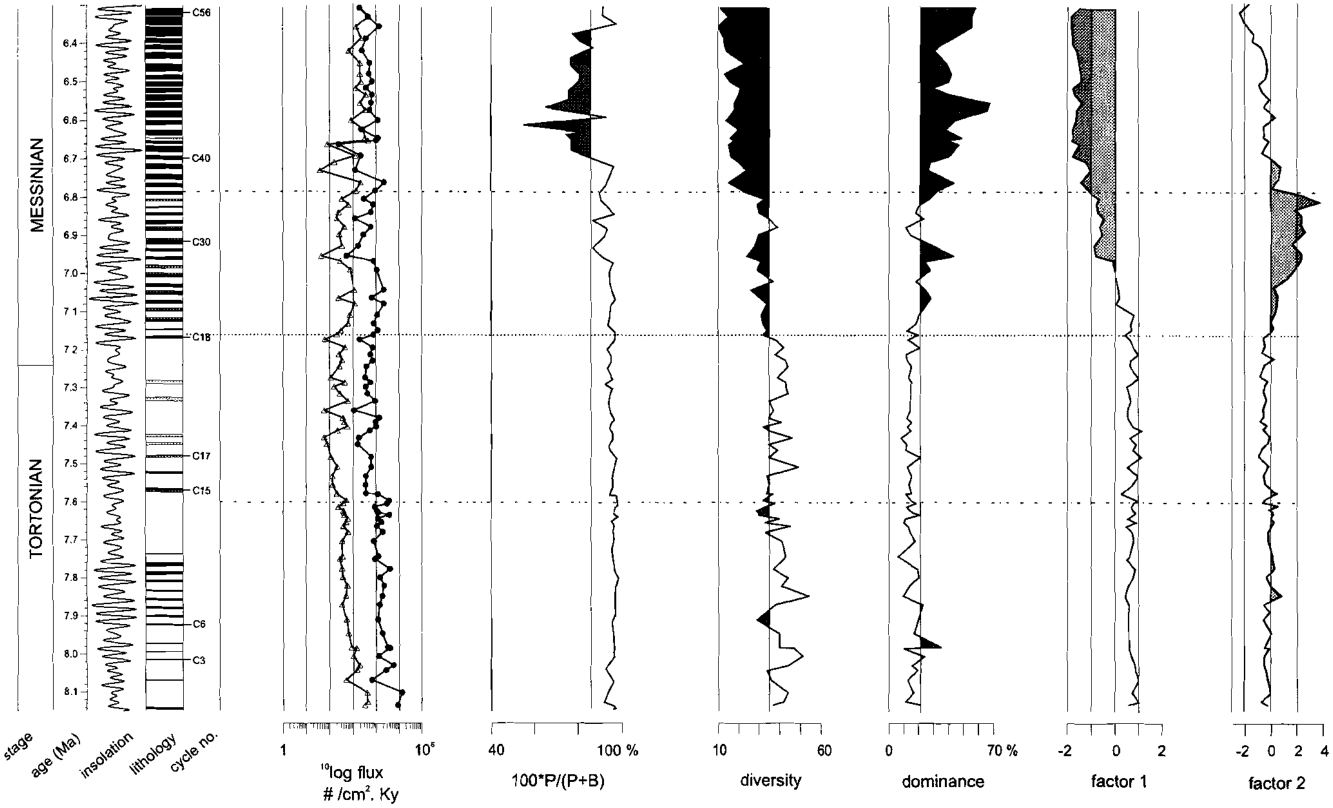

Figure 6. Faunal parameters, together with factor 1 and 2 scores. Data are plotted against age, lithology and the 65^0 northern latitude summer insolation curve. PFAR and BFAR are foraminiferal accumulation rates, calculated with correction for sedimentation rates. Note the log-scale. Triangles are benthos data; dots are plankton data.

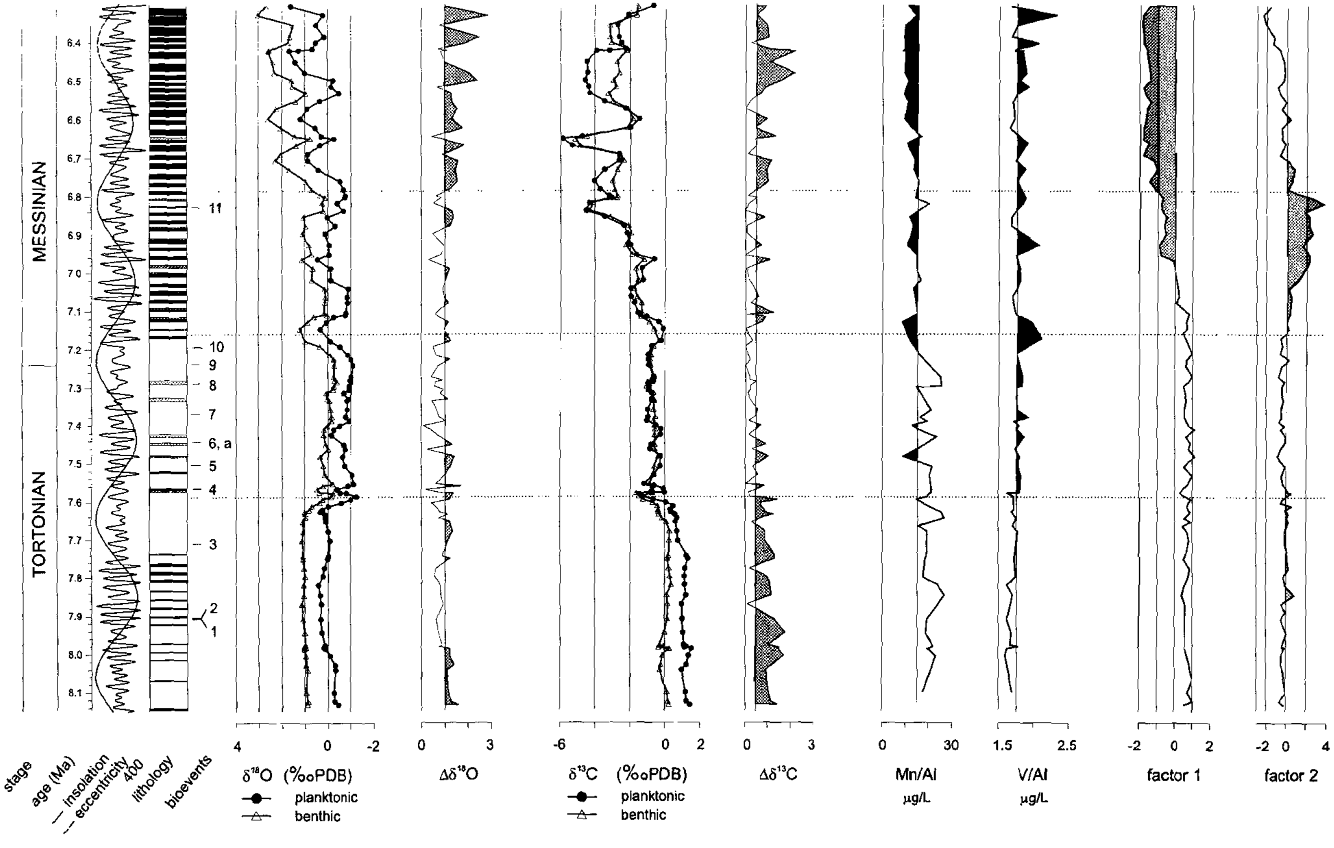

Figure 7. Geochemical data, together with factor scores. Data are plotted against age, lithology and the 65° northern latitude summer insolation curve. Stable isotope data are plotted as three point moving averages. For bioevents see Fig. 2.

Table I. Factor loadings for the species imported into statistical analyses

Species	factor 1	factor 2	Species	factor 1	factor 2
Cibicidoides bradyi	0.71608	0.21200	*Sphaeroidina bulloides*	0.29245	0.37397
Karreriella bradyi	0.67633	-0.09604	miliolids	0.17625	0.10471
Lenticulina spp.	0.65848	-0.05576	*Planulina ariminensis*	0.12630	0.05058
Nodosaria spp.	0.65845	-0.02554	*Globocassidulina subglobosa*	0.01855	0.30894
Heterolepa kullenbergi	0.64590	-0.12813	*Anomalina helicina*	-0.01878	0.56382
Cibicides wuellerstorfi	0.64526	-0.27331	*Sigmoilopsis schlumbergeri*	-0.02256	0.58776
Siphonina reticulata	0.63489	-0.25425	*Bulimina elongata*	-0.15257	-0.17349
Bolivina scalprata miocenica	0.61032	0.02489	*Spiroloculina* spp.	-0.15309	-0.11720
Gyroidina soldanii	0.59619	0.14368	*Clavulina* sp.	-0.22249	0.80122
Cibicides italicus	0.58400	-0.27228	*Uvigerina peregrina*	-0.26625	0.54969
Oridorsalis stellatus	0.56093	-0.03055	*Astrononion* spp.	-0.39469	0.18057
Gyroidina altiformis	0.53164	-0.22564	*Bulimina elegans*	-0.40462	-0.12818
Melonis soldanii	0.51185	0.13418	*Uvigerina cylindrica* sspp.	-0.47569	-0.30306
Eggerella bradyi	0.48595	0.27728	*Bulimina aculeata*	-0.50579	-0.40091
Spiroplectammina spp.	0.39513	-0.08486	*Bolivina dilatata*	-0.52253	-0.42221
Melonis affinis	0.38209	0.22185	*Hanzawaia boueana*	-0.70504	-0.12158
Pullenia bulloides	0.37153	-0.06608	*Heterolepa pseudoungeriana*	-0.78262	0.12785
Uvigerina proboscidea	0.33814	-0.19897	*Bulimina subulata*	-0.81003	-0.34247
Uvigerina rutila	0.32355	0.21931			

maximum values after 6.8 Ma. Between 7.6 Ma and 6.8 Ma the Δ of $\partial^{13}C$ is at a minimum, following a decrease around 7.6 Ma and preceding an increase from ~7.16 Ma onwards.

Trends in the manganese and vanadium concentrations, normalised to the aluminium content of the samples (Mn/Al and V/Al ratios) are shown in Figure 7. Manganese is remobilized in an anoxic environment, and thus expected to be depleted if it is not reprecipitated, whereas vanadium precipitates when the oxic-anoxic boundary resides above the sediment-water interface (Breit and Wanty, 1991; Calvert and Pedersen, 1993; Hastings et al., 1996). The V/Al ratios show an initial increase at 7.6 Ma, and on average remain at a higher level. The Mn/Al ratios show a conspicuous decrease between 7.3 and 7.1 Ma, and generally remain at low levels during the Messinian part of the sequence, especially after 6.8 Ma.

4. Discussion

The shifts in faunal and geochemical parameters, occurring at 7.16 and 6.8 Ma, divide the period recorded in the Monte del Casino section into three major time slices that will be discussed in chronological order. In this section we focus on ongoing, non-cyclic trends. We conclude by comparing data from Monte del Casino section with selected data from the Metochia section on Gavdos.

4.1. 8.145 - 7.16 Ma: predominantly climatic factors

The diverse benthic faunal assemblage found in the lower part of the sequence characterises deeper water environments with sufficient ventilation. This is in agreement with the P/B ratios, that indicate a water depth of ~1000 m. Papers on both recent and fossil benthic foraminifera mention cluster 1 species (Figs. 4, 5) in relation to relatively deep, open marine, oxic environments with normal salinity (*Cibicides wuellerstorfi, Cibicidoides italicus, C. bradyi* and *C. robertsonianus*, *Siphonina reticulata, Uvigerina proboscidea*: Lutze, 1977; Van der Zwaan, 1982; Lutze and Thiel, 1989; Verhallen, 1991; Sjoerdsma and Van der Zwaan, 1992; Kaiho, 1994; but for *U. proboscidea* see Gupta and Srinivasan, 1992). Lutze et al. (1986) mention *C. robertsonianus* as a thermophilic species. Additional species present in this part of the sequence are apparently a little more tolerant and have been related to slightly suboxic conditions (*Gyroidina altiformis, G. soldanii, Lenticulina* spp., *Melonis soldanii, Sphaeroidina bulloides*: Jonkers, 1984; Mackensen et al., 1993; Kaiho, 1994; Loubère, 1994, 1996).

4.1.1. Changes at 7.6 Ma

A minor shift in species composition at 7.6 Ma is accompanied by a small and temporary decrease in species diversity, and is mainly caused by a shift between species in clusters 1 and 3 (Figs. 4, 5). The planktonic flux shows a sharp decrease at 7.6 Ma that is less clearly reflected in the benthic flux. The oxygen and carbon stable isotopes point to a change in environmental conditions (Fig. 7). The positive correlation of $\partial^{18}O$ and $\partial^{13}C$ suggests a common control on both isotope species; in such cases, the ultimate control is likely to be climatic (see Van der Zwaan and Gudjonsson, 1986 for a discussion of models). If the $\partial^{18}O$ patterns are interpreted as dominantly governed by a temperature effect, the shift towards lighter values at 7.6 Ma indicates a warming. The LCO of *Globorotalia menardii 4* at 7.507 Ma and the FO of *G. menardii 5* at 7.369 Ma (Krijgsman, 1997; Fig. 2) also indicate a temperature increase. Hodell et al. (1994), who worked on Moroccan (extra - Mediterranean) material, found benthic isotopic evidence for a warming trend, that started a bit later and crossed the Tortonian/Messinian boundary.

The shift of the carbon isotopes towards lighter values is most pronounced in the planktonic foraminiferal record, i.e. in surface waters. A reduction of the biological production in surface waters is expected to lead to more negative carbon isotope values, and is in agreement with the coincident decrease in planktonic flux (Fig. 6). Since a (lesser) shift to lighter $\partial^{13}C$ is also present in the benthic foraminiferal record, the total water column was apparently affected by an additional change. We assume that together with a warming, the vertical circulation slowed down: upon ageing of the water mass, light carbon may accumulate at the seafloor. A similar scenario was postulated earlier by Vergnaud-Grazzini (1983). Constriction of the Atlantic-Mediterranean connections could further contribute to increasing residence time of deeper waters. Gebhardt (1994), summarizing data from the Betic Cordillera in Spain, mentions uplift of (part of) the Betic Street in the late Miocene. Unfortunately, his data are inadequately constrained to allow us to correlate them with our faunal data, but this could prove to be a first step in the isolation of the Mediterranean, although the Rifian Corridor is suspected to have opened and deepened from ~8 Ma onwards (Krijgsman et al., 1999).

4.1.2. 7.29 - 7.16 Ma: first signs of major perturbations

On approaching the Tortonian/Messinian boundary interval, the more or less stable conditions present before were subject to more profound changes. A short influx of *G. menardii 4* at 7.28 Ma, and the subsequent influx of *G. conomiozea* at 7.24 Ma, the Tortonian/Messinian boundary, suggest biogeographical changes related to cooling (Zachariasse, 1979; Chamley et al., 1986). A cooling is also recorded in the oxygen isotope data. The extra-Mediterranean isotope record of Hodell et al. (1994) suggests a more prolonged cool period than our record, but the start of the *'siphon event'* (influx of deep, cold Atlantic waters through the Rifian Corridor) proposed by Benson et al. (1991) can be biostratigraphically correlated to this cooling. The manganese- and vanadium records both indicate reduced ventilation of the deep Mediterranean waters (Fig. 7).

4.2. 7.16 - 6.8 Ma: development of environmental stress

4.2.1. Indications for increasing dysoxia

The major shift towards more restricted benthic faunas starts during the earliest Messinian, during deposition of the sapropel of cycle C18, around 7.17 Ma. A number of species that represent normal marine conditions, have disappeared or shortly disappear from the record: *Cibicides wuellerstorfi*, *Cibicidoides italicus*, C. *bradyi*, *Siphonina reticulata*, and *Uvigerina proboscidea* (marked in cluster 1 (Fig. 4) with an asterisk). Subsequently, the abundances of the remaining cluster 1 species decline and this group is gradually replaced by successive groups of species represented by clusters 2, 3, 4, and 5 (Fig. 4, 5). A number of these species was mentioned in relation to varying degrees of oxygen and salinity stress, e.g. *Oridorsalis umbonatus*, var. *stellatus* (Van der Zwaan, 1982; Jonkers, 1984; Boersma, 1986; Kaiho, 1994; Loubère, 1996), *Sphaeroidina bulloides* (Mackensen et al., 1993; Kaiho, 1994; Loubère, 1994, 1996), and *Hanzawaia boueana* (Van der Zwaan, 1982). *Uvigerina peregrina* is considered to proliferate under raised organic flux, and/or a decreased oxygen content, and maybe also increased salinity (Van der Zwaan, 1982; Lutze and Coulbourn, 1984; Verhallen, 1991; Sjoerdsma and Van der Zwaan, 1992; Loubère, 1994, 1996). The faunal trends indicate that oxygen levels at the seafloor diminished further. This is in agreement with the decreasing manganese- and increasing vanadium contents of the sediments (Fig. 7).

4.2.2. The 'Carbon Shift' in the progressively isolated Mediterranean

After ~7.16 Ma the close correlation between oxygen and carbon isotopes is lost. Furthermore, the $\Delta\partial$ of both the oxygen and carbon isotopes starts to increase. The oxygen isotopes temporarily shift back to lighter values. After a temporary excursion towards heavier values, the carbon isotopes shift persistently to light ones, in surface as well as bottom waters. This carbon shift has been recognised globally, and has been explained by a eustatic sea-level lowering, or by a shift from C3-dominated to C4-dominated ecosystems on land, related to increased aridity (see discussion in Hodell et al., 1994). We do not see any indications in our data for a substantial sea-level lowering at this point. Comparing our record with that of Hodell et al. (1994; their figure 6*)*, it can be seen that the carbon isotopes reach much lighter values within the Mediterranean, than at the Atlantic side of the Rifian Corridor, indicating that at least a part of the shift toward lighter values within the Mediterranean may have been caused by progressive isolation of the basin from 7.16 Ma onward. A similar discrepancy between intra- and extra-Mediterranean isotope values was noticed by Van der Zwaan and Gudjonsson (1986). Increasing isolation of the Mediterranean will have led to increased residence times of water masses and accumulation of light organic carbon. Krijgsman et al. (1999) present evidence that between 7.2 and 7.1 Ma, the Taza-Quercif Basin, at the southern margin of the Rifian Corridor, shallowed to near-shore depths, and that at ~6.0 Ma at least this part of the Rifian Corridor was uplifted above sea level. Benson et al. (1991) considered the Rifian Corridor blocked during the Messinian, from around the start of the Gilbert Chron, which was then dated at ~5.3 Ma. It was recently re-dated to ~6 Ma (W. Krijgsman, pers. comm.).

Increasing isolation of the Mediterranean basin would be in agreement with the development of the sapropels. Starting with the sapropel of cycle C18, around 7.17 Ma, all insolation maxima are correlated to sapropels. The sapropels increase in thickness relative to the homogeneous intervals, and these in turn obtain a greenish-brown colour. Apparently the boundary conditions for sapropel formation were more easily fulfilled after ~7.17 Ma.

4.3. 6.8 - 6.3 Ma: increasing environmental stress

4.3.1. 6.8 Ma: cooling; stratification

At ~6.85 Ma a new phase of cooling is indicated by the shift towards heavier oxygen isotope values. More or less simultaneously, the $\Delta\partial^{18}O$ and $\Delta\partial^{13}C$ increased (Fig. 7), suggesting that this cooling phase was accompanied by increasing stratification of the water column. Simple species diversity dropped and species from clusters 1 to 4, present in diminishing frequencies until this time, gradually disappeared (Figs. 4, 5, 6). Biconvex, epifaunal species from cluster 5 dominated the assemblage, and species from cluster 6 gradually showed increasing abundances. A number of the latter species have been reported to show opportunistic behaviour and a tolerance to dysoxia, but also to elevated bottom water salinity (*Bolivina dilatata*, e.g., Van der Zwaan, 1982; Verhallen, 1991; Jorissen et al., 1992; Kaiho, 1994; Loubère, 1996, 1997; *Bulimina subulata* (syn. *B. aculeata minima*: see Verhallen, 1991): Van der Zwaan, 1982; Verhallen, 1991; Kaiho, 1994). As the shift of the oxygen isotopes is rather large (2 permil) to be explained only by cooling, and co-occurred with increasing abundances of salinity-tolerant species, we suspect that bottom-water salinity may have increased at the same time. Both planktonic and benthic fluxes decreased temporarily shortly after 6.8 Ma, but planktonic foraminiferal diversity remained at the same level (Calieri, 1997), and thus fails to indicate increased surface water salinity.

4.3.2. 6.7 Ma: shallowing

At 6.7 Ma, shallowing is indicated by decreasing P/B ratios, and increasing abundances of species associated with shallower-water environments (*Astrononion* spp., *Bulimina subulata*, *Heterolepa pseudoungeriana*), together with an increasing percentage of shallow-water, allochthonous elements in the sapropels (e.g. *Elphidium* spp., *Discorbis* spp., *Asterigerina planorbis*; Appendix). The declining P/B ratios are followed by a restoration of the planktonic flux to earlier levels and an increased benthic flux, the latter being in agreement with shallowing. Van der Meulen et al. (in press) consider shallowing at this site to be for the greater part a local phenomenon. They estimated the shallowing to be 483 ±180 m, and related it to isostatic uplift of the region after an inferred phase of slab detachment. Although the major part of this shallowing is probably local, a minor shallowing (tens of meters) is visible in the eustatic curve (Haq et al., 1988). The events at 6.7 Ma concur with deposition of the first diatomites on Gavdos (F.J. Hilgen, pers. comm.).

At ~6.65 Ma the planktonic and benthic carbon isotopes shift to extremely light values. Diagenetic overprint can not be excluded, although we have no indications for extremely bad preservation of sample material. The light values may be related to a sudden relative sea-level lowering due to uplift. Isotopically light carbon is expected to remobilise from the shelf in these circumstances (e.g., Vincent et al., 1980, 1985). The shift in the carbon isotopes is preceded by a peak in the frequency of *Globigerina bulloides* (50%; Calieri, 1997), a species that is related to increased productivity in surface waters.

4.3.3. Brine formation?

We have some indications for hypersaline bottom waters developing in the deeper depressions of the basin. However, the Monte del Casino section may have been temporarily uplifted above the interface between saline and less saline waters at 6.7 Ma. Species from cluster 5 still dominated the benthic faunal assemblage; only after 6.55 Ma these diminished and gradually disappeared. The faunal diversity then decreased to a minimum, and the infaunal, salinity-tolerant species of cluster 6 remained, that already started to proliferate at ~6.8 Ma (Figs. 4, 5). Increasing dysoxia is indicated by the manganese and vanadium records. The recurrent shifts to heavy oxygen isotopes are difficult to explain by cooling alone. The increase of the $\Delta\partial^{18}$O indicates increasing stratification of the water column. Faunal and geochemical evidence thus indicate increasing salinity at reduced depth levels.

The deepening suggested by the P/B ratios after 6.4 Ma is probably an artefact. As bottom-water stress is developing, the P/B ratios are no longer reliable paleodepth-indicators, since declining benthic faunas could erroneously suggest apparent deepening (see Van der Zwaan et al., 1990).

4.4. A step-wise onset of the Messinian salinity crisis? - Comparison with the Metochia section

4.4.1. Benthic foraminifera in the Metochia section

The Metochia section (Gavdos, near Crete), described by Seidenkrantz et al. (subm.) spans the period of 9.78 - 6.66 Ma and thus overlaps in part with the Monte del Casino section. Depositional water depth at both sites was similar during the late Tortonian and early Messinian, and is estimated to be ~1000 m. The insolation-linked sapropel patterns can be correlated over this geographical distance (Hilgen et al., 1995; Krijgsman et al., 1995, 1997; Fig. 8).

Faunal development during the late Tortonian and the early Messinian was similar at both locations. The benthic foraminiferal fauna present at Metochia during the late Tortonian has much in common with the fauna at Monte del Casino, and mainly consists of species present in clusters 1 - 3 of the Monte del Casino section. Most important, at 7.16 Ma, within the resolution of sampling and counting, nearly the same deeper-water species have disappeared from the record in both sections. Thus, the same event appears to affect both locations simultaneously. Faunal development after this event is also comparable at both locations: although different species proliferate in the Metochia and the Monte del Casino sections during the Messinian, they both evidence a period of ongoing shifts in faunal composition between 7.16 and 6.8 Ma, and a similar sequence of increasing environmental stress.

These stress-intolerant species disappear in more Mediterranean sections of similar depth (e.g., Falconara and Gibliscemi on Sicily; unpublished data). Some species, however, (e.g. *S. reticulata*) persist in shallower waters (e.g. the Cretan Vrysses/Exopolis sections: Van der Zwaan, 1982; Potamidha: Wonders and Van der Zwaan, 1979). The deepest waters (e.g. as reflected by the Falconara and Gibliscemi sections) were affected most by the event at ~7.16 Ma: we noticed an almost complete disappearance of all benthic fauna (Van der Zwaan, 1982, and unpublished data). This could imply a salinity increase, starting in the deepest basins as early as ~7.16 Ma.

4.5. 400-ky eccentricity versus ongoing trends

Both at Monte del Casino and Metochia, the environmental deterioration started during deposition of the sapropel at ~7.17 Ma and gradually proceeded until the Messinian salinity crisis was a fact. Important steps in the evolution of both sites are recorded at 7.16 Ma and ~6.8 Ma. Another shift in faunal and geochemical parameters is recorded at Monte del Casino at ~7.6 Ma. These discrete steps in the development of the paleoenvironment occurred at times when the amplitude of the insolation curve, due to interference with the 400-ky eccentricity curve, started to increase, i.e. after an eccentricity minimum and the concurrent carbonate maximum (Figs. 5, 7). The Monte del Casino section represents too little time to evaluate this 400-ky trend over a longer period of time. Although the environmental change at 7.16 Ma is probably related to uplift in the Rifian Corridor area, it appears reasonable to assume that the ongoing

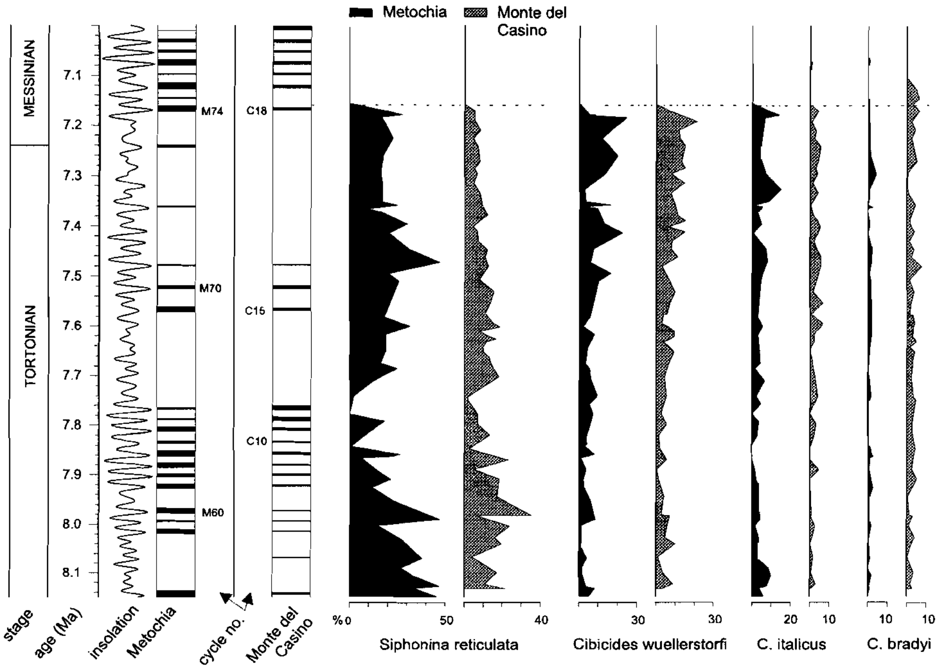

Figure 8. The species that nearly simultaneously leave the record in the Monte del Casino and Metochia sections at 7.17 Ma.

trend towards the salinity crisis was superimposed upon a 400-ky climatic cyclicity.

5. Conclusions

Our evidence indicates a step-wise isolation of the Mediterranean deep water mass, leading to ageing of that water, and at a later stage to increasing salinity at a waterdepth of ~1000 meters: the depositional depth of both the Monte del Casino and Metochia sections during the latest Tortonian and the early Messinian. Apparently the Mediterranean was predominantly influenced by climatic factors between ~8.0 and ~7.16 Ma, but from ~7.16 Ma onwards, gateway dynamics seem to be the dominating factor influencing the paleoenvironment.

At 7.6 Ma a warming may have led to a first slowing-down of the vertical circulation of the Mediterranean water masses. There may be a relation with the closure of the northern Betic Street, although this closure can not be precisely constrained.
Between 7.29 and 7.16 Ma a cooling phase is evident, both inside and outside the Mediterranean. The start of the 'siphon event', proposed by Benson et al. (1991) can be biostratigraphically correlated to this cooling.

A further isolation of the deep Mediterranean waters occurred around 7.16 Ma, when in several sections the synchronous exit of a number of stress-intolerant deep-water benthic species is recorded. In the Monte del Casino section the first indications for increasing water-mass stratification are visible around 6.8 Ma. A major component of the shallowing at 6.7 Ma is probably related to tectonic causes, though at the same time the first diatomites are recorded on Gavdos. Major steps in paleoenvironmental degradation seem to concur with periods following 400 ky eccentricity minima. Each of these events is in some way recorded in the benthic foraminiferal distribution patterns.

Acknowledgements

We wish to thank all people involved in sampling of the sections discussed in this paper. T.K. especially thanks R. Calieri, S. Ferretti, and C. Terzi for their hospitality, and their assistance and the discussions in the field. G. van 't Veld, G. Ittmann, P. Anten, H. de Waard, and A. van Dijk are acknowledged for sample preparation and geochemical analyses. A. Okx picked a large part of the samples, and T. van Hinte helped with the figures. L. Lourens provided the astronomical curves. F. Hilgen provided bioevents, and insight in problems associated with cyclostratigraphic and biostratigraphic correlation. Critical reading by W. Krijgsman, F. Hilgen, and M.J. van der Meulen greatly improved an earlier version of the manuscript. A. Almogi-Labin and W.A. Berggren are gratefully acknowledged for their constructive reviews.

Chapter 4

Miocene Mediterranean:
Metochia (Gavdos)

Benthic foraminifera as indicators of changing Mediterranean-Atlantic water exchange in the late Miocene

Abstract

Benthic foraminifera and stable isotopes from homogeneous sediments in an Upper Miocene (Tortonian-lower Messinian) cyclic succession of homogeneous marls and sapropels from the Island of Gavdos (Greece) show significant changes in bottom-water oxygenation, presumably related to changes in the Mediterranean-Atlantic water exchange.

The benthic foraminifera prove to be excellent indicators of variations in the oxygen contents of the bottom waters, even more so than the stable isotopes. Our data indicate a stepwise restriction of the Mediterranean-Atlantic water exchange resulting in increasing sluggishness of deep-water circulation. The first indication of restricted circulation is seen at 8.5 Ma, which may correspond to a severe restriction of the external zone of the Betic Strait. A second event, which had a very serious influence on the fauna in the deeper Mediterranean, occurred at 7.16 Ma. This event was presumably linked to the partial closure of the Rifian Corridor. The restricted Mediterranean-Atlantic connection also seems to have led to a gradual salinity increase and possibly to the formation of a brine in the deepest basins, thus marking the first development towards the Messinian Salinity Crisis.

M.-S. Seidenkrantz, T. J. Kouwenhoven, F. J. Jorissen, N. J. Shackleton & G. J. van der Zwaan, Marine Geology, in press

1. Introduction

The Miocene was a period in which the Mediterranean underwent substantial changes. In the early Miocene, the proto-Mediterranean was connected through seaways to the Atlantic and Indian Oceans as well as to the Paratethys, but the ongoing convergence between the African and European Plates resulted in a narrowing of these seaways during the middle to late Miocene. Due to the approaching African block, the eastern connection to the Indian Ocean was lost at about 14 Ma (cf. Hsü and Bernoulli, 1978; Berggren, 1982; Adams et al., 1983; Vrielynck et al., 1997). The connection to the Paratethys became more and more confined, and this former part of the Tethys seaway became dominated by fresh-water run-off from the European continent (Orszag Sperber et al., 1993) (Fig. 1).

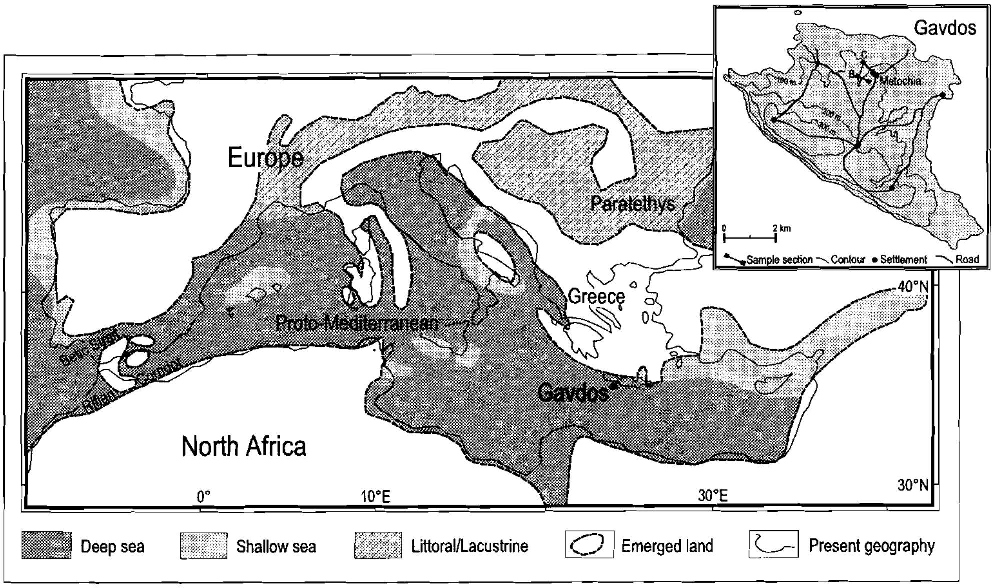

Figure 1. The palaeogeography of the Mediterranean region during the upper Tortonian (redrawn after Orszag Sperber et al., 1993) superimposed on the modern geography. The insert map shows the present geography of the island of Gavdos with the location of the trajectories of the Metochia B and C subsections on the island Gavdos (after Krijgsman et al., 1995).

Also the Mediterranean-Atlantic connection changed. The formerly wide entrance became constricted during the middle and late Miocene (cf. Dercourt et al., 1993; Vrielynck et al., 1997) and the western passages, the Betic Strait (southern Spain) and the Rifian Corridor (Morocco) (Fig. 1), closed gradually during the early to late Messinian (Benson et al., 1991; Krijgsman et al., 1998). Consequently, the water exchange between the Mediterranean and the adjoining ocean progressively diminished, and, because of the negative water budget of the Mediterranean, an anti-estuarine type of circulation was established (e.g., Benson, 1991). The almost complete cut-off of connections to the surrounding oceans in the late Messinian led to the accumulation of a huge series of evaporites during the late Miocene (the Messinian Salinity Crisis) (Selli, 1960; Benson, 1991).

Although the general picture is very well known, the onset and the precise series of events leading to the Salinity Crisis are still much debated. The number of suitable exposures and the dating of the regional geological events are still not precise enough to get a close grip on the timing of the closure of the Mediterranean entrances. It is clear that the closure of the connection to the Indian Ocean and the Paratethys led to a more sluggish, and possibly anti-estuarine type, circulation pattern already in the middle to late Miocene (cf. Vergnaud-Grazzini, 1983; Chamley et al., 1986; Van der Zwaan and Gudjonsson, 1986; Gebhardt, 1999). It is therefore not surprising that from about that time onwards, the pelagic sequences became characterised by the periodic occurrence of sapropels. These sapropel patterns were recently shown to be correlated to the precession and eccentricity cycles (Hilgen, 1991; Hilgen et al., 1995; Sierro et al., 1998). Sapropels clearly show the existence of short-term variations in oxygenation. However, benthic faunas from late Tortonian-Messinian, deep-water sequences in Italy show that variations due to decreasing oxygen contents also occurred in the homogeneous sediments (Kouwenhoven et al., 1999).

It is generally accepted that deep-water benthic foraminifera are excellent indicators of stress. In fact, the deep-water assemblages can be seen as stenotopic (cf. Van der Zwaan, 1983; Van der Zwaan et al., 1999). Normally the benthic deep-water species are adapted to stable conditions and already slight changes in bottom water oxygenation or salinity are reflected in the faunal compositions. In order to assess whether we could detect substantial fluctuations in bottom-water oxygenation not related to sapropel formation, we studied the benthic foraminiferal assemblages from the homogeneous intervals of deep-water sediments from an eastern Mediterranean site on the Isle of Gavdos (Fig. 1). The section covers the time span from 9.8-6.7 Ma, a period of supposedly substantial changes in the Mediterranean-Atlantic connections.

In this paper we present the following: 1) Both the near closure of the outer Betic Strait at ca. 8.5 Ma and the raise in sill depth through the Rifian Corridor at 7.2-7.1 Ma can be detected in the benthic foraminiferal fauna as a decrease in bottom-water oxygenation. 2) The increasing restriction in the Mediterranean-Atlantic water exchange led to a gradual increase in salinity and possibly to brine formation in the deep basins of the Eastern Mediterranean, thus giving the first warning of the Messinian Salinity Crisis.

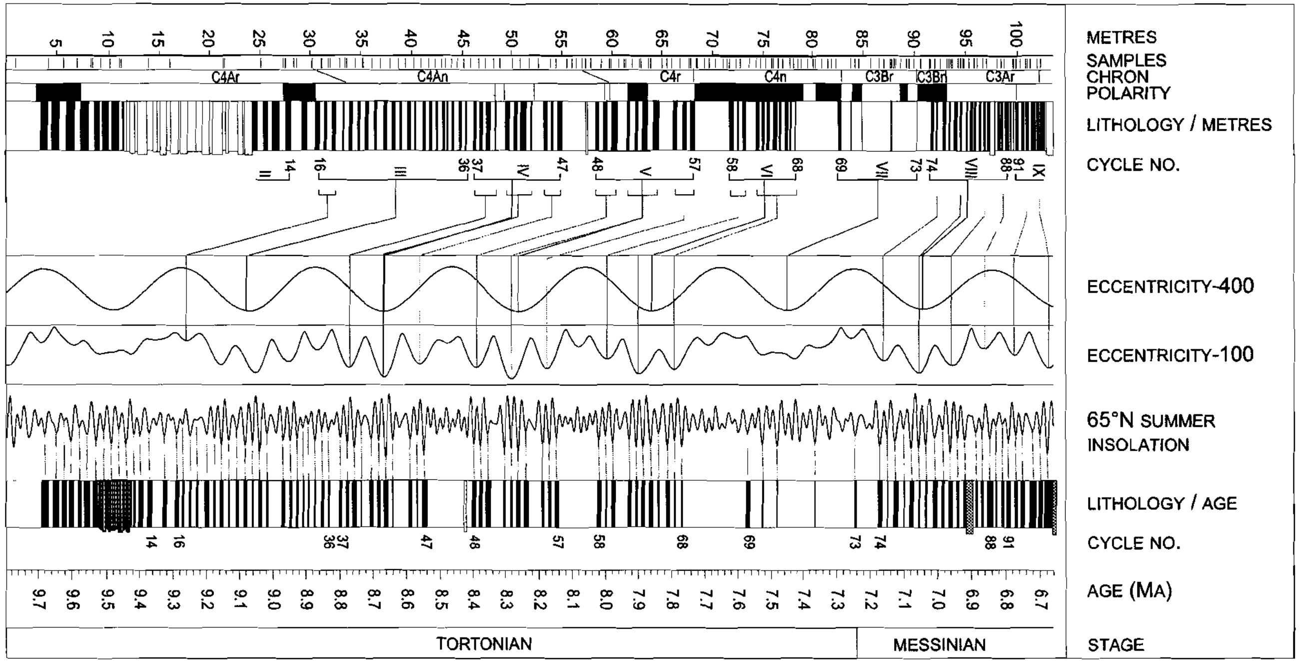

Figure 2. The composite Metochia section, Gavdos. Sample distance, magnetic polarity (from Krijgsman et al., 1995), and lithology (black = sapropels; white = homogeneous intervals; dots = sandy intervals) plotted versus depth. Lithology, and astronomical curves (65°N summer insolation, 100-kyr and 400-kyr eccentricity curves (from Hilgen et al., 1995)) plotted against age. In the polarity column, black denotes normal polarity zones and white indicates reversed polarity; shaded intervals denote zones with undefined polarity. Sedimentary cycles: Arabic numerals mark 20-kyr cycles; Roman numericals mark the large-scale sapropel clusters, correlated to the 100- and 400-kyr eccentricity cycles.

2. Sediment and Chronology

The basal part of the approximately 100 m thick section at Metochia consists of a palaeosol followed by estuarine to shallow-marine sands (Postma et al., 1993). Deep-marine sediments overlie these near-shore deposits. The main part of the section consists of alternating light grey-blue, homogeneous, hemipelagic marls and brown, organic-rich, laminated beds (sapropels) (Fig. 2). The sapropels occur in both small- and large-scale clusters separated from each other by intervals where sapropels are not or only very weakly developed. The small-scale clusters generally contain 3-4 sapropels, whereas the large-scale clusters typically encompass 3-4 small-scale clusters (Fig. 2) (Hilgen et al., 1995). Prior to 7.16 Ma these sapropel clusters are separated by intervals of no or only weak sapropel formation; after 7.16 Ma sapropels are a much more regularly occurring feature.

The chronology of the deposits is based on a combination of magnetostratigraphic, biostratigraphic (planktonic foraminifera and dinoflagellates), and cyclostratigraphic data (Hilgen et al., 1995; Krijgsman et al., 1995). The Neogene Mediterranean sedimentary cycles have been shown to be linked to variations in solar insolation (Hilgen, 1991; Postma et al., 1993) and an astronomically calibrated time scale for the Metochia section has been established through correlation to the 65°N summer insolation curve of $La90_{(1,1)}$ (Laskar, 1990; 1993; Hilgen et al., 1995; Lourens et al., 1996). Each sapropel/marl cycle is, thus, correlated with the precession cycle with periodicities of 19 and 23 kyr (average 21.7 kyr) (Hilgen et al., 1995), whereas the small- and large-scale clusters correlate to the 100-kyr and 400-kyr eccentricity cycles, respectively (Fig. 2) (Hilgen et al., 1995).

The Tortonian/Messinian boundary is usually recognised at the First Regular Occurrence (FRO) of the planktonic foraminiferal group *Globorotalia conomiozea* (d'Onofrio et al., 1975; Colalongo et al., 1979; Krijgsman et al., 1994) at 7.24 Ma (Hilgen et al., 1995).

3. Objectives, material, and methods

The objective of this paper was not to study the conditions during sapropel deposition, but instead to investigate longer-term changes in the palaeoceanography of the Eastern Mediterranean during the times represented by the hemipelagic marl portion of each cycle. Thus, we analysed the foraminifera in one sample from each homogeneous layer (i.e. about one sample per 21.7 kyr) (Fig. 2). Where possible, we used samples from the mid-point between two sapropels. In view of the relatively high sedimentation rate (1-6 cm/kyr or between 20 and 120 cm per cycle; Fig. 4) mixing of material from the sapropelic sediments into the homogeneous marls should normally be negligible.

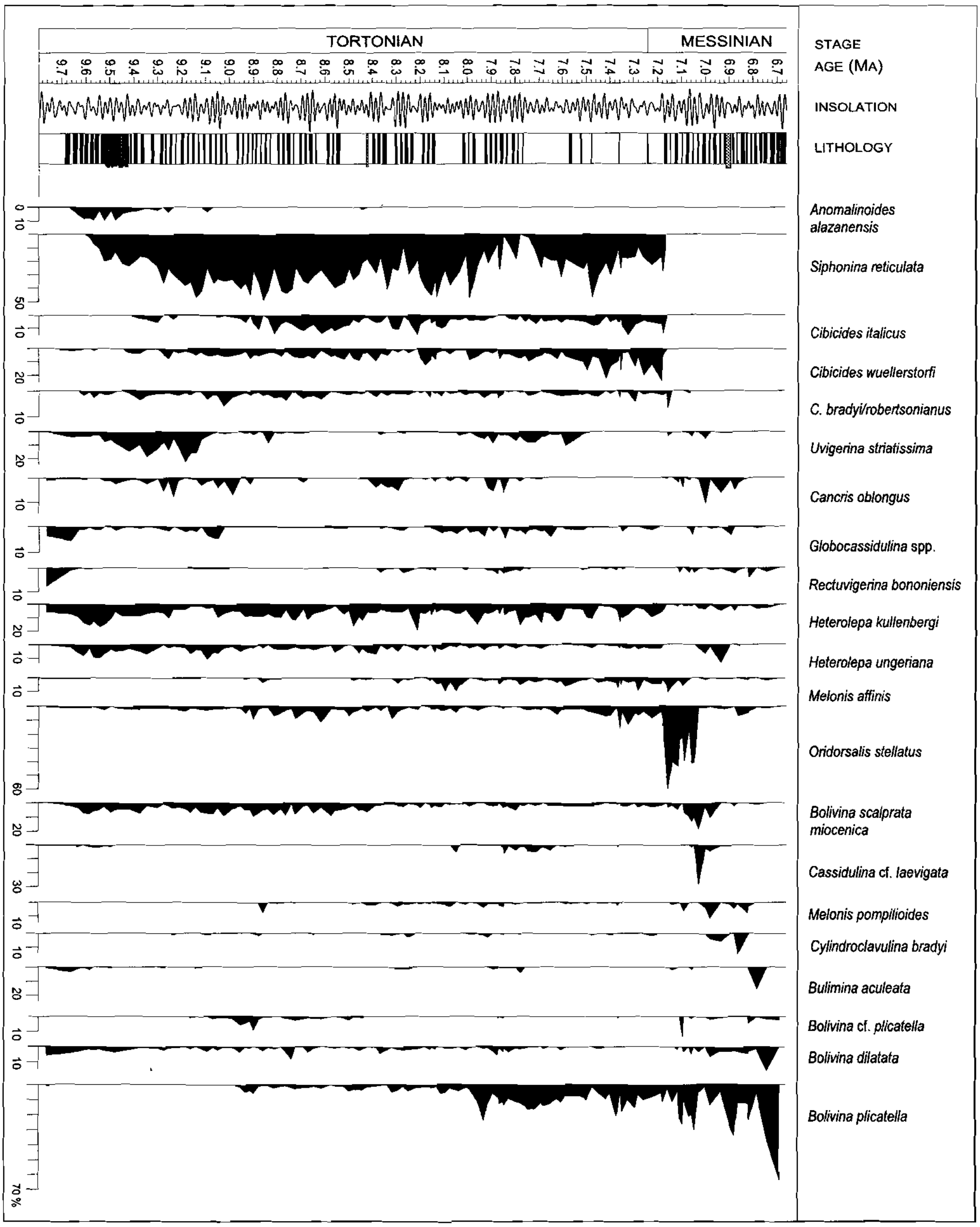
STAGE
TORTONIAN
MESSINIAN
AGE (MA)
9.7
9.6
9.5
9.4
9.3
9.2
9.1
9.0
8.9
8.8
8.7
8.6
8.5
8.4
8.3
8.2
8.1
8.0
7.9
7.8
7.7
7.6
7.5
7.4
7.3
7.2
7.1
7.0
6.9
6.8
6.7
INSOLATION
LITHOLOGY
Anomalinoides alazanensis
0 10
Siphonina reticulata
50
Cibicides italicus
10
Cibicides wuellerstorfi
20
C. bradyi/robertsonianus
10
Uvigerina striatissima
20
Cancris oblongus
10
Globocassidulina spp.
10
Rectuvigerina bononiensis
10
Heterolepa kullenbergi
20
Heterolepa ungeriana
10
Melonis affinis
10
Oridorsalis stellatus
60
Bolivina scalprata miocenica
20
Cassidulina cf. laevigata
30
Melonis pompilioides
10
Cylindroclavulina bradyi
10
Bulimina aculeata
20
Bolivina cf. plicatella
10
Bolivina dilatata
10
Bolivina plicatella
70 %

3.1 Data collection and faunal analysis

The material for this study was collected from two profiles, Metochia B and Metochia C (Fig. 1), which have been combined to a composite record of approximately 100 m thickness. Sampling was carried out during fieldwork in November 1991 (Metochia B) and June 1992 (Metochia C).

The samples were washed through sieves with mesh diameters of 63 and 125 µm at the Department of Earth Sciences, University of Utrecht, The Netherlands. The >125 µm fraction was examined for its benthic foraminiferal content. Where possible, at least 300 specimens were counted in each sample, although the generally low concentration of benthic foraminifera, especially in the topmost samples, often did not allow this (see Appendix 1).

The relative frequencies of individual species (Fig. 3) are calculated in percent of the total benthic foraminiferal fauna. Shallow-water epiphytic taxa such as *Elphidium* spp., *Asterigerinata* spp., *Discorbis* spp., and *Cibicides lobatulus* are grouped together as allochthonous (Fig. 4). The concentrations of planktonic and benthic (allochthonous and autochthonous grouped separately) foraminifera are calculated as number of specimens per gram of dry sediment. The B/P ratio (Fig. 4) is expressed as a calculation of $(B/(B+P))*100$ (the percentage of autochthonous benthic foraminifera of the total foraminiferal population). Samples with less than 30 benthic specimens were excluded from plots and statistical treatments. The low number of specimens in some samples means risking an artificial overrepresentation of certain species. However, the relative frequency of specific species does not vary significantly between neighbouring samples with different foraminiferal concentrations. For counts and original author names of the benthic foraminifera see Appendix 1.

3.2. Multivariate statistics

Standard SPSS software was used to perform statistical faunal analysis on the relative percentage data. The original dataset contains 109 species and species groups, including both autochthonous and allochthonous taxa (Appendix 1). Of these, species, which never reached frequencies of 4%, were omitted. In order to avoid overrepresentation of the remaining taxa, no new closed sum was calculated. The reduced dataset, consisting of 48 variables, was introduced into a hierarchical cluster analysis (between-group, Pearson correlation), in order to define major benthic groups (Figs. 5, 6).

Figure 3. Selected benthic foraminifera from the Metochia section, Gavdos, plotted versus age. The relative frequencies of the species are calculated as percentage of the total benthic fauna. To the left is shown the lithology (black = sapropels; white = homogeneous intervals; dots = sandy intervals) and the 65°N summer insolation curve (from Hilgen et al., 1995).

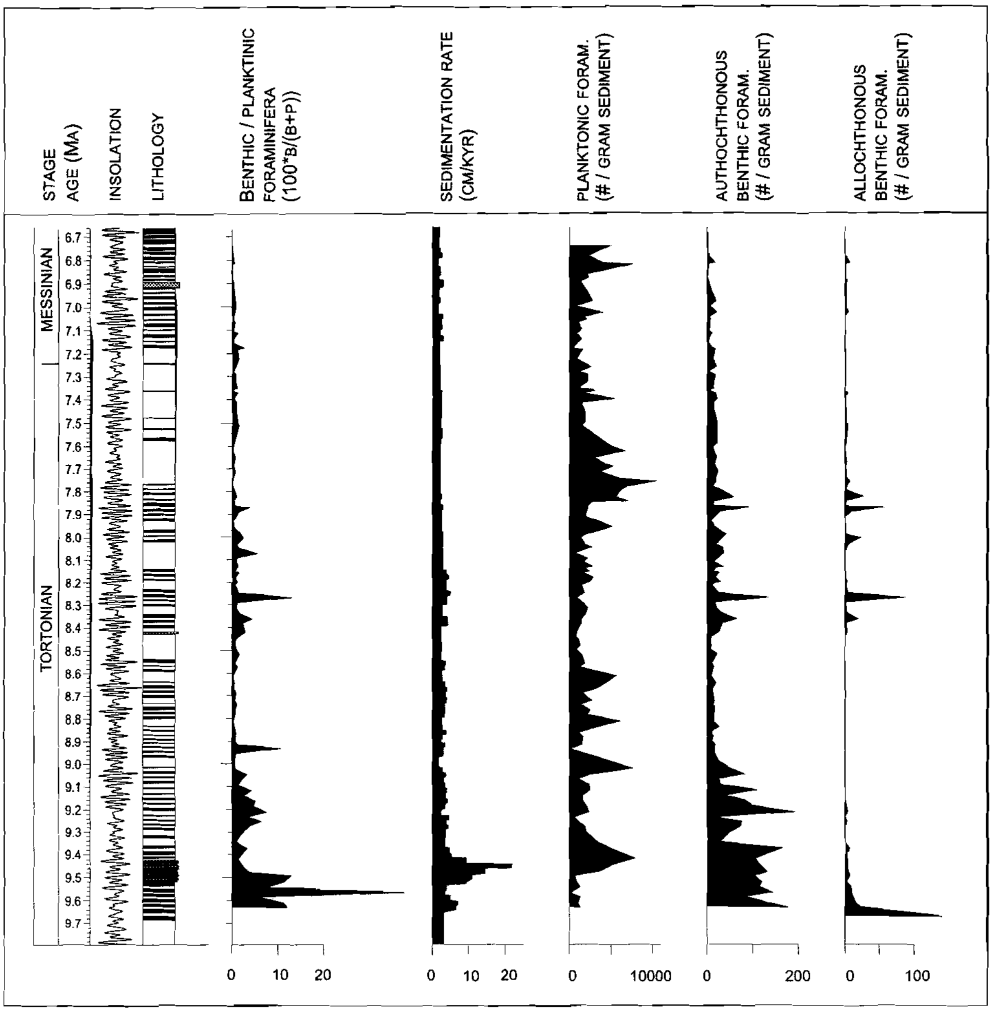

Figure 4. Sedimentation rate, concentrations (numbers/gram sediment) of autochthonous and allochthonous benthic foraminifera and of planktonic foraminifera, and B/P-ratios plotted against age. The lithology (black = sapropels; white = homogeneous intervals; dots = sandy intervals) and the 65°N summer insolation curve (from Hilgen et al., 1995) are also illustrated.

3.3. Stable isotopes

Stable isotope measurements (Fig. 7) were carried out on the planktonic species *Globigerinoides obliquus* Bolli and the benthic taxa *Cibicides wuellerstorfi* and *Heterolepa*. The measurements on *Heterolepa* were carried out on *H. kullenbergi* and *H. ungeriana*, where the former was most common in the Tortonian and the latter more common in the Messinian part of the section (Fig. 3). The measurements were carried out in part at Cambridge University, U.K., and in part at Utrecht University, The Netherlands. The samples processed in Cambridge were cleaned with hydrogen peroxide and then analysed on a VG PRISM mass spectrometer after reaction in a MULTIPREP reaction system in which each sample is reacted with orthophosphoric acid, injected into in an individual vial and the evolved gas extracted by a hollow needle. The specimens processed at Utrecht University were first roasted in vacuum and thereafter treated with hydrophosphoric acid at 100°C for 90 minutes. The measurements were carried out on a VG SIRA 24 mass spectrometer. At both laboratories, both planktonic and benthic (*C. wuellerstorfi* as well as *Heterolepa* in Utrecht, only *C. wuellerstorfi* in Cambridge) isotope measurements were carried out. All the data were reported as deviations from the PDB standard.

On samples prior to 7.16 Ma, benthic isotope measurements were in general (66 out of 110 samples) carried out on both *C. wuellerstorfi* and *Heterolepa* spp., mainly *H. kullenbergi*. Benthic isotope values of *C. wuellerstorfi* were preferably used for the record (Fig. 7) because of its calcification in equilibrium with ambient sea water (see Zahn et al., 1986), and because of its generally epifaunal habitat (Lutze and Thiel, 1989; but see Mackensen et al., 1993). *Heterolepa* samples were added where *C. wuellerstorfi* was scarce. Samples younger than 7.16 Ma only contained *Heterolepa* spp. Different microhabitat preferences may cause an offset between *Cibicides wuellerstorfi* and the *Heterolepa* species, but no correction was made, as Farrell (1991, ref. in Shackleton et al., 1995) argued that for *C. wuellerstorfi* and *H. kullenbergi*, isotope values are interchangeable.

Where possible, at least 50 planktonic and 15-20 benthic specimens were picked. However, due to small original sample sizes and relatively low number of specimens, samples with fewer specimens were occasionally analysed. Poor preservation (e.g. recrystallisation) was reason to omit five samples from the record. A difference between *C. wuellerstorfi* and *H. kullenbergi* values exceeding 0.5 permil was ground to reject two more samples. Remaining outliers are defined as values deviating more than three standard deviations from the mean value and are indicated in figure 7. These samples were also excluded from the three-point-moving-averages in the figure.

4. Results

4.1. Foraminifera

A rich, diverse benthic foraminiferal fauna occurs in most of the Metochia section (Fig. 3). Except for the shallow-marine lower part (Postma et al., 1993), comparison of the species composition with recent and other fossil data indicate a water depth of about 1000 m (cf. Parker, 1958; Berggren and Haq, 1976; Massiota et al., 1976; Cita and Zocchi, 1978; Lohmann, 1978; Wright, 1978; Barbieri, 1998; De Rijk et al., 1999).

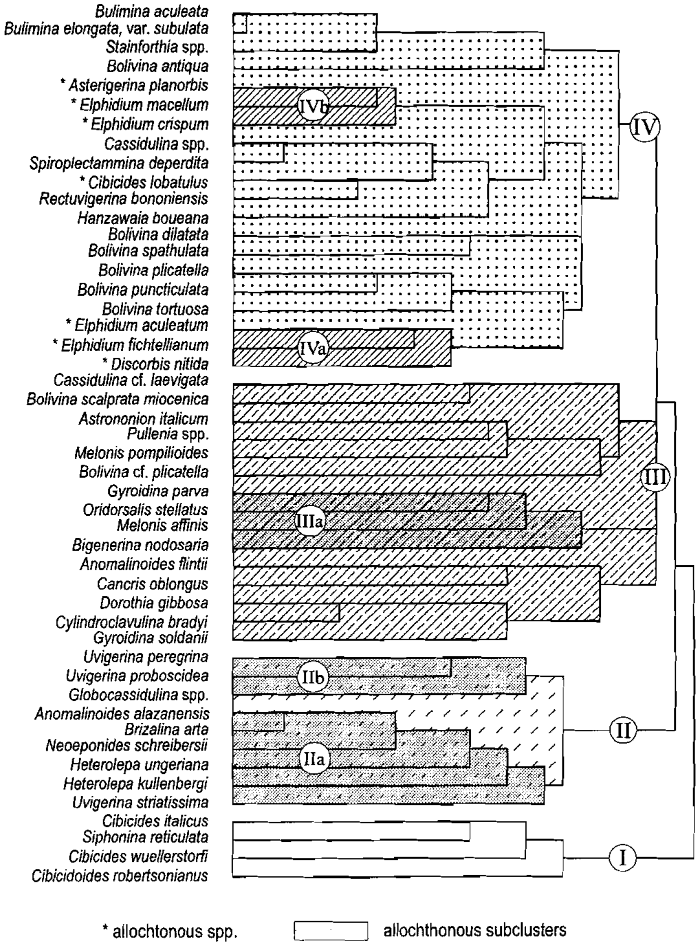

Figure 5. Dendrogram resulting from hierarchical clustering (between-group, Pearson correlation). Clustering divided the benthic foraminiferal faunas into four main clusters, which could again be subdivided into subclusters.

The hierarchical cluster analysis divides the benthic foraminiferal faunas into four major groups, of which three, Clusters I, II, and III, show maximum frequencies in distinct periods in time (Figs. 5, 6).

The first two groups (Clusters I and II) in general dominate the fauna during the Tortonian and earliest Messinian prior to 7.16 Ma (Fig. 3), and the foraminiferal assemblage is in general rich and diverse. The constituents of Cluster I disappear during the deposition of the sapropel of cycle 74 at 7.17 Ma, the first sample devoid of Cluster I species being at 7.16 Ma (Figs. 3, 6). These species are *Siphonina reticulata,* *Cibicides wuellerstorfi*, *Cibicides italicus*, *Cibicidoides robertsonianus,* and *Cibicidoides bradyi* (Figs. 3, 5). The foraminifera suggest a well-oxygenated palaeoenvironment with a normal salinity (Van der Zwaan, 1982; Katz and Thunell, 1984). Cluster II separates species occurring in the shallow depositional environment at the basis of the section (Figs. 3, 6); first dominated by Subcluster IIb (*Uvigerina peregrina*, *Uvigerina proboscidea,* and *Globocassidulina* spp.) and later by Subcluster IIa (e.g., *Neoeponides schreibersii, Anomalinoides alazanensis,* and *Brizalina arta*) (Fig. 5).

The third group (Cluster III, Figs. 5, 6) is made out by taxa that successively peak in relative frequencies from 7.16 to 7.0 Ma, e.g., *Oridorsalis stellatus*, *Cassidulina* cf. *laevigata*, and *Bolivina scalprata miocenica* (Fig. 3). These species are also present in the earlier part of the section, but only in low percentages. *O. umbonatus* is among the first species to recolonise the Mediterranean in the early Pliocene after the Messinian Salinity Crisis (Wright, 1979) and the species seems tolerant to high salinities (Van der Zwaan, 1983). *O. stellatus* is morphologically very close to *O. umbonatus* and may have the same environmental preferences. *C. laevigata* is a stress-tolerant species, which thrives under unstable conditions (Conradsen et al., 1994).

The fourth group (Cluster IV, Figs. 4, 5) is composed of species that show maximum abundances at the base of the sequence, between 8.4 and 7.8 Ma, and in the period after approximately 7.0 Ma (e.g., *Bolivina* (mainly *B. dilatata*), *Bulimina* spp., *Rectouvigerina bononiensis* group, *Stainforthia* spp., *Globocassidulina subglobosa,* and *Cancris oblongus*). Many of the species in this assemblage consist of taxa that are tolerant to high environmental stress, especially a low oxygen content (e.g., Van der Zwaan, 1982; Katz and Thunell, 1984; Sprovieri et al., 1986; Sen Gupta et al., 1989; Murray, 1991; Sen Gupta and Machain-Castillo, 1993). Intervals with an increase in this assemblage often coincide with increased concentrations of planktonic foraminifera (Fig. 4), indicating increased primary production. After approximately 7.0 Ma, *Bolivina plicatella* and *Bolivina* spp., especially *Bolivina dilatata*, dominate the foraminiferal assemblage (Fig. 3). Van der Zwaan (1982) suggests that *B. plicatella* is highly tolerant to raised salinities and oxygen deficiencies, while Van der Zwaan and Den Hartog Jager (1983) consider *B. plicatella* an epiphytic species. In our material the distribution of *B. plicatella* does not covary with the allochthonous, epiphytic species, and we therefore consider it *in situ. B. dilatata* may tolerate high salinities combined with low oxygen contents (Van der Zwaan, 1983: included in *B. spathulata*).

Subclusters IVa and IVb represent shallow-water species such as *Elphidium* spp. (e.g. *E. aculeatum, E. crispum, E. fichtelianeum,* and *E. macellum*), *Asterigerinata planorbis*, and *Discorbis nitida* (Figs. 5, 6). These species all have an epiphytic habitat and are commonly found displaced to greater depths in Mediterranean sediments (e.g., Todd, 1958; Van der Zwaan, 1983; Jorissen, 1987). They were presumably transported to the site by seaweed, and may be considered to be a measure of the surface water current activity. Although it did not group with Subclusters IVa or IVb, also *Cibicides lobatulus* is considered an allochthonous species.

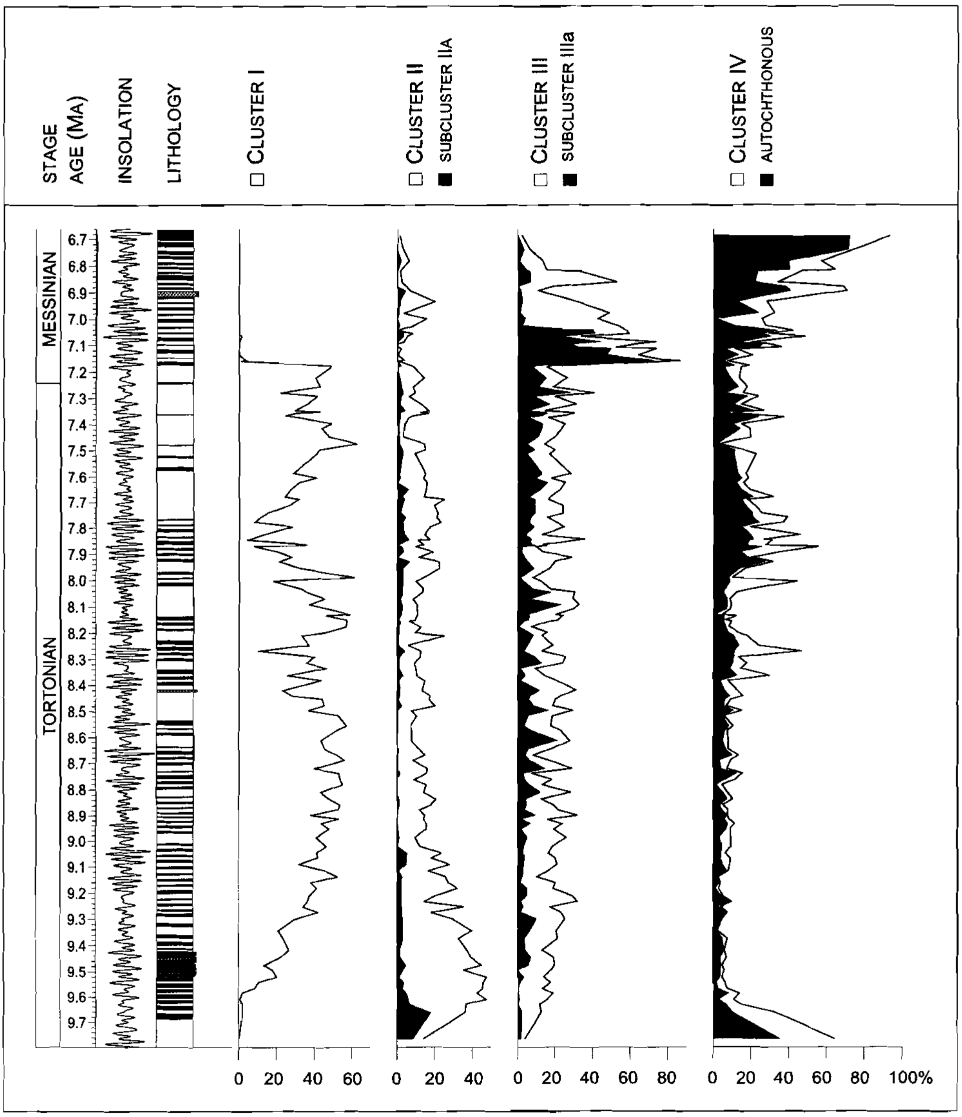

Figure 6. The main clusters and subclusters of the dendrogram plotted versus age. The lithology (black = sapropels; white = homogeneous intervals; dots = sandy intervals) and the 65°N summer insolation curve (from Hilgen et al., 1995) are indicated to the left.

4.2. Stable isotopes

The benthic $\delta^{18}O$ values show very little scatter about a line that shows a trend towards more positive values at the top of the section, the overall change being about 0.5 ‰ over 3 my (Fig. 7). The mean value of about +1.0 ‰ for the period between 9 and 7.3 Ma is only about 0.5 ‰ lighter than would be found in the Mediterranean Sea today. The fact that there is not a significant change in values over the lowest part of the section, when the benthic faunas give evidence for an increasing water depth, suggests that the water column may have been relatively homogeneous as it is at present, implying deep-water formation within the basin. Thus, the trend towards more positive values at the top of the section might imply a gradual increase in the bottom water salinity during the non-sapropel intervals. The shifts in the planktonic $\delta^{18}O$ are comparatively large, and could be attributed to changing surface water temperatures, salinity, or a combination of these factors.

In the main part of the section, the mean benthic $\delta^{13}C$ value is around +1.0 ‰, similar to the value for the planktonic $\delta^{13}C$, again supporting the hypothesis that deep water was forming within the basin and that there was a vigorous ventilation of the bottom waters. Values for both benthic and planktonic $\delta^{13}C$ increase by about one permil between 9.6 and 9.3 Ma, possibly related to deepening, and thus increasing distance to shore and decreasing productivity. At the top of the section there is a significant change to lighter benthic $\delta^{13}C$ values above the 7.16 Ma level of faunal change, and a lesser change in the planktonic values. This implies a sudden drop in ventilation and thus in deep-water dissolved oxygen, as is also implied by the faunal data discussed above.

5. Discussion

5.1. 9.8-9.3 Ma: Tectonically determined deepening phase

At the base of the Metochia section, a palaeosol is overlain by estuarine sediments (Postma et al., 1993). The lower part of the marine section (approximately 9.8-9.5 Ma) is characterised by a high influx of shallow-water, epiphytic foraminifera (Cluster IVa,b) and a high B/P-ratio (Fig. 4), which agrees with a close proximity to land. The upwards decrease of the B/P-ratio and the decreasing influx of allochthonous, epiphytic shallow-water benthic foraminifera (change from Cluster IV to Cluster I and II, Fig. 6) indicate a gradual deepening already in the lower part of the Metochia section. This is supported by a concurrent lithological change from sands to hemipelagic marls (Fig. 2) (Postma et al., 1993). In agreement with deepening, a decreasing productivity is indicated by the increase in benthic and planktonic $\delta^{13}C$ values (Fig. 7) and the diminishing planktonic and benthic foraminiferal concentrations (Fig. 4). A few species, such as *Anomalinoides alazanensis* (Fig. 3) and *Anomalinoides pompilioides* (Appendix 1) are restricted to this basal part of the section.

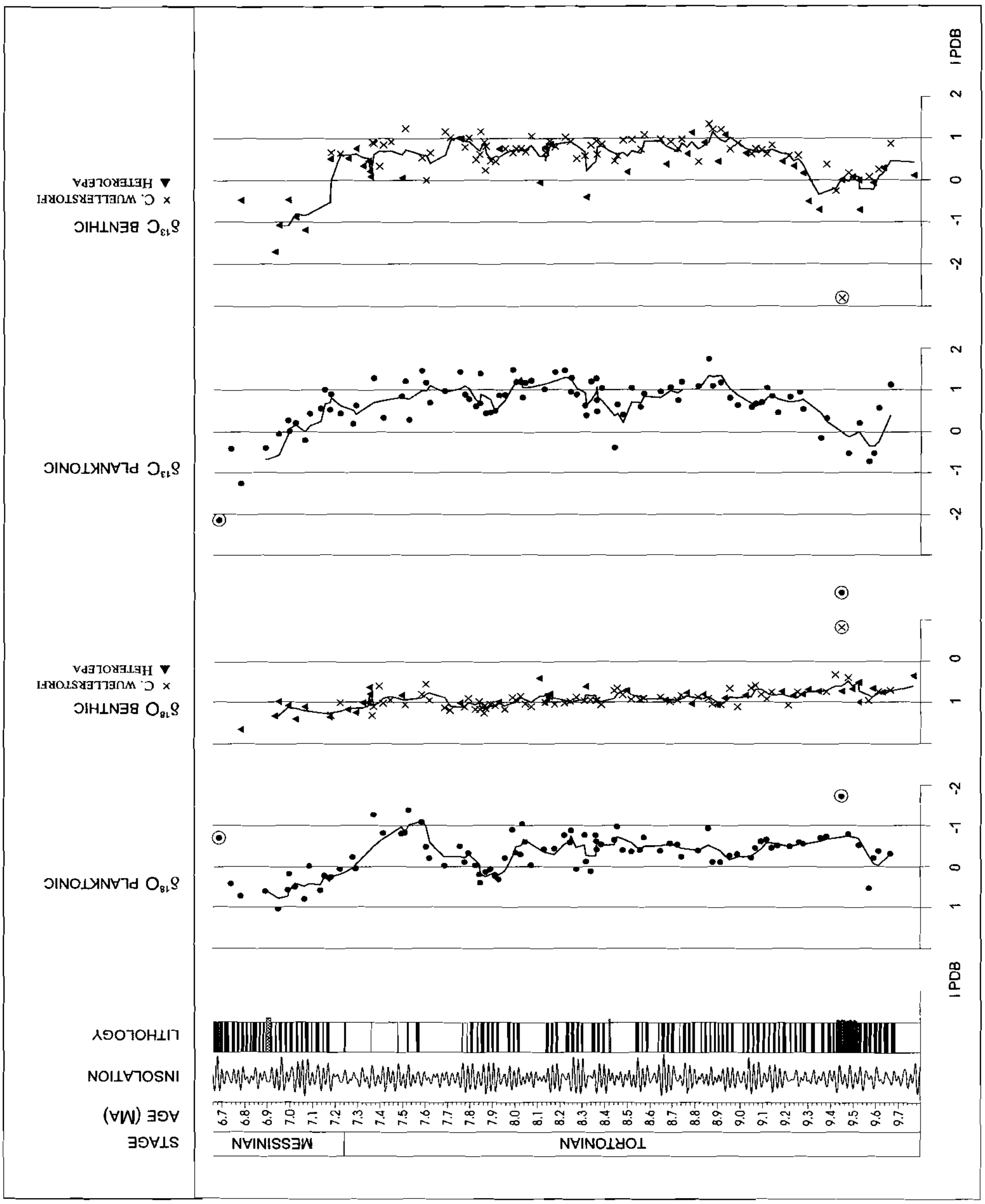

Figure 7. Stable oxygen and carbon isotope data from Metochia, shown as actual measurements (points) and as a three point moving average curve. Planktonic isotopes were measured on *G. obliquus*. Benthic isotopes were measured on *Cibicides wuellerstorfi* (crosses) and *C. pseudoungerianus* (triangles). Outlyers were not included in the three point moving average and are marked by circles. Lithology and 65⁰ N summer insolation curve to the left.

The formation of the marine basin at Gavdos during this period is presumably linked to the extensive tectonic activity that characterised the Miocene (cf. Meulenkamp et al., 1979; Ten Veen, 1998).

5.2. 9.3-7.17 Ma: Severe restriction of the Betic Strait

At 9.3 Ma, the tectonic subsidence of the Gavdos region had halted and the water depth stabilised at about 1000 m. Concurrently, the *S. reticulata* assemblage of Cluster I indicates normal marine and generally well-oxygenated bottom waters indicating a good Atlantic-Mediterranean water exchange as also previously suggested by Gebhardt (1999). From 9.3 to 8.5 Ma both benthic foraminifera and isotope data suggest that the environment was relatively stable with only subtle faunal changes.

Between ~8.5 and ~8.2 Ma, the general increase in mainly infaunal, low-oxygen species (Cluster IV; Fig. 6) and a decrease in importance of the normal-marine, high-oxygen Clusters I and II indicate a period of general increase in oxygen stress. Also the scarce, deep-sea ostracod fauna indicates decreased oxygenation (J.P. Peypouquet, pers. comm. 1995). After a temporary return to more ameliorated conditions, the oxygen stress was further accentuated from about 7.9 to 7.6 Ma (see Cluster I, Fig. 6), where also the autochthonous ostracods disappeared (J.P. Peypouquet, pers. comm. 1995). Planktonic $\delta^{13}C$ temporarily shifted to lighter values during these intervals, indicating increased surface production of light carbon. The fact that the benthic $\delta^{13}C$ values (measured on epifaunal species that prefer relatively high dissolved oxygen levels) show little change (Fig. 7), suggests a gradient between infaunal (as illustrated by the low-oxygen species) and epifaunal conditions (as illustrated by the $\delta^{13}C$).

Gebhardt (1994) showed that the external zone of the Betic Strait closed gradually during the middle to late Tortonian sometime between 9 and 7.5 Ma, with the western part closing earlier than the eastern. This event must have had a severe impact on the Mediterranean environment. We suggest that the more sluggish circulation indicated by the Metochia data, is a result of the shallowing of the Betic Strait influencing the water exchange with the Atlantic, and that the severe restriction of the main passageway of the Betic Strait can therefore be dated to about 8.5 Ma.

As Gavdos is located relatively far from the Betic Strait region, the high influx of allochthonous specimens from about 8.4 to 7.8 Ma (Fig. 4) cannot in itself have been caused by the changes in sill depth and lifting of the Betic Strait region. There is no evidence in the stable isotope values for an increased freshwater run-off from land that could have explained this high influx either (Fig. 7). Instead, we suggest that the high amount of allochthonous foraminifera was caused by a regional uplift as Crete was subjected to constant tectonic movements during the late Miocene (e.g., Ten Veen, 1998). The concurrent increase in autochthonous foraminifera (Fig.4) might be due to reworking of specimens that cannot be distinguished from the *in-situ* fauna. Alternatively, this increase may also be explained by a higher influx of nutrients washed out into the sea from tectonically uplifted shelves resulting in increased food availability.

After ~7.6 Ma a decrease in low-oxygen tolerant species (e.g., *C. oblongus*, Fig. 3) and an increase in high oxygen species (Cluster I, Fig. 6) occurred, indicating a return to normal marine, oxygenated conditions. The benthic oxygen isotope values suggest a gradual increase in bottom water salinity from ~7.3 Ma onwards. The planktonic $\delta^{18}O$ may indicate increasing surface-water temperatures between 7.9 and 7.6 Ma, followed by a cooling trend that lasted well into the Messinian.

5.3. 7.17-6.7 Ma: Partial closing of the Rifian Corridor

The top part of the sequence, representing the period between 7.16 and 6.7 Ma, shows evidence of strongly increasing stress in the benthic environment. The basin remained deep, as is evident from the B/P ratios (Fig. 4), and the stress increase thus still took place in deep waters.

A group of benthic foraminifera suddenly decreases in abundance and several disappear totally at 7.16 Ma. The most prominent species, which disappear, are *S. reticulata*, *C. wuellerstorfi,* and *C. italicus* (Cluster I). All these species are indicative of a well-ventilated environment. After the disappearance of the *S. reticulata* assemblage, *O. stellatus*, *C.* cf. *laevigata*, and *B. scalprata miocenica* (Cluster III; Figs. 3, 6) successively follow each other as the dominant species. Finally, the fauna changes to a poor, low-diversity assemblage and the fauna in the uppermost part of the section (section top: 6.7 Ma) contains almost only *B. plicatella* and *B. dilatata* (Cluster IV; Figs. 3, 6). A close sampling shows that the main faunal change, with the disappearance of *S. reticulata* and the development towards the more restricted foraminiferal fauna, occurred between the deposition of the homogeneous intervals of cycles 74 and 73, that is within less than 10.000 years. A similar disappearance of the *Siphonina reticulata* assemblage at approximately 7.16 Ma has also been recorded in a number of Mediterranean deeper-water sections (Kouwenhoven et al., 1998), amongst those Monte del Casino in Italy (Kouwenhoven et al., 1999). This "7.16-Ma" faunal event thus seem to occur synchronously throughout the deeper Mediterranean basins. Shallower locations are less affected (e.g., Van der Zwaan, 1982). At locations at the Betic Strait and the Rifian Corridor some effect is seen on the benthic fauna at this time, too (Berggren and Haq, 1976; Kouwenhoven et al., 1998; R. Sprovieri, pers. comm., 1997, unpublished data), although the event as such has not been recorded on the Atlantic side of the Rifian Corridor (Barbieri, 1998).

Apparently, the 7.16-Ma event is caused by a substantial decline in ocean ventilation, leading to diminished deep-water dissolved oxygen. This is also supported by the increased density of sapropels after 7.16 Ma and by the marked shift to lighter values in the benthic and to a lesser degree in the planktonic carbon isotope values (Fig. 7). This carbon isotope shift is a global phenomenon, which has been explained by, amongst others, eustatic sea-level lowering (see discussion in Hodell et al., 1994). The intra-Mediterranean carbon shift is, however, about twice as large as the carbon shift seen in the Atlantic (cf. Hodell et al., 1994), a fact also noted by Van der Zwaan and Gudjonsson (1986) and Kouwenhoven et al. (1999). In our data there is no evidence of a significant sea-level drop nor of increased oxygen consumption due to raised production (no increase in planktonic foraminiferal concentrations; Fig. 4). This indicates that a progressive isolation of the Mediterranean basin, and the resulting decreasing ventilation of especially the deeper waters, caused at least part of the intra-Mediterranean carbon shift. The probably Mediterranean-wide occurrence of the event suggests that the sluggish circulation be related to lesser water inflow caused by relative uplift of the sill of the Atlantic-Mediterranean waterway. There is strong evidence that the Rifian Corridor became constricted due to vertical movements between 7.2 and 7.1 Ma. Krijgsman et al. (1998, 1999) and Kouwenhoven et al. (1999) assume that uplift at that time eventually led to obstruction of inflowing Atlantic waters through the Rifian Corridor.

There is no concurrent shift in the benthic oxygen isotope values at 7.16 Ma. However, the benthic $\delta^{18}O$ indicates a gradual increase in salinity throughout the upper part of the section. We believe that the very poor benthic foraminiferal fauna, with dominance of *B. plicatella,* near the top of the section is a result of this increase in salinity and that it may reflect the gradual formation of a deep brine caused by the diminishing of the Mediterranean-Atlantic water exchange.

6. Conclusions

The benthic foraminiferal data provide evidence for a step-wise decrease of the Mediterranean-Atlantic water exchange. In this respect, especially the deep-water benthic foraminifera proved to be a very sensitive tool, even more so than the stable isotopes. If we summarise our evidence, it seems likely that the first severance in water exchange took place at about 8.5 Ma. This was followed at 7.16 Ma by a second very significant restriction of the water exchange.

Hitherto, there has been surprisingly little evidence for the exact time when the respective connections were severed. The Tortonian was in general a period of relatively stable environmental conditions and well-oxygenated waters (Gebhardt, 1999). However, it seems clear from Gebhardt (1994) that the wide and very important waterway, formed by the external Betic Zone and the main constituent of the so-called Betic Street, was gradually closing from early Tortonian times onward. In the middle Tortonian only isolated patches of full marine waters remained, suggesting that tectonic uplift had closed the passage. Based on the data of Gebhardt (1994), this event occurred between 9.0 and 7.5 Ma, but more precisely, our own data suggest that 8.5 Ma would be the time that the main passage was blocked. The benthic foraminifera point to a first step of decreased and unstable circulation at that level. At that time, also the basins in the internal Betic Zone were probably uplifted, as testified by extensive erosional surfaces (Van de Poel, 1992; Baggley, 1998). At ~7.2-7.1 Ma, the Rifian Corridor, the other important connection, was severely restricted, while marine sediments were deposited in the Sorbas and Nijar basins (see Krijgsman et al., 1998; Riding et al., 1998), later followed by restriction and evaporite deposition. Our data suggest that the net result of the events was a further reduction in water exchange and circulation, as both benthic foraminifera and stable isotopes indicate a significant decrease in deep-water circulation at 7.16 Ma. The lower evaporites formed from the definitive onset of the Messinian Salinity Crisis at 5.96 Ma and onwards were still of marine origin , and the total closure of the Mediterranean-Atlantic passage did probably not occur before about 5.59 Ma (Krijgsman et al., 1999).

The increasing restriction in the Mediterranean-Atlantic water exchange seems to have led to not only the step-wise development of oxygen deficiency but also a gradual increase in salinity throughout the Tortonian and early Messinian. After approximately 7.0 Ma the salinity increase was severe enough to influence the deep benthic community and it may also have caused the formation of a brine in the deep basins.

Acknowledgements

We would like to thank F. J. Hilgen and W. J. Zachariasse, University of Utrecht, who provided the samples and who together with L. Lourens, University of Utrecht, further aided us in our work. We also thank A. Antonarakou, University of Athens, and J. P. Peypouquet, University of Bordeaux, for putting the planktonic foraminifera and ostracod data, respectively, at our disposal. We are grateful to K. L. Knudsen, University of Aarhus, and W. Krijgsman, University of Utrecht for carefully reading through the manuscript. We are grateful to G. Ittman, G. van't Veld, and A. van Dijk, University of Utrecht, for carrying out the laboratory analyses and to J. Gissel-Nielsen, University of Aarhus, for preparing earlier versions of some of the drawings. R. Barbieri, University of Bologna, and F. J. Sierro, University of Salamanca, are gratefully acknowledged for their reviews and valuable suggestions. The study was carried out in the context of the EEC Human Capital and Mobility Program "MIOMAR" (MIOcene Marine Archives Reading) and further funded by the Danish Natural Science Research Council (MSS).

Chapter 5

A transfer function for oxygenation

A transfer function for bottom-water oxygenation based on benthic foraminifera: A case study of late Miocene data

Abstract

All modern methods to reconstruct oxygen contents of bottom waters in fossil settings lead to semi-quantitative estimates at best. A new approach to arrive at quantitative estimates was developed recently. The method is based on the use of benthic foraminiferal taxa from oxyphilic habitats. These taxa inhabit the top levels of the sediment column, and to them oxygen is a limiting factor. This observation has been employed to construct a transfer function that leads to quantitative oxygen estimates and appears to be independent of trophic regimes. Since the transfer function is based on modern data, we attempt to validate the method for fossil application in this study. For this purpose, the transfer function was applied to a late Miocene Mediterranean sequence, for which benthic foraminiferal counts as well as geochemical oxygenation proxies were available. Application of the method led to a realistic reconstruction of bottom-water oxygenation, that is not in conflict with conventional proxies for oxygenation. This suggests that careful application of the transfer function may lead to reliable quantitative oxygen reconstructions of highly varying paleoceanographic settings.

1. Introduction

Over the past decades much effort has been put into reconstructions of bottom-water oxygenation in fossil settings (see for overview Bernhard, 1986; Kaiho, 1994, 1999; Sen Gupta and Machain Castillo, 1993; Van der Zwaan et al., 1999). Many of the methods applied however, have considerable limitations and none of them gives a quantitative estimate of the actual amount of free oxygen at for instance the sediment-water interface. Yet, proper models of paleo-circulation partly rely upon such quantitative estimates (e.g. Marchitto et al., 1998), and so do realistic reconstructions of paleoenvironmental change.

At this stage the most readily applicable methods to reconstruct oxygen contents of bottom waters include stable carbon isotopes, redox-sensitive elements, and benthic foraminiferal abundances. These methods, however, lead to semi-quantitative estimates at best. Kaiho (1994 and 1999) developed a method leading to quantitative results, which is based on the occurrence of a large number of taxa in a wide range of environments. An objection to this method could be that his analysis is based on a comparison between the occurrences of dead assemblages and the temporal oxygenation state based on ill-defined measurements. Furthermore, it is not clear how his index should be applied to widely differing assemblages, as the index is based on multiple regression in which the role of individual taxa is not well defined.

Recently, Van der Zwaan et al. (submitted) developed another approach to arrive at quantitative estimates. The authors studied abundances of living (Rose Bengal stained) foraminifera from the Indian Ocean, Atlantic Ocean and two Mediterranean localities: the Adriatic Sea and the Levantine Basin. They could distinguish three main groups of benthic foraminifera. A first group of species, the so-called epifauna group, appears to inhabit the top levels of the sediment column. A second group, well known from many earlier studies (e.g., Corliss and Emerson, 1990; Jorissen et al., 1995), preferably resides at the deep redox boundary and apparently consists of facultative anaerobes. A third group of, potentially infaunal, species lives at varying depths in the sediment, and is able to resist oxygen deficiency over rather long time spans (see Barmawidjaja et al., 1992; De Stigter et al., 1998). The occurrences of individual species were compared to in situ measurements of oxygen, carried out with microprobes. The authors found strong indications that a number of the epifauna species are obligate oxygen dependent. This observation was translated into a regression function that appeared to be independent of trophic regimes and specific oceanographic settings (Van der Zwaan et al., submitted). The ultimate goal of the transfer function is its application in fossil settings, so as to create the possibility to quantify the oxygenation history of oceanic basins in various paleoceanographic settings and time slices. This paper reports on an attempt to validate the method in a late

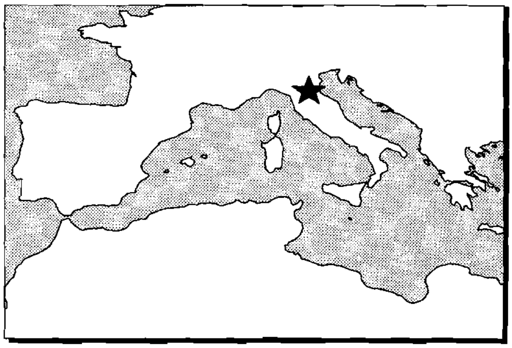

Figure 1. Location of the Monte del Casino section.

Miocene Mediterranean setting, using a sequence that has been well described, and for which benthic foraminiferal counts as well as geochemical proxies of oxygenation were at our disposal.

The Miocene is a period during which the stage completely altered in the Mediterranean area. Due to closure of the Mediterranean connection to the Indian Ocean the marine circulation must have changed completely. A logical assumption is, that at some time the circulation turned from estuarine to anti-estuarine. Subsequently the formerly rather well-connected Paratethys region became more and more isolated due to tectonic movements in the Carpathian Arc. Within the Mediterranean proper the Italian landmass emerged and the separation of eastern and western basins began to take shape. Later, the connecting seaways to the Atlantic Ocean in the extreme western part of the Mediterranean were modified substantially. Uplift led to shoaling of the Betic and Rif Streets and gradually to constriction of the outflowing deep Mediterranean waters by the more pronounced sills. Eventually this resulted in isolation of the basin, and the Messinian salinity crisis. This stepwise process and the profound effects of increasing isolation on the vertical circulation of the Mediterranean waters were mentioned in a number of papers (see for instance Selli, 1960; Hsü et al., 1973; Benson et al., 1991; Hodell et al., 1994; Krijgsman et al., 1999a,b; Kouwenhoven et al., 1999; Seidenkrantz et al., in press).

Evidence has been presented that at 7.16 Ma a considerable decrease in deep-water ventilation took place in the central and eastern Mediterranean (Kouwenhoven et al., 1999; Seidenkrantz et al., in press). The geographical extent of the ventilation change (i.e. central and eastern basins) suggests that it was related to obstruction of deep-water circulation, possibly at the western sills. The absolute magnitude of the change in oxygen contents, however, is not clear at all. In this paper we attempt to reconstruct the deep-water oxygenation over a period of about 2 Ma, using data from the Italian Monte del Casino section (Fig. 1). We selected this section not only because of its faunal assemblages that are reasonably well preserved and already quantified (Kouwenhoven et al., 1999), but also because it is situated in a geodynamical context that is rather clear. Recently, Van der Meulen et al. (1999) elaborated on the geodynamic changes that took place during its deposition. Moreover, we have data on the distribution of important redox elements and carbon isotopes of foraminiferal carbonate, which provide an additional tool to check the quantitative oxygen contents as reconstructed using foraminifera. In this sense, this paper reports on a pilot study in which for the first time Miocene deep-water oxygenation is reconstructed quantitatively. Therefore, we will start with justifying the methods used.

2. The oxygen transfer function

2.1 Oxygen and modern benthic foraminifera

In a recent study Van der Zwaan et al. (submitted) plotted the Average Living Depth position of all species from a wide range of environments. The plots reveal that the sediment column is closely and continuously inhabited (Fig. 2a, b: Atlantic and Indian Ocean, respectively) suggesting that taxa must have rather wide overlap of the niche dimensions. This indicates that many species do not have very specific environmental requirements. In a review of the proxy value of benthic foraminifera, Van der Zwaan et al. (1999) reached a similar conclusion. In general, all species display highest abundances at the sediment-water interface. Van der Zwaan et al. (1999), partly following Jorissen et al., (1995), explained this by assuming that in-sediment distribution patterns are the result of the balance between preference for food and tolerance to lowered oxygenation. It seems logical to assume that all species prefer to reside at the sediment-water interface where the most labile organic matter accumulates. This organic matter is exploited as source of food, either directly or indirectly by feeding upon bacterial stocks. Competitive interference appears to lead to the displacement of less competitive species deeper into the sediment column (Ernst et al., 1999): the deeper a species lives in the sediment column, the less competition it has to endure. At the same time it has to accept food of lower quality and should be able to tolerate the more hostile conditions, specifically the decreasing oxygen contents. Some species are clearly able to do so: their ALD indicates that at least during part of the year they live below the level down to which free oxygen occurs. These species are referred to as "potential infauna group", in line with earlier terminology of Barmawidjaja et al. (1992). A plot of the average living position of the epifauna group versus that of the potential infauna group (Fig. 3) shows that the latter is below the level of free oxygen. The plot also shows that concomitant with increased downward penetration of oxygen in the sediment column, the environmental gradient inhabited by the foraminifera expands. This is primarily due to the shift of the potential infauna group to deeper parts. On the average, the epifauna group remains in the shallowest, best-aerated sediment layer.

2.2 The transfer function

Taxa that were considered to be almost exclusively epifaunal in the Adriatic and Levantine Basins (Mediterranean Sea) were followed over time by Jannink (in prep.) and Duijnstee (in prep.). Their in-sediment distribution patterns were

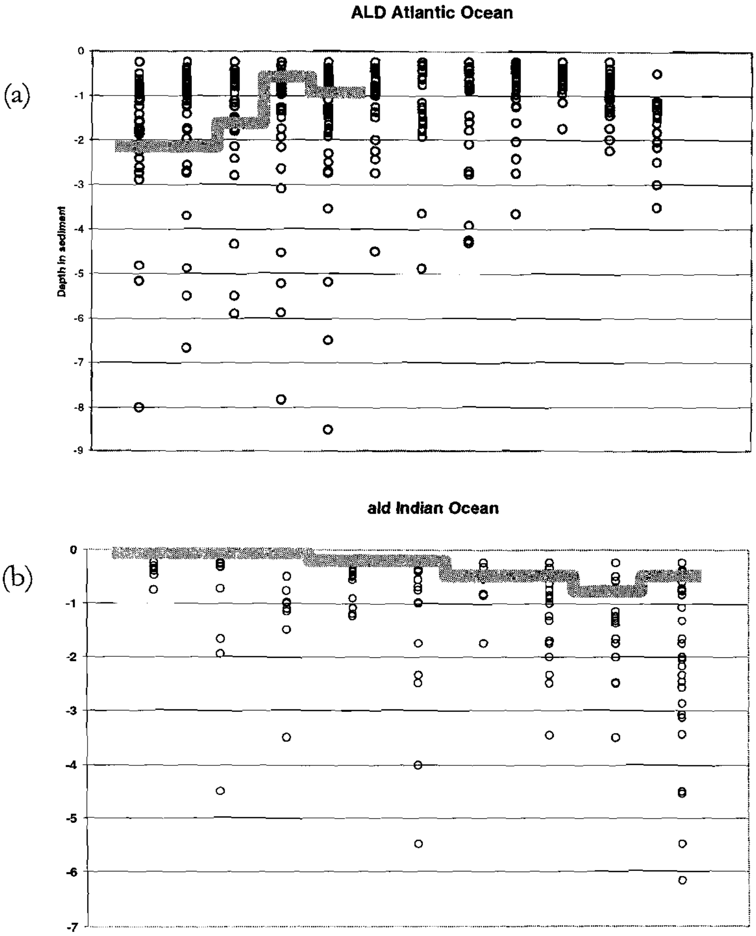

Figure 2. Average Living Depth of benthic foraminiferal species from the Atlantic **(a)** and Indian **(b)** Oceans. Data from Jannink et al., 1998 (Indian Ocean) and Guichard, 1997 (Atlantic Ocean). Level of penetration of free oxygen is indicated with full line.

compared to the oxygen concentrations in the sediment column as measured by microprobes. As was noticed earlier, oxygen seems to be a limiting factor for these species. Most abundant patches of epifauna occur in the top sediment layer during periods when oxygen penetration in the sediment column is deepest. Van der Zwaan et al. (op cit) conclude that the taxa belonging to this group are apparently oxyphilic, i.e. dependent on the presence of free oxygen.

Van der Zwaan et al. (op cit.) observed a correlation between oxygen and modern oxyphilic taxa from the Mediterranean, Atlantic and Indian Oceans. The taxa from deeper water sites that were considered to be oxyphilic were *Cibicides*

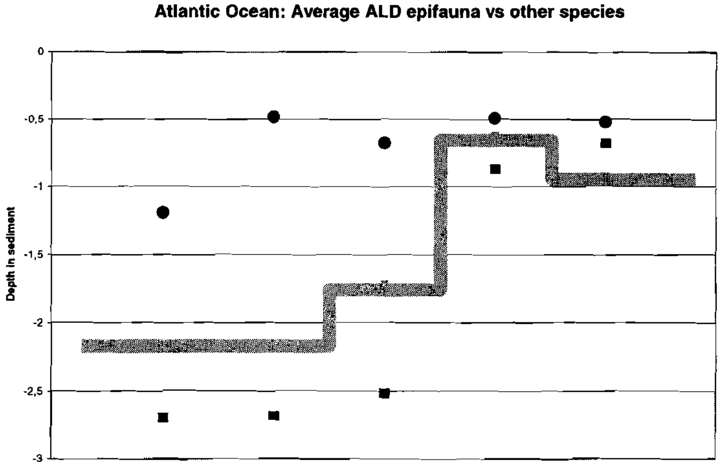

Figure 3. Average ALD of all epifaunal taxa and all "potentially" infaunal taxa in the Indian Ocean. Level of oxygen penetration is indicated with full line. Data from Guichard, 1997.

(not *C. bradyi*), *Gavelinopsis* spp., *Rosalina* spp., miliolids, *Lenticulina* spp., *and Sphaeroidina bulloides*. Agglutinated taxa were omitted because of the evident fragility and rather low preservation potential of a number of them. Therefore, in the plot the proportion of only calcareous species belonging to the oxyphilic assemblage is regarded, versus oxygen. It appears that in spite of the widely differing trophic regimes of the areas considered, the joint abundances of this group correlate with the oxygen contents at the sediment-water interface according tot the formula:

$$[\text{Oxygen content } \mu\text{Mol/L}] = 7.9602 + 5.95\ [\%\ \text{oxyphilic taxa}]$$

2.3 Application to late Miocene data

We applied the oxygen transfer function to the benthic faunas of the Monte del Casino section (N-Italy). We selected a group of calcareous oxyphilic species (Table I) in order to reconstruct the oxygen contents of the bottom waters. Basically, we used the same species that were used in the modern analysis and we will further justify the use of these species, and of the transfer function, in the discussion.

Data of the Monte del Casino section were published in a previous paper (Kouwenhoven et al., 1999). Details pertaining to methods used in foraminiferal and geochemical analyses are given there. The lithology of the section consists of an alternation of homogenous marls, and sapropels. It is important to note that we omitted sapropel samples from the data set, because we were particularly interested in the ventilation history of the site under non-sapropel conditions. In this paper we consider the frequencies of abundant taxa, stable carbon isotopes of benthic foraminiferal carbonate, and the most important redox elements, manganese and vanadium.

3. Results

The result of the oxygen transfer function as applied to data from the Monte del Casino sequence is presented in Figure 4. In this figure we show the calculated oxygen content at the sediment-water interface and conventional proxies for bottom-water oxygenation, versus the lithology and age column of the Monte del Casino section. The dendrogram resulting from hierarchical clustering of taxa with relative frequencies of 5% and more is shown in Fig. 5a. The distribution in time of relevant groups of species is summarized in Fig. 5b.

The reconstructed oxygen curve suggests that before 7.16 Ma the oxygen content of the bottom waters was relatively stable. A gradual decrease between 8 and 7.75 Ma is reflected in the benthic counts, but not in the geochemical redox proxies. According to the transfer function oxygenation more or less stabilized around 200-300 μMol/L between 7.7 and 7.2 Ma. A relatively minor drop in oxygen contents, as indicated by the elements and the carbon stable isotopes at ~7.6 Ma is not reflected in the benthic foraminiferal counts and the reconstructed oxygenation curve. All tools point at the fact that we are dealing with an overall rather well ventilated water column during most of the older part of the sequence.

Fig. 5b shows that a major faunal turnover was initiated during deposition of the sapropel of sedimentary cycle 18, around 7.17 Ma. Most striking is the virtual disappearance of an important group of species dominated by *Cibicides wuellerstorfi* and *Siphonina reticulata* c.s. (marked in Fig. 5a with an asterisk; white in Fig. 5b, cluster 1). According to the results of the oxygen transfer function (Fig. 4), at ~7.16 Ma the oxygen contents dropped from 300 to ~125 μMol/L, and later to even lower values. Two reconstructions are made for the period following the event at 7.16 Ma. If the relative frequencies of *Cibicides pseudoungerianus* are included in the calculation (solid line in Fig. 4), this drop of oxygen levels was followed by a steep increase until 6.95 Ma. This is in line with the patterns found in the redox elements: both manganese and vanadium indicate rapidly changing oxygen conditions during this period. If the relative frequencies of *C. ungerianus* are

---

Figure 4. (next page) Bottom-water oxygenation proxies for the Monte del Casino section, with lithology, age model, and the 65 °N summer insolation curve (see Hilgen et al., 1995; Krijgsman et al., 1995, 1997). $\delta^{13}C$ of benthos is a three point running average curve. Manganese is depleted in sediments under anoxic conditions. Vanadium is enriched when the oxic/anoxic boundary is situated at the sediment-water interface or in the water column. Quantitative oxygen reconstructions are calculated including (solid line) and excluding (dashed line) the relative frequency of *C. pseudoungerianus*.

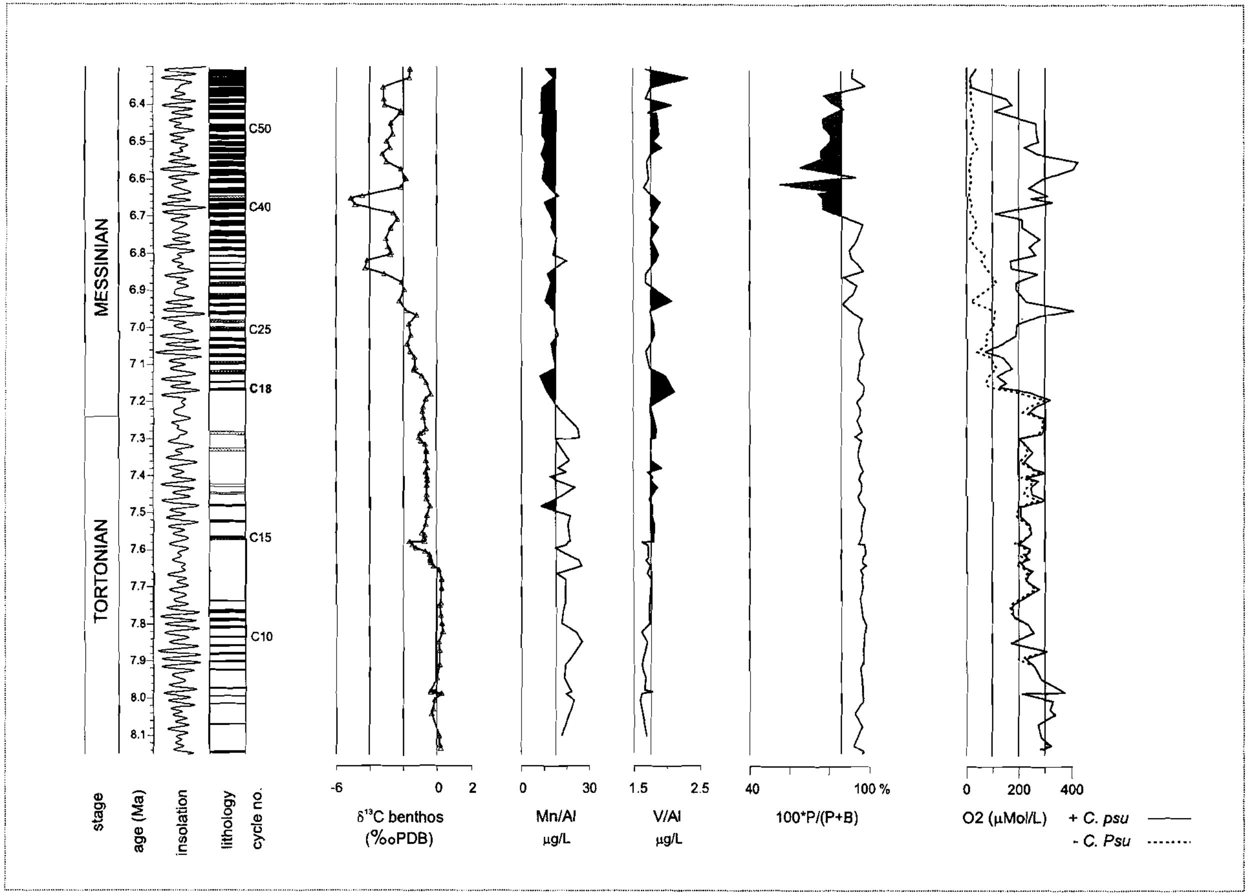
MESSINIAN
TORTONIAN
6.4
6.5
6.6
6.7
6.8
6.9
7.0
7.1
7.2
7.3
7.4
7.5
7.6
7.7
7.8
7.9
8.0
8.1
C50
C40
C25
C18
C15
C10
stage
age (Ma)
insolation
lithology
cycle no.
-6
0
2
δ13C benthos
(‰PDB)
0
30
Mn/Al
µg/L
1.5
2.5
V/Al
µg/L
40
100 %
100*P/(P+B)
0
200
400
O2 (µMol/L)
+ C. psu
- C. Psu

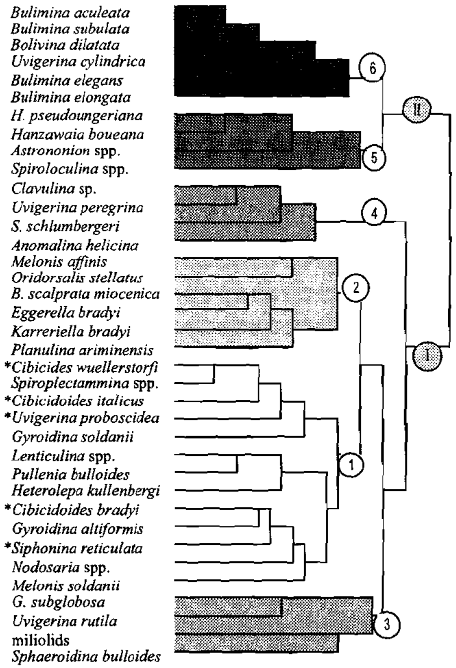
Bulimina aculeata
Bulimina subulata
Bolivina dilatata
Uvigerina cylindrica
Bulimina elegans
Bulimina elongata
H. pseudoungeriana
Hanzawaia boueana
Astrononion spp.
Spiroloculina spp.
Clavulina sp.
Uvigerina peregrina
S. schlumbergeri
Anomalina helicina
Melonis affinis
Oridorsalis stellatus
B. scalprata miocenica
Eggerella bradyi
Karreriella bradyi
Planulina ariminensis
*Cibicides wuellerstorfi
Spiroplectammina spp.
*Cibicidoides italicus
*Uvigerina proboscidea
Gyroidina soldanii
Lenticulina spp.
Pullenia bulloides
Heterolepa kullenbergi
*Cibicidoides bradyi
Gyroidina altiformis
*Siphonina reticulata
Nodosaria spp.
Melonis soldanii
G. subglobosa
Uvigerina rutila
miliolids
Sphaeroidina bulloides
6
5
4
2
1
3
II
I

5a

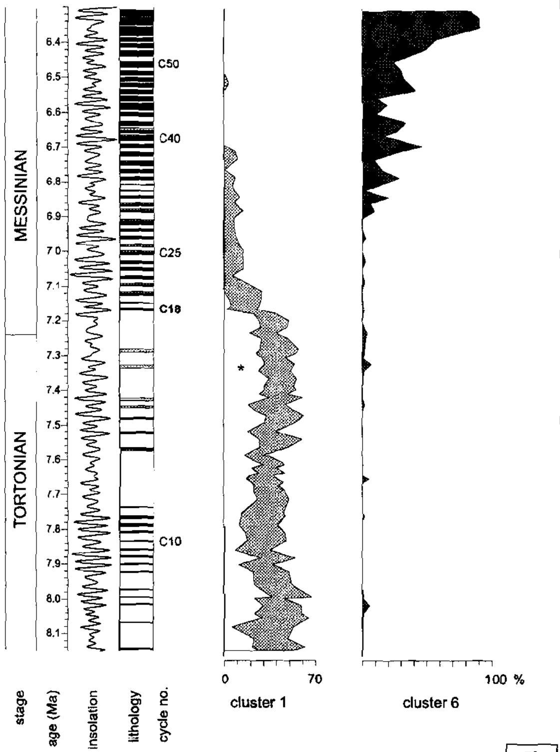
MESSINIAN
TORTONIAN
6.4
6.5
6.6
6.7
6.8
6.9
7.0
7.1
7.2
7.3
7.4
7.5
7.6
7.7
7.8
7.9
8.0
8.1
C50
C40
C25
C18
C10
*
0
70
100 %
cluster 1
cluster 6
stage
age (Ma)
insolation
lithology
cycle no.

5b

excluded from the calculations, reconstructed oxygen contents remain below ~100 μMol/L. This would be more in line with the continuous decrease in the carbon isotopes of benthic carbonate, that shift to values well below the average Tortonian value of about 0 $^{o}/_{oo}$.

At Monte del Casino the temporal distribution pattern of the benthic foraminifera, and thus of the related oxygen reconstruction based on the transfer function, is complicated by the fact that the geodynamical setting of the section changed drastically following the events at 7.16 Ma (Van der Meulen et al., 1999). A relative shallowing of about 400 meters was established during the early Messinian. Temporal increase of oxygenation as reflected in the oxygen reconstruction when *C. pseudoungerianus* is included (solid line) could reflect uplift of the site into a better-aerated part of the water column after the low-oxygen event at 7.16 Ma. The reconstructed oxygen record further suggests that after about 6.6 Ma the oxygen levels steadily dropped to minimum values. This is in line with the trend in both the redox-sensitive elements and the carbon isotopes, and the development of a stress-tolerating benthic foraminiferal fauna in the top of the section.

4. Discussion

We know that substantial changes in the oxygenation of the bottom waters took place during the deposition of the Monte del Casino sequence (Kouwenhoven et al., 1999). In the light of these changes, we have to discuss use of the transfer function, which was established using modern living foraminiferal patterns. Furthermore, we have to justify our selection of oxyphilic foraminifera used for the construction of a late Miocene oxygen record.

4.1 Recent oxyphilic taxa

The correlation of the oxyphilic taxa with oxygen contents of bottom waters is not based on a simple physiological relationship. Experimental research already suggested that most foraminifera have wide tolerance ranges for variations in oxygenation (Alve and Bernhard, 1995; Moodley et al., 1998a,b). On the basis of this evidence Van der Zwaan et al. (1999) argued that most foraminifera have a narrow range in which oxygen limitation starts to be effective. Above this limit variation in oxygenation does not seem to affect abundances (e.g. Jorissen et al., 1995). Below this limit species apparently cannot survive. In this sense oxygen

Figure 5. (previous page) **(a)** Dendrogram resulting from hierarchical cluster analysis of relative frequencies of 5% and more in homogeneous sediments. Two main groups and six clusters are indicated by shading. **(b)** Joint frequencies of cluster 1 and cluster 6 species. The white area in cluster 1 denotes species disappearing during deposition of cycle C18 (~7.17 Ma), and corresponds to joint frequencies of taxa indicated with an asterisk in the dendrogram (a).

seems to be a parameter mostly deciding on presence/absence, and not on abundances. The correlation is therefore not easily understood in terms of oxygen alone. However, it becomes acceptable if we consider the effects following a change in bottom water oxygen concentrations. An increase in oxygen contents leads to a deeper penetration of free oxygen in the sediment. Together with the downward shift of the redox fronts, this results in an increased inhabitable zone for oxyphilic taxa. Figure 3 shows that such an expansion of the inhabited zone indeed takes place. If this is taken into account, the relationship of abundance versus oxygenation is understandable in terms of increasing abundances of oxyphilic taxa coinciding with increased inhabitable volume of sediment. This renders the relationship independent of place and time, and it is therefore acceptable to apply it in the context of fossil settings.

Table I. Miocene species used as input for the transfer function calculating bottom-water oxygenation.

included in oxyphilic group	doubtful
miliolids	*C. pseudoungerianus*
Lenticulina spp.	*Oridorsalis stellatus*
Anomalina helicina	
Siphonina reticulata	
Sphaeroidina bulloides	
Cibicides kullenbergi	
C. ungerianus	
C. italicus	
C. wuellerstorfi	
C. robersonianus	
C. dutemplei	

4.2 Selection of Miocene oxyphilic taxa

The selection of late Miocene species to be considered as oxyphilic is more difficult to justify. Extensive fauna analysis in a wide variety of environmental settings reveals consistent patterns of correlations between benthic species. In various dendrograms (e.g. Van der Zwaan, 1982, 1983; Kouwenhoven et al., 1999; this thesis, Ch. 7; Seidenkrantz et al., in press) Miocene species intolerant to oxygen depletion cluster consistently together.

The similarity between the modern and Miocene assemblages, together with the supporting quantitative analyses of a wide array of Miocene faunas, justifies the application of the oxygen transfer function using Miocene taxa. Since the function is based on calcareous species only, preservational effects caused by early disintegration of agglutinated species does not play a role.

During the Miocene we find the same species as the modern ones mentioned by Van der Zwaan et al. (submitted) to be oxyphilic. Most important among these are *Cibicides wuellerstorfi* and *C. ungerianus*, species consistently indicative of well-ventilated environments. Miliolids also cluster in the group of species intolerant to low oxygen conditions. However, under Miocene conditions these species are rather infrequent. Further we included *Siphonina reticulata*, a species which is always prominent in assemblages from well-aerated deeper Miocene environments, but highly infrequent in modern assemblages.

We omitted *Oridorsalis umbonatus* var. *stellatus* from the index. Although the species is characterised by Guichard (1997) as shallow-living, we suspect that it is stress tolerant under certain circumstances and may even live in deeper sediment layers. Brief but severe dominance of *O. stellatus* (60%) was described in the Metochia section just after the event at 7.17 Ma (Seidenkrantz et al., in press). For the time being we decided not to include this species in the oxyphilic group. Another problematic species is *Cibicides pseudoungerianus*. Belonging to the *C. ungerianus* group, it is usually considered to be epifaunal. The distribution pattern of this species in the Monte del Casino section, and its overall tendency to cluster with potentially infaunal species, renders this questionable. Therefore we made one reconstruction with, and another without *C. pseudoungerianus* (Fig. 4).

4.3 The reconstructed oxygen record

4.3.1 The overall trend

Between 8.1 and 7.16 Ma the reconstructed record of bottom-water oxygenation indicates values around 250-300 µMol/L, a value which is comparable to the modern day values in the Eastern Mediterranean (around 4–5 ml/L, or 175-250 µMol/L at ~1000 meters; see Miller et al., 1970; Lacombe and Tchernia, 1972; Tchernia, 1980; Béthoux, 1993). Between 8 and 7.8 Ma the oxygen content decreased by ~100 µMol/L. Evaluating data from the Metochia section (Gavdos, south of Crete), Seidenkrantz et al. (in press) noticed two periods of diminished bottom-water oxygenation, around ~8.5 and ~7.9 Ma. They attributed these to diminishing circulation due to the constriction of the Betic Street from ~8.5 Ma onwards. The second period of decreased oxygenation in Metochia can be correlated to the ~100 µMol/L drop observed in Monte del Casino. This temporary decrease is reflected in the frequencies of the species in cluster 1, but is not seen in the records of the redox-sensitive elements, and the stable carbon isotopes. The reconstructed oxygen curve stabilised after ~7.7 Ma at bottom-water oxygen contents around 250 µMol/L. The geochemical proxies indicate a small drop in oxygen contents at about 7.6 Ma, which is not reflected in the faunal record. No severe disturbances are recorded during this period, and all tools point to the fact that we are dealing with an overall rather well ventilated water column during most of the older part of the sequence. At first sight there are no reasons why we should not accept the quantitative oxygen estimates as based on the transfer function.

The faunal turnover that was initiated during deposition of the sapropel of sedimentary cycle C18 led to the virtual disappearance of an important group of epifaunal species dominated by *Cibicides wuellerstorfi* and *Siphonina reticulata* c.s. (figures 5a, 5b: cluster 1). The disappearance of these species occurred at several deep-water sites and was earlier interpreted as evidence of decreased deep-water ventilation (Kouwenhoven et al., 1999; Seidenkrantz et al., in press), as there were no indications for a sudden increase in productivity, neither planktonic nor benthic. The cause of decreasing circulation was assumed to be the uplift of the western Mediterranean sill in the Rifian Corridor. Krijgsman et al. (1999a) showed that uplift took place between 7.2 and 7.1 Ma. This corresponds to the time that the group of open marine species mentioned disappeared from the deep Mediterranean in Monte del Casino and other sections. All oxygenation proxies indicate the onset of major environmental changes at this stage. Manganese, which remobilizes under anoxic conditions, decreased. Vanadium, indicative of oxygen deficiency at the sediment-water interface, increased on the average. A position of the redox front at or above the sediment-water interface probably occurred during the Messinian, and is in line with the oxygen estimates. Fe, present in the form of pyrite after 7.3 Ma and a dominating feature after 7.16 Ma, indicates that negative redox potentials occurred high in the sediment column or even above the sediment-water interface. During such conditions the deeper redox fronts, as for instance the sulfide producing front, will have resided close to the sediment water interface, or even in the water column. In that context it is remarkable that the group of deep redox dwellers as *Globobulimina* and *Chilostomella* is not well represented in the Monte del Casino samples. For this phenomenon we have no other explanation than to assume that such deep redox dwellers were not so prominent yet as they are in modern assemblages.

4.3.2 Shallowing as a complicating factor

After 7.16 Ma the geodynamical setting of the section became a complicating factor. Van der Meulen et al. (1999) convincingly argued that the region underwent considerable uplift, and estimate the shallowing of the Monte del Casino area at 400 meters: from about 1000 meters water depth between 7.9 and 7.1 Ma, to about 600 meters at 6.7 Ma. They related this uplift to rebound after slab detachment, which led to a lateral shift of depocenters in the course of the evolution of the Apennines. This implies that at 7.16 Ma, the time of decreasing deep water ventilation, the section was still within reach of these deep waters, but was situated in a completely different part of the water column shortly afterwards, in better ventilated waters somewhat deeper than the shelf break. Shallowing strongly influenced the composition of benthic foraminiferal faunas, which had been characterized by a transitional composition after 7.16 Ma (cluster 4, Fig.5a). The first signs of unstable bathymetry are seen around 6.95 Ma (Fig. 4), and coincide with indications of diminishing bottom-water oxygenation reflected by the geochemical proxies. *Cibicides pseudoungerianus* suddenly dominated the benthic faunal assemblage, and continued to do so until, after 6.4 Ma, an assemblage composed of *Bolivina*, *Bulimina* and *Uvigerina* species was established (Fig. 5a: cluster 6).

This sequence of events immediately affects the oxygen reconstruction. *C. pseudoungerianus* is usually considered to be epifaunal, but shows opportunistic behaviour in the Monte del Casino section. If this taxon is excluded from the transfer function, the reconstructed oxygen levels are definitely too low (dashed line in Fig. 4). In this case the reconstructed oxygen levels permanently fall below 50 μMol/L after 6.8 Ma. Such levels are probably sufficiently low to trigger sapropel conditions (Rosenberg, 1980, ref. in Béthoux, 1993). The reconstructed values for bottom-water oxygenation are comparatively high if relative frequencies of *C. pseudoungerianus* are included in the calculation (solid line in Fig. 4), exceeding 400 μMol/L at two occasions. We are inclined to distrust these peak values at ~6.95 and ~6.55 Ma, and ascribe them to, for the moment unexplained, reflections of rapid environmental change. The mean values of 200-250 μMol/L, discarding the peak values, seem acceptable for the setting as reconstructed for this site. For the moment we prefer to include *C. pseudoungerianus* in the calculations, but to look at the results with caution. The increase of really stress-tolerant benthic faunas (Fig. 5a: cluster 6) in the top part of the sequence suggests decreasing oxygen values, which is in line with the sedimentological development of the sequence: in the uppermost twelve cycles all sediments, laminated or not, are of a dark green-brown colour and smell of hydrocarbons.

In all, the values for bottom-water oxygenation as reconstructed by use of the transfer function do not contradict the patterns as seen in the conventional proxies for oxygenation The transfer function may even provide a more reliable reconstruction than redox-sensitive elements, which can be remobilised, and carbon stable isotopes, which are always multi-interpretable and prone to diagenesis.

5. Conclusion

The oxygen transfer function based on modern assemblages, and tested on data from the late Miocene Monte del Casino secton, proves to be promising. At first sight the reconstructed oxygen values seem reliable, and the method leads to realistic values. Closer observation of earlier reconstructed events, and comparison with conventional methods of oxygen reconstruction, each with their particular sensitivity, reveals no major contradictions. However, the method needs further validation in different settings and time slices before it can be used as reliable input to constrain the outcome of modelling experiments.

Acknowledgements

I am indebted to N. Jannink, I. Duijnstee and B. van der Zwaan for putting the information at my disposal and for valuable discussions on the feasibility of this validation test.

Chapter 6

Mediterranean paleocirculation

A reconstruction of late Miocene Mediterranean circulation patterns

Abstract

In spite of extensive research concerning the late Miocene Mediterranean, questions remain on the Mediterranean water circulation patterns. Knowledge of, preferably quantitative, oxygen contents of water masses could be of help to reconstruct this circulation, and solve questions on the causes of the Mediterranean salinity crisis. Bottom-water oxygenation is usually estimated qualitatively, or semi-quantitatively at best, from abundances of infaunal benthic foraminifera, and from stable carbon isotope data or redox-sensitive elements. It now appears that relative percentages of oxyphilic benthic foraminifera are a rather straightforward measure of bottom water oxygenation, as recent data show that a transfer function translates relative percentages of oxyphilic foraminifera to oxygen concentrations expressed in µMol/L (Van der Zwaan et al., subm.). Using this method, we made an attempt to reconstruct the Mediterranean water circulation, employing benthic foraminiferal data from five Mediterranean sections and one site located at the Atlantic side of the Rifian corridor. We find that during the late Miocene an anti-estuarine circulation is likely, but that this simple pattern is complicated by geographic changes affecting the central part of the basin. Deep-water formation appears to have existed in the central northeastern part of the basin, probably less intensive from 7.6 Ma onwards. At about 7.16 Ma constriction of the Atlantic portals led to restricted exchange of Mediterranean and Atlantic water masses and to decreasing bottom water ventilation.

1. Introduction

During the Miocene the Mediterranean area was the scene of profound geographical and environmental change: the former Tethyan Seaway was transformed from a corridor accommodating a circum-equatorial flow into a series of semi-enclosed basins. Between the early and middle Miocene the connection to the Indo-Pacific was closed (see a.o. Adams, 1983; Vergnaud-Grazzini, 1983; Rögl, 1999) and around the NN5-NN6 transition (~14 Ma) the connection of the present Mediterranean basin to the Paratethys was severed or closed as well (Rögl, 1999). It is significant that this roughly coincides with the onset of sapropel formation in the Mediterranean basin (Chamley et al., 1986). Water mass exchange with the Atlantic remained intact through the Rifian and Betic corridors (Fig.1a).

An anti-estuarine circulation probably developed in the proto-Mediterranean, at some time after closure of the connection to the Indo-Pacific. Assuming an analogy with the present-day situation, evaporation probably exceeded precipitation plus runoff, and additional surficial inflow from the Atlantic was necessary to compensate for water loss. In this model, the Mediterranean evolved into a concentration basin and to some extent this notion is supported by stable isotope evidence (Vergnaud-Grazzini, 1983). As an additional feature, modern Mediterranean circulation includes deep-water formation on the Adriatic shelf and in the Liguro-Provençal Basin during winter (Miller et al., 1970; Lacombe and Tchernia, 1972; Robinson et al., 1992; Béthoux, 1993; Rohling, 1994 with references cited therein).

Miocene Mediterranean circulation patterns were probably not only subject to interactions with major ocean basins, but also to geographic changes within the basin. Based on paleomagnetic reconstructions of plate rotations, Duermeyer et al. (1998) estimated that the Tyrrhenian basin opened between 8.6 and 7.6 Ma. The first sediments in the basin were dated at 7.8 Ma (Duermeyer et al., 1998: data of Kastens et al., 1987 recalibrated to Hilgen et al., 1995) suggesting that the basin had reached a depth allowing detectable sediment infill by that time. Shaping of the basin into its present configuration continued well into the Plio-Pleistocene (Duermeijer et al., 1998 and subm). The development of the Italian landmass and the central Mediterranean sill (e.g. Van der Meulen, 1999) was crucial in separating the eastern and western basins, and must have had consequences for late Miocene circulation patterns. During the Messinian the restriction of the basin from surrounding major ocean basins led to the deposition of massive evaporites, of which the geographical distribution is closely tied to the paleogeography of that time (Fig. 1b). This event provides additional evidence for the prevailing circulation pattern, since an estuarine circulation would lead to flushing of deeper waters, thus inhibiting evaporite deposition (Sonnenfeld, 1984; but see Tchernia, 1980).

Figure 1. (a) Paleogeography of the late Miocene Mediterranean (redrawn after Orszag-Sperber, et al., 1993). **(b)** Approximate extension of evaporite deposits (after Nesteroff, 1973). Stars indicate the sections for which detailed data are available.

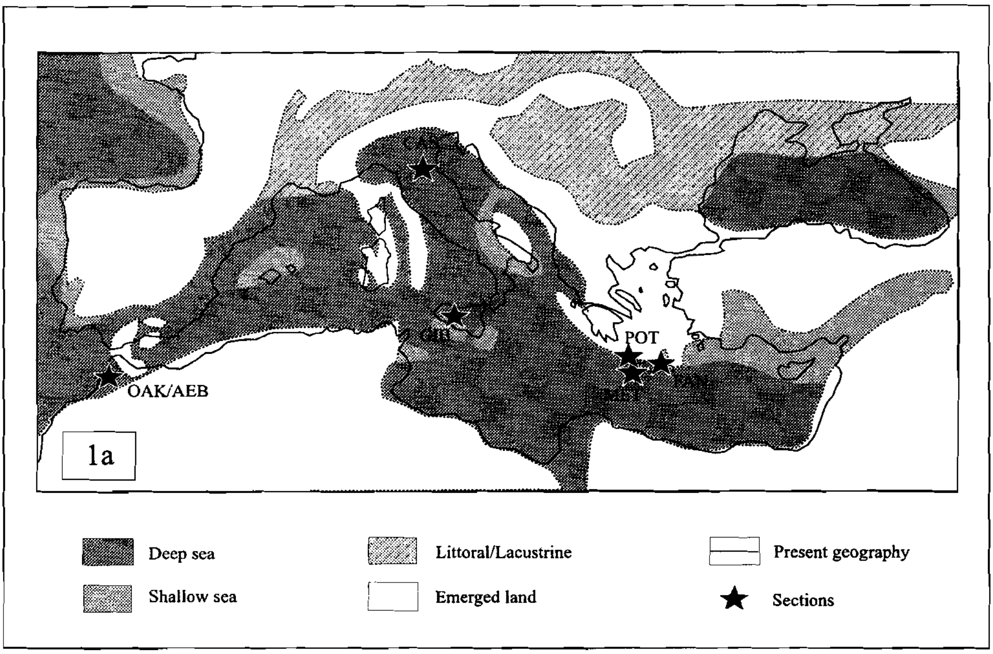
CAS
GIB
POT
MET
FAN
OAK/AEB
1a
Deep sea
Shallow sea
Littoral/Lacustrine
Emerged land
Present geography
Sections

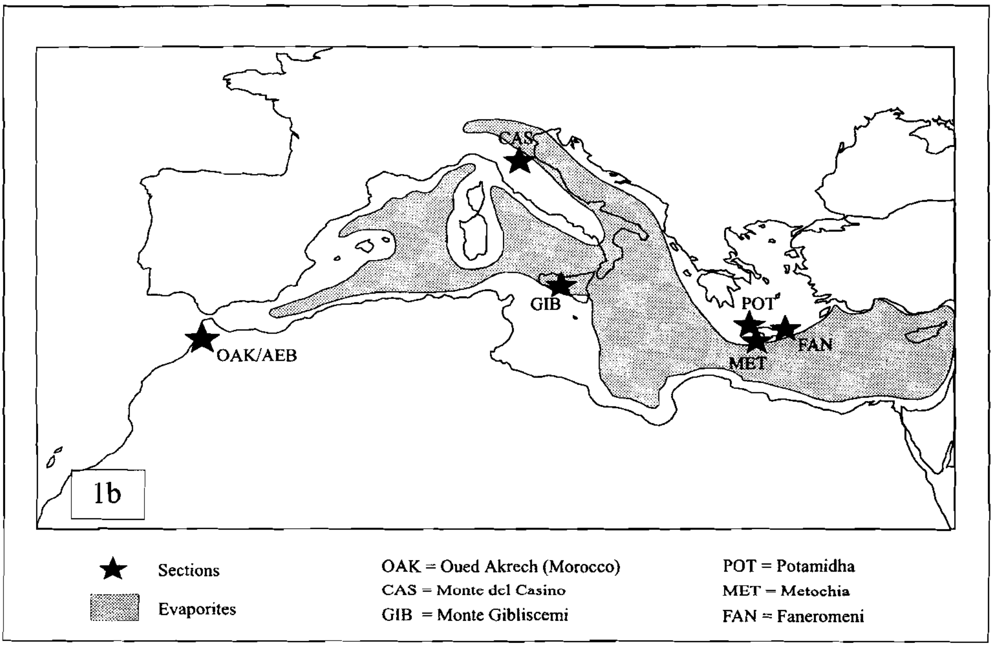
CAS
GIB
POT
MET
FAN
OAK/AEB
1b
Sections
Evaporites
OAK = Oued Akrech (Morocco)
CAS = Monte del Casino
GIB = Monte Gibliscemi
POT = Potamidha
MET = Metochia
FAN = Faneromeni

Recently we acquired more insight in the processes preceding the onset of the salinity crisis and detailed information has become available about the situation at the portals towards the Atlantic (Hodell et al., 1994; Barbieri, 1998; Krijgsman et al., 1999a,b). Previous research has indicated that a significant paleoenvironmental event at about 7.16 Ma initiated the onset of the salinity crisis (Kouwenhoven et al., 1999; Seidenkrantz et al., in press), and can be correlated to shallowing in the eastern part of the Rifian Corridor (Krijgsman et al., 1999a). At that time the oxygenation of deeper waters must have diminished dramatically. Data suggest that shortly afterwards the bottom water salinity started to increase in the deeper parts of the basin.

In this paper we integrate data from five late Miocene Mediterranean sections and one bordering the Atlantic (Oued Akrech, Morocco). Our purpose is to reconstruct Mediterranean circulation patterns and to trace whether and how these contributed to the Messinian Salinity Crisis. For this we employed quantitative estimates of water-mass oxygenation using an oxygen transfer function based on benthic foraminifera. The oxygenation records of all sections studied can be correlated in detail employing cyclostratigraphical patterns (Fig. 2; see also Hilgen et al., 1995; Krijgsman et al., 1995, 1997).

2. Material and methods

Detailed benthic foraminiferal counts are available of five Mediterranean sections and one section located in the Atlantic realm (for locations see Fig. 1). The sections cover different time slices, but all include the Tortonian/Messinian boundary (dated at 7.24 Ma; see Hilgen et al., 1995), and the earliest Messinian (Fig. 2). The lithology of the Mediterranean sections consists of an alternation of homogeneous and sapropelitic sediments. For the Moroccan section, where no sapropels are developed, duplets of white and reddish strata were correlated to homogeneous/sapropel duplets within the Mediterranean (Meijer, 1998). In this paper we concentrate on samples taken from homogeneous sediments (white in Oued Akrech, Morocco), as our purpose is to determine long-term trends, and not differences between homogeneous and sapropelitic sediments. For all sections, samples were disintegrated in water and washed over 63, 125, and 595 µm sieves. Benthic foraminiferal counts were performed on the 125-595 µm fraction, and relative percentages were calculated for all taxa. Paleobathymetry was calculated for each sample by introducing P/B ratios based on epifaunal species, in the equation of Van der Zwaan et al. (1990). Depositional depth of the sections varies from around 300 m to 1000-1200 m (Fig. 3a). It should be emphasised that bathymetrical reconstructions are less sensitive at the shallow (~0 m) and deep end (~1200 m) of the reconstructed range, and evidence of (oxygen) stress

Figure 2. Plots of lithology against age of the sections discussed. Sedimentary cycles are correlated to the 65°N summer insolation curve (Hilgen et al., 1995). In Oued Akrech reddish layers are developed instead of sapropels and grey layers.

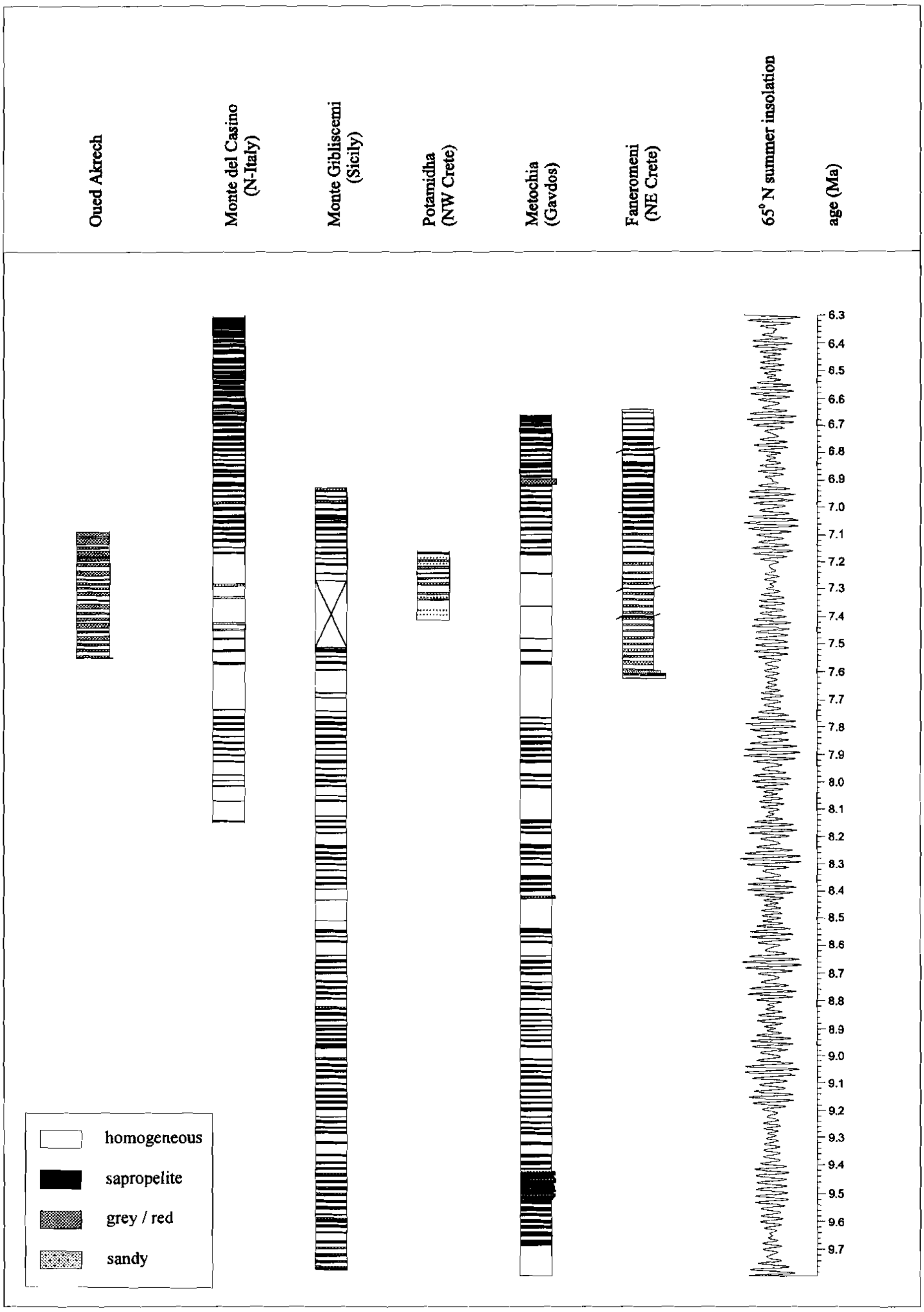
Oued Akrech
Monte del Casino (N-Italy)
Monte Gibliscemi (Sicily)
Potamidha (NW Crete)
Metochia (Gavdos)
Faneromeni (NE Crete)
65° N summer insolation
age (Ma)
6.3
6.4
6.5
6.6
6.7
6.8
6.9
7.0
7.1
7.2
7.3
7.4
7.5
7.6
7.7
7.8
7.9
8.0
8.1
8.2
8.3
8.4
8.5
8.6
8.7
8.8
8.9
9.0
9.1
9.2
9.3
9.4
9.5
9.6
9.7
homogeneous
sapropelite
grey / red
sandy

is a reason to regard the reconstruction with the utmost caution (see Van der Zwaan et al., 1990).

For the Monte del Casino and Metochia sections planktonic and benthic stable isotope records are available. The record is monospecific for Metochia (*G. obliquus* and *Heterolepa* or *Cibicides*) but measurements were carried out on multi-species samples for Monte del Casino. For the Monte del Casino and Faneromeni sections, element analysis provided records of the redox-sensitive elements vanadium and manganese. Detailed information about handling of samples for benthic foraminiferal counts and geochemical analyses can be found elsewhere (Wonders and Van der Zwaan, 1979; Kouwenhoven et al., 1999; Seidenkrantz et al., in press).

A quantitative estimate of bottom water oxygenation was made according to the method as outlined in Van der Zwaan et al. (submitted). This approach to calculate quantitative oxygen levels of bottom waters was recently tested for application to fossil sequences using data from the Monte del Casino section (this thesis, Chapter 5). In order to calculate oxygen levels, agglutinated and allochthonous species were omitted from the census counts and a new closed sum was calculated. From the percentage of oxyphilic taxa the oxygen levels were calculated using the equation (seeVan der Zwaan et al., submitted, and Chapter 5 of this thesis):

$$[\text{Oxygen concentration } \mu\text{Mol/L}] = 7.9602 + 5.95\ [\%\ \text{oxyphilic taxa}]$$

4. Results

Figure 3a shows calculated paleodepths for four Mediterranean sections and the section bordering the Atlantic. For the Potamidha section P/B ratios were not available. All sections except for Monte del Casino show rather stable paleodepths. In the central Mediterranean area Monte del Casino and Gibliscemi were deposited in relatively deep waters. In the eastern Mediterranean Faneromeni and Metochia appear to be shallow-intermediate, and deep water sites, respectively. Faunal evidence (Wonders and Van der Zwaan, 1979) suggests that the Potamidha sediments were deposited at approximately 600 metres. Potamidha can thus be regarded as an eastern Mediterranean intermediate water site, if compared to Recent water-mass distribution (compare a.o. Rohling et al., 1994, and references mentioned therein). Paleo-oxygenation patterns of bottom waters, based on the oxygen transfer function, are shown in Fig. 3b. For species imported into the transfer function, see Table I in Chapter 5 of this thesis. In the case of the Faneromeni section we added to these shallow water, epiphytic species.

Figure 3. **(a)** Depth reconstructions, based on the method in Van der Zwaan et al. (1990). OAK=Oued Akrech; CAS=Monte del Casino; GIB=Monte Gibliscemi; POT=Potamidha; MET=Metochia; FAN=Faneromeni. **(b)** Quantitative reconstructions of bottom-water oxygenation based on the oxygen transfer function (Van der Zwaan et al., subm.).

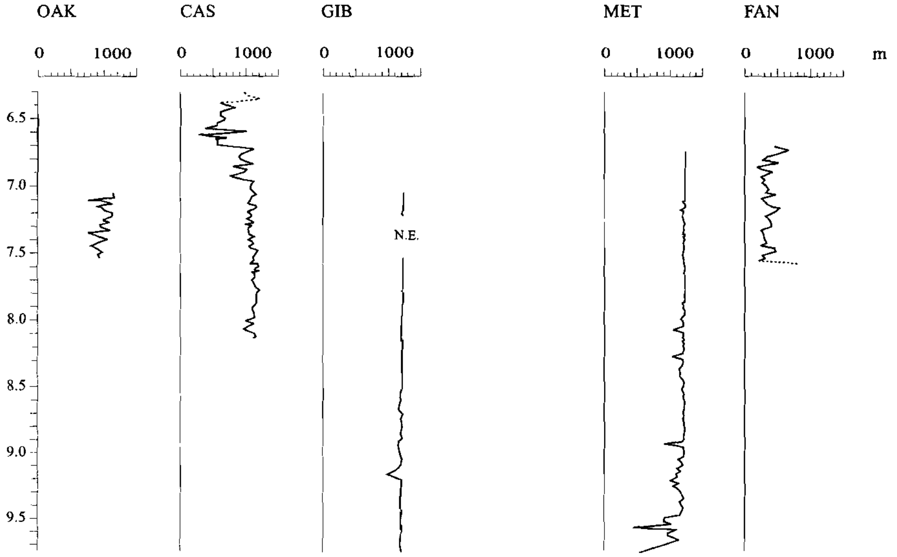
OAK
CAS
GIB
MET
FAN
0
1000
m
6.5
7.0
7.5
8.0
8.5
9.0
9.5
N.E.

3a

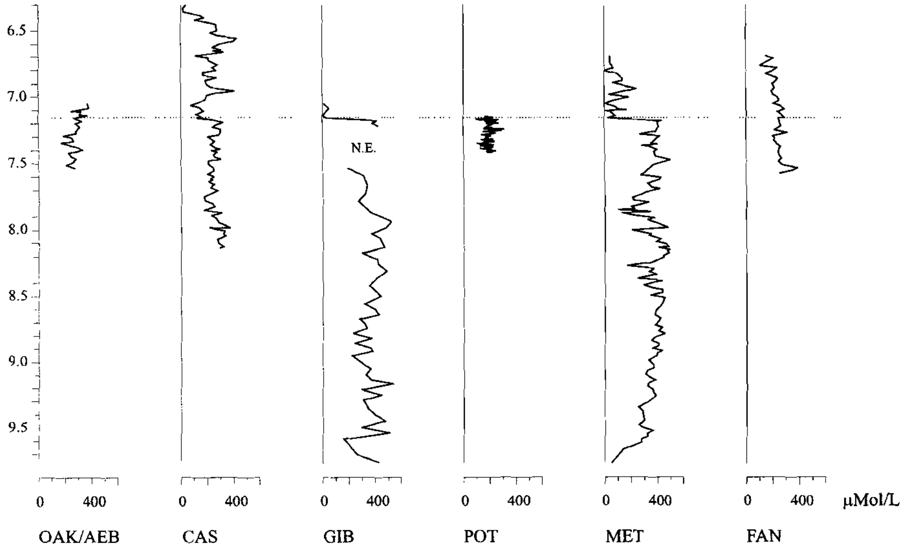
6.5
7.0
7.5
8.0
8.5
9.0
9.5
N.E.
0
400
µMol/L
OAK/AEB
CAS
GIB
POT
MET
FAN

3b

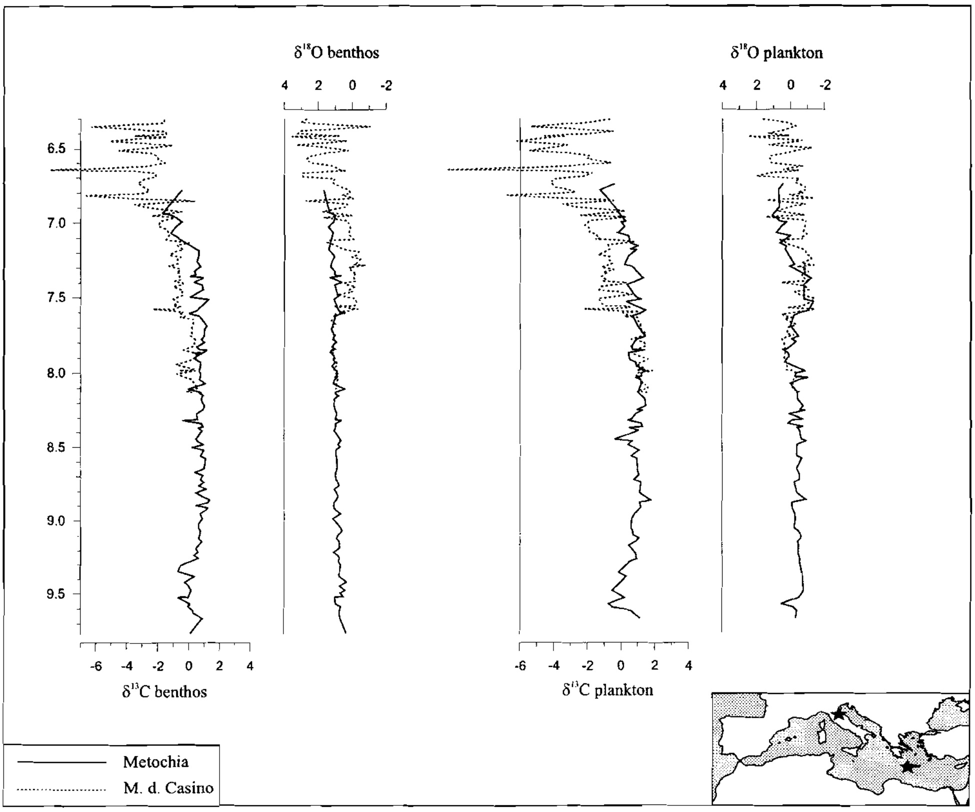

Figure 4. Benthic and planktonic stable isotope records of the Monte del Casino and Metochia sections (solid line=Metochia; dashed line=M. d. Casino). Carbonate of the planktonic species *G. obliquus* was analysed in both sections. Analyses of benthic carbonate were performed on *Cibicides* spp. fot Metochia and on multi-species samples for M. d. Casino.

A correlation is apparent between depth and oxygenation: the deepest sites are best ventilated. A second feature that is immediately evident, is the near-disappearance of oxygen in the deepwater sections of Gibliscemi and Metochia at 7.16 Ma. At Monte del Casino the drop in oxygenation is somewhat less drastic, and in the shallower sites of Potamidha and Faneromeni, and in Oued Akrech, it is not prominent at all.

Figure 4 gives plots of isotope records of planktonic and benthic foraminiferal carbonate for the Monte del Casino and Metochia sections. These sections were located at more or less similar water depths (around 1000 m) for most of the time span considered (until the uplift of Monte del Casino after 6.7 Ma, see discussion). Judging the near-identical isotope composition prior to 7.6 Ma, these sites were covered by very similar water masses. From 7.6 Ma onwards a clear offset is seen between both the carbon and oxygen isotope records of the two sections. Since at Monte del Casino the oxygen isotopes shift to lighter values, surface and bottom waters apparently became warmer, or the salinity decreased, or both. At the same time the carbon isotope values at Monte del Casino shift more strongly to lighter values than the gradual shift visible in the Metochia record. Long-term trends before and afterwards 7.6 Ma are similar, $\delta^{13}C$ becoming lighter and $\delta^{18}O$ heavier after 7.16 Ma.

Figure 5 gives plots of the redox elements manganese (Mn/Al) and vanadium (V/Al) for the Monte del Casino and Faneromeni sections. Of these sections, depositional depths differ some 700-800 m as based upon P/B ratios and faunal composition (see Chapter 7 of this thesis). The trends of the redox-sensitive elements are in agreement with the trends in oxygen reconstructions based on the oxygen transfer function. In Monte del Casino, a decrease in bottom-water oxygen content is evidenced in both proxies; around 7.16 Ma most clearly in the manganese record. Faneromeni is affected less by this event, but a decrease of bottom-water oxygen content around 7.16 Ma is reflected in the manganese record.

4. Discussion

4.1. Basin configuration and circulation

Between 9 and 6 Ma, the sections described in this paper were not situated at precisely the present locations, and the basin configuration was quite different from today (see Fig. 1a). The Corsica-Sardinia plate was probably more or less in its present position after 15 Ma, but the Tyrrhenian Sea had not opened or was opening (Van der Voo, 1993; Duermeijer et al., 1998). Crete and related elements of the Hellenic Arc were probably located more to the north. In the central Mediterranean area a barrier was developing between western and eastern basins (Italian landmass; Sicilian Sill).

It is evident that in the time slice considered here, the Mediterranean was already a semi-enclosed basin, connected to the Atlantic Ocean with gateways that became increasingly confined during the late Miocene. If the Mediterranean has been acting as a concentration basin since its semi-enclosure, an estuarine circulation is not probable (see a.o. Lacombe and Tchernia, 1972; Tchernia, 1980; Vergnaud-Grazzini, 1983). Especially in the context of late Miocene events, Sonnenfeld (1984) convincingly argued that an anti-estuarine circulation must be regarded as a prerequisite for evaporite deposition, as an estuarine circulation would flush the basin. A gradual trend towards heavier oxygen isotope compositions in the Messinian (Fig. 4) indicates increasing bottom water salinity. An estuarine circulation would further lead to upwelling in the east, a feature that would lead to notable high productivity deposits, for which we see no indications. We are therefore inclined to accept an anti-estuarine circulation type as starting point of our discussion.

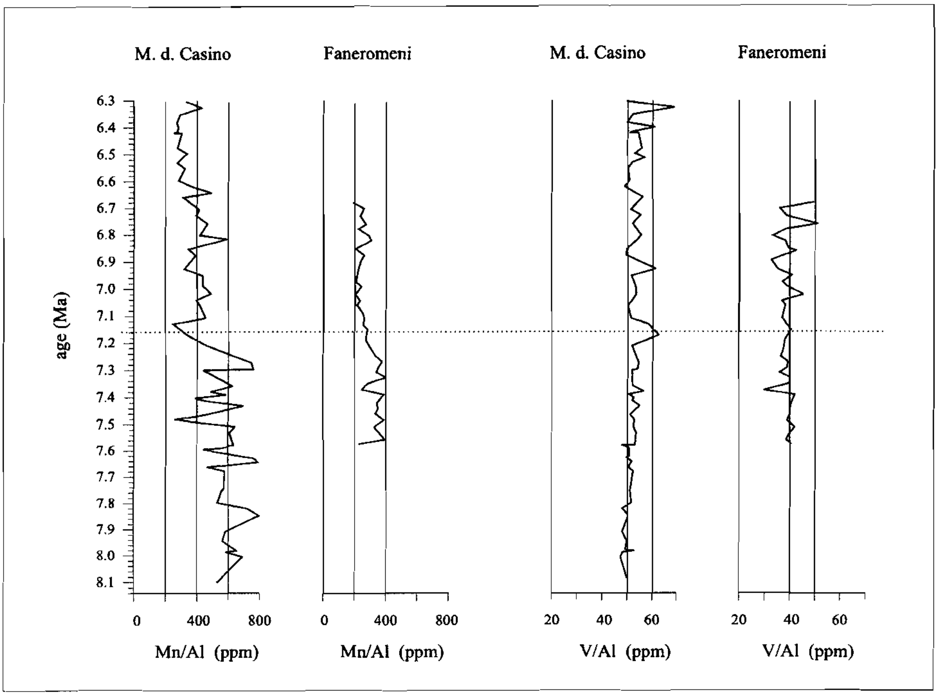

Figure 5. Plots of the redox-sensitive elements Mn and V for the Monte del Casino and Metochia sections. Elements concentrations are corrected for terrestrial input by calculating the ratio with aluminium.

4.2. Simple two-layered model of anti-estuarine circulation

In its simplest form, an anti-estuarine circulation in the late Miocene Mediterranean would consist of a surface water mass flowing from the Atlantic eastwards into the basin, and an outflowing deep water mass flowing to the west. In this simple two-layered system, the inflowing (Atlantic) surface water mass would gain weight (salinity) by evaporation, sink in the eastern Mediterranean, and the bottom water mass transported from east to west would carry Mediterranean characteristics into the Atlantic. In analogy with today, the driving force of this circulation would be the net buoyancy loss due to evaporation. Amendments to this simple representation of paleo-circulation can be made by taking Coriolis forces into account, which lead to cyclonic gyres in surface water circulation. This model is probably an oversimplification, as the phenomena we expect to encounter in that case do not fit our data.

The sections considered here were deposited in intermediate and deeper water in different regions. Although the sites are far apart, we probably may regard them as two groups, one from the central and one from the eastern Mediterranean, although we acknowledge that all types of local influences may have blurred the picture somewhat.

If we compare the oxygenation curves (Fig. 3), it is immediately evident that the typical pattern expected in a simple two layered circulation system, i.e. gradually declining oxygen concentration towards deeper waters, did not prevail. Instead, we find lower concentrations of oxygen in intermediate waters, and higher oxygen concentrations at the deeper sites. Accepting this immediately renders a two-layered model inadequate, and ventilation of deeper waters imperative. The oxygen concentration in the deep water sites is close to recent values. On the average the reconstructed values approach 6-7 ml/L or 300 µMol/L, and higher for the major parts of Monte Gibliscemi and Metochia. The latter values are very high, probably due to the fact that the transfer function is necessarily not very accurate in the high range of oxygen values. This is caused by the fact that in the modern data set used to construct the transfer function, such high values did not occur. Yet, we are inclined to accept the reconstruction as indicating full ventilation and maximal oxygen concentrations. It then necessarily follows that formation of young, oxygen-rich deep waters was already going on in the Late Miocene, just as today.

4.3. Three-layered model: analogue to present circulation

In analogy with present circulation patterns, the mid-northern part of the basin (proto-Adria and Ionian) apparently experienced surficial inflow (cyclonic gyre). The more or less semi-enclosed and shallow parts in the north are potential sites for the formation of deep waters. Under the warm and arid climate (see Chamley et al., 1986) excess evaporation could have led to sinking of heavy waters, and cause deep water formation over the area that is now occupied by Italy and the Adriatic. An oxygen-rich plume of young deep water would pass by Sicily (Monte Gibliscemi; assuming a central Mediterranean position of this site), and could explain the near absence of infauna and the high bottom-water oxygen levels in deep waters near Sicily. Just as today, part of this O_2-rich deep water plume would flow into the eastern Mediterranean, passing by Metochia. In the very east, the plume could have combined with proto-Levantine interme-diate waters to become the Mediterranean intermediate water mass flowing towards the Atlantic, losing its new deep water characteristics on the way. This picture is summarised in Fig. 6. At this stage it is important to note that planktonic foraminifera remained present, even just prior to the formation of evaporites. In a simple two-

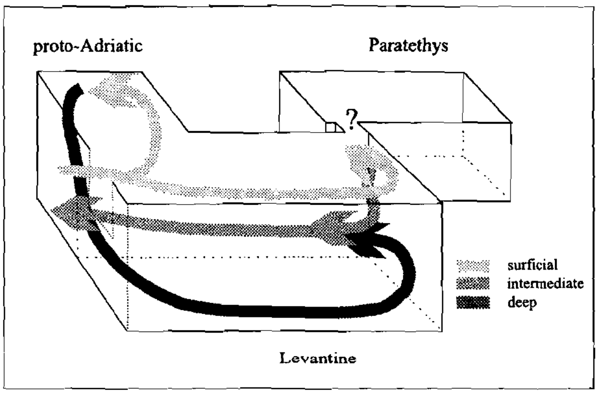

Figure 6. Schematic reconstruction of late Miocene circulation in the central/eastern Mediterranean basin.

layered system this would be impossible since surface water salinities would necessarily be very high (Rohling et al., 1998). In the Mediterranean this was certainly not the case, which supports our notion of a three-layered model. In this model the waters reaching the eastern Mediterranean would have been saline through evaporation and have sunk to intermediate depth to form the proto-Levantine intermediate water. Between deep and intermediate water masses, salt fractionation may have occurred, steadily rendering the deepest waters more saline without affecting the surface water layers or causing a planktic desert.

The moment that either the ambient flow of water masses was obstructed, or the deep water formation ceased, the characteristics of deep water masses, as evidenced by the benthic associations and geochemical proxies, would change. Circulation would slow down, water masses would age and the oxygen content of the deep water mass would decrease. This is what may have happened at 7.16 Ma. Shallower sites, located in the intermediate water mass, were affected less, implying that some surficial inflow, and the formation of intermediate waters, remained more or less intact.

4.4. Deeper sites in more detail

The highest oxygen concentrations were calculated from the transfer function For Metochia and Monte Gibliscemi. Deviating low oxygen levels at the basis of the Metochia section may be related to the fact that the site was located in a deepening basin: the basis of the section consists of shallow water deposits (Postma et al., 1993). Overall oxygen levels were lower at Monte del Casino than at the two deepest sites. Either the site was not located in a trajectory of deep-water formation, or its history as remnant of a foredeep influenced the local paleoenvironmental conditions: the lowermost sedimentary cycles of the Monte del Casino section contain numerous small turbidites (see the more detailed lithology in Kouwenhoven et al., 1999; Van der Meulen et al., 1999). Decreasing oxygen contents at Metochia around 8.3 Ma may also be due to local tectonics (see Seidenkrantz et al., in press). The event correlates with increased influx of shallow and epiphytic species, here considered to be of allochthonous origin, and not accounted for in the oxygen calculations.

Around 7.9 Ma the oxygenation diminished by 150-200 μMol/L in all three deeper water sites (Fig. 3b). Return to earlier oxygenation levels was fast in Metochia, slow in Gibliscemi, and did not occur at all in Monte del Casino. We tentatively attribute these oxygenation changes to vertical movements at the western portals to the Atlantic, or to regional circulation changes due to opening of the Tyrrhenian Basin.

Before 7.6 Ma the isotope records of Metochia and Monte del Casino are similar, but after 7.6 Ma they show an offset (Fig.4). This offset occurred simultaneously in the $\delta^{13}C$ and the $\delta^{18}O$ of plankton and benthos. The effects of diagenetic alteration are more apparent in the isotope records of Monte del Casino, especially after 7.16 Ma where preservation is worse, but this is probably not the cause for the offset. The isotope patterns indicate that the waters in the proto-Adriatic became fresher and/or warmer, and judging the carbon isotope signal, more aged as well, than the eastern

Mediterranean waters. The data suggest that deep-water production slowed, and that older and less saline or warmer waters passed the central Mediterranean sites. This phenomenon could well be related to the emerging Italian landmass and Alpine area, which now started to drain into the proto-Adriatic. Whatever the cause, the consequence of diminishing deep-water formation should be decreasing ventilation of the deeper waters. Part of the Gibliscemi record is not exposed, but around 7.6 Ma the oxygen levels were still low. Comparison with the Metochia record suggests that whatever happened at 7.6 Ma was a central Mediterranean event, and did not drastically affect the general deeper water circulation.

At 7.16 Ma the oxygen content of the deep-water sites dropped, approaching very low values. At the intermediate sites and at Oued Akrech no such effect is apparent in the oxygen reconstructions. This immediately suggests that the rate of deep water formation changed considerably. However, the isotopes do not display drastic changes at this point, suggesting that deep-water formation could not have been affected by a change in climate or precipitation. An alternative cause is a steep increase in bioproduction, which could have resulted in increased oxygen consumption; for this we have no evidence either (see Seidenkrantz et al., in press). The data suggests (see also discussions in Kouwenhoven et al., 1999, and Seidenkrantz et al., in press) that the deep-water outflow was substantially blocked due to constriction of the Rifian portal to the Atlantic (Krijgsman et al., 1999a). As a result the deeper parts of the basin were no longer adequately flushed. Stable oxygen isotopes and faunal compositions indicate that from that time onwards deep-water salinity started to increase. Consequently, the deep water mass may have become inert, and once a critical threshold value was surpassed, the intermediate waters became detached from the deeper waters. The interface between intermediate and deep water masses may have served as a fractionation level via which salinity of the deeper waters steadily increased. Deeper water sites became increasingly populated by stress tolerant taxa and Monte Gibliscemi, the deepest central Mediterranean site, rapidly developed into a benthic desert (see Chapter 7 of this thesis).

4.5. Intermediate sites in more detail

Unfortunately, no data are available for the older Tortonian part of sections Faneromeni and Potamidha. We therefore have no evidence for changes in intermediate water properties before 7.6-7.4 Ma. Mean reconstructed oxygen levels around the Tortonian/Messinian boundary are considerably lower than in the deep waters, which is consistent with a three-layered model.

The 7.16 Ma collapse of oxygenation that is so evident in the deeper sections is hardly seen in the oxygen reconstructions for these intermediate-water sites. The manganese record of Faneromeni supports decreasing oxygenation. In combination the fauna record and the oxygen reconstruction suggest that the intermediate water layers were less affected by the events at 7.16 Ma. The onset of the Messinian salinity crisis proceeded gradually, the salinity increase starting in the deepest parts of the basin.

Later, together with increasing salinities of the deeper waters, the interface between the deep and intermediate waters was probably raised. Evidence for this is found in the Monte del Casino section, that was uplifted to intermediate depth (~600m) after 6.7 Ma (Van der Meulen et al., in press; Kouwenhoven et al., 1999). Here the reconstructed oxygenation of bottom waters returned to pre-7.16 Ma values until 6.6-6.5 Ma. A considerable decrease in oxygen contents then coincided with the development of a benthic fauna tolerating increased salinity and oxygen depletion, and the benthic oxygen isotopes shifted to heavy values (this thesis, Chapters 5 and 7).

5. Conclusions

Employing a combination of tools we constructed a tentative model of late Miocene Mediterranean circulation patterns. Application of an oxygen transfer function to a number of intermediate and deep waters sites led to a reconstruction of ventilation through time. The reconstructed oxygenation records from the central and eastern Mediterranean are in support of a three-layered anti-estuarine circulation model. Is seems likely that deep-water production took place in the proto-Adriatic but diminished somewhat from 7.6 Ma onwards. At 7.16 Ma deep water ventilation decreased drastically. As there is no evidence of decreased deep-water formation or increased productivity, it is likely that obstruction of deep-water outflow played an important role. It is concluded that due to the constriction of the Atlantic portals the residence time of deep waters increased and the deep water mass became increasingly saline. At some stage, the combination of the return flow and deep-water formation were no longer able to flush the deeper parts of the basin. This became ill aerated, and at a later stage too saline to allow benthic life. Sites at intermediate depths were at that time still ventilated by the intermediate water mass flowing westward.

Chapter 7

Late Miocene benthic foraminifera

Assemblage structure and proxy value of late Miocene benthic foraminifera

Abstract

In this paper we compare late Miocene benthic foraminiferal associations from five Mediterranean sections and one section located at the Atlantic side of the Rifian corridor. For all sections, census counts of benthic foraminifera were available in the 125 μm fraction. Stable oxygen and carbon isotopes, and analyses of the redox-sensitive elements manganese and vanadium were available for part of the sections. These proxies were used to constrain paleoecological interpretations of species abundance patterns. Additionally, quantitative reconstructions of bottom-water oxygenation were employed. These were derived from a recently developed transfer function, that is based on the percentages of oxyphilic species in Recent benthic assemblages. Similarities and dissimilarities in faunal development of the sections, that were deposited in different (sub-)basins and water depths, are discussed in relation to well-documented environmental changes. The proxy value of Miocene benthic taxa is discussed in some detail, in particular their use in reconstructing oxygenation, paleodepth and (to a lesser extent) organic flux. Finally, we discuss a microhabitat model for late Miocene benthic foraminifera.

1. Introduction

Over the past decades, attempts to reconstruct the progression of the Messinian Salinity Crisis resulted in numerous papers (e.g. Bandy, 1973; Hsü et al., 1973; Ryan, 1973; Ryan et al., 1974; Vergnaud-Grazzini et al., 1977, 1983; Adams, 1976; Benson, 1976; Berggren and Haq, 1976; Cita, 1976; Ruggieri and Sprovieri, 1976; Adams et al., 1977, 1983; Cita and Ryan, 1979; Vergnaud-Grazzini, 1983; McKenzie et al., 1979/1980; Hodell et al., 1986, 1989, 1994; Müller and Hsü, 1987; Weijermars, 1988; Glaçon et al., 1990; Benson and Rakic El Bied, 1991; Kastens, 1992; Sierro et al., 1993; 1997; Hilgen et al., 1995; Krijgsman et al., 1995, 1997, 1999a, b; Sprovieri et al., 1996; Vai, 1997; Bertini et al., 1998; Foresi et al., 1998). From these it is apparent that the timing of the complex processes leading to formation of evaporites, and presumably to the total desiccation of the Mediterranean, has been a central issue. Since the original discovery and initial publications in the DSDP reports (DSDP Leg 13: Scientific Staff, 1970) huge progress has been made in this field, recently leading to detailed dating of the onset of actual evaporate deposition (Krijgsman et al., 1999b).

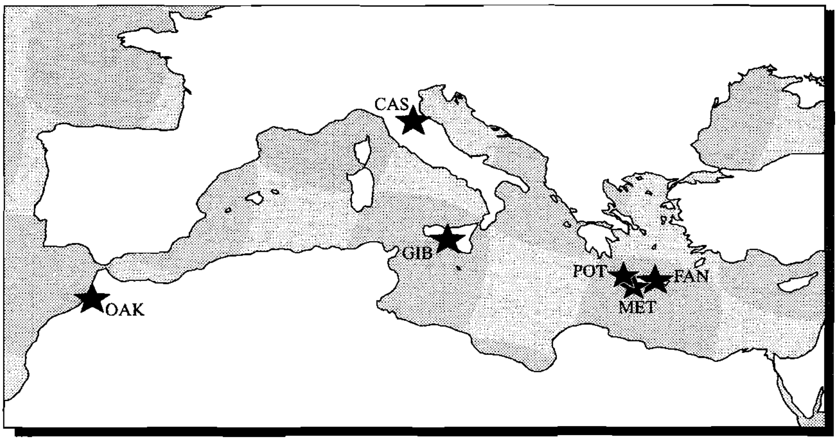

Figure 1. Locations of the sections discussed in this paper. CAS=Monte del Casino; FAN= Faneromeni; GIB=Monte Gibliscemi; MET=Metochia; OAK=Oued Akrech; POT=Potamidha

Although we have a reasonably accurate picture of the chronology by now, many questions concerning the processes acting during this relatively short time span remain unanswered. Among the proxies available to reconstruct these processes, benthic foraminifera play a relatively important role. Their proxy value for bottom-water oxygenation was recently summarised by Gooday and Rathburn (1999), Jorissen (1999), Kaiho (1999) and Van der Zwaan et al (1999). Consequently, they are also good proxies of any process dependent on oxygenation. Variation in paleodepth for instance, can be reflected in benthic assemblages because of co-variation with oxygen contents (Bandy and Chierici, 1966; Van der Zwaan et al., 1990; Van der Zwaan et al., 1999). A second parameter on which benthic assemblages heavily depend is the flux of organic matter (e.g. Berger and Herguera, 1992; Jorissen et al., 1992; Sen Gupta and Machain Castillo, 1993; Gooday et al., 1992; Den Dulk et al., 1998; De Stigter et al., 1998; Van der Zwaan et al., 1999). Flux is taken by many to reflect the amount of available food. Changes in paleobathymetry may in fact be caused by changes in organic flux, since with increasing depth the organic flux decreases (e.g. Suess, 1980; Berger and Diester-Haass, 1988). This indicates that the proxy value of benthic foraminifera is potentially large, but in practice not so easy to apply.

The Messinian is ideal to further constrain the proxy value of benthic foraminifera, since in this period large environmental contrasts existed in many variables. Nevertheless, the number of late Miocene records of benthic foraminifera is surprisingly small, considering the amount of literature devoted to the Messinian. Precise dating of a number of these records proved to be difficult, due to the absence of stratigraphic markers and/or reliable magnetostratigraphy (e.g. Berggren and Haq, 1976; Van der Zwaan, 1982, 1983; Troelstra et al., 1980; Poignant and Moissette, 1992; Van de Poel, 1992; Barbieri, 1998). However, the information presented is indispensible to enlarge our understanding of benthic foraminiferal paleoecology.

The main body of this paper is composed of observations in a number of sections from intermediate to deep water sites, covering the late Tortonian and straddling the Tortonian/Messinian boundary. Our objective is to construct a coherent model, describing the faunal response to environmental change in some detail. The onset of the Messinian salinity crisis started already during the earliest Messinian, as a continuous trend towards more stressed environments. The sections we have at our disposal are well dated and contain information about these long-term environmental changes. The data on benthic foraminifera will be employed in evaluating the development of assemblages towards the salinity crisis. One of the aims is, to separate the effects of different environmental parameters. We strive after a detailed paleoecological interpretation, making maximal use of the information contained in the assemblages when comparing the distribution patterns with a number of other proxies. As a second step we will revert to comparing the outcome with recent studies on the ecology of benthic foraminifera. In this way, potential differences between late Miocene and Recent assemblage structures are not *a priori* blurred and we can use both sources of evidence (modern and fossil) independently.

2. Material and Methods

2.1. The sections

We have census counts of benthic foraminifera at our disposal from five Mediterranean clay/marl sequences, most from rather deep-water environments. One section is located in Morocco on the Atlantic side of the Rifian Corridor (Fig. 1). The taxonomic concepts applied to these data sets are standardised to a high degree, and counts were performed on the 125 - 595 μm fraction in all cases. Age models are

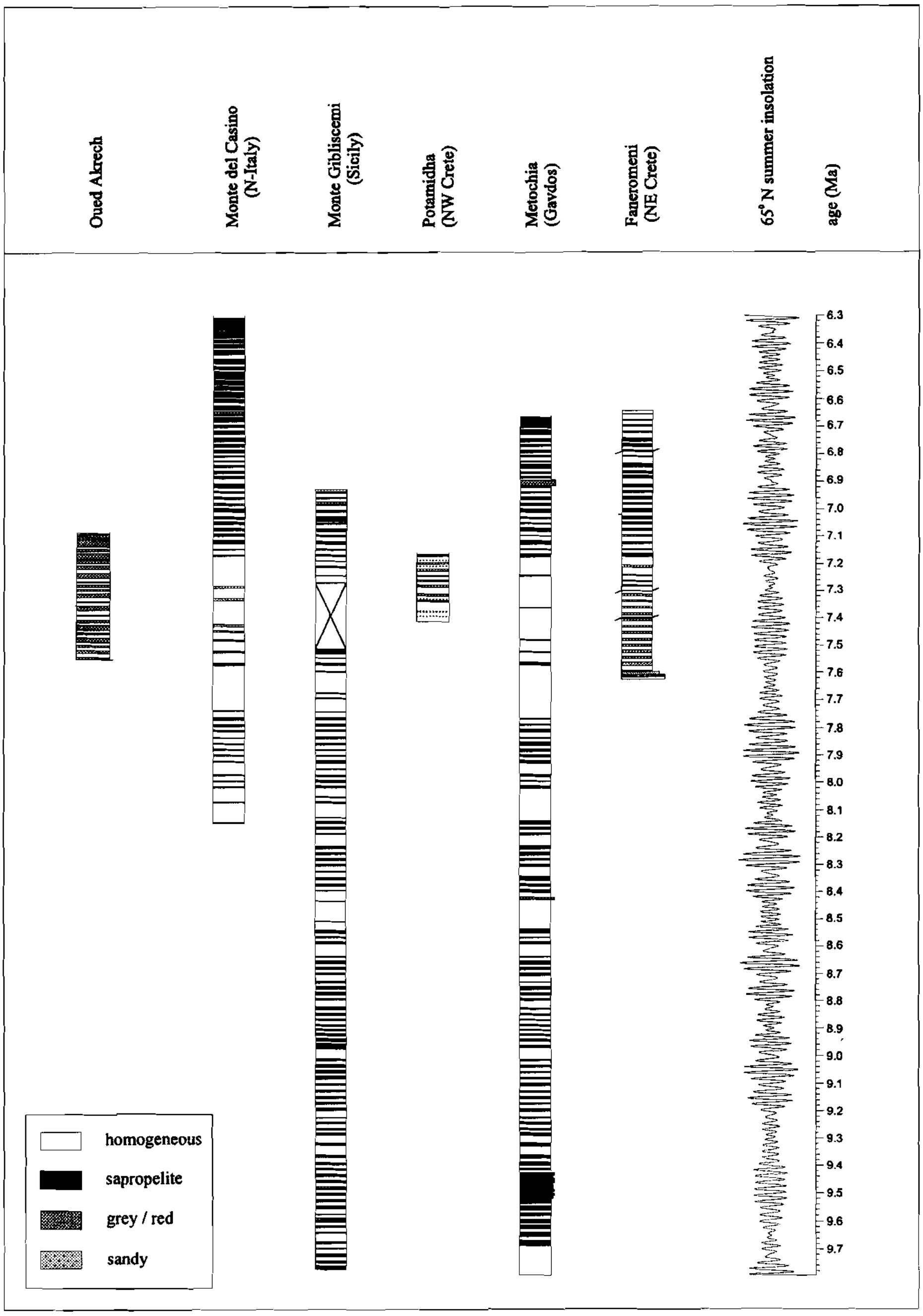

Figure 1. Age models of the sections, with the 65⁰ Northern Hemisphere summer insolation curve

derived from Langereis et al. (1984), Hilgen et al. (1995), Krijgsman et al. (1994, 1995, 1997), and Meijer (1998). All sections are correlated cyclostra tigraphically (Fig. 2). On average we counted one sample per homogeneous interval, which gives an approximate resolution of one sample per 20 ky. In part of the sections, samples derived from sapropelitic beds were counted as well. Details about sample handling and summaries of relevant data on lithology can be found in publications listed below:

Section Faneromeni is located on NE Crete, Greece. Element analysis (ICP-AES) of a detailed transect over three sedimentary cycles containing sapropels and homogeneous sediments was published in Nijenhuis et al. (1996). Data on planktonic foraminifera was published in Calieri (1996). Census counts of benthic foraminifera have not been published before.

Section Metochia is located on Gavdos, a small island near Crete, Greece. Element analysis (ICP-AES) of a detailed transect over three sedimentary cycles containing sapropels and homogeneous levels was published in Schenau et al., 1998. Planktonic foraminiferal assemblages have been studied and the data will be published in the near future. Details pertaining to the sedimentology of the section were described by Postma et al. (1993). Census counts of benthic foraminifera and stable isotope results of planktonic and benthic carbonate can be found in Seidenkrantz et al. (in press).

Section Potamida is located in the Khania province, NW Crete, Greece. The section was subject of detailed study in the framework of the Accuracy in Time project (Drooger et al., 1979). All possible fauna groups of this section were quantified in detail, in combination with magnetostratigraphy and sedimentology. Data on planktonic foraminifera were published in Zachariasse (1979). Census counts of benthic foraminifera can be found in Wonders and Van der Zwaan (1979). Both plankton and benthos records are characterized by a very detailed sample resolution.

Section Monte Gibliscemi is located in the southern part of Sicily, Italy. Planktonic foraminiferal assemblages have been quantified for the Serravallian and early Tortonian part of the section (Hilgen et al., in press; Turco et al., subm.). No plankton census counts are available for the latest Tortonian/Messinian part of the section. Sample resolution for benthic foraminifera in this section is one sample per two cycles, i.e. a resolution of approximately 40 ky. These data have not been published earlier.

Section Monte del Casino is located in northern Italy. Tephra-stratigraphy was published by Laurenzi et al. (1997). Negri and Vigliotti (1997) and Negri et al. (1999) published data on calcareous nannofossils and magnetostratigraphy. Integrated bio-, magneto-, tephra- and cyclostratigraphy was performed by Krijgsman et al. (1997). Planktonic foraminiferal counts will be published by Calieri et al. (in prep.). Data on stable isotopes, redox-sensitive elements and census counts of benthic foraminifera can be found in Kouwenhoven et al. (1999).

Section Oued Akrech is located in the Bou Regreg Valley, NW Morocco. In this section no sapropels were deposited, but an alternation of reddish and white red layers (fresh sediment). Meijer (1998) performed magnetostratigraphy, and assumes that the red layers are correlative to sapropels within the Mediterranean. Census counts of

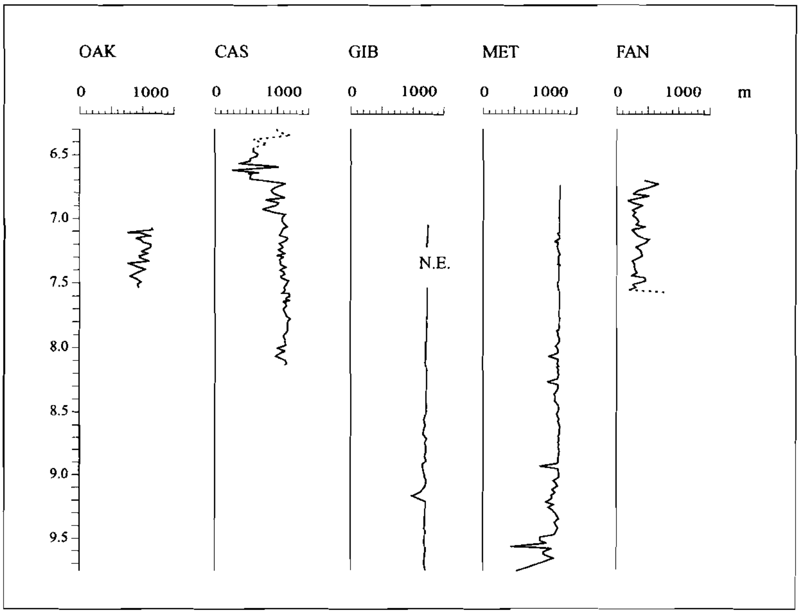

Figure 3. Paleobathymetry of the sections, calculated from P/B ratios (Van der Zwaan et al., 1990)

benthic foraminifera from a different set of samples were published earlier by Barbieri (1998). The data on benthic foraminiferal distribution patterns as discussed here are based on a different and more detailed set of samples.

2.2. Benthic foraminifera

In order to determine the assemblage structures of benthic foraminifera in the sections, we used the census counts and the Shannon diversity index. Hierarchical clustering (standard SPSS software) was employed in order to give the data a statistical background. We used a standard clustering technique for all sections discussed, in order to prevent bias introduced by differing procedures. In the clustering procedure, ill-defined remainder groups were omitted from the data sets. Infrequent taxa (below 3 - 5% in any one sample) were also eliminated. No new closed sum was calculated, in order to avoid overrepresentation of the species that remained in the statistical procedure. The resulting robust, representative data set was imported into cluster analysis, employing Pearson correlation, within-groups linkage.

Environmental parameters based on the foraminiferal counts were constrained. Paleobathymetrical change can be quantified using planktonic and benthic foraminiferal ratios as discussed in Van der Zwaan et al. (1990). For all samples such calculations were performed. Since according to Van der Zwaan et al. (1990) infaunal taxa are not primarily participating in the consumption of organic flux from the mixed layer, these have to be omitted from the closed sum in calculating paleodepth.

Therefore we corrected the P/B ratios for infauna. Further, we calculated the oxygen content at the sediment-water interface, using a transfer function recently developed by Van der Zwaan et al. (subm.). This regression predicts oxygen contents according to the formula

$$[O2\ (\mu Mol/L) = 7.9206 + 5.95 * \ \%\ \text{oxyphilic taxa}]$$

The Miocene taxa considered oxyphilic are listed in Chapter 5 of this thesis. We checked the outcome, if possible, against data from sediment logs, which give supporting information about sediment colour and the presence/absence of bioturbation. Where available, we checked the oxygen reconstructions against geochemical proxies.

2.3. Geochemistry

Stable isotope measurements of planktonic and benthic carbonate were available for the Metochia and Monte del Casino sections. For the Monte del Casino and Faneromeni sections, analyses (ICP-AES) of the redox-sensitive elements manganese and vanadium were performed. The element concentrations were normalised to the aluminium content of the samples in order to correct for terrestrial input (see Nijenhuis et al., 1996). Correlations (Pearson) of single species with redox-sensitive elements were carried out for the Monte del Casino and Faneromeni sections. Occurrences of single species and groups of species were compared with these geochemical parameters.

3. Results

The six sections for which census counts of benthic foraminifera were available all straddle the Tortonian/Messinian boundary and cover at least the earliest part of the Messinian. All sections contain the level at approximately 7.16 Ma where simultaneous environmental changes are reported from deeper-water sections. None of the sections contains the level where evaporite deposition began (5.96 Ma: Krijgsman et al., 1999b).

3.1. Paleobathymetry

Paleobathymetry of the sections was estimated by calculation of paleodepths from P/B ratios (Fig. 3). Only homogeneous levels are included in these calculations, as sapropelitic (dysoxic) conditions influence depth reconstructions (see Van der Zwaan et al., 1990). Given the fact that oxygenation decreased in the deeper Mediterranean

---

Figure 4a-f (next pages). Dendrograms of the sections, with relative frequencies per cluster and the bottom-water oxygen contents, reconstructed with the transfer function (Van der Zwaan et al., subm.)

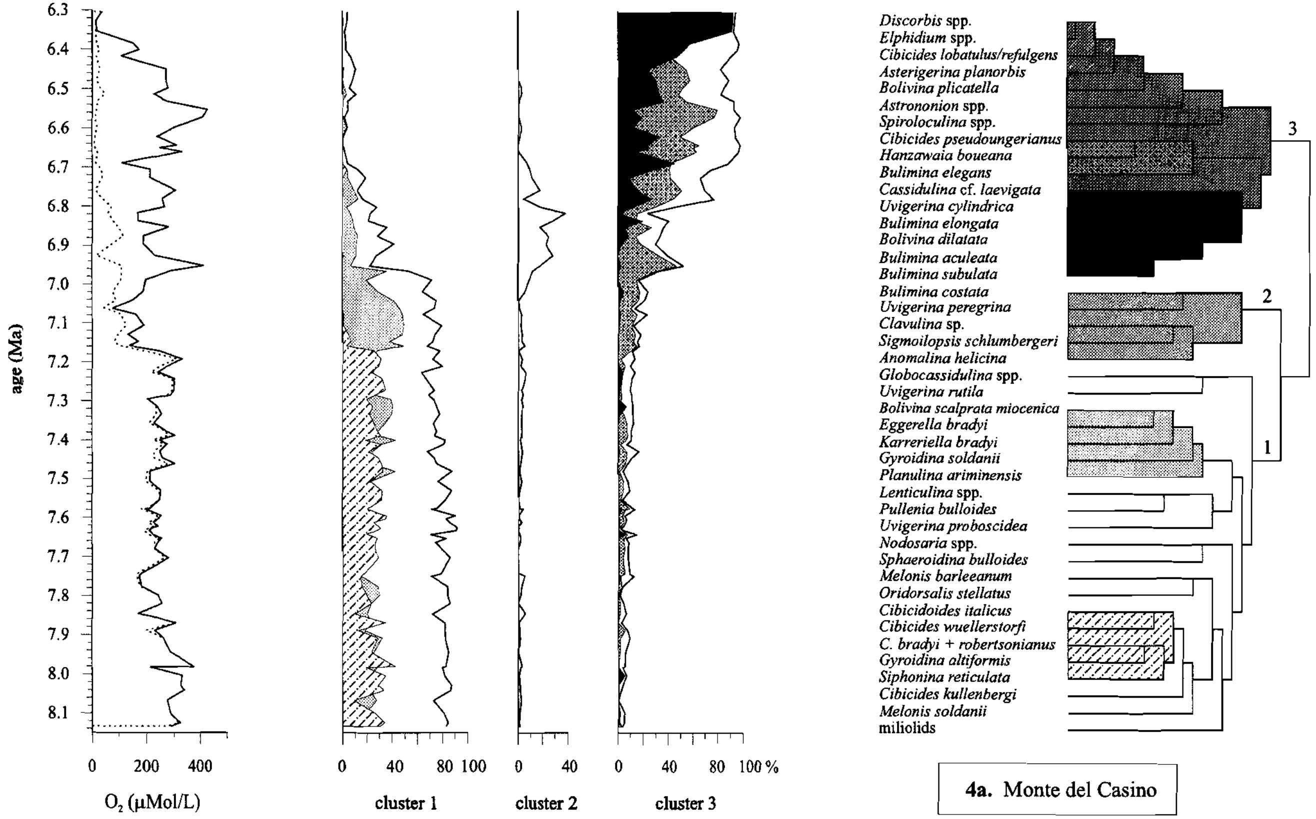

4a. Monte del Casino

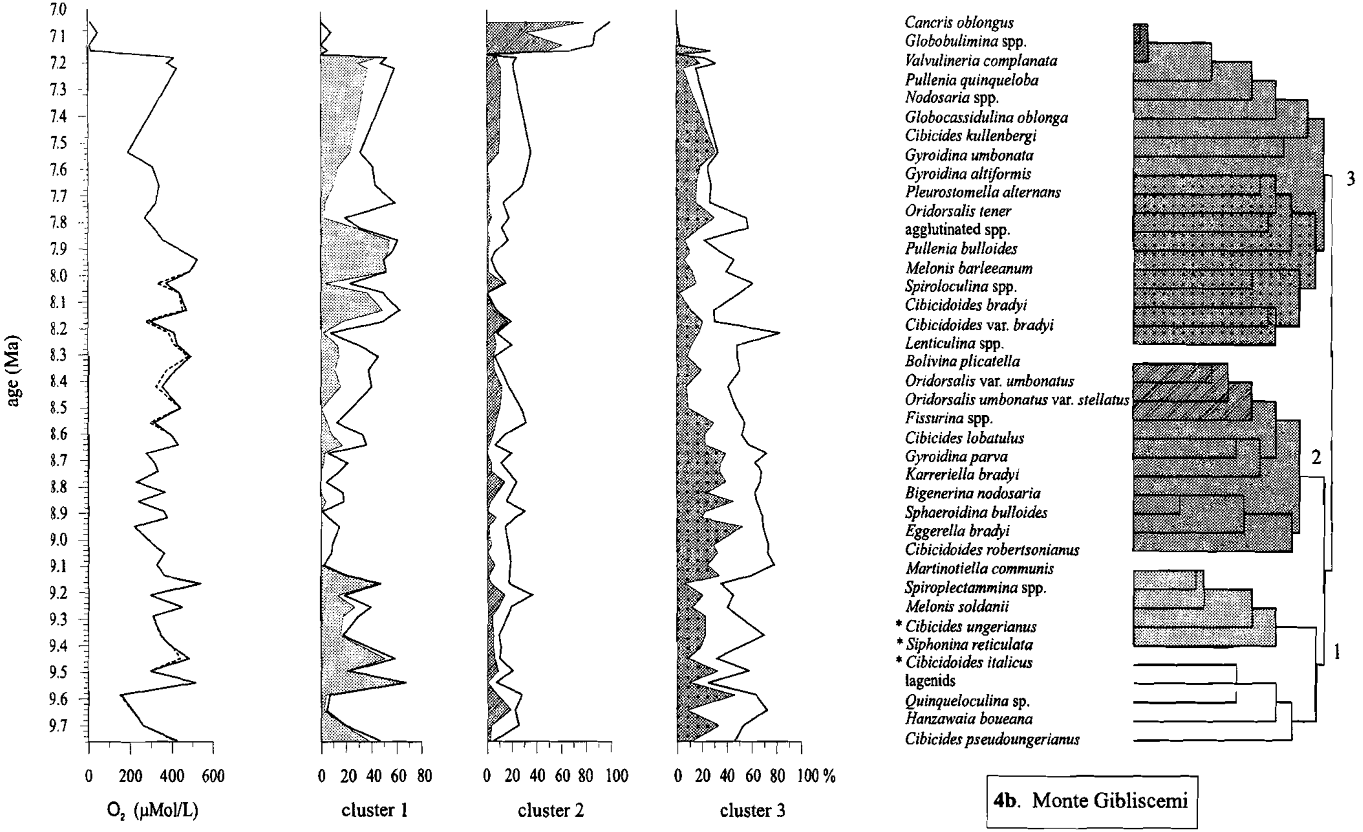

4b. Monte Gibliscemi

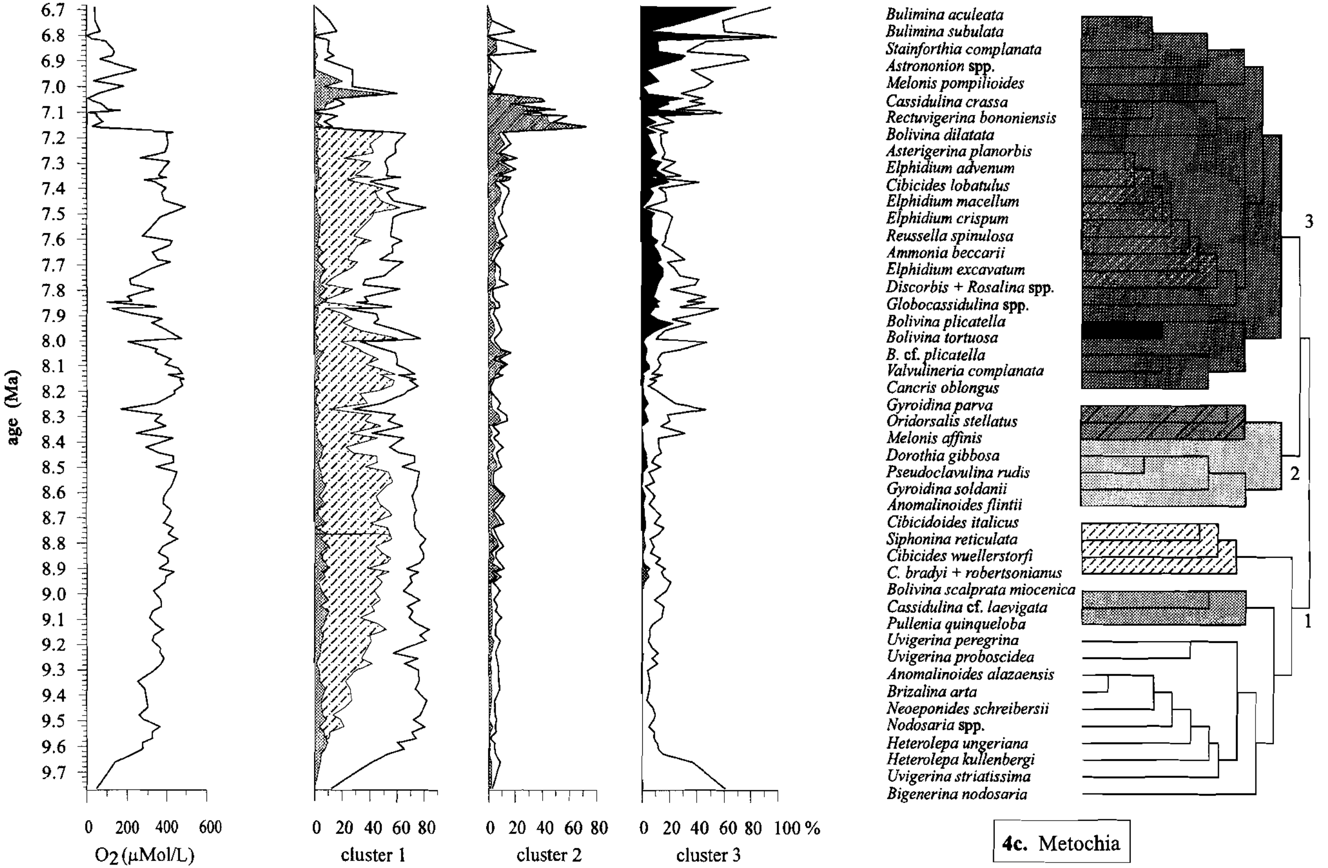
age (Ma)
6.7
6.8
6.9
7.0
7.1
7.2
7.3
7.4
7.5
7.6
7.7
7.8
7.9
8.0
8.1
8.2
8.3
8.4
8.5
8.6
8.7
8.8
8.9
9.0
9.1
9.2
9.3
9.4
9.5
9.6
9.7
0 200 400 600
O2 (μMol/L)
0 20 40 60 80
cluster 1
0 20 40 60 80
cluster 2
0 20 40 60 80 100 %
cluster 3
Bulimina aculeata
Bulimina subulata
Stainforthia complanata
Astrononion spp.
Melonis pompilioides
Cassidulina crassa
Rectuvigerina bononiensis
Bolivina dilatata
Asterigerina planorbis
Elphidium advenum
Cibicides lobatulus
Elphidium macellum
Elphidium crispum
Reussella spinulosa
Ammonia beccarii
Elphidium excavatum
Discorbis + Rosalina spp.
Globocassidulina spp.
Bolivina plicatella
Bolivina tortuosa
B. cf. plicatella
Valvulineria complanata
Cancris oblongus
Gyroidina parva
Oridorsalis stellatus
Melonis affinis
Dorothia gibbosa
Pseudoclavulina rudis
Gyroidina soldanii
Anomalinoides flintii
Cibicidoides italicus
Siphonina reticulata
Cibicides wuellerstorfi
C. bradyi + robertsonianus
Bolivina scalprata miocenica
Cassidulina cf. laevigata
Pullenia quinqueloba
Uvigerina peregrina
Uvigerina proboscidea
Anomalinoides alazaensis
Brizalina arta
Neoeponides schreibersii
Nodosaria spp.
Heterolepa ungeriana
Heterolepa kullenbergi
Uvigerina striatissima
Bigenerina nodosaria
3
2
1
4c. Metochia

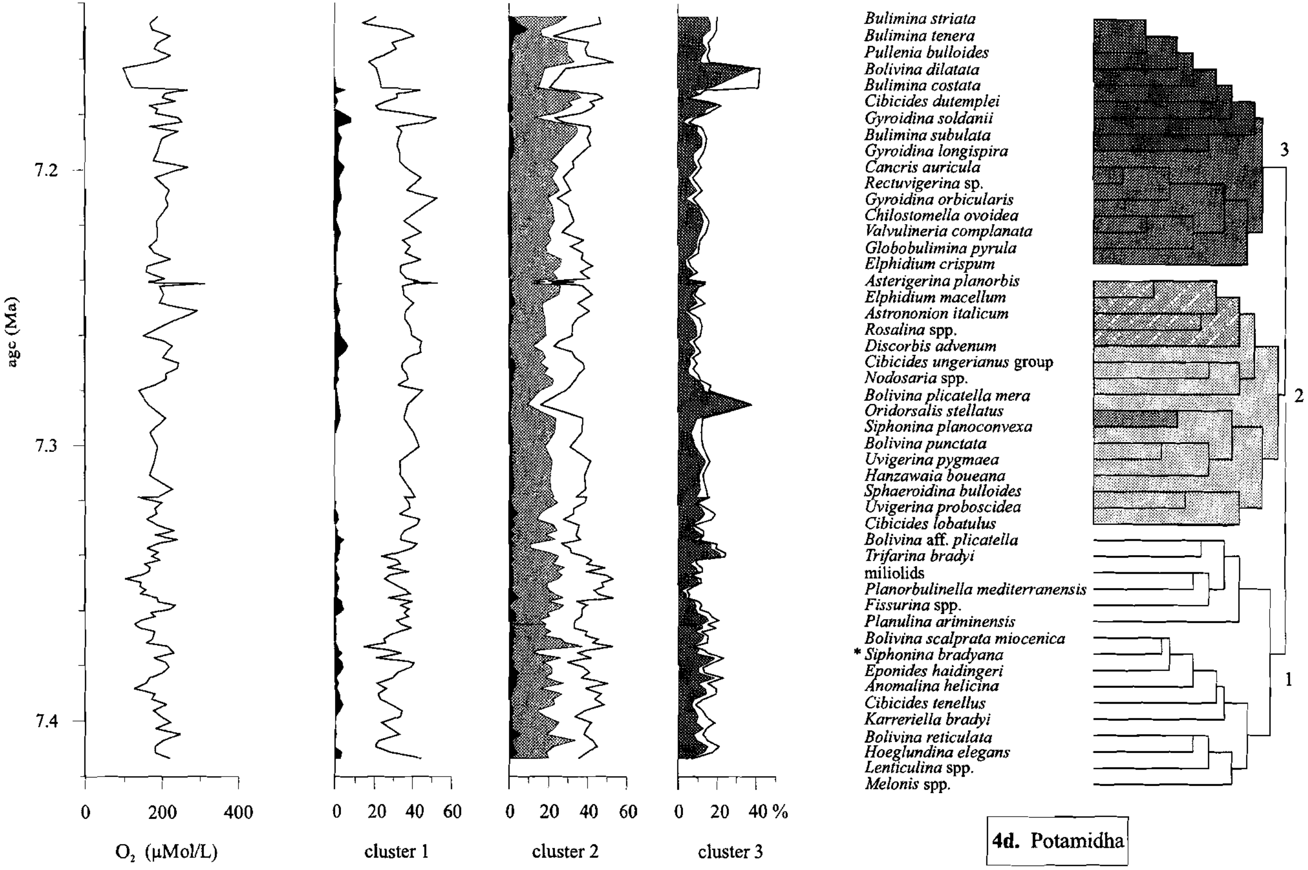
age (Ma)
7.2
7.3
7.4
0
200
400
O₂ (µMol/L)
0
20
40
60
cluster 1
0
20
40
60
cluster 2
0
20
40 %
cluster 3
Bulimina striata
Bulimina tenera
Pullenia bulloides
Bolivina dilatata
Bulimina costata
Cibicides dutemplei
Gyroidina soldanii
Bulimina subulata
Gyroidina longispira
Cancris auricula
Rectuvigerina sp.
Gyroidina orbicularis
Chilostomella ovoidea
Valvulineria complanata
Globobulimina pyrula
Elphidium crispum
Asterigerina planorbis
Elphidium macellum
Astrononion italicum
Rosalina spp.
Discorbis advenum
Cibicides ungerianus group
Nodosaria spp.
Bolivina plicatella mera
Oridorsalis stellatus
Siphonina planoconvexa
Bolivina punctata
Uvigerina pygmaea
Hanzawaia boueana
Sphaeroidina bulloides
Uvigerina proboscidea
Cibicides lobatulus
Bolivina aff. plicatella
Trifarina bradyi
miliolids
Planorbulinella mediterranensis
Fissurina spp.
Planulina ariminensis
Bolivina scalprata miocenica
* Siphonina bradyana
Eponides haidingeri
Anomalina helicina
Cibicides tenellus
Karreriella bradyi
Bolivina reticulata
Hoeglundina elegans
Lenticulina spp.
Melonis spp.
3
2
1
4d. Potamidha

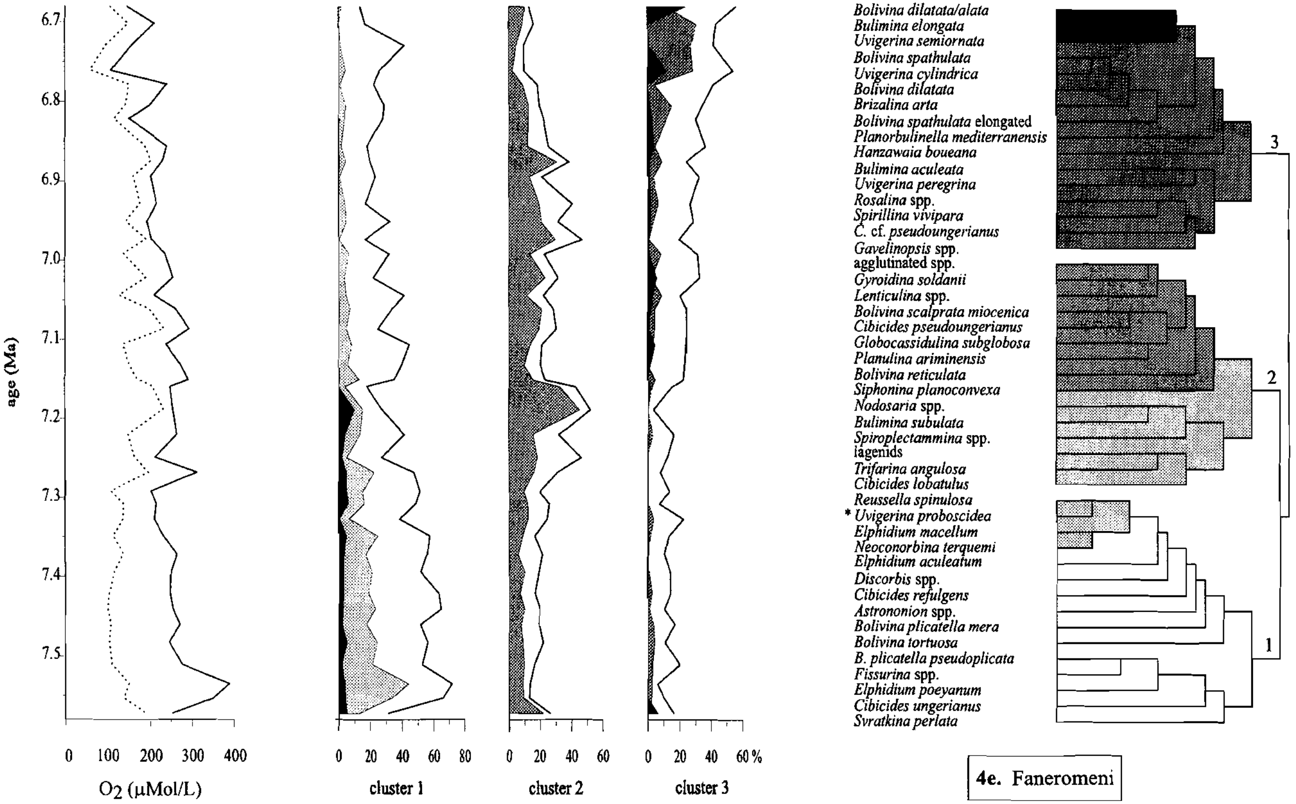
6.7
6.8
6.9
7.0
7.1
7.2
7.3
7.4
7.5
age (Ma)
0
100
200
300
400
O2 (µMol/L)
0
20
40
60
80
cluster 1
0
20
40
60
cluster 2
0
20
40
60 %
cluster 3
Bolivina dilatata/alata
Bulimina elongata
Uvigerina semiornata
Bolivina spathulata
Uvigerina cylindrica
Bolivina dilatata
Brizalina arta
Bolivina spathulata elongated
Planorbulinella mediterranensis
Hanzawaia boueana
Bulimina aculeata
Uvigerina peregrina
Rosalina spp.
Spirillina vivipara
C. cf. pseudoungerianus
Gavelinopsis spp.
agglutinated spp.
Gyroidina soldanii
Lenticulina spp.
Bolivina scalprata miocenica
Cibicides pseudoungerianus
Globocassidulina subglobosa
Planulina ariminensis
Bolivina reticulata
Siphonina planoconvexa
Nodosaria spp.
Bulimina subulata
Spiroplectammina spp.
lagenids
Trifarina angulosa
Cibicides lobatulus
Reussella spinulosa
* Uvigerina proboscidea
Elphidium macellum
Neoconorbina terquemi
Elphidium aculeatum
Discorbis spp.
Cibicides refulgens
Astrononion spp.
Bolivina plicatella mera
Bolivina tortuosa
B. plicatella pseudoplicata
Fissurina spp.
Elphidium poeyanum
Cibicides ungerianus
Svratkina perlata
3
2
1
4e. Faneromeni

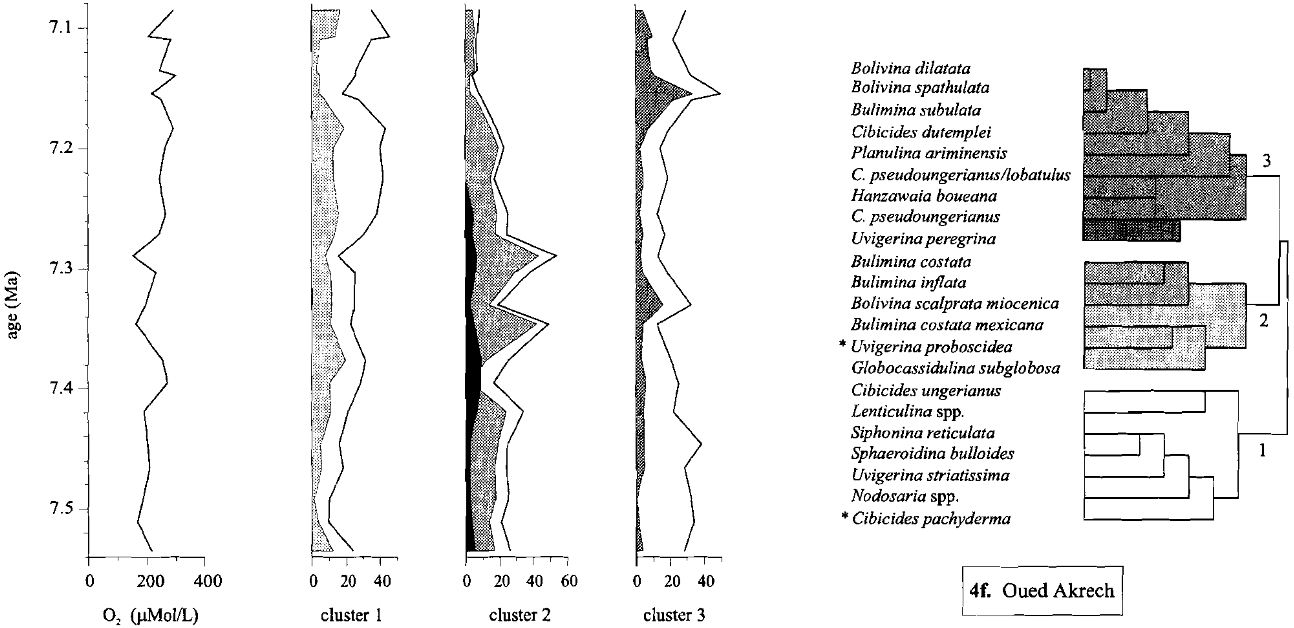
7.1
7.2
7.3
7.4
7.5
age (Ma)
0
200
400
O$_2$ (μMol/L)
0
20
40
cluster 1
0
20
40
60
cluster 2
0
20
40
cluster 3
Bolivina dilatata
Bolivina spathulata
Bulimina subulata
Cibicides dutemplei
Planulina ariminensis
C. pseudoungerianus/lobatulus
Hanzawaia boueana
C. pseudoungerianus
Uvigerina peregrina
Bulimina costata
Bulimina inflata
Bolivina scalprata miocenica
Bulimina costata mexicana
* *Uvigerina proboscidea*
Globocassidulina subglobosa
Cibicides ungerianus
Lenticulina spp.
Siphonina reticulata
Sphaeroidina bulloides
Uvigerina striatissima
Nodosaria spp.
* *Cibicides pachyderma*
3
2
1
4f. Oued Akrech

basins after ~7.16 Ma (Kouwenhoven et al., 1999; Seidenkrantz et al., in press), these depth reconstructions are of lesser value after that point. However, they do give a fair indication of depositional depths during the Tortonian and earliest Messinian. For the Faneromeni section, depositional depth is estimated at 300-400 m. For Potamidha, no P/B ratios were available, but Wonders and Van der Zwaan (1979) estimate depth of deposition to be around 600 m. Major parts of the Oued Akrech, Monte del Casino, Monte Gibliscemi and Metochia sections were deposited in estimated water depths of 1000 m or more. At depths around ~1200 m the method we used is no longer reliable, as it loses sensitivity and the errors are large.

Most sections at our disposal can be regarded as from relatively deep waters in which small sea level movements would not immediately be apparent. However, large-scale sea level movements should certainly be reflected, either directly or by the side effects of increasing supply of sediments and/or shallow-water benthic foraminifera from the coastal areas.

3.2. Benthic faunal trends

The dendrograms resulting from hierarchical clustering of the data sets are shown in Figure 4(a-f). All dendrograms display a major subdivision into three main clusters. Relative frequencies of species that are characteristic for the late Tortonian parts of the sections, and presumably reflecting normal marine conditions (clusters 1), have been summed and put beside plots of Shannon diversity in Figure 5. In all sections, the relative frequency of this group of species diminishes around 7.16 Ma. Benthic faunas of the deepest Mediterranean locations (Monte Gibliscemi, Metochia, Monte del Casino) were affected by decreasing ventilation after ~7.16 Ma, and faunal diversities in these sections decreased from that moment onward. In contrast with this, the diversity at the Atlantic site (Oued Akrech) is hardly affected. Similarly, in the shallower sites of Faneromeni and Potamidha no effects are seen in the diversity trends.

Two other clusters are prominent in all sections. At Monte del Casino and Metochia these clusters evidently represent more stress-tolerant faunas, developing after the deposition of the sapropel at 7.17 Ma. Faneromeni shows a similar, but less rigorous change in faunal development. At Monte Gibliscemi no really stressed faunas develop, as the samples are more or less barren after a transitional stage dominated by *Oridorsalis* spp. The Potamidha section contains too few samples above the level of major change. At the Atlantic side of the Rifian corridor (Oued Akrech), we see only minor, temporary signs of environmental disturbance.

Apparently, the event at ~7.16 Ma affected the deepest sites most, and as bottom-water conditions deteriorated, assemblages with increasingly stress tolerant taxa predominated. In this sense, the statistical outcome is clearly dominated by the time series effect of a continuous environmental change, that started already in the late Tortonian, and persisted into the Messinian.

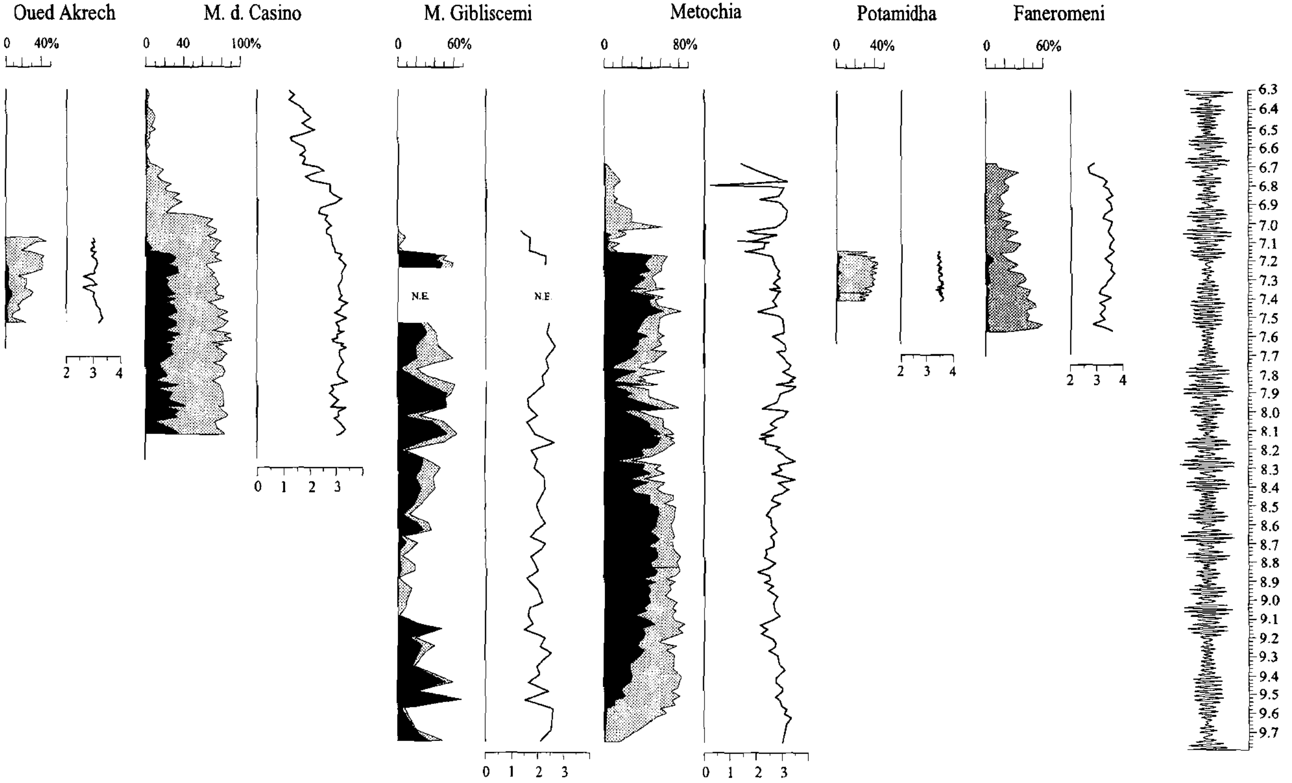

Figure 5. Joint frequencies of species in cluster 1 (left) and Shannon diversity (right) for all sections.

3.3. Geochemical proxies

3.3.1. Clusters versus stable isotope data

For the Metochia and Monte del Casino sections stable isotope data are shown beside relative frequencies of cluster 1 taxa in Figure 6(a, b). Both the oxygen and carbon isotopes indicate the environmental change that took place from 7.16 Ma onwards. Kouwenhoven et al. (1999) and Seidenkrantz et al (in press) interpreted the carbon and oxygen isotope patterns as the result of progressive isolation of the Mediterranean, decreasing bottom water ventilation and increasing bottom water salinity, especially in deeper waters. In both sections there is a clear positive correlation of the pattern of the carbon isotopes from benthic foraminiferal carbonate with the relative frequencies of cluster 1 species, and a negative correlation with cluster 3 species.

Comparison with the benthic oxygen isotope data gives a less clear picture. Increasing bottom-water salinity is most clearly indicated in the Monte del Casino section, where the shift towards heavy oxygen isotopes is comparatively large and coincides with a regular increase of species tolerating increased salinity (*Uvigerina cylindrica, Bulimina subulata, Bolivina dilatata* : Van der Zwaan, 1982).

3.3.2. Taxa and groups versus redox-sensitive elements

Manganese and vanadium are often used as geochemical proxies for oxygen depletion of bottom waters (e.g. Reichart et al., 1998; Den Dulk et al., 1998 and subm.). Manganese is remobilised from the sediment under dysoxic/anoxic conditions, while vanadium is enriched when the oxic-anoxic front is situated above the sediment-water interface (Breit and Wanty, 1991; Calvert and Pederson, 1993; Nijenhuis et al., 1996; Schenau et al., 1998). Table I shows correlations (Pearson) of taxa from the Monte del Casino section that were imported into cluster analysis, with these redox-sensitive elements. Joint percentages of taxa displaying significant positive correlations with redox-sensitive elements ($r > 0.4$ for Mn/Al and $r > 0.3$ for V/Al) are shown next to plots of Mn/Al and V/Al in Figure 7a. The pattern displayed by the Mn/Al ratio is reflected in the joint percentages of *Siphonina reticulata*, *Cibicides wuellerstorfi*, *Lenticulina* spp., *Pullenia quinqueloba*, and *Melonis soldanii*. The joint percentages of *Bolivina dilatata*, *Bulimina elongata* and *Uvigerina cylindrica gaudryinoides* correlate with the increase in the V/Al ratio after 6.7 Ma. The peak values of V/Al around 7.2 and 6.9 Ma are not clearly mirrored by species with a good correlation with the V/Al ratio, although these peaks most probably indicate periods of dysoxia.

Correlations of Faneromeni taxa with the V/Al and Mn/Al ratios are given in Table II. Joint percentages of species showing a positive correlation with the redox-sensitive elements are shown in Figure 7b. Joint percentages of *Bolivina spathulata*, *B dilatata/alata*, *Bulimina elongata* and *Uvigerina cylindrica cylindrica* ($r > 0.4$) show a similar trend as the

---

Figure 6. Stable isotopes of benthic foraminiferal carbonate, with joint frequencies of cluster 1 and cluster 3 species. **(a)** Metochia section; **(b)** Monte del Casino section.

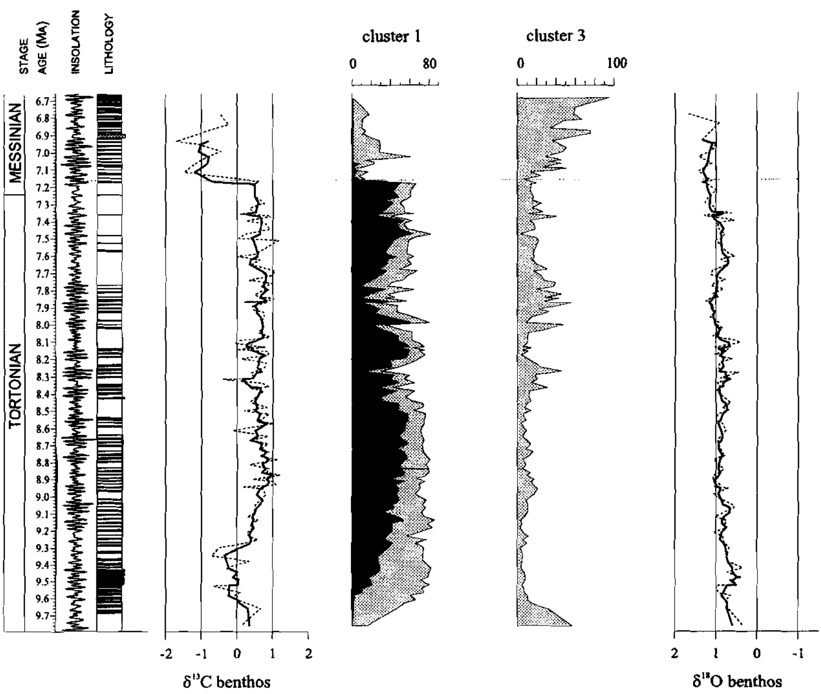
STAGE
AGE (MA)
INSOLATION
LITHOLOGY
MESSINIAN
TORTONIAN
6.7
6.8
6.9
7.0
7.1
7.2
7.3
7.4
7.5
7.6
7.7
7.8
7.9
8.0
8.1
8.2
8.3
8.4
8.5
8.6
8.7
8.8
8.9
9.0
9.1
9.2
9.3
9.4
9.5
9.6
9.7
cluster 1
0 80
cluster 3
0 100
-2 -1 0 1 2
δ^{13}C benthos
2 1 0 -1
δ^{18}O benthos

6a

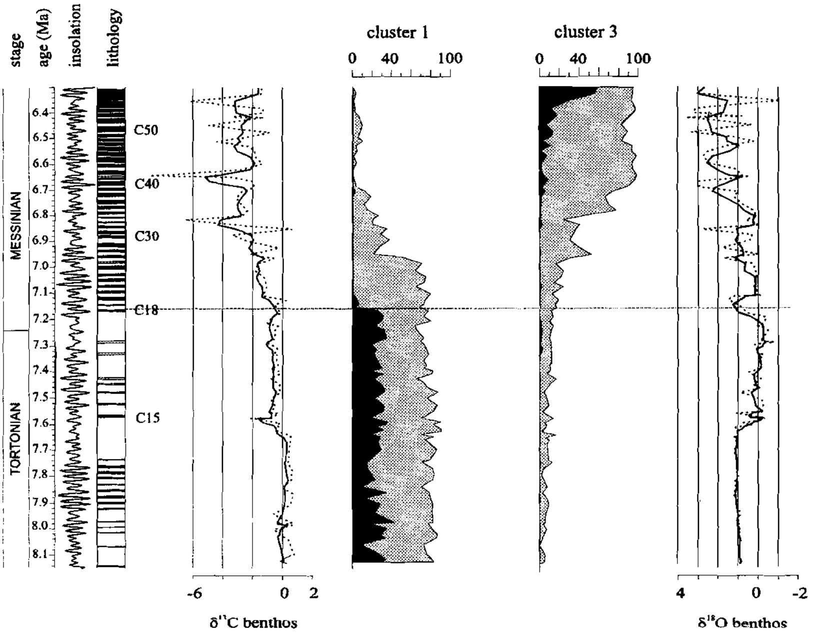
stage
age (Ma)
insolation
lithology
MESSINIAN
TORTONIAN
6.4
6.5
6.6
6.7
6.8
6.9
7.0
7.1
7.2
7.3
7.4
7.5
7.6
7.7
7.8
7.9
8.0
8.1
C50
C40
C30
C18
C15
cluster 1
0 40 100
cluster 3
0 40 100
-6 0 2
δ^{13}C benthos
4 0 -2
δ^{18}O benthos

6b

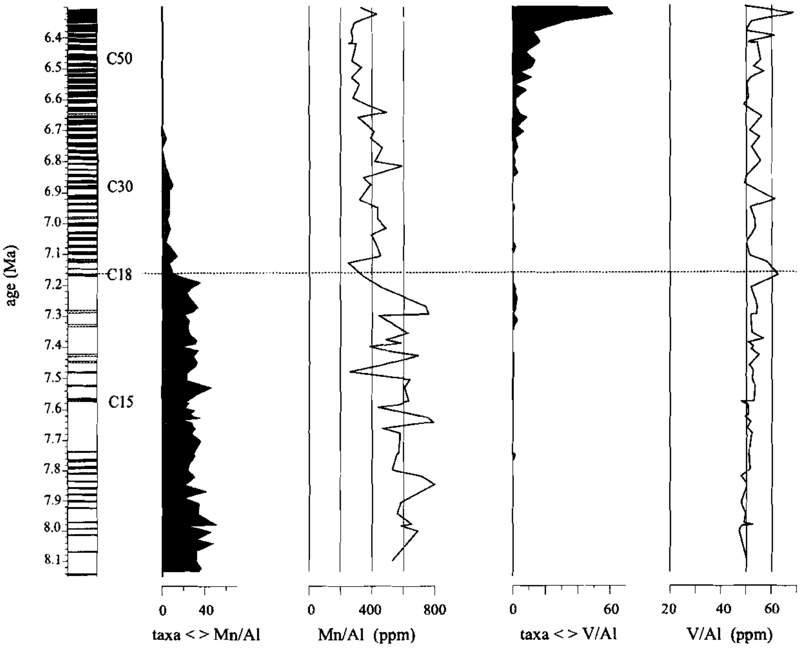
age (Ma)
6.4
6.5
6.6
6.7
6.8
6.9
7.0
7.1
7.2
7.3
7.4
7.5
7.6
7.7
7.8
7.9
8.0
8.1
C50
C30
C18
C15
0
40
taxa < > Mn/Al
0
400
800
Mn/Al (ppm)
0
60
taxa < > V/Al
20
40
60
V/Al (ppm)

7a

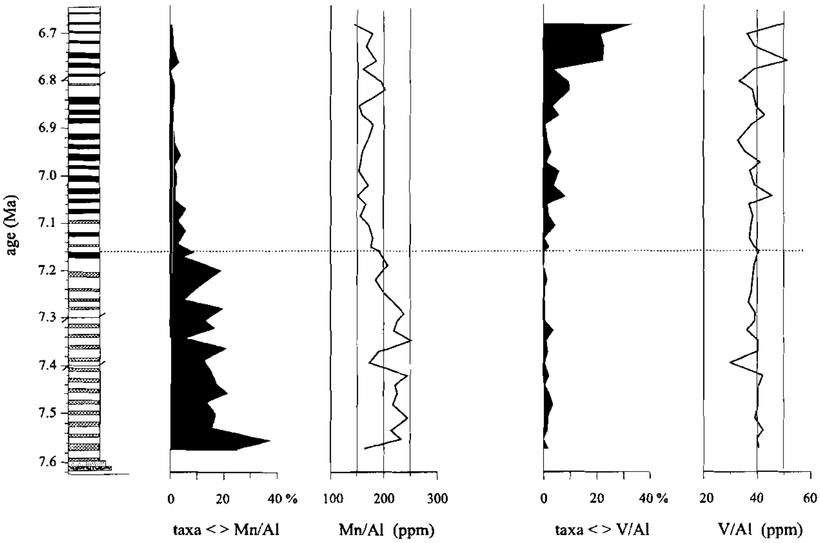
age (Ma)
6.7
6.8
6.9
7.0
7.1
7.2
7.3
7.4
7.5
7.6
0
20
40 %
taxa < > Mn/Al
100
200
300
Mn/Al (ppm)
0
20
40 %
taxa < > V/Al
20
40
60
V/Al (ppm)

7b

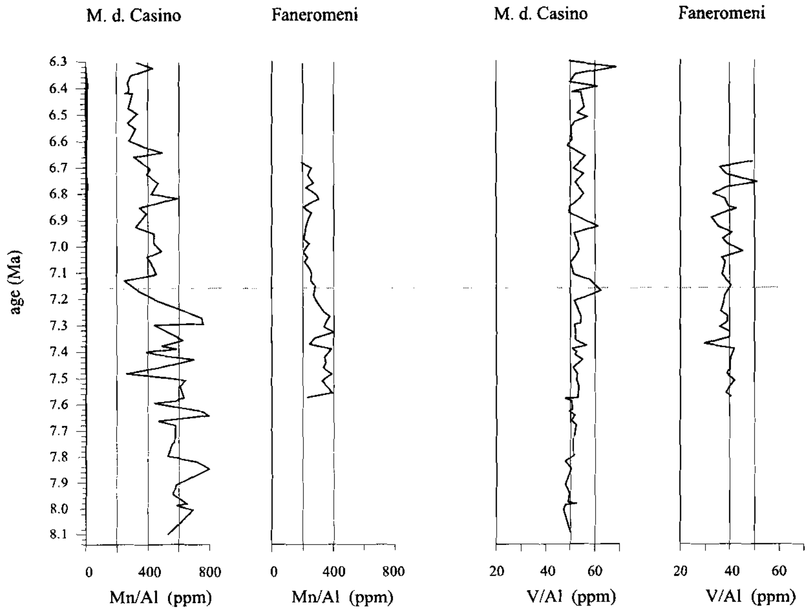

Figure 8. Comparison of trends in the concentrations of Mn and V in the Monte del Casino (~1000m) and Faneromeni (~300m) sections.

V/Al ratio. *U. cylindrica cylindrica* and *B. dilatata/alata* show a positive correlation with V/Al and a negative correlation with Mn/Al. Joint percentages of *Bolivina tortuosa, Cibicidoides bradyi, Neoconorbina terquemi, Reussella spinulosa, Siphonina reticulata* and *Uvigerina proboscidea* mirror the Mn/Al ratio.

In Figure 8 we compare the patterns of Mn/Al and V/Al in both sections. The benthic associations of the Faneromeni section display minor change, if compared to deeper sites, but the combined benthic and geochemical records indicate that the shallower site at Faneromeni was also affected by the event at 7.16 Ma.

3.4 The oxygenation index

The oxygenation state of the bottom waters at the sediment-water interface was calculated using the regression of Van der Zwaan et al. (subm). The frequencies of obligate oxic, epifaunal species were summed and introduced into the transfer function. It appears that at the Monte Gibliscemi and Metochia, and to a lesser extent the Monte del Casino sections, the bottom waters were extremely well aerated preceding the

---

Figure 7. Redox-sensitive elements Mn and V, corrected for terrestrial input by calculating the ratio with Al. Trends in element concentrations are compared to joint relative frequencies of taxa with significant correlation to the element concentrations (r > 0.4). **(a)** Monte del Casino section; **(b)** Faneromeni section.

Table I. Significant correlations of taxa with redox-sensitive elements: Monte del Casino.

Species	Mn/Al: r / p	V/Al: r / p
Bolivina dilatata	-.3238 / .003	.3237 / .001
Bulimina elongata		.4889 / < .001
Bulimina subulata	-.4958 / < .001	
Cibicidoides bradyi	.3190 / .003	
C. italicus	.3430 / .002	
Cibicides kullenbergi	.3482 / .002	
C. pseudoungerianus	-.5591 / < .001	
C. ungerianus	.3168 / .004	-.3654 / .001
C. wuellerstorfi	.4982 / < .001	
Gyroidina altiformis 2	.3776 / < .001	
Gyroidina soldanii	.3041 / .005	
Hanzawaia boueana	-.4832 / < .001	
Karreriella bradyi	.3232 / .003	
Lagenids	.3330 / .002	
Lenticulina spp.	.5357 / < .001	
Melonis soldanii	.5283 / < .001	
Pullenia quinqueloba	.5815 / < .001	
Siphonina reticulata	.5974 / < .001	-.3561 / .001
Sphaeroidina bulloides	.3181 / .004	-.3194 / .003
Uvigerina cylindrica gaudryinoides		.4599 / < .001
Uvigerina rutila	.3087 / .005	

Table II. Significant correlations of taxa with redox-sensitive elements: Faneromeni

Species	Mn/Al: r / p	V/Al: r / p
Anomalinoides flintii		-.4506 / .004
Anomalinoides sp.1	-.5480 / < .001	
Bolivina dilatata/alata	-.3210 / .043	.6106 / < .001
Bolivina tortuosa	.4865 / .001	
Bolivina spathulata		.4593 / .003
Brizalina arta		.4860 / .001
Bulimina costata	.3462 / .029	
Bulimina elongata		.4302 / .006
Cibicidoides bradyi	.4631 / .003	
Cibicides dutemplei	-.4141 / .008	
C. pseudoungerianus mc	-.5507 / < .001	
Lenticulina spp.		-.3407 / .031
Neoconorbina terquemi	.5077 / .001	
Reussella sp.1	.3492 / .027	
Reussella spinulosa	.6289 / < .001	
Siphonina reticulata	.4813 / .002	
Spiroplectammina spp.	-.3374 / .033	
Uvigerina cylindrica cylindrica	-.4383 / .005	.4701 / .002
Uvigerina peregrina	-.4687 / .002	
Uvigerina proboscidea	.6836 / < .001	

Tortonian/Messinian boundary (Fig. 4). Around 7.16 Ma the bottom-water oxygenation dropped dramatically at all three deeper-water sites. In Potamidha the drop in oxygen content is far less conspicuous, and in Faneromeni and the Atlantic site (Oued Akrech) there is hardly any change in the oxygenation curve.

3.5. Salinity

The stable oxygen isotopes of the Monte del Casino and Metochia sections start shifting to more positive values after 7.16 Ma, and continue to do so after ~6.8 Ma. At the moment we have no plankton data at our disposal to disciminate between a temperature and a salinity effect. In Monte del Casino we assumed the shift to be too large (~3 permil) to be explained by cooling alone (Kouwenhoven et al., 1999), and we interpreted this in terms of increasing bottom-water salinity. In Metochia the stable isotope record is less reliable after 6.85 Ma, due to poor preservation of the fauna. However, after 6.8 Ma benthic foraminifera are present in both sections, that have been mentioned to tolerate increased salinity (e.g. Van der Zwaan, 1982): *Bulimina aculeata*, *Bolivina dilatata* and *B. plicatella* in Metochia, and *B. dilatata*, *Bulimina subulata*, and *B. elongata* in Monte del Casino. Santarelli et al. (1998) found evidence in the dinoflagellate record of Faneromeni for increasing salinity, starting at 6.68 Ma.

4. Discussion

4.1. Organic flux

Although the flux of organic matter to the benthic environment is generally considered to be one of the main factors structuring benthic assemblages, we have indications that the events at 7.16 Ma had little to do with increased primary producitvity. Neither planktonic nor benthic foraminiferal numbers show an increase at or around the event (Kouwenhoven et al., 1999, Fig. 6; Seidenkrantz et al., in press, Fig. 4). In this sense, organic flux is a relatively minor factor. However, organic flux has been paramount in three aspects. It probably determines to a great extent the differences between eastern and central Mediterranean assemblages. BFAR's (benthic foraminiferal accumulation rates) indicate that the eastern sites were more productive. Secondly, the difference between assemblages from intermediate and deep waters (for instance, lower percentages of bi- and triserially arranged species at deeper sites) is linked to the lower flux arriving in deeper water. Thirdly, the drop in productivity in the course of the Messinian probably plays a role in the faunal development, although we think that salinity is an overriding factor after ~6.8 Ma.

4.2. Paleobathymetry

Paleobathymetrical reconstructions of the sections are based on the proportion of planktonic foraminifera in the total assemblages (P/B ratios; Fig. 3). These paleodepth values are an approximation of true depths, as the calculation used is not precise at depths exceeding 1200 m. The reconstruction also fails when bottom-water oxygenation decreases. Depth estimates will be too low in case of a benthic 'bloom', and too high when a benthic desert develops, as is often the case in sapropels. Alternative methods are based on benthic faunal composition, and on benthic 'marker species' that are characteristic for certain depth levels. Marker species are often chosen for analogy with Recent depth distributions, but this method is not altogether reliable. Indications exist, that species have changed their depth preferences through time (e.g. *Uvigerina peregrina*, Van der Zwaan, 1982; Murray, 1991). A further disadvantage is that benthic faunal compositions are sometimes biased, particularly in cases where the benthic environment is stressed. Opportunistic species occur over large depth ranges. They are apparently able to migrate tens to hundreds of meters in a relatively short period if stress develops, or if a former 'benthic desert' is repopulated (see Speijer and Van der Zwaan, 1996, for a Paleocene example). These restrictions taken into consideration, it is very well possible to make a reasonably accurate depth reconstruction using all available information, including sediment characteristics and diversity trends. Table III shows paleo-depth distributions for a number of benthic foraminifera, based on data from the six Mediterranean sections. These are usually in line with, but sometimes contradict data from the literature.

4.2.1. Bathymetry and diversity

In general a bathymetric trend in diversity is expected, highest diversities occurring in deeper waters. In our material this is not clearly the case. In the Potamidha and Faneromeni sections diversities are highest, followed by the - deeper - Monte del Casino section. Gibliscemi, the deepest section, shows lowest diversities. An obvious assumption would be that restricting conditions towards deeper waters prevent higher diversities. However, considering the oxygen reconstructions (Fig. 4), this is probably not the case: the deeper water localities are generally better ventilated than the shallower ones. If we compare per region, this deviating diversity pattern from shallow to deep water is also present. The eastern Mediterranean faunas are more diverse than those in the central Mediterranean are. The fauna of the deeper water Metochia section is characterised by diversities that are equal to or lower than those in the shallower Potamidha and Faneromeni sections. Among the central Mediterranean sections, the deeper Gibliscemi section clearly shows lower faunal diversities than Monte del Casino. If an unidentified stress factor in the deeper waters is not preventing the expected high diversity, we have to conclude that these Miocene deeper water sites deviate from the general trend that diversity is highest in stable, deep water environments.

Modern deep-water environments are not only characterised by diversified assemblages, but often also by assemblages composed of specialised species. In the Miocene bathymetric range chart (Table III) a substantial number of species is characteristic for deeper water. Such species would be adapted to relatively stable (trophic) conditions. In view of the higher degree of specialisation, environmental change is most keenly felt in these deeper environments. The event at 7.16 Ma is most evident in the deeper water sections. This can be explained in a straightforward way by assuming that the event exclusively affects deep-water sites. An alternative explanation is, however, that deep-water communities are more prone to reflect environmental change. This notion will be further discussed below. In most of the Mediterranean sections fauna remained present after the 7.16 Ma change, but in Monte Gibliscemi and in the neighbouring deep-water localities Falconara and Giammoia (Sicily), the 7.16 Ma change led to near-extinction of the deep-water assemblage. These sites remained devoid of benthic foraminifera until the late Messinian, when invasion of shallow water, tolerant species *(B. aculeata)* repopulated of the environment (Van der Zwaan, unpublished data).

4.3. Oxygenation

Oxygenation of bottom waters is usually reconstructed on basis of benthic faunal associations and geochemical proxies, such as redox-sensitive elements and carbon stable isotopes. These proxies are all semi-quantitative at best, and moreover, the geochemical proxies are prone to diagenesis and remobilisation. A quantitative measure of bottom-water oxygenation, recently developed and evaluated on data of, among others the Monte del Casino section (Van der Zwaan et al., subm.; this thesis, Chapter 5), was applied to all six sections described in this paper (Fig. 4). The recon structions show the event at ~7.16 Ma in most sections, and add a quantitative measure of bottom-water oxygenation. After thorough evaluation, paleo-circulation reconstructions can be based on these oxygenation curves (see Chapter 6 of this thesis) and the quantitative data can eventually be used to constrain the outcome of modelling experiments.

4.4. Assemblage structure

4.4.1. Bathymetry and oxygenation

Based on the paleobathymetric estimates (Fig. 3), the Faneromeni and Potamidha sections are the shallowest, deposited at estimated water depths of around 3-400 and 600 m. The other sections were deposited in somewhat deeper waters (1000-1200 m). This difference is expressed in the data matrices and cluster-diagrams of the sections. In the Faneromeni section the proportion of epiphytes and other shallow-water species (*Discorbis, Cibicides refulgens/ lobatulus, Elphidium* spp.) is relatively high, and these taxa do not cluster together consistently. Although the shallow fauna does group together in the other sections, we find no separate clusters of shallow water species in any of the sections. This indicates that the water was too deep for the epiphytes to proliferate, and the distance to shore too large to allow substantial rafting. Especially in the deeper Monte del Casino and Metochia sections, epiphytes tend to group at the side of the more stressed assemblages. This is probably related to the decreasing standing stocks associated with the development of stressed conditions. Rafted (allochthonous) elements will then represent a more substantial percentage of the assemblages.

In most sections we find a rather clear-cut grouping of benthic assemblages. Generally this subdivision is related to the increase of oxygen stress, as summarised in Figure 4. In this figure, the distribution of the assemblages is plotted versus time, and versus the calculated oxygen contents at the sediment-water interface. In all deep-water sections but the extra-Mediterranean section Oued Akrech, we find evidence for diminishing bottom water ventilation. The substantial decrease of the oxygen content in the deep-water realm at 7.16 Ma is most evident. The shallower-water sections Potamidha and Faneromeni do not reflect such strong shifts in oxygenation, although Faneromeni shows steadily decreasing oxygenation of the bottom-water environment over time. The Potamidha section stratigraphically only just covers the event at 7.16 Ma, but the Faneromeni section should reflect it. This leads to the conclusion that shallow waters were less affected by the event than deep waters. The faunal assemblages in most sections are clearly organised along an oxygen stress gradient. The joint abundances of the species comprising the (sub-)clusters co-vary with the oxygenation trend, indicating the overriding importance of oxygen in structuring the assemblages.

4.4.2. Temporal variation and in-sediment distribution of oxygen

Time series analysis of benthic foraminifera is complicated by the fact that two types of response patterns interfere. When oxygen concentrations at the sediment-water interface decrease through time, this leads to a response of the faunal assemblages. At the same time, decreasing oxygen contents at the sediment-water interface cause the redox fronts to rise, and the participation of infaunal taxa in the processes operating in the topmost sediment layer to increase. Ordination of species along a stress gradient reflects the pattern of temporal environmental change in the sections. At the same time, this ordination can be used to assess the distribution of species along an oxygen gradient from the sediment-water interface down to the redox front. The (sub)-assemblages in the cluster analysis can then be viewed either as increasingly stress tolerant, or as characteristic for deeper parts of the sediment column. The latter also requires a high degree of stress tolerance. This aspect of the cluster analysis touches upon the microhabitat structure of the assemblages and is discussed in the last part of this paper.

Cluster analysis of the assemblages from each of the sections results in a number of clusters that can be regarded as representative of a range of environments: from a normal marine to a stressed environment. However, when comparing these clusters one has to bear in mind that the outcome of the cluster analyses cannot be compare in a straightforward way. The stress-tolerant cluster 3 of, for instance, Potamidha is from much better aerated waters than the corresponding cluster 3 from Monte del Casino. The Gibliscemi section is another illustration. Instead of a stress fauna, a benthic desert developed at this site. Thus, the most stress-tolerant cluster (3) of Monte Gibliscemi is from an environment in which oxygenation values are almost as high as they are in the best ventilated part of the Monte del Casino section. We will take this difference into account in the following discussion.

4.4.3. Equilibrium assemblages

Fossil as well as Recent benthic assemblages from open marine, undisturbed sites display similar characteristics: diversity is relatively high and dominance is low (e.g. Phleger and Soutar, 1973; Murray, 1991). Such assemblages characterise the late Tortonian sequences in the deeper Mediterranean at Monte Gibliscemi and Metochia, and to a lesser extent, Monte del Casino. For the Tortonian parts of these sequences, high oxygen contents were calculated. Characteristic species for these assemblages are for instance *C. ungerianus*, miliolids, *C. italicus*, *S. reticulata*, *Melonis soldanii* and higher agglutinants. It is assumed that such species are keen competitors, living preferably at the sediment-water interface (Jorissen et al., 1992; Den Dulk et al., 1998; Jorissen, 1999; Van der Zwaan et al., 1999 and references therein). These species occur in relatively low frequencies in relatively high-diversity assemblages. Such assemblages are sensitive to stress. As was mentioned earlier, this is probably related to the extremely narrow niche dimensions of these taxa, which causes them to respond immediately to environmental change. With increasing pressure of stress, for instance when oxygen contents decrease, they will be replaced. It is remarkable that the replacing species in deeper waters were also predominantly trochospiral taxa that probably preferably lived as epifauna. Prominent among these are *Oridorsalis umbonatus*, *Gyroidina* species, *Karreriella bradyi* and *Cibicidoides bradyi*, all of which are representative of the first stages in the development of deep-water stress.

The notion of *K-selection* (see e.g. Pianka, 1978) has been attached to the equilibrium assemblages (Van der Zwaan, 1982; Jorissen, 1988; Murray, 1991; Hottinger, 1983), implying that they combine a narrow tolerance range with a low offspring and slow reproduction. For benthic foraminifera, most of these characteristics are ill known, and it seems therefore best to retain the phrase ‘equilibrium taxa’. Relatively few tri- and biserial taxa, species classically regarded as infauna, occur in these assemblages. A characteristic of equilibrium taxa is that their highest abundances occur at the sediment water interface, as will be discussed in the final part of this paper.

4.4.4. Stress assemblages: the role of oxygen

Faunal assemblages living under certain amounts of stress are characterised by lowered diversity and increased dominance. In many cases, standing stocks, and thus BFAR’s are high, but these may very well be low when a site develops towards a benthic desert. The latter is for instance the case in a well-developed oxygen minimum zone (see Den Dulk et al., subm.), or in sapropelitic sediments. Oxygen as a stress factor has been extensively studied and several methods have been employed to represent stress in an efficient way. Berggren and Haq (1976), for instance, used an index based upon the number of spiral species present in a series of samples. This method, as well as others, was based upon the assumption that bi-and triserially arranged species (e.g. *Bulimina*, *Bolivina* and *Uvigerina* spp.) represent infauna and are thus more resistant to stress.

The proportional increase of infauna occurring as bottom-water oxygenation decreases is thought to be related to rising redox fronts. Standing stocks of infaunal species probably increase rapidly, if the deep redox front shifts as high as the sediment level where labile organic matter is abundant. High frequencies of infauna are thus not only the result of a closed-sum effect caused by the reduced presence of other species, but just as well of their ability to profit from the prevailing environmental conditions. Oxygen stress is specific in the sense that macrofaunal elements are more readily affected by reduced oxygen contents, so that predation pressure decreases. This may also contribute to higher standing stocks of stress taxa (Verhallen, 1991).

In older associations, potential stress markers and components of stress faunas are often spirally arranged species (for instance, Paleocene: Berggren and Aubert, 1975; Aubert and Berggren, 1976; Speijer and Van der Zwaan, 1996; Speijer et al., 1996). Indications exist that infaunal habitats were hardly explored by benthic foraminifera before the middle Miocene (see Douglas and Woodruff, 1981; Van der Zwaan et al., 1986, Thomas, 1986; Chapter 8 of this thesis).

Though taxa tolerant to oxygen stress are often potentially infaunal, the ultimate effect of stress on these species depends on the stretch of time this stress is acting. Some taxa are only tolerant to short term changes in oxygen content and in this sense may be better identified as ruderal. The longer a taxon is able to live under stress, the more it approaches characteristics of true stress species (*S-species* sensu Grime, 1973; see also Jorissen, 1988). These taxa are predicted to have a low population turnover and long generation lengths.

4.4.5. Salinity stress

Small salinity changes normally have no influence on assemblage characteristics. Van der Zwaan (1982) extensively discussed the effects of salinity change in the context of the Messinian events. It appears that in the shallow water realm only substantial differences lead to hyper- or hyposaline assemblages. In general, large deviations from normal salinity seem virtually impossible in deeper waters. However, the oxygen isotope records of Metochia and Monte del Casino suggest that a rather substantial salinity increase occurred at deeper Mediterranean sites during the early Messinian. At 7.16 Ma, ventilation decreased, leading to lowered oxygen contents at the sediment water interface. It appears that oxygen is the prime parameter leading to the faunal change observed. However, the subsequent development of stress faunas in both Monte del Casino and Metochia is probably to a large extent related to changes in salinity. In the period in which these faunal changes occurred in succession, the carbon isotopes indicate only minor changes in ventilation (Fig. 6). This is confirmed by the redox proxies, which suggest that the main decrease in oxygenation took place around 7.16 Ma (Fig. 7). We are therefore inclined to consider the salinity changes after 7.16 Ma as a factor contributing to a faunal assemblage which progressively impoverished. As was discussed earlier, oxygen stress is expexted to result in a high proportion of tri- and biserial taxa. In contrast, salinity stress in deeper waters seems to lead to progressive abundances of *C. pseudoungerianus* and other trochospiral taxa. This suggests that not all taxa tolerating oxygen stress are able to withstand salinity increase as well, and vice versa.

4.4.6. Ruderals and repopulation

Ruderals, also described as *r-strategists*, are able to repopulate vacated niches in a very short period of time. There is a difference between these taxa and so-called opportunistic species. As soon as a niche is repopulated to a certain extent, the ruderals are replaced by opportunistic taxa if food is abundant and/or oxygen low, and eventually by equilibrium taxa if normal marine conditions are restored. Ruderals are commonly epifaunal taxa, contrary to opportunists. Because a characteristic feature of repopulation events is that they are usually of relatively short duration, (Alve, 1999, and references therein), they will be missed in a fossil setting when sampling resolution is low. Fossil examples of re-population events are numerous in the Mediterranean since the Miocene, as sapropels are often barren (e.g. Rohling et al., 1993).

When evaluating samples around the 7.16 Ma level, we encountered a short-lived dominance of *Oridorsalis stellatus* in two deeper-water sections (Fig. 9: Monte Gibliscemi, Metochia). In the Metochia section, the youngest sample of the sapropel deposited around 7.17 Ma contains no spirally arranged taxa at all. The sample directly above this sapropel contains 293 *Oridorsalis stellatus* of a total of 553 specimens. In Gibliscemi, the sapropel at the same level is barren, and the first sample collected above this sapropel contains 44 *O. stellatus* of a total of 93 specimens. *O. umbonatus* has been found repopulating the Mediterranean in the earliest Pliocene (Wright, 1979; Sprovieri & Hasegawa, 1990). The species is apparently an *r-selected* recoloniser in deeper waters, but from our data it is not clear whether it is tolerant to lowered oxygenation. In both sections there are more species that flourish for a short period after the 7.16 event, but they are not as dominant as *O. stellatus* (see Fig. 9). In Gibliscemi the samples eventually become more or less barren. In Metochia the benthic fauna is eventually dominated by stress taxa, indicating decreased ventilation and possibly increased salinity.

5. Microhabitats of late Miocene benthic foraminifera

As was mentioned earlier, time series analysis of benthic foraminiferal patterns always has two aspects. One is the variation in time as a response to changing environmental variables. The other aspect is related to the fact that the same ordination as along stress gradients through time, takes place at each point in time, from the sediment-water interface downwards. Therefore, we can employ the cluster analysis as presented in Figure 4 to unravel the microhabitat patterns of Miocene benthic foraminifera. In the shallowest sections Potamidha and Faneromeni,.but also in

---

Figure 9. (next page) Taxa dominating in the Metochia and Gibliscemi sections directly after deposition of the sapropel at 7.17 Ma.

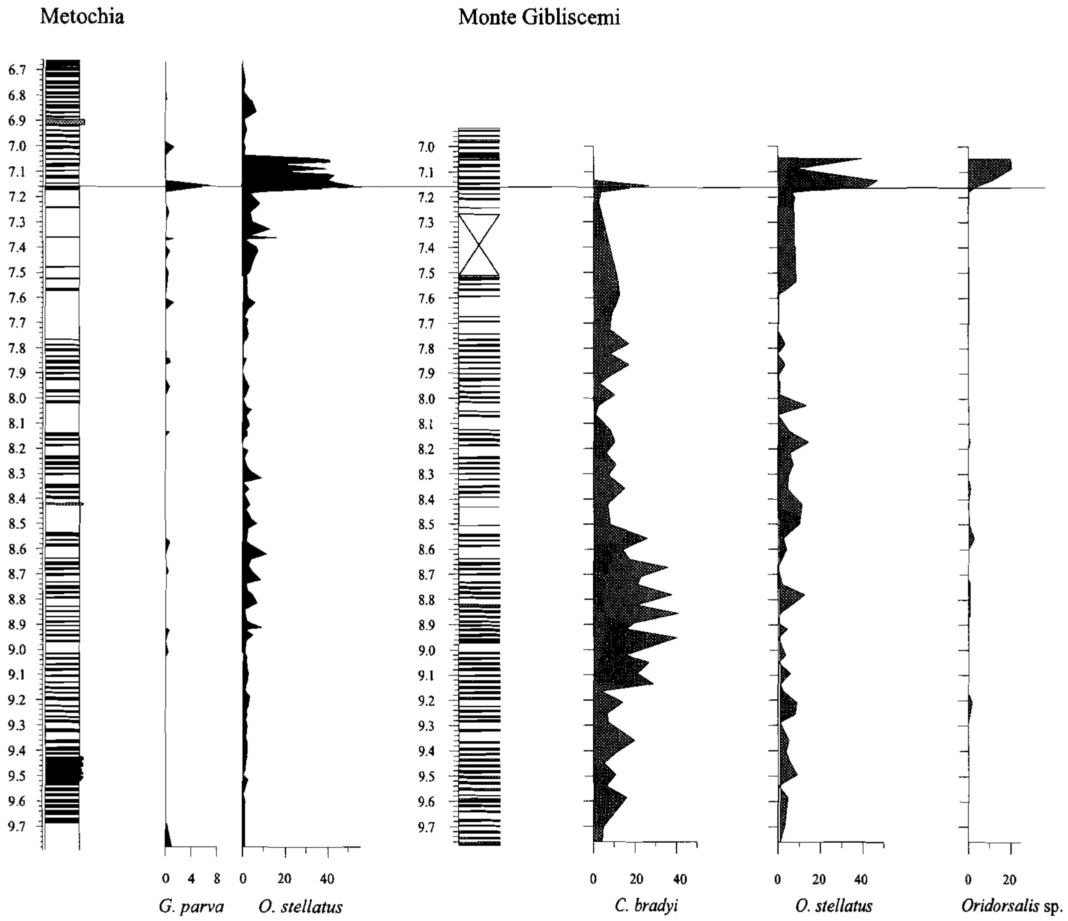
Metochia
Monte Gibliscemi
6.7
6.8
6.9
7.0
7.1
7.2
7.3
7.4
7.5
7.6
7.7
7.8
7.9
8.0
8.1
8.2
8.3
8.4
8.5
8.6
8.7
8.8
8.9
9.0
9.1
9.2
9.3
9.4
9.5
9.6
9.7
0 4 8
G. parva
0 20 40
O. stellatus
0 20 40
C. bradyi
0 20 40
O. stellatus
0 20
Oridorsalis sp.

Table III. Paleobathymetric list of regularly occurring species.

taxa	shelf	upper bathyal	middle bathyal	lower bathyal
Elphidium spp.	———			
Discorbis spp.	———			
Asterigerina spp.	———			
Neoconorbina terquemi	———			
Gavelinopsis lobatula	······	———		
Spirillina vivipara	······	———		
Cibicides lobatulus	······	———		
Cibicides refulgens	······	———		
Anomalinoides alazanensis		———		
Neoeponides schreibersii		———		
Cibicides ungerianus	······	———	······	
Bolivina reticulata		———	······	
Bolivina tortuosa		———	······	
Brizalina arta		———	······	
Bulimina elegans		———	······	
Cibicides dutemplei		———	······	
Reussella spinulosa		———	······	
Rosalina spp.		———	······	
Bolivina plicatella mera	······	———	———	
B. plicatella ssp. *pseudoplicata*	······	———	———	
Svratkina perlata		———	———	
Trifarina angulosa		———	———	
Planorbulinella mediterranensis		———	———	
Hanzawaia boueana		———	———	
Rectuvigerina bononiensis		———	———	
Uvigerina cylindrica		———	———	
Siphonina planoconvexa		———	———	
Bulimina aculeata		———	———	
Bulimina aculeata var. *Lappa*		———	———	
Bulimina elongata		———	———	
Bulimina subulata		———	———	
Bolivina dilatata		———	———	
Bolivina spathulata		———	———	
Uvigerina peregrina		———	———	
Planulina ariminensis		———	———	
Astrononion spp.		———	———	
Cibicides pseudoungerianus		———	———	
Uvigerina proboscidea		———	———	
Uvigerina pygmaea		———	———	
Bolivina scalprata miocenica		———	———	
Gyroidina orbicularis		———	———	
Pullenia quinqueloba		———	———	
Gyroidina soldanii		———	———	
Globocassidulina spp.		———	———	······
Bulimina striata		······	———	
Bolivina punctata		······	———	
Uvigerina rutila		······	———	
Uvigerina striatissima			———	
Sigmoilopsis schlumbergeri			———	
Bigenerina nodosaria			———	
Anomalina helicina			———	
Cibicides kullenbergi		······	———	———
Melonis barleeanum			———	———
Melonis soldanii			———	———
Valvulineria spp.			———	———
Pullenia bulloides			———	———
Sphaeroidina bulloides			———	———
Chilostomella spp.			———	———
Cibicides bradyi			———	———
Cibicides robertsonianus			———	———
Cibicides pachyderma			———	———
Eggerella bradyi			———	———
Gyroidina altiformis			———	———
Gyroidina parva			———	———
Karreriella bradyi			———	———
Melonis pompilioides			———	———
Oridorsalis stellatus			———	———
Cibicides wuellerstorfi			······	———
Siphonina reticulata			······	———
Cancris spp.			······	———
Globobulimina spp.			······	———
Quinqueloculina seminula			······	———

Metochia and Monte del Casino, there are well-defined clusters consisting of *Bolivina*, *Bulimina* and *Uvigerina* species. These stress tolerant taxa represent the potential infauna part of the assemblage (Van der Zwaan et al., 1999 and references therein). Species belonging to this group are able to migrate to deeper sediment layers and employ less labile organic matter stored there. *Bolivina spathulata* is one of the species persistently occurring in the most stressed part of the sequences and can be considered as the species that lives at the deepest redox fronts.

So-called modern deep infauna, composed of species as *Globobulimina* and *Chilostomella* does not frequently occur in our Miocene sequences, in spite of the fact that some sapropelitic samples were counted. Some of these species had already evolved, for instance *Globobulimina, Chilostomella*, and rare *Cassidulinoides* species. This deep infauna group gains in importance from the late Miocene onwards. The Miocene group of potential infauna is rather large and already quite comparable to the modern one.

The most abundant group next to potential infauna is a group of taxa that can be characterised as epifauna. Most of these species are planispiral or trochospiral and they are known from the literature as living predominantly at the sediment-water interface. Dominance of this group indicates well-ventilated bottom water environments and a rather deep position of the redox front. Van der Zwaan et al. (1999) assume that these species are not so tolerant to oxygen stress, but very well able to compete for food. This explains their prominent position at the sediment water interface under normal conditions. The number of species belonging to this group increases substantially towards deeper water environments. In the Tortonian and earliest Messinian part of the Monte Gibliscemi and Metochia sections, the number of potential infauna species is low and the number of epifauna species relatively high. This illustrates an important prediction of the Trox-1 and Trox-2 models (Jorissen et al, 1995; Van der Zwaan et al., 1999): with increasing water depth, nutrients become limitative. As a consequence of the limited amount of organic flux reaching deep environments, less organic matter is stored in the sediment, rendering the deeper sediment layers a less profitable environment for potential infaunal species. One should bear in mind, however, that in this context the name 'epifauna' is somewhat deceptive, since in deeper waters where the redox front resides deep, these 'epifauna' species may occur below the sediment-water interface.

All taxa that occur at the sediment-water interface in deeper waters have a more or less similar life style. This raises the question how microhabitats are partitioned there. In shallower waters, microhabitat partitioning is with sediment depth, creating substantial spatial subdivision and allowing rather high diversities. Such partitioning is clearly less effective in the more homogeneous deeper water environment. In spite of that, more taxa are living in a smaller environmental range than in shallower water. This apparent contradiction can only be solved if we assume very narrow niche dimensions of the deeper water taxa, and thus extremely specialised life styles. This notion is supported by what we observe if stress affects the benthic communities: the deeper water assemblages react far more sharply on environmental change than assemblages living in shallower waters.

6. Conclusions

Evaluation of benthic faunal development in six late Miocene mudd y sequences enabled determination of a sequence of events affecting the paleo-Mediterranean, and clarified the benthic assemblage structures. In the relatively stable late Tortonian, differences in paleoproductivity and faunal diversity existed between sites located at different depths, as well as between sites located in the central and the eastern part of the basin. The decrease of ventilation beginning at 7.16 Ma affected all Mediterranean sites, but the deepest sites show a considerably larger disturbance of benthic faunas than the shallower ones. These deep sites may have been affected most strongly by the event. At the same time, the equilibrium faunas from deep waters were probably more prone to environmental perturbations, due to their more specialised nature.

For most sections, a clear subdivision can be made between equilibrium and stress assemblages. Apart from temporal trends in the oxygenation state of bottom waters, this subdivision also provides insight in the community structure and microhabitat partitioning of Miocene benthic faunas. Many elements we know from Recent benthic faunas were already present: epifauna and potential infauna groups are comparable to their Recent counterparts. Deep redox dwellers were, however, not so frequent as today. Apparently this microhabitat had not been explored to its present extent.

Acknowledgements

We wish to thank all people who contributed to this research. F. Hilgen, W. Krijgsman and L. Lourens did most of the sampling. Laboratory assistance was provided by G. van 't Veld, G. Ittmann, A. van Dijk and H. de Waard. D. van den Akker, A. Okx, M. Rauhé and J. de Wit picked samples. W. den Hartog made SEM-pictures and made up the plates that illustrate our taxonomic concepts. Astronomical curves are from L. Lourens. Discussions with F. Hilgen, W. Krijgsman, W.J. Zachariasse, M.-S. Seidenkrantz, and M.J. van der Meulen on many subjects related to this research were most valuable.

Chapter 8

Synthesis

Survival under stress: benthic foraminiferal patterns and Cenozoic biotic crises

1. Introduction

The subject of this thesis is the development of Cenozoic benthic foraminiferal faunas in relation to major disturbances of the marine environment in the area that is presently occupied by the Mediterranean Sea. As such, this research is part of a longer-term programme, aimed at comparing the effects of major Cenozoic crises on marine biota. Earlier studies in the context of this programme were directed at the Cretaceous/ Paleogene and the Paleocene/ Eocene boundary events (Speijer and Van der Zwaan, 1996; Speijer et al, 1996a, b; Speijer and Schmitz, 1998), the terminal Miocene development on approaching the Messinian Salinity Crisis (Van der Zwaan, 1982, 1983), and the late Pliocene faunal turnover (e.g. Verhallen, 1991). These studies provided insight in the relationship between the nature and degree of stress in the marine environment, and the effects on associations of benthic foraminifera. The environmental factors contributing to these effects, and their relative importance, are not always clear from fossil studies alone. Therefore, fossil data gathering went hand in hand with field- and laboratory studies on living foraminifera (e.g. Jorissen, 1988; Van der Zwaan and Jorissen, 1991; Barmawidjaja et al., 1992; De Stigter, 1997, 1998a, b; Jannink et al., 1998). In recent years experimental studies contributed considerably to the understanding and interpretation of fossil patterns (e.g. Moodley et al., 1997, 1998a, b, Ernst et al., 1999; Van der Zwaan et al., 1999).

This thesis lays an emphasis on two different periods: the Paleocene and, as the main focus, the late Miocene. All material is derived from the Tethyan/Mediterranean area, of which the configuration changed profoundly in the course of the Cenozoic. The early Paleocene faunas reflect the recovery from a worldwide crisis, the Cretaceous/Paleogene boundary event. Both the Paleocene and the Miocene ended with a major turnover of benthic foraminifera, the Paleocene/Eocene benthic extinction and the Messinian alinity crisis, respectively. The former occurred on a wordwide scale; of the latter the effect was more localised to the Mediterranean basin per se. Nature and duration of these events were different, and are not the subject of this research. Our aim was twofold: we wanted to detect the points in time at which environmental changes set in, and what factors contributed to these changes. At the same time we expected to learn more about the development through time of benthic species recording stress. Therefore we studied benthic foraminiferal associations in the periods preceding and following the actual crises.

2. Data

The basis for this synthesis is formed by data from the Paleocene El Kef section in Tunisia, and six late Miocene sections, of which five are located in the central and eastern Mediterranean and one borders the Atlantic. The data from El Kef cover the Paleocene between the major extinction events at the Cretaceous/ Paleogene and the Paleocene/Eocene boundaries, respectively. Data from the late Miocene sequences document the faunal changes preceding the Messinian salinity crisis. As the data are not from a geographically and temporally homogeneous area, a bias is introduced which may hinder comparison of the faunal patterns. However, all data are derived from locations in the same bioprovince: the part of the Tethyan area that eventually developed into the Mediterranean faunal province. Moreover, all assemblages described and referred to are derived from predominantly muddy sequences, characterised by a relatively high sediment supply, and a relatively large distance to shore. The sequences described were all deposited at water depths between 200 and 1200 metres, and thus well below the photic layer. Therefore, influences of processes playing a role at shallow water depths need not be taken into account (e.g. continuous deposition of coarse clastics, light penetration, presence of algal symbionts, wave motion/action and regular short-term disturbances). In these deeper waters, the effects of stress (in particular oxygen stress) and organic flux are relatively important in structuring the benthic assemblages.

Especially in the Miocene sequences we rely on precise dating, provided by a combination of bio- magneto- and cyclostratigraphy (e.g. Hilgen et al., 1995; Krijgsman et al., 1995, 1997). This allows detailed correlations and provides a firm grip on the temporal evolution of environments and their biota towards crises, in this case the Messinian salinity crisis.

When evaluating the Miocene data sets, and reconstructing late Miocene events and water circulation patterns, we found that assemblage characteristics rather than marker species are fit for use to solve the issues encountered. The comparison of the Miocene with the Paleocene data also relies mainly on such assemblage characteristics. Faunal compositions in similar depth ranges differ for the late Miocene and the Paleocene. Indications exist that the environmental preferences of genera and of single species may have changed within the last 50 Ma. Therefore, discussion and comparison of Paleocene and Miocene faunal trends is bound to lack great detail, the more so as quantitative faunal data covering the period in-between (Eocene, Oligocene and earlier Miocene) are scarcely available. Yet, such comparisons are needed in order to increase our knowledge of the evolution of benthic foraminifera and the underlying ecological principles.

3. Major perturbations during the Cenozoic

To put our data in a wider context, we will first briefly sketch the events that most prominently affected the benthic communities during the Cenozoic (see Fig. 1).

3.1. "Catastrophic events" in the Cenozoic benthic environment

Major crises, or catastrophes, in the marine environment bear a number of similar characteristics. The onset of these crises, except for the most instantaneous ones (possibly the K/Pg boundary), is characterised by diminishing diversity, and increasing dominance of stress tolerating benthic foraminiferal species. Post-crisis development includes repopulation of the benthic environment. Contrary to recurrent and reversible perturbations, related to the Earth's orbital parameters (sapropel formation in the

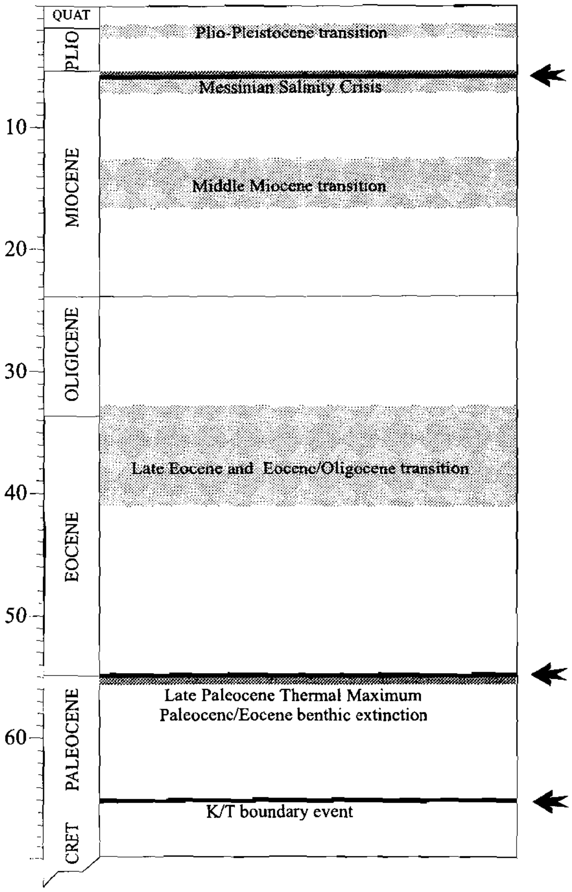

Figure 1. Overview of main disturbances of the benthic environment during the Cenozoic. Light grey shading indicates gradual turnovers (Eocene/Oligocene, middle Miocene, Plio-Pleistocene). Dark grey shading indicates periods preceding or following benthic extinction levels. Arrows indicate levels of actual crises.

Mediterranean since the Miocene), the effects are irreversible. Many of the repopulating taxa were already present in the previous time slice, but new species also appear.

3.1.1. Cretaceous/Paleogene boundary extinction event

The Cretaceous/Paleogene boundary event affected terrestrial as well as marine biota. As recorded in the El Kef section (Tunisia), the event seems to have taken place more or less instantaneously, i.e. almost within the resolution of sampling (e.g. Speijer and Van der Zwaan, 1996, but see a.o. Keller, 1988). It led to the extinction of planktonic taxa and temporary disappearance of a large number of formerly common benthic species. Recovery of the benthic environment after the event is characterised by discrete steps in the build-up of the benthic associations (e.g. Speijer and Van der Zwaan, 1996; Chapter 2). Dominant species in the earliest Paleocene record are *Hormosina* spp. (~30%, a very short-lived dominance) and, throughout the P1a planktonic foraminiferal zone, *Cibicidoides pseudoacutus*. Both taxa were already present in low numbers in the Cretaceous samples. Starting at the P1a-P1b transition, the frequency of *C. pseudoacutus* diminished and gradually a diverse benthic association was re-established. This association consisted of a mix of Cretaceous taxa that remained present throughout the boundary interval, a number of so-called "Lazarus species" that reappeared after the P1a zone, and new species that were not recorded at the site prior to the K/Pg event.

3.1.2. Paleocene/Eocene boundary benthic extinction event

Contrary to the crisis at the Cretaceous/Paleogene boundary, the event at the Paleocene/Eocene transition affected the deep oceanic benthic environment most profoundly (Speijer et al., 1997; Thomas, 1998). The benthic records in the Tethyan area also reveal that its nature was quite different from the K/Pg event. Environmental instability already started during the late Paleocene (Speijer et al., 1996a, b; Schmitz et al., 1997; Speijer and Schmitz, 1998; this thesis, Chapter 2). The actual crisis, however, occurred within a relatively short time span (Schmitz et al., 1997; Norris and R hl, 1999: ~150 kyr). It was attributed to global warming (e.g. Kennett and Stott, 1990; Zachos et al., 1994; Bralower et al., 1995; Norris and R hl, 1999), volcanism (Bralower et al., 1997), decreasing oxygenation of deeper waters, and changing deep oceanic circulation (Kaiho, 1991; Schmitz et al., 1997). The event had a different expression at different water depths. The turnover in the moderate to deep benthic environment was more dramatic than the one at the Cretaceous/Paleogene boundary, and caused many permanent exits (e.g. Speijer et al., 1996a, Schmitz et al., 1997). At neritic sites , however, no extinctions were recorded (Speijer et al., 1996b). Diversity diminished well before the actual event and a number of temporary (Lazarus) extinctions were recorded. Post-crisis species composition differed from site to site and was probably related to depth. At Gebel Aweina (Egypt; paleodepth approximately 200-300 m) the immediate post-crisis benthic environment was dominated by *Bulimina* species, with some *Cibicides* and other spiral taxa (Speijer and Schmitz, 1998). At Zumaya (northern Spain) and in deep Atlantic sites, temporary predominance of *Nuttalides truempyi* occurred (Tjalsma & Lohmann, 1983; Thomas and Shackleton, 1996; Schmitz et al., 1997). New species gradually evolved during the Eocene (a.o. *Globocassidulina subglobosa*).

3.1.3. Late Miocene: the Messinian Salinity Crisis

Although the effects of the Messinian salinity crisis were probably not restricted to the Mediterranean area, evaporite deposition was local and most prominently affected the Mediterranean semi-enclosed basin (see Chapter 6, Fig. 1). Evaporite deposition lasted from 5.96 to 5.33 Ma (Lourens et al., 1996; Krijgsman et al., 1999b) and left the benthic environment practically devoid of foraminifera. Ongoing development towards this crisis started as early as ~7.16 Ma, more than a million years before actual evaporite deposition, and was recorded by benthic faunas in the deeper Mediterranean basins (this thesis, Chapters 3, 4, 7). Recovery of the benthic environment after the Messinian salinity crisis mainly consisted of the gradual return of Lazarus taxa (Wright, 1978, 1980; Brolsma, 1978; Van der Zwaan, 1983; Sprovieri and Hasagawa, 1990). Earliest Pliocene deeper-water assemblages were dominated by *Oridorsalis umbonatus* (Wright, 1980; Sprovieri and Hasagawa, 1990). No permanent extinctions were reported, and no new species entered immediately after the event. In this sense, the event was the least dramatic of the three.

3.2. Gradual changes during the Cenozoic: replacement of benthic species and genera

The periods in which more gradual turnover of benthic species occurred, bear different characteristics than the events mentioned above. In fact, no events in the true sense are involved in the Mediterranean area. Instead, gradual replacement of species is seen, by others that were probably better adapted to the prevailing environmental conditions. The time spans involved are much longer than during the "catastrophic" events just discussed. Although difficult to assess precisely, the effects of the gradual turnovers appear to be as substantial and long lasting as the more eye-catching catastrophic events.

3.2.1. Middle to late Eocene and transition into the Oligocene

Gradual extinctions and originations of benthic species characterise the second part of the Eocene. On approaching the Eocene/Oligocene boundary, only the turnover of larger benthic foraminifera was more or less abrupt (Adams et al., 1986), and associated with hiatuses in the shallow marine record. Close to the Eocene/Oligocene boundary a sudden decrease in size of smaller benthic foraminifera was described, followed by the extinction of a few species (a.o. *Nuttalides truempyi*; Nocchi et al., 1986; see also Lohman, 1978; Thomas, 1986). This loss of species was balanced by the origination of new species (a.o. within the genera *Uvigerina*, *Sphaeroidina*). The gradual trend towards more enriched $\delta^{18}O$ culminated just after the Eocene/Oligocene boundary. This conspicuous isotope excursion was not correlated with an abrupt faunal turnover, neither planktonic nor benthic (e.g. Boersma, 1986). It has been attibuted to the onset of Southern Hemisphere glaciation (e.g. Boersma, 1986) and according to Mackensen and Ehrmann (1992) can be fully attributed to an ice volume effect.

3.2.2. The middle Miocene faunal transition

During the middle Miocene the preveously open connection between the Tethys and the adjacent Indo-Pacific was gradually closed, transforming a part of the old Tethys into the semi-enclosed Mediterranean basin. The formation of sapropels started around that time (Chamley et al., 1986), and continued to be a dominating feature of the Mediterranean sediments. Literature on smaller benthic foraminifera is scarce, but trends in larger foraminifera imply the development of increasing endemism in benthic associations (Adams et al., 1983; Hottinger, 1983; Drooger, 1995). Meulenkamp and Van der Zwaan (1988) assume that at mid-Burdigalian times the Mediterranean biota were profoundly affected by increasing nutrient supply related to the emerging Alpine relief. Data on *Uvigerina* (Van der Zwaan et al., 1986) show that the middle Miocene was a time of substantial change in Atlantic, Mediterranean and Paratethys assemblages. Mediterranean and oceanic sequences (e.g. Thomas, 1986; Woodruff and Savin, 1989; Ramsay et al., 1998) have in common that the faunal changes were gradual and took place over an extended period of time.

3.2.3. The late Pliocene and the Pliocene/Pleistocene transition

The Late Pliocene and the Pliocene/Pleistocene transition in the Mediterranean marine record show a sequence of extremely well-developed sapropels. Sapropels represent a disturbance of normal marine conditions in the Mediterranean basin, but most post-sapropel environments show the return of the conditions prevailing before. A change in the total assemblage composition in the Late Pliocene overprints these intensive but short-term perturbations of deeper marine muddy systems. Van der Zwaan (1983) demonstrated on the basis of quantitative data that the Late Pliocene climate cooling resulted in increasing dominance of opportunistic and stress-tolerant species. Verhallen (1991) elaborated this picture and reported gradual immigrations of new species. Moreover, he noticed a specific and rapid evolution of other taxa and demonstrated that the environmental changes were paramount in the evolution of for instance *B. marginata*.

4. General assemblage characteristics

Notwithstanding differences in species composition, there are general faunal characteristics with which the Cenozoic benthic associations can be described and compared. Diversity is the most obvious one. Paleocene assemblages from the Mediterranean domain contain as many species as Miocene and Pleistocene ones, especially if similar benthic environments are considered (compare Chapter 2, Fig. 2; Chapter 7, Fig. 5). In most sections covering the range of open marine outer shelf to slope environments, Shannon diversity is in the order of 3 (see Chapter 7, Fig. 5; compare a.o. Den Dulk et al., 1998). Any gross deviation from this number indicates departure from equilibrium conditions: in this sense diversity is an excellent marker of stress in the benthic environment (see also Boltovskoy and Wright, 1976; Murray, 1991). As soon as equilibrium conditions at a site are disturbed, diversity will decrease and certain species may start to dominate assemblages. Dominance - expressed as the relative frequency of the most common taxon - is another rather independent measure of stress in the benthic environment. This stress may pertain to food quality or quantity, oxygen deficiency, deviations from normal salinity or any other disturbance. Calculation of diversity and dominance gives no (or minor) insight in the direct causes for stress.

Cenozoic "catastrophic" events show a (short or long) prelude in which these general effects on benthic faunas can be noticed. Disturbances in the benthic environment preceding both the terminal Paleocene and Miocene events in the Mediterranean area are characterised by decreasing

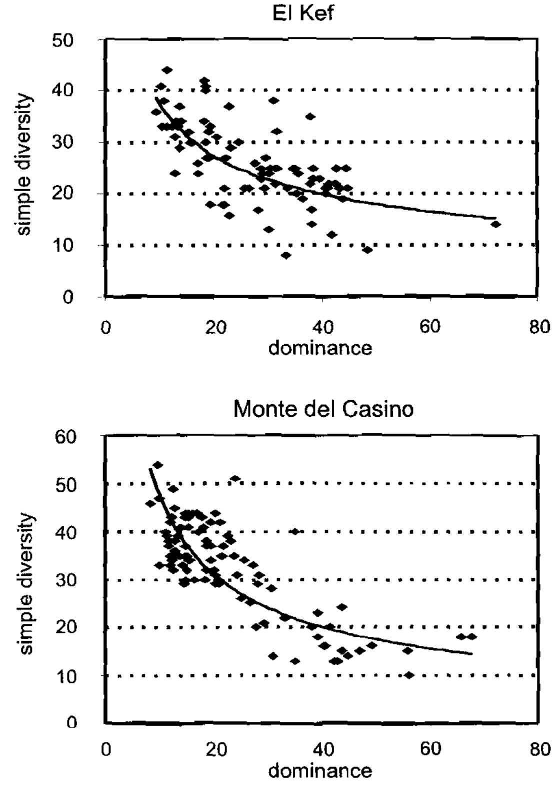

Figure 2. **(a)** Plot of diversity versus dominance of species in the El Kef section (Paleocene). **(b)** Idem for the Monte del Casino section (late Miocene). At a certain point (simple diversity ~20-25, Shannon diversity ~2), diversity no longer diminishes, and increasing dominance indicates stressed environment.

diversity, and increasing dominance of one or more taxa (Chapter 2, Fig. 2; Chapter 3, Fig. 6; Chapter 4, Fig. 4). There seems to be a critical threshold value. When the Shannon diversity falls below 2 (corresponding to a simple diversity of ~20-25), the equitability of the assemblages begins to change (Fig. 2), and the balance in the assemblages is distorted by high dominances of a few stress tolerant taxa. The Miocene sequences illustrate that a gradual (linear) change in salinity results, in the end, in a non-linear response of the fauna characteristics. The assemblages are transformed in a relatively short interval of time through the rapidly increasing dominance of salinity tolerant species (Chapter 7, Fig. 6).

During the more gradual faunal turnovers, for instance in the Late Pliocene, such distinct changes in diversity or dominance did not occurr. In this sense they are completely different and are typically replacement events: elements of the older assemblage became extinct or emigrated, and their place was taken by newly arrived immigrants or locally evolving taxa.

5. Statistical analyses of the total assemblage: ecological structure

Statistical analysis of benthic faunal communities is usually directed at efficient description of general assemblage characteristics, changes in these, and their possible causes. Hierarchical clustering divides the associations into manageable groups. Such groups have certain characteristics in common, often interpreted as similar environmental preferences or even rather similar microhabitats. Factor analysis aims at determining the causes of major environmental trends on the basis of the response of foraminifera to changes in the benthic environment. The latter method proves to be more efficient in younger environments. Time control is better in more recent periods and more of the original components of faunas are preserved. Moreover, younger faunas have more species in common with Recent faunas, which facilitates paleoenvironmental interpretations.

The clustering method for the Paleocene and Miocene sections described in Chapters 2 and 7 is standardised. Although clustering inevitably includes the effect of time, it differentiates in most cases between equilibrium groups at one end of the spectre and stress (or opportunistic) groups at the other (see also Van der Zwaan, 1983). Considering the findings of our studies, we tend to conclude that the basic assemblage structures have not changed through time. Oxygen and food appear to be the main structuring parameters in all cases, and species are basically distributed along these environmental gradients. However, the group of stress tolerant, or opportunistic, taxa seems to be growing over time. Compared with the Paleocene assemblages, a larger number of Miocene species is able to cope with stressed conditions (see Fig. 3a: percentage of bi- and triserially arranged taxa). Comparison of Paleocene and Miocene assemblages makes another feature evident: stress taxa or opportunistic taxa can be recognised by their abundancy patterns. The equilibrium taxa occur in low and regular frequences, but the opportunistic taxa display large fluctuations in relative frequencies and have high peak abundances.

Considering our data and those from the literature, the main impression is that cluster analysis is a good method to decipher the ecological structure of the benthic assemblages. Moreover, comparing Paleocene and late Miocene data, it appears that the main assemblage structure basically remained unchanged over the past 50 my.

6. Characteristics at generic and species level

Comparing the relative frequency data and the cluster diagrams from the late Miocene and the earliest and late Paleocene, it is evident that different taxa indicate environmental stress (see Speijer and Van der Zwaan, 1996; Speijer et al., 1996a, b; Speijer and Schmitz, 1998; this thesis, Chapters 2 and 7). During the Paleocene, *Bolivina* and *Uvigerina* species were not frequent; this includes the intervals following the Cretaceous/Paleogene boundary event, and preceding and following the Paleocene/Eocene benthic extinction. Costate and smooth-walled buliminids were present and dominated certain intervals during the late Paleocene, but most prominent in the earliest Paleocene of El Kef was *Cibicides pseudoacutus*. Spiral taxa (*Anomalina*, *Cibicides* and *Valvulineria* spp.) still played an important role in the late Paleocene and early Eocene stressed environments, together with *Bulimina* spp. in the older parts of El Kef and Gebel Aweina (Speijer at al., 1996a; Speijer et al., 1998; this thesis, Chapter 2).

6.1. Cenozoic genera and groups: specialisation?

Only primitive uvigerinids are recorded in the Paleocene sections. Tall and slender (e.g. *Coryphostoma* and *Loxostomoides* spp.) as well as short and broad bolivinids (e.g. *Bolivinoides draco draco* (Cretaceous of El Kef), evidently ecological predecessors of taxa as *Bolivina*, were present but never frequent. All were ornamented, and the short and broad types at best resemble the Miocene to Recent reticulate bolivinids, that are in their turn not related to extremely stressed conditions either. It appears that during the Eocene the *Bolivina* and *Uvigerina* species gained importance (Fig. 3a). Van der Zwaan et al. (1986) give an overview of *Uvigerina* development during the Cenozoic in the Tethys and Paratethys areas, showing the first numerically important occurrences of the *Uvigerina semiornata* group during the Eocene. Grünig (1977) describes development in *Bolivina* and *Uvigerina* species towards more "modern" forms during the Eocene, together with increasing frequencies of these species in sections in Italy and Spain. She found a subdivision of ornamentation in *Uvigerina*, with spinose *Uvigerina* in deeper waters and costate to smooth types at shallower depths. Van Leeuwen (1986) found a

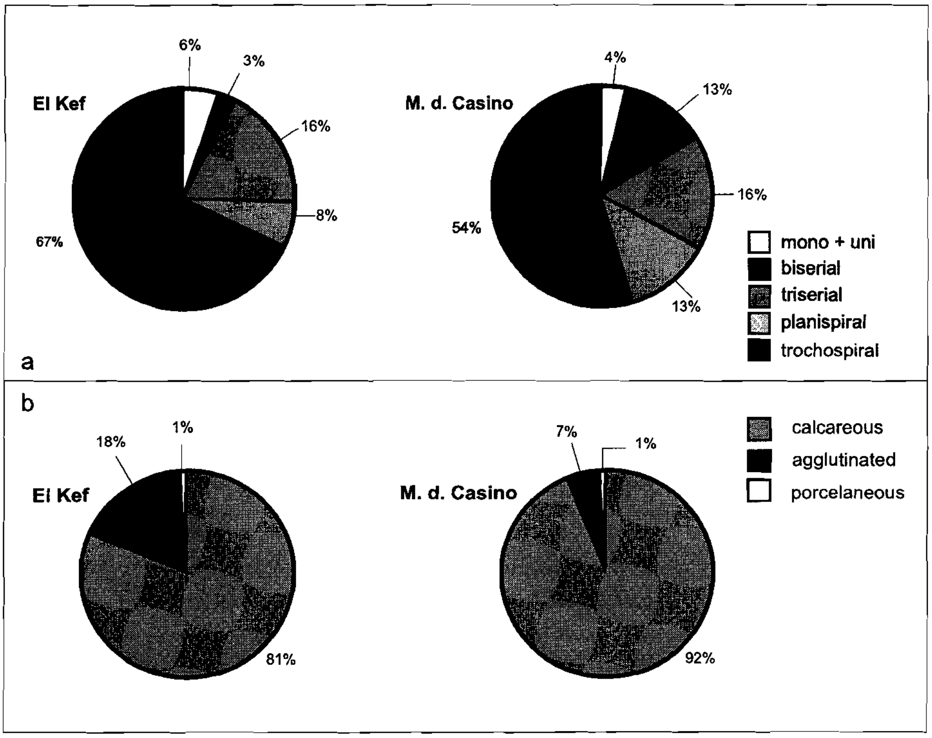

Figure 3. **(a)** Joint relative frequencies of five major perforate benthic fauna groups in a Paleocene (El Kef) and a late Miocene (Monte del Casino) section. An increase in the proportion of biserial taxa is seen, at the cost of uniserial and trochospiral taxa. **(b)** Joint relative frequencies of porcelaneous, perforate and agglutinated taxa in a Paleocene (El Kef) and a late Miocene (Monte del Casino) section. Relative percentages of porcelaneous taxa have remained more or less unchanged. The proportion of trochospiral taxa apparently expanded at the expense of agglutinated forms.

similar distribution of ornamentation versus depth for recent and subrecent *Uvigerina peregrina* in the Angola Basin. Grünig (1977) also describes a development in *Bolivina* species, that co-occurs with increasing frequencies of these taxa in the sections she studied (e.g. *Bolivina antegressa angulata - B. dentata*, *Bolivina nobilis - B. gracilis*). In this case the development is probably related to shallowing. Pika Biolzi and Rögl (1996) described benthic foraminifera from the Paleogene/Neogene boundary GSSP at Lemme-Carrosio (Italy), that was deposited at > 1000 m. The samples contain *Uvigerina*, mainly spinose and spinicostate, but *Bolivina* occurs only in low numbers. This may be related to deposition in an open marine equilibrium environment. In the open ocean "modern" stress taxa are also scarce. In the southern Atlantic *Bolivina* spp. were only present in low abundances from Eocene to early Miocene (Boersma, 1977).

Bulimina species, costate as well as smooth-walled (*B. midwayensis*, *B. strobila/ farafraensis*, *Turrilina brevispira*, *B. quadrata/ovata* plexus, *Sporobulimina eocaena*) were well represented during the Paleocene. Some of these taxa indicated more or less stressed environments by showing high relative frequencies in assemblages with decreasing diversity (*B. midwayensis*, *B. strobila/farafraensis*, *B. quadrata/ovata* plexus: Speijer et al., 1996a, b; Speijer and Schmitz, 1998; this thesis, Chapter 2). Costate *Bulimina* species in Miocene and Recent assemblages indicate moderate stress. Extremely stress-tolerant forms like *B. aculeata* and relatives were not yet present in the Paleocene and were not mentioned in the Eocene or earliest Miocene (see Grünig, 1977; Pika Biolzi and Rögl, 1996). *B. aculeata* may have evolved during the early to middle Miocene, and evolved into *B. marginata* during the Pliocene (Verhallen, 1991).

Agglutinated taxa were found in considerable frequencies (sometimes >70%) in shallow Paleocene and Eocene sequences (Grünig, 1977; Speijer et al., 1996a, b; Speijer and Schmitz, 1998; this thesis, Chapter 2). They include well-cemented *Spiroplectammina/Spiroplectinella*, *Vulvulina* and *Haplophragmoides* spp., the latter mainly dominating the shallower environments prior to the Paleocene/ Eocene boundary event. Today, similar precentages of agglutinated taxa are found in hyper-or hyposaline marsh environments. Pika Biolzi and Rögl (1996) found finely agglutinated taxa (e.g. *Karreriella*) in the Lemme-Carrosio section, dwelling at depths exceeding 1000 m. Some Miocene sections also contain a fair amount of agglutinated foraminifera, the maximum being some 25% (Gibliscemi: mainly *Karreriella* and *Eggerella*). Miocene agglutinants occured at all depths, but not in the percentages that were found in shallow Paleocene material (Fig. 3b). Over the whole, there seems to be a difference between Paleocene and Miocene proportions of agglutinants, except maybe for the extremely stressed shallow (but still marine) environments. Under modern conditions, these environments are often inhabited by calcareous taxa, amongst others *Buliminella*, *Stainforthia* and *Cancris* (Van der Zwaan and Jorissen, 1991; Alve, 1995), and not by agglutinants.

Porcelaneous taxa (mainly miliolids) are not frequent in Paleocene assemblages. Grünig (1977) recorded moderate frequencies of miliolids in Eocene assemblages, in material from lagoonal environments from Northern Italy and Northern Spain. During the late Miocene, miliolids reach frequencies of 20% in some open marine slope environments (e.g. Monte Gibliscemi), but this is an exception in our material. Notwithstanding the scattered record, it appears that the minimum-maximum proportion of miliolids remained rather constant during the Cenozoic (Fig. 3b). In Plio-Pleistocene assemblages from the Arabian Sea, a relation was found between the presence of certain types of miliolids and bottom-water oxygenation (Den Dulk et al., subm.).

The Cenozoic development of epiphytic taxa is illustrated by the differences between the Paleocene and Miocene sections. Epiphytic taxa are rare in Paleocene sections. The late Miocene Faneromeni section (~300-400 m) contains up to 30% of epiphytic and shallow-water taxa belonging to several genera (e.g. *Elphidium*, *Asterigerina*, *Discorbis*, *Gavellinopsis*). Grünig (1977) found *Asterigerina* spp. in Eocene material, together with rare *Elphidium*. These taxa probably evolved during the Eocene, and continued evolving in the Plio-Pleistocene. *Ammonia* spp. are rarely found in Miocene samples, but are a dominant feature of the Pliocene to Recent shallow Mediterranean (e.g. Hageman, 1979; Jorissen, 1988).

6.2. Depth migration: marginalisation?

Depth migration was mentioned as a factor in Eocene changes in benthic foraminiferal associations (Boersma, 1977). Indications exist that the development of new species is associated with migration of pre-existing species to greater depths. An example may be *Siphonina prima* (*Pulsiphonina prima*) as compared to *Siphonina reticulata* (*S. bradyana*). *S. prima* is found in Paleocene and Eocene assemblages at moderate depths (~200-300 m). Its Miocene counterpart, *S. reticulata*, is abundant in Miocene open marine environments at water depths of 500 m and (much) more. *Anomalina* and *Anomalinoides* species are on the whole more scarce in Miocene to Recent material than they are in older sediments, and their occurrence became more restricted to deeper- water environments. *Nodosaria* spp., *Stilostomella* spp. and monothalamous taxa were abundant and sometimes dominant in Eocene environments (e.g. Grünig, 1977), but in the Miocene-Pliocene and Recent assemblages they are only abundant in deeper water environments. The reason may be that these taxa were unable to adapt to the more specialised habitat occupation that developed in shelf- and upper bathyal environments during the Cenozoic, and were forced into the deeper and more remote oceanic areas.

6.3. Cenozoic development of microhabitat partitioning?

In the course of the Cenozoic, a shift has occurred in benthic taxa that record stressed bottom-water environments. Many of the new taxa that evolved are now known to be stress-tolerant: *Bolivina*, *Uvigerina*, and a number of *Bulimina* spp. Many of these taxa live as potential or deep infauna (e.g. Corliss and Emerson, 1990; Barmawidjaja et al., 1992; De Stigter et al., 1998a, b). Comparison of dominant morphogroups in, for instance, Paleocene and Miocene environments gives the impression that deep infaunal habitats were not yet occupied in the Paleocene. The development of stress during the late Paleocene is characterised by peak frequencies of costate and smooth buliminids, and *Cibicidoides* and *Anomalinoides* species. Late Miocene assemblages representing stressed conditions at the sea floor contain large relative frequencies of smooth-walled *Bulimina* and *Bolivina* spp., and sometimes rectuvigerinids. Only a few spiral taxa are associated with moderate stress during the Miocene (e.g. *Cibicides pseudoungerianus* at moderate depths). In spite of gaps in the geological record, the development of benthic associations appears to be characterised by exploration of deeper sediment layers and increasing partitioning of the benthic habitat. The main step in this evolution seem to have taken place during the middle Miocene, when many modern and specialised forms apparently invaded the deeper sediment layers exploring for food.

References

Adams, C.G., 1976. Larger foraminifera and the late Cenozoic history of the Mediterranean region. Palaeogeography, ~climatology, ~ecology, 20: 47-66.

Adams, C.G., Benson, R.H., Kidd, R.B., Ryan, W.B.F., and Wright, R.C., 1977. The Messinian salinity crisis and evidence of late Miocene eustatic changes in the world ocean. Nature, 269: 383-386.

Adams, C.G., Gentry, A.W. and Whybrow, P.J., 1983. Dating the terminal Tethyan event. In: J.E. Meulenlamp (Ed.), Reconstruction of marine paleoenvironments. Utrecht Micropaleont. Bull., 30: 273-298.

Adams, C.G., Butterlin, J. and Samanta, B.K., 1986. Larger Foraminifera and events at the Eocene-Oligocene boundary in the Indo-West Pacific region. In: Ch. Pomerol and I. Premoli Silva (Eds.): Terminal Eocene Events. Developments in Palaeontology and Stratigraphy, 9: 237-252.

Adelseck, C.G., Jr. and Berger, W.H., 1975. On the dissolution of planktonic foraminifera and associated microfossils during settling and on the sea floor. Cushman Found. Foram Res., Spec. Publ., 13: 70-81.

Alve, E., 1995. Benthic foraminiferal distribution and recolonisation of formerly anoxic environments in Drammersfjord, southern Norway. Mar. Micropaleont., 25: 2-3.

Alve, E., 1999. Colonization of new habitats by benthic foraminifera: a review. Earth Science Reviews, 46(1-4): 167-185.

Alve, E. and Bernhard, J.M., 1995. Vertical migratory response of benthic foraminifera to controlled oxygen concentrations in an experimental mesocosm. Marine Ecology Progress Series, 116: 137-151.

Aubert, J. and Berggren, W.A., 1976. Paleocene benthic foraminiferal biostratigraphy and paleoecology of Tunisia. Bull. Centre Rech. Pau – SNPA, 10: 379-469.

Baggley, K.A., 1998. The Late Tortonian - Early Messinian foraminifera record of the Abad Member (Turre Formation), Sorbas Basin, Almería, southeastern Spain. Ph.D. Thesis, University of Greenwich, 145 pp.

Bandy, O.L., 1973. Chronology and paleoenvironmental trends, late Miocene - early Pliocene, western Mediterranean. In: C.W. Drooger (Ed.), Messinian Events in the Mediterranean. KNAW - Geodynamics Scientific Report, 7, North-Holland Publishing Co., Amsterdam: 21-25.

Bandy, O.L. and Chierici, M.A., 1966. Depth-temperature evaluation of selected California and Mediterranean bathyal foraminifera. Mar. Geol., 4: 259-271.

Barbieri, R., 1998. Foraminiferal paleoecology at the Tortonian/Messinian boundary, Atlantic coast of northwestern Morocco. J. of Foram. Res., 28(2): 102-123.

Barmawidjaja, D.J., Jorissen, F.J., Puskaric, S., Van der Zwaan, G.J., 1992. Microhabitat selection by benthic foraminifera in the northern Adriatic Sea. Journal of Foraminiferal Research, 22(4): 297-317.

Benson, R.H., 1976. Changes in the Ostracodes of the Mediterranean with the Messinian salinity crisis. Palaeogeography, ~climatology, ~ecology, 20: 147-170.

Benson, R.H., 1991. Messinian Salinity Crisis. Encyclopedia of Earth System Science 3, 161-167.

Benson, R.H. and Rakic El Bied, K., 1991. The Messinian parastratotype at Cuevas del Almanzora, Vera Basin, SE Spain: Refutation of the deep-basin, shallow-water hypothesis? Micropaleontology, 37: 289-302.

Benson, R. H., K. Rakic-El Bied, and G. Bonaduce, 1991, An important current reversal (influx) in the Rifian Corridor (Morocco) at the Tortonian-Messinian boundary: The end of Tethys Ocean, Paleoceanography, 6(1): 164-192.

Berger, W. H., and Vincent, E., 1986, Deep-sea carbonates: Reading the carbon-isotope signal. Geol. Rundschau, 75: 249-269.

Berger, W.H. and Diester-Haass, L., 1988. Paleoproductivity: the benthic/planktonic ratio in foraminifera as a productivity index. Mar. Geol., 81: 15-25.

Berger, W.H. and Herguera, J.C., 1992. Reading the sedimentary record of the ocean's productivity. In: P.G. Falkowski and A.D. Woodhead (Eds.), Primary Productivity and Biogeochemical Cycles in the Sea. Plenum Press, New York.

Berggren, W.A., 1974a. Late Paleocene-Early Eocene benthonic foraminiferal biostratigraphy and paleoecology of Rockall Bank. Micropal., 20: 426-448.

Berggren, W.A., 1974b. Paleocene benthonic foraminiferal biostratigraphy, biogeography and paleoecology of Libya and Mali. Micropal., 20: 449-465.

Berggren, W.A., 1982. Role of ocean gateways in climatic changes, Studies in Geophysics, Climate in Earth History. National Academy of Sciences Press, Washington, D.C., pp. 43-54.

Berggren, W.A. and Aubert, J., 1975. Paleocene benthonic foraminiferal biostratigraphy, paleobiogeography and paleoecology of Atlantic-Tethyan regions: Midway-type fauna. Palaeogeography, ~climatology, ~ecology, 18: 73-192.

Berggren, W.H. and Haq, B.U., 1976. The Andalusian Stage (late Miocene): Biostratigraphy, biochronology and paleoecology. Palaeogeography, ~climatology, ~ecology, 20: 67-129.

Berggren, W.A. and Miller, K.G., 1988. Paleogene tropical planktonic foraminiferal biostratigraphy and magnetobiochronology. Micropaleontology, 34: 362-380.

Berggren, W.A., Kent, D.V., Swisher, C.C. and Aubry, M.-P., 1995. A revised Cenozoic geochronology and chronostratigraphy. S.E.P.M. Spec. Publ., 54: 129-212.

Bernhard, J.M., 1986. Characteristic assemblages and morphologies of benthic foraminifera from anoxic, organic-rich deposits; Jurassic through Holocene. J. Foram. Res., 16(3): 207-215.

Bertini, A., Londeix, L., Maniscalco, R., Di Stefano, A., Suc, J.-P., Clauzon, G., Gautier, F. and Grasso, M., 1998. Paleobiological evidence of depositional conditions in the Salt Member, Gessoso-Solfifera Formation (Messinian, Upper Miocene) of Sicily. Micropaleontology, 44(4): 413-433.

Béthoux, J.-P., 1993. Mediterranean sapropel formation, dynamic and climatic viewpoints. Oceanol. Acta, 16(2): 127-133.

Boersma, A., 1977. Eocene to early Miocene benthic foraminifera, DSDP Leg 39, South Atlantic. In: P.R. Supko, K. Perch-Nielsen et al., Init. Res. DSDP, 39. US Gov. Printing Office.

Boersma, A., 1986a. Eocene-Oligocene Atlantic paleo-oceanography, using benthic foraminifera. In: Ch. Pomerol and I. Premoli Silva (Eds.): Terminal Eocene Events. Developments in Palaeontology and Stratigraphy, 9: 225-236.

Boersma, A., 1986b, Biostratigraphy and biogeography of Tertiary bathyal benthic foraminifers: Tasman Sea, Coral Sea and on the Chatham Rise, In: J.P. Kennett, C. von der Borch et al. (Editors), Init. Rep. DSDP, 90, 961-1035.

Boltovskoy, E. and Wright, R., 1976. Recent foraminifera. Dr. W. Junk b.v., The Hague, U.S.A.

Bou Dagher, M., 1987. The Stainforthidae (Foraminifera) in the Late Paleocene and Early Eocene of Tunisia. Bull. Centre Rech. Expl. Prod. Elf-Aquitaine, 11: 133-152.

Bralower, T.J., Zachos, J.C., Thomas, E., Parrow, M., Paull, C.K., Kelly, D.C., Premoli Silva, I., Sliter, W.V. and Lohmann, K.C., 1995. Late Paleocene to Eocene paleoceanography of the equatorial Pacific Ocean: Stable isotopes recorded at Ocean Drilling Program Site 865, Allison Guyot. Paleoceanography, 10(4): 841-865.

Bralower, T.J., Thomas, D.J., Zachos, J.C., Hirschmann, M.M., Röhl, U., Sigurds- son, H., Thomas, E. and Whitney, D.L., 1997. High-resolution records of the late Paleocene thermal maximum and circum-Caribbean volcanism: Is there a causal link? Geology, 25(11): 963-966.

Breit, G. H. and Wanty, R.B., 1991. Vanadium accumulation in carbonaceous rocks: A review of geochemical controls during deposition and diagenesis. Chem. Geol., 91: 83-97.

Brinkhuis, H. and Zachariasse, W.J., 1988. Dinoflagellate cysts, sea level changes and planktonic foraminifers across the Cretaceous-Tertiary boundary at El Haria, Northwest Tunisia. Mar. Micropal., 13: 153-191.

Brinkhuis, H., Romein, A.J.T., Smit, J. and Zachariasse, W.J., 1994, Danian-Selandian dinoflagellate cysts from lower latitudes with special reference to the El Kef section, NW Tunisia. GFF, 166: 46-48.

Brolsma, M.J., 1978. Quantitative foraminiferal analysis and environmental interpretation of the Pliocene and topmost Miocene on the south coast of Sicily. Utrecht Micropaleont. Bull., 18, 159 pp.

Calieri, R., 1996. Planktonic foraminiferal biostratigraphy and cyclostratigraphy of the Tortonian-Messinian boundary: preliminary results from the Faneromeni section (Crete). Palaeopelagos, 6: 329-338.

Calieri, R., 1997. Biostratigrafia e cicli paleoclimatologici del Messiniano inferiore (confronta tra i sedimenti del versante Adriatico e guelli del Mediterraneo orientale). Doctoral Thesis, University of Bologna.

Calvert, S. E., and Pedersen, T.F., 1993. Geochemistry of Recent oxic and anoxic marine sediments: Implications for the geological record. Mar. Geol., 113: 67-88.

Cande, S.C. and Kent, D.V., 1992. A new Geomagnetic Polarity Time Scale for the Late Cretaceous and Cenozoic, J. Geoph. Res., 97: 13917-13951.

Cande, S.C. and Kent, D.V., 1995. Revised calibration of the Geomagnetic Polarity Time Scale for the Late Cretaceous and Cenozoic, J. Geoph. Res., 100: 6093-6095.

Chamley, H., Meulenkamp, J.E., Zachariasse, W.J. and Van der Zwaan, G.J., 1986. Middle to Late Miocene marine ecostratigraphy: clay minerals, planktonic foraminifera and stable isotopes from Sicily. Oceanologica Acta, 9(3): 227-238.

Cita, M.B., 1976. Biodynamic effects of the Messinian Salinity Crisis on the evolution of planktonic foraminifers in the Mediterranean. Palaeogeography, ~climatology, ~ecology, 20: 23-42.

Cita, M. B., 1979. Lacustrine and hypersaline deposits in the deep sea and their bearing on paleoenvironment and paleoecology, In: M. Talwani et al. (Editors), Deep Sea Drilling Results in the Atlantic Ocean: Ocean Crust, Maurice Ewing Ser., 2, AGU Washington, DC: 402-419.

Cita, M.B. and Zocchi, M., 1978. Distribution patterns of benthic foraminifera on the floor of the Mediterranean sea. Oceanol. Acta, 1: 445-462.

Cita, M.B. and Ryan, W.B.F., 1979. Late Neogene environmental evolution. In: U. von Rad and W.B.F. Ryan (Eds.): DSDP, Initial Reports, 47A: 447-459.

Colalongo, M.L., di Grande, A., d'Onofrio, S., Gianelli, L., Iaccarino, S., Mazzei, R., Poppi, B., M. F., Romeo, M., Rossi, A., Salvatorini, G., 1979, A proposal for the Tortonian-Messinian boundary. Ann. Géol. Pays. Hellén. Tome hors ser.: 285-294.

Conradsen, K., Bergsten, H., Knudsen, K.L., Nordberg, K. and Seidenkrantz, M.-S., 1994. Recent benthic foraminiferal distribution in the Kattegat and the Skagerrak. Scandinavia. Cushm. Found. Foramin. Res., Spec. Publ. 32: 53-68.

Corliss, B.H. and Chen, C., 1988. Morphotype patterns of Norwegian Sea deep sea benthic foraminifera and ecological implications. Geology, 16: 716-719.

Corliss, B.H. and Emerson, S., 1990. Distribution of Rose Bengal stained deep-sea benthic foraminifera from the Nova Scotia continental margin and Gulf of Maine. Deep-Sea Research, 37: 381-400.

De Jager, J. (1979), The relation between tectonics and sedimentation along the 'Sillaro Line', Geologica Ultraiectina, 19.

De Rijk, S., Troelstra, S. R., Rohling, E. J., 1999. Benthic foraminiferal distribution in the Mediterranean Sea. J. Foramin. Res. 29, 93-103.

Den Dulk, M., Reichart, G.J., Memon, G.M., Roelofs, E.M.P., Zachariasse, W.J. and Van der Zwaan, G.J., 1998. Benthic foraminiferal response to variations in surface water productivity and oxygenation in the northern Arabian Sea. Mar. Micropaleont., 35: 43-66.

Den Dulk, M., Reichart, G.J., Van Heyst, S., Zachariasse, W.J. and Van der Zwaan, G.J. (subm). Benthic foraminifera as proxies of organic matter flux and bottom water oxygenation? – A case history from the northern Arabian Sea.

Dercourt, J., Ricou, L.E., Vrielynck, B. (Editors), 1993. Atlas Tethys Palaeoenvironmental Maps. Gauthier Villars, Paris, 307 pp.

De Stigter, H.C., Jorissen, F.J. and Van der Zwaan, G.J., 1998a. Bathymetric distribution and microhabitat partitioning of live (Rose Bengal stained) benthic foraminifera along a shelf to deep sea transect in the southern Adriatic Sea. Journal of Foraminiferal Research, 28: 40-65.

De Stigter, H.C., Van der Zwaan, G.J. and Langone, L., 1998b. Differential rate of benthic foraminiferal test production in surface and subsurface sediment habitats in the southern Adriatic Sea. Journal of Foraminiferal Research,

D'Onofrio, S., Gianelli, L., Iaccarino, S., Morlotti, E., Romeo, E., Salvatorini, G., Sampo, M.,Sprovieri, R., 1975. Planktonic foraminifera of the Upper Miocene from some Italian sections and the problem of the lower boundary of the Messinian. Boll. Soc. Paleontol. Ital. 14: 177-196.

Donze, P., Colin, J.P., Damotte, R., Oertli, H.J., Peypouquet, J.-P. and Said, R., 1982. Les ostracodes du Campanien terminal à l'Eocène inférieure de la coupe du Kef, Tunisie Nord-Occidentale. Bull. Centre Rech. Expl. Prod. Elf-Aquitaine, 6: 273-307.

Douglas, R.C. and Woodruff, F., 1981. Deep-Sea Benthic Foraminifera. In: C. Emiliani (Ed.), The Oceanic Lithosphere. The Sea, Vol. 7: 1233-1327.

Drooger, C.W., 1979. Marine connections of the Neogene Mediterranean deduced from the evolution and distribution of larger foraminifera. Ann. Géol. Du Pays Hell., Tôme hors Série, vol. 1: 361-369.

Drooger, C.W., 1995. Radial foraminifera: morphometrics and evolution. Verhandelingen der Koninklijke Nederlandse Akademie van Wetenschappen, Afd. Natuurkunde, Eerste Reeks, 41: 1-242.

Drooger, M. M., 1982. Quantitative range chart analysis. Utrecht Micropal. Bull., 26.

Duermeijer, C.E., Van Vught, N., Langereis, C.G., Meulenkamp, J.E. and Zachariasse, W.J., 1998. A major late Tortonian rotation phase of the Crotone Basin using AMS as tectonic tilt correction and timing of the opening of the Tyrrhenian Basin. Tectonophysics, 287: 233-249.

Duermeijer, C.E. and Langereis, C.G. The late Neogene to Recent geodynamic evolution of the central Mediterranean and the role of the African promontory: a paleomagnetic approach. Tectonics (subm.).

Ernst, S.R., Duijnstee, I.A.P., Jannink, N.T. and Van der Zwaan, G.J. Experimental study of microhabitat preferences and mobility of benthic foraminifers, with special reference to *Leptohalysis scotti*. Fifth Int. Workshop on Agglutinated Foraminifers, Plymouth, Sept. 1997. Grzybowski Foundation, Spec. Publ., 7, in press.

Ferretti, S., and Terzi, C., 1995. Late Miocene isotope stratigraphy and astronomical calibration of the Monte del Casino section (northern Apennines, Italy), Giornale di Geol., Ser. 3a, 57(1,2): 99-112.

Foresi, L.M., Iaccarino, S., Mazzei, R. and Salvatorini, G., 1998. New data on middle to late Miocene calcareous plankton biostratigraphy in the Mediterranean area. Riv. It. Pal. Strat., 104(1): 95-114.

Gebhardt, H., 1994. Die Tap-mergel in der Provinz Alicante (Südostspanien, Langhium bis Tortonium): Biostratigraphie, Paläogeographie und Paläoökologie. Berliner Geowissenschaftliche Abhandlungen, Reihe A: Geologie und Paläontologie 163: 1-149.

Gebhardt, H., 1999. Middle to Upper Miocene benthonic foraminiferal palaeoecology of the Tap Marls (Alicante Province, SE Spain) and its palaeoceanographic implications. Palaeogeography, -climatology, -ecology, 145: 141-156.

Gibson, T.G., Bybell, L.M. and Owens, J.P., 1993. Latest Paleocene lithologic and biotic events in neritic deposits of southwestern New Jersey. Paleoceanography, 8: 495-514.

Glaçon, G., Vergnaud-Grazzini, C., Iaccarino, S., Rehault, J.P., Randrianasolo, A., Sierro, F.J. and Weaver, P., 1990. Planktonic foraminiferal events and stable isotopic record in the Upper Miocene of the Tyrrhenian Sea, ODP Site 654, Leg 107. In: K.A. Kastens, J. Mascle et al. (Eds.): Proceedings ODP, Scientific Results, 107. College Station, Texas: 415-427.

Gooday, A.J. and Rathburn, A.E., 1999. Temporal variability in living deep-sea benthic foraminifera: a review. Earth Science Reviews, 46(1-4): 187-212.

Gooday, A., Levin, L., Linke, P. and Heeger, T., 1992. The role of benthic foraminifera in deep-sea food webs and carbon cycling. In: G.P. Rowe (Ed.): Deep-Sea Food Chains and the Global Carbon Cycle. Kluwer Academic Publishers, The Netherlands: 62-91.

Grime, J.P., 1973. Evidence for the existence of three primary strategies in plants and its relevance to ecological and evolutionary theory. The Am. Nat., 111: 1169-1194.

Grünig, A., 1977. Palaeoökologische untersuchungen an Eozaenen benthonischen kleinforaminiferen aus Norditalien und Nordspanien. Ph.D. thesis, University of Bern.

Guichard, S., 1997. Evolution de l'environnement dans la zône de l'upwelling Mauritanien pendant les derniers 236,000 ans: le témoignage de l'écosystème benthique. Ph.D. thesis, Bordeaux University, 476 pp.

Gupta A.K. and Srinivasan, M. S., 1992. Uvigerina proboscidea abundances and paleoceanography of the northern Indian Ocean DSDP Site 214 during the Late Neogene, Mar. Micropal., 19: 355-367.

Hageman, J., 1979. Benthic foraminiferal assemblages from Plio-Pleistocene open bay to lagoonal sediments of the western Peloponnesus (Greece). Utrecht Micropaleont. Bull., 20, 171 pp.

Haq, B.U., Hardenbol, J. and Vail, P.R., 1987. Chronology of fluctuating sea levels since the Triassic. Science, 325 : 1156-1167.

Haq, B. U., Hardenbol, J. and Vail, P. R., 1988. Mesozoic and Cenozoic chronostratigraphy and cycles of sea-level change, SEPM Spec. Pub., 42: 71-108.

Hastings, D. W., Emerson, S. R. and Mix, A. C., 1996. Vanadium in foraminiferal calcite as a tracer for changes in the areal extent of reducing sediments, Paleoceanography, 11(6): 665-678.

Hilgen, F.J., 1991. Astronomical calibration of Gauss to Matuyama sapropels in the Mediterranean and implications for the Geomagnetic Palarity Time Scale. Earth Planet. Sci. Lett. 104: 226-244.

Hilgen, F.J., Krijgsman, W., Langereis, C.G., Lourens, L.J., Santarelli, A., and Zachariasse, W.J., 1995. Extending the astronomical (polarity) time scale into the Miocene. Earth Plan. Sc. Lett., 136: 495-510.

Hilgen, F.J., Krijgsman, W., Raffi, I., Turco, E. and Zachariasse, W.J. Integrated stratigraphy and astronomical calibration of the Serravallian/Tortonian boundary section at Monte Gibliscemi (Sicily, Italy). Mar. Micropaleont., in press

Hodell, D.A. and Kennett, J.P., 1986. Late Miocene-early Pliocene stratigraphy and paleoceanography of the south Atlantic and southwest Pacific Oceans: A synthesis, Paleoceanography, 1: 285-311.

Hodell, D.A., Elmstrom, K.M. and Kennett, J.P., 1986. Latest Miocene benthic $d^{18}O$ changes, global ice volume, sea level an the 'Messinian salinity crisis'. Nature, 320: 411-414.

Hodell, D.A., Benson, R.H., Kennett, J.P. and Rakic-El Bied, K., 1989. Stable isotope stratigraphy of latest Miocene sequences in northwest Morocco: the Bou Regreg section. Paleoceanography, 4: 467-482.

Hodell, D.A., Benson, R.H., Kent, DV., Boersma, A. and Rakic-El Bied, K., 1994. Magnetostratigraphic, biostratigraphic, and stable isotope stratigraphy of an Upper Miocene drill core from the Salé Briqueterie (northwest Morocco): A high-resolution chronology for the Messinian stage. Paleoeanography, 9: 835-855.

Hottinger, L., 1983. Processes determining the distribution of larger foraminifera in space and time. In: J.E. Meulenkamp (Ed.): Reconstruction of marine paleoenvironments. Utrecht Micropaleont. Bull., 30: 239-254.

Hsü, K.J. and Bernoulli, D., 1978. Genesis of the Tethys and the Mediterranean. In: R.B. Kidd, P.J. Worstell et al., Init. Repts. DSDP, 42: 943-949. U.S. Govt. Printing Office, Washington.

Hsü, K. J., Cita, M. B. and Ryan, W. B. F., 1973. The origin of the Mediterranean evaporites. Init. Rep., DSDP, XIII ; 1203-1231.

Jannink, N.T., Zachariasse, W.J. and Van der Zwaan, G.J., 1998. Living (Rose Bengal stained) benthic foraminifera from the Pakistan continental margin (northern Arabian Sea). Deep-Sea Research I, 45: 1483-1513.

Jonkers, H. A., 1984. Pliocene benthic foraminifera from homogeneous and laminated marls on Crete. Utrecht Micropaleont. Bull., 31.

Jorissen, F.J., 1987. The distribution of benthic foraminifera in the Adriatic Sea. Mar. Micropaleontol. 12: 21-48.

Jorissen, F.J., 1988. Benthic foraminifera from the Adriatic Sea; principles of phenotypic variation. Utrecht Micropaleont. Bull., 37: 174 pp.

Jorissen, F.J., 1999. Benthic foraminiferal successions across Late Quaternary Mediterranean sapropels. Mar. Geol., 153: 91-101.

Jorissen, F.J., Barmawidjaja, D.M., Puskaric, S. and Van der Zwaan , G.J., 1992. Vertical distribution of benthic foraminifera in the northern Adriatic Sea: the relation with organic flux. Mar. Micropaleont., 19: 131-146.

Jorissen, F.J., De Stigter, H.C. and Widmark, J.G.V., 1995. A conceptual model explaining benthic foraminiferal habitats. Mar. Micropaleont., 22: 3-15.

Kaiho, K., 1991. Global changes of Paleogene aerobic/anaerobic benthic foraminifera and deep-sea circulation. Palaeogeography, ~climatology, ~ecology, 83: 65-85.

Kaiho, K., 1994. Benthic foraminiferal dissolved-oxygen index and dissolved-oxygen levels in the modern ocean. Geology, 22: 719-722.

Kaiho, K., 1999. Effect of organic carbon flux and dissolved oxygen on the benthic foraminiferal oxygen index (BFOI). Marine Micropaleontology, 37: 67-76.

Kastens, K.A., 1992. Did glacio-eustatic sealevel drop trigger the Messinian salinity crisis? New evidence from Ocean Drilling Program site 654 in the Tyrrhenian Sea. Paleoceanography, 7: 333-356.

Kastens, K.A., Mascle, J., Auroux, C., et al., 1987. Proceedings ODP., Init. Reports, 107, Part A. College Station, Texas.

Katz, M.E. and Thunell, R.C., 1984. Benthic foraminiferal biofacies associated with Middle Miocene to Early Pliocene oxygen-deficient conditions in the eastern Mediterranean. J. Foramin. Res. 14: 187-202.

Katz, M.E. and Miller, K.G., 1991. Early Paleogene benthic foraminiferal assemblages and stable isotopes in the Southern Ocean. In: P.F. Ciesielski, Y. Kristoffersen et al. (Eds): Proceedings of the Ocean Drilling Program, Scientific Results, 114: 481-512.

Keigwin, L. D., 1987. Toward a high-resolution chronology for latest Miocene paleoceanographic events. Paleoceanography, 2(6): 639-660.

Keller, G., 1988. Biotic turnover in benthic foraminifera across the Cretaceous/ Tertiary boundary at El Kef, Tunisia. Palaeogeography, ~climatology, ~ecology, 66: 153-171.

Keller, G., 1992. Paleoecologic response of Tethyan benthic foraminifera to the Cretaceous/Tertiary boundary transition. In: Y. Takayanagi and T. Saito (Editors): Studies in Bebthic Foraminifera. Benthos '90 Sendai, 1990. Tokai University Press, Tokyo: 77-91.

Keller, G. and Lindinger, M., 1989. Stable isotope, TOC and $CaCO_3$ record across the Cretaceous/Tertiary boundary at El Kef, Tunisia. Palaeogeography, ~climatology, ~ecology, 73: 243-265.

Kennett, J.P. and Stott, L.D., 1990. Proteus and proto-Oceanus: Ancestral Paleogene oceans as revealed from Antarctic stable isotopic results; ODP Leg 113. In: P.F. Barker, J.P. Kennett et al., Proc. ODP, Sci. Res., 113: 865-880.

Kellough, G.R., 1965. Paleoecology of the Foraminiferida of the Wills Point Formation (Midway Group) in northeast Texas. Gulf Coast Assoc. Geol. Socs., Trans., 15: 73-153.

Kennett, J.P. and Stott, L.D., 1991. Abrupt deep-sea warming, palaeoceanographic changes and benthic extinctions at the end of the Palaeocene. Nature, 353: 225-229.

Kouwenhoven, T.J., Seidenkrantz, M.-S. and Van der Zwaan, G.J., 1998. The prelude to the Messinian salinity crisis, 6th International Conference on Paleoceanography, 23-29.8.98, Lisbon, Portugal, p.144.

Kouwenhoven , T.J., Seidenkrantz, M.-S. and Van der Zwaan, G.J., 1999. Deep-water changes: The near-synchronous disappearance of a group of benthic foraminifera from the late Miocene Mediterranean. Palaeogeography, ~climatology, ~ecology, 152: 259-281.

Krijgsman, W., Hilgen, F.J., Langereis, C.G., Santarelli, A., Zachariasse, W.J., 1994. The age of the Tortonian/Messinian boundary. Earth Planet. Sci. Lett. 121, 533-547.

Krijgsman, W., Hilgen, F.J., Langereis, C.G., Santarelli, A., Zachariasse, W.J., 1995. Late Miocene magnetostratigraphy, biostratigraphy and cyclostratigraphy in the Mediterranean. Earth Planet. Sci. Lett. 136, 475-494.

Krijgsman, W., Hilgen, F.J., Negri, A., Wijbrans, J.R. and Zachariasse, W.J., 1997. The Monte del Casino section (Northern Apennines, Italy): a potential Tortonian/ Messinian boundary stratotype? Palaeogeography, ~climatology, ~ecology, 133: 27-47.

Krijgsman, W., Langereis, C.G., Zachariasse, W.J., Bocaletti, M., Moratti, G., Gelati, R., Iaccarino, S., Papani, and Villa, G., 1999a. Late Neogene evolution of the Taza-Quercif Basin (Rifian Corridor, Morocco) and implications for the Messinian salinity crisis. Marine Geology, 153: 147-160.

Krijgsman, W., Hilgen, F.J., Raffi, I., Sierro, F.J. and Wilson, D.S., 1999b. Chronology, causes and progression of the Messinian salinity crisis. Nature, 400: 652-655.

Lacombe, H. and Tchernia, P., 1972. Caractères Hydrologiques et Circulation des Eaux en Méditerranée. In: D.J. Stanley (Ed.): The Mediterranean Sea: A Natural Sedimentation Laboratory. John Wiley & Sons, Inc.

Langereis, C.G., Zachariasse, W.J. and Zijderveld, J.D.A., 1984. Late Miocene magnetobiostratigaphy of Crete. Mar. Micropaleont., 8: 261-281.

Laskar, J., 1990. The chaotic motion of the solar system: A numerical estimate of the size of the chaotic zones. Icarus 88, 266-291.

Laskar, J., Joutel, F., Boudin, F., 1993. Orbital, precessional, and insolation quantities for the Earth from -20 Myr to +10 Myr. Astron. Astrophys. 270, 522-533.

Laurenzi, M.A., Tateo, F., Villa, I.M. and Vai, G.B., 1997. New radiometric datings bracketing the Tortonian/Messinian boundary in the Romagna potential stratotype sections (northern Apennines, Italy). In: A. Montanari, G.S. Odin and R. Coccioni (Eds.), Miocene Stratigraphy, An Integrated Approach. Developments in Palaeontology and Stratigraphy, 15: 493-520.

Linke, P. and Lutze, G.F., 1993. Microhabitat preferences of benthic foraminifera: a static concept or a dynamic adaptation to optimize food aquisition? Mar. Micropaleont., 20: 215-234.

Lohmann, G.P., 1978. Abyssal benthonic foraminifera as hydrographic indicatiors in the western South Atlantic Ocean. J. Foramin. Res., 8: 6-34.

Loubère, P., 1994. Quantitative estimation of surface ocean productivity and bottom water oxygen concentration using benthic foraminifera. Paleoceanography, 9(5): 723-737.

Loubère, P., 1996. The surface ocean productivity and bottom water oxygen signals in deep water benthic foraminiferal assemblages. Mar. Micropaleont., 28: 247-261.

Loubère, P., 1997. Benthic foraminiferal assemblage formation, organic carbon flux and oxygen concentrations on the outer continental shelf and slope, J. Foram. Res., 27(2): 93-100.

Lourens, L.J., Antonarakou, A., Hilgen, F.J., Van Hoof, A.A.M., Vergnaud-Grazzini, C. and Zachariasse, W.J., 1996. Evaluation of the Plio-Pleistocene astronomical timescale. Paleoceanogr. 11: 391-413.

Luger, P., 1985. Stratigraphie der marinen Oberkreide und des Alttertiärs im südwestlichen Obernil-Becken (SW-Ägypten) unter besonderer Berücksichtigung der Mikropaläontologie, Palökologie und Paläogeographie. Berliner Geowissensch. Abh., Reihe A: Geol. Paläont., 63.

Lutze, G. F., 1977,.Neogene benthonic foraminifera from site 369, Leg 41, DSDP. Init. Rep. DSDP, 41: 659-666.

Lutze, G. F., and Coulbourn, W. T., 1984. Recent benthic foraminifera from the continental margin off northwest Africa: community structure and distribution. Mar. Micropaleont., 8: 361-401.

Lutze, G. F. and Thiel, H., 1989. Epibenthic foraminifera from elevated microhabitats: *Cibicidoides wuellerstorfi* and *Planulina ariminensis*. J. Foram. Res., 19(2): 153-158.

Lutze, G. F., Pflaumann, U. and Weinholz, P., 1986. Jungquartäre Fluktuationen der benthischen Foraminiferenfaunen in Tiefsee-Sedimenten vor NW-Afrika - Eine Reaktion auf Produktionsänderungen im Oberflächenwasser. Meteor Forschungergebnisse, Reihe C: Geologie und Geophysik, 40: 163-180.

Mackensen, A. and Ehrmann, W.U., 1992. Middle Eocene through Early Oligocene climate history and paleoceanography in the Southern Ocean: Stable oxygen and carbon isotopes from ODP sites on Maud Rise and Kerguelen Plateau. Marine Geology, 108: 1-27.

Mackensen, A., Hubberten, H.-W., Bickert, T., Fischer, G., Fütterer, D.K., 1993a. The d^{13}C in benthic foraminiferal tests of *Fontbotia wuellerstorfi* (Schwager) relative to the d^{13}C of dissolved inorganic carbon in Southern Ocean deep water: implications for glacial ocean circulation models. Paleoceanography, 8: 587-610.

Mackensen, A., Hubberten, H.-W., Scheele, N. and Schlitzer, R., 1993a. Decoupling of d^{13}C$_{SCO2}$ and phosphate in Recent Weddell Sea deep and bottom water: Implications for glacial Southern Ocean paleoceanography, Paleoceanography, 11(2): 203-215.

Marchitto, T.M. Jr., Curry. W.B., and Oppo, D.W., 1998. Millenial-scale changes in North Atlantic circulation since the last glaciation. Nature, 393: 557-561.

Martini, E., 1971. Standard Tertiary and Quaternary calcareous nannoplankton zonation. In: A. Faranacci (Ed): Proceedings of the 2nd Planktonic Conference, Roma, 1970, Vol. 2. Tecnoscienza, Roma, Italy: 739-785.

Massiota, P., Cita, M.B. and Mancuso, M., 1976. Benthonic foraminifers from bathyal depths in the eastern Mediterranean. 1st. Int. Symp. on Benthonic Foraminifera of Continental Margin, Part A: Ecology and Biology. Maritime Sediments, Spec. Publ. 1: 251-262.

McKenzie, J.A., Jenkyns, H.C. and Bennett, G.G., 1979/1980. Stable isotope study of the cyclic diatomite-claystones from the Tripoli Formation, Sicily: a prelude to the Messinian salinity crisis. Palaeogeography, ~climatology, ~ecology, 29: 125-141.

Meijer, R., 1998. Astronomical dating of the late Miocene Oued Akrech and Ain el Beida sections (Atlantic margin, northwest Morocco). Graduate thesis, Utrecht University.

Meulenkamp, J.E., and Van der Zwaan, G.J., 1988. On Mediterranean late Cenozoic biotic crises, tectonic events and relative changes of sea level. Paléobiologie Continent., Montpellier XVII: 95-106.

Meulenkamp, J.E., Jonkers, A. and Spaak, P., 1979. Late Miocene to Early Pliocene development of Crete, Proceedings of the VI colloquium on the Geology of the Aegean Region, Athens, pp. 137-149.

Miller, A.R., Tchernia, P., Charnock, H. and Mc Gill, D.A., 1970. Mediterranean Atlas of Temperature, Salinity, Oxygen: Profiles and data from cruises of R.V. Atlantis and R.V. Chain, with distribution of nutrient chemical properties. Edited by A.E. Maxwell et al., Alpine, Braintree, MA, 190 pp.

Moodley, L., Van der Zwaan, G.J., Herman, P.M.J., Kempers, A.J. and Van Breugel, P., 1997. Differential response of Benthic meiofauna to anoxia with special reference to Foraminifera (Protista: Sarcodina). Marine Ecology Progress Series, 158: 151-163.

Moodley, L., Van der Zwaan, G.J., Rutten, G.M.W., Boom, R.C.E. and Kempers, L., 1998a. Subsurface activity of benthic foraminifera in relation to porewater oxygen content: laboratory experiments. Mar. Micropaleont., 34: 91-106.

Moodley, L., Schaub, B.E.M., Van der Zwaan, G.J. and Herman, P.M.J., 1998b. Resistance of benthic foraminifera (Protista: Sarcodina) to hydrogen sulphide. Mar. Ecol. Progress Series, 169: 77-86.

Müller, D. W., and Hsü, K. J., 1987. Event stratigraphy and paleoceanography in the Fortuna Basin (Southeast Spain): A scenario for the Messinian Salinity Crisis, Paleoceanography, 2(6): 679-696.

Murray, J.W., 1991. Ecology and paleoecology of benthic foraminifera. Longman Scientific & Technical., U.K., 397 pp.

Negri, A. and Vigliotti, L., 1997. Calcareous nannofossil biostratigraphy and paleomagnetism of the Monte Tondo and Monte del Casino sections (Romagna Apennine, Italy), In: A. Montanari, G. S. Odin, and R. Coccioni (Eds.), Miocene Stratigraphy, An Integrated Approach, Elsevier, Amsterdam: 477-492.

Negri, A., Giunta, S., Hilgen, F.J., Krijgsman, W. and Vai, G.B., 1999. Calcareous nannofossil biostratigraphy of the M. del Casino section (northern Apennines, Italy) and paleoceanographic conditions at times of late Miocene sapropel formation. Mar. Micropaleont., 36: 13-30.

Nesteroff, W.D., 1973. Mineralogy, petrography, distribution, and origin of the Messinian Mediterranean evaporites. In: W.B.F. Ryan, K.J. Hsü et al., Init. Reports DSDP, Vol. 13, Washington (US Gov. Printing Office).

Nijenhuis, I. A., Schenau, S. J., Van der Weijden, C. H., Hilgen, F. J., Lourens L. J. and Zachariasse, W. J., 1996. On the origin of upper Miocene sapropelites: a case study from the Faneromeni section, Crete (Greece). Paleoceanography, 11(5): 633-645.

Nocchi M., Parisi, G., Monaco, P., Monechi, S., Madile, M., Napoleone, G., Ripepe, M., Orlando. M., Premoli Silva, I. and Bice, D.M., 1986. The Eocene-Oligocene boundary in the Umbrian pelagic sequences. In: Ch. Pomerol and I. Premoli Silva (Eds.): Terminal Eocene Events. Developments in Palaeontology and Stratigraphy, 9:25-40.

Norris, R.D. and Röhl, U., 1999. Carbon cycling and chronology of climate warming during the Paleocene/Eocene transition. Nature, 401: 775-778.

Olsson, R.K. and Wise, S.W., Jr., 1987. Upper Paleocene to middle Eocene depositional sequences and hiatuses in the New Jersey Atlantic Margin. In: C.A. Ross and D. Haman (Eds): Timing and Depositional History of Eustatic Sequences: Constraints on Seismic Stratigraphy. Cushman Foundation for Foraminiferal Research, Special Publication, 24: 99-112.

Orszag-Sperber, F., Butterlin, J., Clermonte, J., Colchen, M., Giraud, R., Poisson, A., and Ricou, L.E., 1993. Tortonian palaeoenvironments (11.5 - 6 Ma). In: J. Dercourt, L.E. Ricou, B. Vrielynck (Eds.): Atlas Tethys Palaeoenvironmental Maps. Gauthier Villars, Paris.

Ott d'Estevou, Ph., and Montenat Ch., 1990. Le bassin de Sorbas-Tabernas, Doc. Et Trav. IGAL no. 12-13: 101-128.

Parker, F.L., 1958. Eastern Mediterranean Foraminifera. Reports of the Swedish Deep-Sea Expedition 8: 219-283.

Perch-Nielsen, K., 1981. Nouvelles observations sur les nannofossiles calcaires à la limité Crétacé-Tertiaire, près de El Kef, Tunisie. Cah. Micropaléont., 3: 25-36.

Phleger, F.B. and Soutar, A., 1973. Production of benthic foraminifera in three east Pacific oxygen minima. Micropaleontology, 19: 110-115.

Pianka, E.R., 1978. Evolutionary Ecology. Harper and Row, 2nd edition, 397 pp.

Pika Biolzi, M. and Rögl. F., 1996. Benthic Foraminifera of the Paleogene/Neogene Boundary Section Lemme-Carrosio, Italy. Giorn. Geol., Ser. 3a, 58(1,2): 71-80.

Peypouquet, J.-P., Grousset, F. and Mourquiart, P., 1986. Paleooceanography of the Mesogean Sea based on ostracods of the northern Tunisian continental shelf between the Late Cretaceous and Early Paleogene. Geol. Rundschau, 75: 159-174.

Pflum, C.E. and Frerichs, W.E., 1976. Gulf of Mexico deep-water foraminifers. Cushman Found. Foram. Res., Spec. Publ., 14.

Platt, J. P., and Vissers, R. L. M., 1989. Extensional collapse of thickened continental lithosphere: A working hypothesis for the Alboran Sea and Gibraltar arc. Geology, 17: 540-543.

Poignant, A. and Moissette, P., 1992. Benthic Foraminifera from interbedded marls in a diatomaceous series of the Messinian of Algeria. Neues Jahrbuch für Geologie und Paläontologie, Monatshefte, 11: 657-674.

Postma, G., Hilgen, F.J., Zachariasse, W.J., 1993. Precession-punctuated growth of a late Miocene submarine fan lobe on Gavdos (Greece). Terra Nova 5: 438-444.

Ramsay, A.T.S., Smart, C.W. and Zachos, J.C., 1998. A model of early to middle Miocene deep ocean circulation for the Atlantic and Indian Oceans. In: A. Cramp, C.J. McLeod, S.V. Lee and E.J.W. Jones (Eds.): Geological evolution of ocean basins: results from Ocean Drilling Program. Geol. Soc. Spec. Publ., 131:55-70.

Reichart, G. J., 1997. Late Quaternary variability of the Arabian Sea monsoon and oxygen minimum zone. Geologica Ultraiectina, 154.

Reichart, G.J., Lourens, L.J. and Zachariasse, W.J., 1998. Temporal variability in the northern Arabian Sea Oxygen Minimum Zone (OMZ) during the last 225,000 years. Paleoceanography, 13: 607-621.

Ricci Lucchi, F., 1975. Miocene paleoceanography and basin analysis in the Periadriatic Apennines. In: C. H. Squyres (Editor): Geology of Italy, The Earth Sciences Society of the Lybian Republic: 129-236.

Ricci Lucchi, F., 1986. The Oligocene to Recent foreland basins of the northern Apennines, Spec. Publ. Int. Ass. Sediment., 8: 105-139.

Riding, R., Braga, J.C., Martín, J.M., and Sánchez-Almazo, I.M., 1998. Mediterranean Messianian Salinity Crisis: constraints from a coeval marginal basin, Sorbas, southeastern Spain. Mar. Geol. 146: 1-20.

Robinson, A.R., Malanotte-Rizzoli, P., Hecht, A., Michelato, A., Roether, W., Theocharis, A., Ünlüata, Ü., Pinardi, N., Artegiani, A., Bergamasco, A., Bishop, J., Brenner, S., Christianidis, S., Gacic, M., Georgopoulos, D., Golnaraghi, M., Hausmann, M., Junghaus, H.-G., Lascaratos, A., Latif, M.A., Leslie, W.G., Lozano, C.J., O—uz, T., Özsoy, E., Papageorgiou, E., Paschini, E., Rozentroub, Z., Sansone, E., Scarrazato, P., Schnitzler, R., Spezie, G.-C., Tziperman, E., Zodiatis, G., Athanassiadou, L., Gerges, M. and Osman, M. (The POEM-group), 1992. General circulation of the Eastern Mediterranean. Earth-Science Reviews, 32: 285-309.

Rögl, F., 1999. Circum-Mediterranean paleogeography. In: G.E. Roessner and K. Heissig (Eds.): The Miocene land mammals of Europe. Pfeil Verlag, Munich: 339-348.

Rohling, E.J., De Stigter, H.C., Vergnaud-Grazzini, C. and Zaalberg, R., 1993. Temporary repopulation by low-oxygen tolerant benthic foraminifera within an upper Pliocene sapropel: Evidence for the role of oxygen depletion in the formation of sapropels. Mar. Micropaleont., 22: 207-219.

Rohling, E.J., 1994. Review and new aspects concerning the formation of eastern Mediterranean sapropels. Marine Geology, 122, 1-28.

Rohling, E.J. and Bigg, G.R., 1998. Paleosalinity and $\delta^{18}O$: a critical assessment. J. Geophys. Res., C: Oceans, 103: 1307-1318.

Ruggieri, G. and Sprovieri, R., 1976. Messinian salinity crisis and its paleogeographical implications. Palaeogeography, ~climatology, ~ecology, 20: 13-21.

Ryan, W.B.F., 1973. Geodynamic implications of the Messinian crisis of salinity. In: C.W. Drooger (Ed.), Messinian events in the Mediterranean. North Holland, N.Y.: 26-38.

Ryan, W. B. F., Cita, M.B., Rawson, M.D., Burckle, L.H. and Saito, T., 1974. A paleomagnetic assignment of Neogene stage boundaries and the development of isochronous datum planes between the Mediterranean, the Pacific and Indian Oceans in order to investigate the response of the World Ocean to the Mediterranean "Salinity Crisis". Riv. It. Paleont. Stratigr., 80: 631-688.

Saint-Marc, P., 1993. Biogeographic and bathymetric distribution of benthic foraminifera in Paleocene El Haria Formation of Tunisia. J. Afr. Earth Sc., 15: 473-487.

Saint-Marc, P. and Berggren, W.A., 1988. A quantitative analysis of Paleocene benthic foraminiferal assemblages in Central Tunisia. J. Foram. Res., 18: 97-113.

Salaj, J., Pozaryska, K. and Szczechura, J., 1976. Foraminiferida, zonation and subzonation of the Paleocene of Tunisia. Acta Palaeont. Pol., 21: 127-190.

Salaj, J., 1980. Microbiostratigraphie du Crétacé et du Paléogène de la Tunisie Septentrionale et Orientale (Hypostratotypes Tunisiens). Institut Géologique de Dionyz Stúr, Bratislava, Slovakia, 238 pp.

Salaj, J., 1986. The new Postrugoglobigerina praedaubjergensis zone at the base of the stratotype of the marine Paleocene (El Kef, Tunisia). Geologica Carpathica, 37: 35-48.

Salaj, J., 1994. Contribution à l'étude microbiostratigraphique du Paléocène Moyen (=l'Harien) de la région du Kef (Tunisie septentrionale). Zemní plyn a nafta, 38, 4: 261-289.

Santarelli, A., Brinkhuis, H., Hilgen, F.J., Lourens, L.J., Versteegh, G.J.M. and Visser, H., 1998. Orbital signatures in a Late Miocene dinoflagellate record from Crete (Greece). Marine Micropaleontology, 33: 273-297.

Schenau, S.J., Antonarakou, A., Hilgen, F.J., Lourens, L.J., Nijenhuis, I.A., Van der Weijden, C.H. and Zachariasse, W.J., 1998. Organic-rich layers in the Metochia section (Gavdos, Greece): evidence for a single mechanism of sapropel formation during the past 10 Myr.

Scientific Staff, D. L. 1., Deep Sea Drilling Project: Leg 13, Geotimes, 12-15, 1970.

Schmitz, B., Asaro, F., Molina, E., Monechi, S., Von Salis, K. and Speijer, R.P., 1997. High-resolution iridium, $d^{13}C$, $d^{18}O$, foraminifera and nannofossil profiles across the latest Paleocene benthic extinction event at Zumaya, Spain. Palaeogeography, ~climatology, ~ecology, 133: 49-68.

Seidenkrantz, M.-S., Kouwenhoven, T.J., Jorissen, F.J., Shackleton, N.J., and Van der Zwaan, G.J. Benthic foraminifera as indicators of changing Mediterranean-Atlantic water exchange in the late Miocene. Marine Geology, in press.

Selli, R., 1960. Il Messiniano Mayer-Eymar 1867. Proposta di un neostratotipo. Giorn. Geol., Ser. 2, 28: 1-33.

Sen Gupta, B.K. and Machain Castillo, M.L., 1993. Benthic foraminifera in oxygen-poor habitats. Mar. Micropaleont., 20: 183-201.

Sen Gupta, B.K., Lee, R.F., May, M.S., III, 1989. Upwelling and unusual assemblage of benthic foraminifera on the northern Florida continental slope. J. Paleontol. 55: 853-857.

Shackleton, N.J., Hall, M.A., Pate, D., 1995. Pliocene stable isotope stratigraphy of site 846. In: Pisias, N.G., Mayer, L.A., Janacek, T.R., Palmer-Julson, A., van Andel, T.H., et al., Proc. ODP, Sci. Results, 138: College Station, TX (Ocean Drilling Program), 337-353.

Shackleton, N. J., Crowhurst, S., Hagelberg, T., Pisias, N.G. and Schneider, D.A., 1995. A new late Neogene time scale: Application to Leg 138 sites, In: N. G. Pisias, L. A. Mayer, T. R. Janacek, A. Palmer-Julson, and T. H. Van Andel (Eds.), Proc. ODP, Sci. Res., 138: 517-533.

Sierro, F.J., Flores, J.A., Civis, J., Gonzáles Delgado, J.A. and Francés, G., 1993. Late Miocene globorotaliid event-stratigraphy and biogeography in the NE-Atlantic and Mediterranean. Mar. Micropaleont., 21: 143-168.

Sierro, F. J., Flores, J. A., Zamarreno, I., Vazquez, A., Utrilla, R., Frances, G., Hilgen, F. J. and Krijgsman, W., 1997. Astronomical cyclicity and sapropels in the pre-evaporitic Messinian of the Sorbas basin (western Mediterranean). Geogaçeta, 21: 199-202.

Sierro, F.J., Flores, J.A., Zamarreño, I., Vázquez, A., Utrilla, R., Francés, G., Hilgen, F.J., Krijgsman, W., 1998. Messinian pre-evaporate sapropels and precession-induced oscillations in western Mediterranean climate. Mar. Geol. 153: 137-146.

Sjoerdsma, P. G. and Van der Zwaan, G. J., 1992. Simulating the effect of changing organic flux and oxygen content on the distribution of benthic foraminifers, Mar. Micropaleont., 19: 163-180.

Sonnenfeld, P., 1984. Brines and evaporites. Academic Press, Inc., Orlando, Florida / London, 613 pp.

Speijer, R.P., 1994a. Extinction and recovery patterns in benthic foraminiferal paleocommunities across the Cretaceous/Paleogene and Paleocene/Eocene boundaries. Geologica Ultraiectina, 124: 191 pp.

Speijer, R.P., 1994b. Paleocene sea-level fluctuations recorded in benthic foraminiferal assemblages from Gebel Oweina (Esna, Egypt): local, regional or global patterns? G.F.F., 116: 63-65.

Speijer, R.P., 1995. The late Paleocene benthic foraminiferal extinction as observed in the Middle East. In: P. Laga (Editor): Paleocene-Eocene Boundary Events. Bull. Soc. Belge Geol., 103: 267-280.

Speijer, R.P. and Van der Zwaan, G.J., 1996. Extinction and survivorship of southern Tethyan benthic foraminifera across the Cretaceous/Paleogene boundary. In: M.B. Hart (Ed.), Biotic recovery from mass extinction events, Geol. Soc. Spec. Publ., 102: 343-371.

Speijer, R.P. and Schmitz, B., 1998. A benthic foraminiferal record of Paleocene sea level and trophic/redox conditions at Gebel Aweina, Egypt. Palaeogeography, ~climatology, ~ecology, 137: 79-101.

Speijer, R.P., Schmitz, B., Aubry, M.-P. and Charisi, S., 1996a. The latest Paleocene benthic extinction event: Punctuated turnover in outer neritic foraminiferal faunas from Gebel Aweina, Egypt. Isr. J. Earth Sc., 44: 207-222.

Speijer, R.P., Van der Zwaan, G.J. and Schmitz, B., 1996b. The impact of Paleocene/Eocene boundary events on middle neritic benthic foraminiferal assemblages from Egypt. Mar. Micropaleont., 28: 99-132.

Sprovieri, R., Thunell, R.C. and Howell, M., 1986. Paleontological and geochemical analysis of three laminated sedimentary units of late Pliocene-early Pleistocene age from the Monte San Nicola section in Sicily. Riv. It. Paleont. Strat. 92: 401-434.

Sprovieri, R. and Hasegawa, S., 1990. Plio-Pleistocene benthic foraminifer stratigraphic distribution in the deep-sea record of the Tyrrhenian Sea (ODP Leg 107). In: Kastens, K.A., Mascle, J. et al. (Eds.), Proceedings ODP, Sci. Res., 107: 429-459.

Sprovieri, R., Di Stefano, E. and Sprovieri, M., 1996. High resolution chronology for late Miocene Mediterranean stratigraphic events. Riv. It. Paleont. Stratigr., 102(1): 77-104.

Suess, E., 1980. Particulate organic carbon flux in the oceans – surface productivity and oxygen utilisation. Nature, 288: 260-263.

Tchernia, P., 1980. Descriptive Regional Oceanography. J.C. Swallow (Editor), Pergamon Marine Series, 3, Pergamon Press, 253 pp.

Ten Veen, J., 1998. Neogene outer-arc evolution in the Cretan segment of the Hellenic Arc: tectonic, sedimentary and geodynamic reconstructions. Geologica Ultraiectina, 160, 191 pp.

Thomas, E., 1986. Early to middle Miocene Benthic foraminiferal faunas from DSDP sites 608 and 610, North Atlantic. Geol. Soc. London, Spec. Publ., 21, 205-218.

Thomas, E., 1998. Biogeography of the Late Paleocene Benthic Foraminiferal Extinction. In: M.-P. Aubry, S.G. Lucas and W.A. Berggren (Eds.): Late Paleocene – early Eocene climatic and biotic events in the marine and terrestrial records. Columbia University Press: 214-242.

Thomas, E. and Shackleton, N.J., 1996. The Paleocene-Eocene benthic foraminiferal extinction and stable isotope anomalies. In: R.W.O'B. Knox, R.M. Corfield and R.E. Dunay (Eds.): Correlation of the Early Paleogene in Northwest Europe. Geol. Soc. Spec. Publ., 101: 401-441.

Todd, R., 1958. Foraminifera from western Mediterranean deep-sea cores. Reports of the Swedish Deep-Sea Expedition 8: 169-215, Tables 1-19, plates 1-3.

Tjalsma, R.C. and Lohmann, G.P., 1983. Paleocene-Eocene bathyal and abyssal foraminifera from the Atlantic Ocean. Micropaleontology, Spec. Publ., 4, 94 pp.

Troelstra, S.R., Van de Poel, H.M., Huisman, C.H.A., Geerlings, L.P.A. and Dronkert, H., 1980. Paleoecological changes in the latest Miocene of the Sorbas basin, S.E. Spain. Géologie Mediterranée, Tome 7(1): 115-126.

Turco, E., Hilgen, F.J., lourens, L.J., Scackleton, N.J. and Zachariasse, W.J. (subm). Punctuated evolution of global climate cooling during the late Middle to early late Miocene: High-resolution planktonic foraminiferal and oxygen isotope records from the Mediterranean.

Vai, G. B., 1989. A field trip guide to the Romagna Apennine geology. The Lamone valley. Boll. Soc. Paleontol. Ital., 28(2,3): 343-367.

Vai, G. B., and Ricci Lucchi , F., 1977. Algal crusts, autochtonous and clastic gypsum in a cannibalistic evaporite basin: a case history from the Messinian of Northern Apennines, Sedimentology, 24: 211-244.

Vai, G. B., Villa, I. M. and Colalongo, M. L., 1993. First direct radiometric dating of the Tortonian/Messinian boundary, C. R. Acad. Sci. Paris, Ser. II, 316: 1407-1414.

Vai, G.B., 1997. Cyclostratigraphic estimate of the Messinian Stage duration. In: A. Montanari, G. S. Odin, R. Coccioni (Eds.), Miocene Stratigraphy: An Integrated Approach. Elsevier, Amsterdam: 463-476.

Van Couvering, J.A., Berggren, W.A., Drake, R.E., Aguirre, E. and Curtis, G.H., 1976. The terminal Miocene event. Mar. Micropaleont., 1 ; 263-286.

Van der Meulen, M.J., 1999. Slab detachment and the evolution of the Apenninic Arc (Italy). Geologica Ultraiectina, 170, 136 pp.

Van der Meulen, M. J., Meulenkamp, J. E. and Wortel, M. J. R., 1998. Lateral shifts of Apenninic foredeep depocentres reflecting detachment of subducted lithosphere. Earth Planet. Sci. Lett., 154: 201-218.

Van der Meulen, M.J., Kouwenhoven, T.J., Van der Zwaan, G.J., Meulenkamp, J.E. and Wortel, M.J.R. Late Miocene uplift in the Romagnan Apennines and the detachment of subducted lithosphere. Tectonophysics, in press.

Van de Poel, H.M., 1992. Foraminiferal biostraigraphy and paleoenvironments of the Miocene-Pliocene Carboneras-Nijar Basin (SE Spain). Scripta Geol., 102: 1-32.

Van der Voo, R., 1993. Paleomagnetism of the Atlantic, Tethys and Iapetus oceans. Cambridge University Press, 411 pp.

Van der Zwaan, G.J., 1982. Paleoecology of late Miocene Mediterranean foraminifera. Utrecht Micropaleontol. Bull., 25: 201 pp.

Van der Zwaan, G.J., 1983. Quantitative analyses and the reconstruction of benthic foraminiferal communities. In: J.E. Meulenkamp (Ed.): Reconstruction of marine paleoenvironments. Utrecht Micropaleontol. Bull., 30: 49-70.

Van der Zwaan, G.J., and Thomas, E., 1980. Late Miocene environmental evolution in the Mediterranean area: stable isotopes of planktonic and benthic foraminifera from Crete. Proc. Kon. Ned. Acad. Wetensch., Ser. B., 83(3): 327-343.

Van der Zwaan, G.J. and Den Hartog Jager, D., 1983. Paleoecology of Late Miocene Sicilian benthic foraminifera. Proceedings KNAW, Series B, 86(2): 211-223.

Van der Zwaan, G.J., and Gudjonsson, L., 1986. Middle Miocene - Pliocene stable isotope stratigraphy and paleoceanography of the Mediterranean, Mar. Micropaleont., 10: 71-90.

Van der Zwaan, G.J. and Jorissen, F.J., 1991. Biofacial patterns in river-induced shelf anoxia. In: R.V. Tyson and T.H. Pearson (Eds.): Modern and ancient continental shelf anoxia. Geol. Soc. Spec. Publ.,

Van der Zwaan, G.J., Jorissen, F.J., Verhallen, P.J.J.M. and Von Daniels, C.H., 1986. *Uvigerina* from the eastern Atlantic, North Sea Basin, Paratethys and Mediterranean. Utrecht Micropal.. Bull., 35: 7-20.

Van der Zwaan, G.J., Jorissen, F.J. and De Stigter, H.C., 1990. The depth dependency of planktonic/benthic foraminiferal ratios: Constraints and applications. Marine Geology, 95: 1-16.

Van der Zwaan, G.J., Duijnstee, I.A.P., Den Dulk, M., Ernst, S.R., Jannink, N.T. and Kouwenhoven, T.J., 1999. Benthic foraminifers: proxies or problems? A review of paleoecological concepts. Earth Science Reviews, 46(1-4): 213-235.

Van der Zwaan, G.J., Almogi-Labin, A., Jannink, N.T., Duijnstee, I.A.P., and Jorissen, F.J. (subm.). Apparent oxyphilic benthic foraminifera: a new proxy in paleoceanography for quantitative reconstruction of oxygen content.

Van der Zwaan, G.J., Almogi-Labin, A., Jannink, N.T., Duinstee, I.A.P., and Jorissen, F.J. (subm.). Apparent oxyphilic benthic foraminifera: a new proxy in paleoceanography for quantitative reconstruction of oxygen content.

Van Leeuwen, R.J.W., 1986. The distribution of Uvigerina in the late Quaternary sediments of the deep Eastern South Atlantic. Utrecht Micropaleont. Bull., 35: 47-66.

Vergnaud-Grazzini, C., 1978. Miocene and Pliocene oxygen and carbon isotopic changes at DSDP Sites 372, 374, and 375: Implications for the Pre-Messinian History of the Mediterranean, In: Init. Rep., DSDP, 42A, US Government Printing Office, Washington, DC: 829-836.

Vergnaud-Grazzini, C., 1983. Reconstruction of Mediterranean Late Cenozoic hydrography by means of carbon isotope analysis. Utrecht Micropaleont. Bull., 30: 25-47.

Vergnaud-Grazzini, C., Ryan, W.B.F. and Cita, M.B., 1977. Stable isotope fractionation, climate change and episodic stagnation in the eastern Mediterranean Sea. Sed. Geol., 28: 81-93.

Verhallen, P.J.J.M., 1991. Late Pliocene to early Pleistocene Mediterranean mud-dwelling foraminifera; influence of a changing environment on community structure and evolution. Utrecht Micropaleont. Bull., 40.

Vincent, E., Killingley, J.S. and Berger, W.H., 1980. The magnetic epoch-6 carbon shift: a change in the ocean's $^{13}C/^{12}C$ ratio 6.2 million years ago. Mar. Micropaleont., 5: 185-203.

Vincent, E., Killingley, J.S. and Berger, W.H., 1985. Miocene oxygen and carbon isotope stratigraphy of the tropical Indian Ocean, in: J. P. Kennett (Editor), The Miocene Ocean: Paleoceanography and Biogeography. GSA Memoir, 163: 103-130.

Vrielynck, B., Odin, G.S. and Dercourt, J., 1997. Miocene palaeogeography of the Tethys Ocean: Potential global correlations in the Mediterranean. In: A. Montanari, G.S. Odin, R. Coccioni (Eds.), Miocene Stratigraphy: An Integrated Approach. Development in Palaeontology and Stratigraphy. Elsevier Science B. V., Amsterdam, 157-165.

Weijermars, R., 1988. Neogene tectonics in the western Mediterranean may have caused the Messinian salinity crisis and associated glacial event. Tectonophysics, 148: 211-219.

Wonders, A.A.H. and Van der Zwaan, G.J.. 1979. The smaller benthic foraminifera in the section Potamidha I. Utrecht Micropaleont. Bull., 21: 27-58.

Woodruff, F. and Savin, S.M., 1989. Mid-Miocene isotope stratigraphy in the deep sea: high-resolution correlations, paleoclimatic cycles, and sediment preservation. Paleoceanography, 6: 755-806.

Wortel, M. J. R., and Spakman, W., 1992. Structure and dynamics of subducted lithosphere in the Mediterranean region. Proc. Kon. Ned. Akad. Wetensch., 95: 325-347.

Wright, R., 1978. Neogene paleobathymetry of the Mediterranean based on benthic foraminifers from DSDP Leg 42A. In: K.J. Hsü, L. Montadert et al., Init. Rep. DSDP 42, Pt. 1, U.S. Govern. Printing Office (Washington): 837-847.

Wright, R., 1980. Benthic foraminiferal repopulation of the Mediterranean after the Messinian (Late Miocene) event. Palaeogeography, -climatology, -ecology, 29: 189-214.

Zachariasse, W.J., 1979. Planktonic foraminifera from section Potamidha I: Taxonomic and phyletic aspects of keeled globorotaliids and some paleoenvironmental estimates. Utrecht Micropaleont. Bull., 21: 129-166.

Zachos, J.C., Stott, L.D. and Lohmann, K.C., 1994. Evolution of early Cenozoic temperatures. Paleoceanography, 9(2): 353-387.

Zahn, R., Winn, K. and Sarnthein, M., 1986. Benthic foraminiferal 13C and accumulation rates of organic carbon: *Uvigerina peregrina* group and *Cibicidoides wuellerstorfi*. Paleoceanography 1: 27-42.

Zhang, J. and Scott, D.B., 1996. Integrated stratigraphy and paleoceanography of the Messinian (latest Miocene) across the North Atlantic Ocean. Mar. Micropaleont., 29: 1-36.

Faunal reference list

Below follow faunal reference lists of Paleocene and late Miocene taxa. Nomenclature follows Loeblich and Tappan, 1964 in most cases. References at the end of this section pertain to Miocene species only.

Selected Paleocene species from the El Kef section

Relative frequencies of abundant species are given in Chapter 2, Figure 3. A number of species are pictured in Speijer (1994), and Speijer and Van der Zwaan (1994). Most other species are pictured in Aubert and Berggren (1976), and Luger (1985).

Allomorphina trigona Reuss (Aubert and Berggren, 1976, p. 428, Pl. 7, Fig. 12).
Ammomarginulina aubertae Gradstein and Kaminski (Speijer, 1994, p. 44, Pl. 9, Fig. 5).
Anomalinoides affinis (Hantken) (Speijer, 1994, p. 58, Pl. 6, Fig. 1; p. 162, Pl. 3, Fig. 6). We follow Salaj et al.(1976) in considering *A. welleri* (Plummer) as a junior synonym.
Anomalinoides ekblomi(Brotzen) (Speijer, 1994, p. 58, Pl. 8, Fig. 2).
Anomalinoides praeacutus (Vasilenko) (Speijer, 1994, p. 60, Pl. 8, Fig. 1; p. 164, Pl. 7, Fig. 2).
Anomalinoides rubiginosus (Cushman) (Speijer, 1994, p.60, Pl.8, fig.3; p.164, Pl.1, Fig.5). We follow Van Morkhoven et al.(1986) in considering A. danica Brotzen as a junior synonym.
Anomalinoides simplex (Brotzen) (Speijer, 1994, p.60, Pl.9, Fig.1).
Anomalinoides susanaensis (Browning) (Aubert and Berggren, 1976, p.432, Pl.11, Fig.2a-c; Speijer, 1994, p.62, Pl.10, Fig.3).
Anomalinoides cf. *acutus* (Plummer) (Speijer, 1994, p.58, Pl.10, Fig.2).
Anomalinoides cf. *aegyptiacus* = *Anomalinoides* cf. *aegyptiacus* (LeRoy) (Speijer, 1994, p.116, Pl.5, Fig.2).
Anomalinoides cf. *praeacutus* = cf. *Anomalinoides praeacutus* (Vasilenko). This taxon differs from A. Praeacutus in having pores all over the spiral side.
Arenoturrispirillina sp. 1 = *Ammodiscoides* sp.? *Arenoturrispirillina* sp.? (Aubert and Berggren, 1976, p. 407, Pl. 1, Fig. 2; Speijer, 1994, p. 44, Pl. 9, Fig. 3).
Bolivinoides decoratus (Jones) (Speijer, 1994, p. 46, Pl. 9, Fig. 2)
Bulimina midwayensis Cushman and Parker (Speijer, 1994, p.110, Pl.1, Fig.9).
Bulimina quadrata-ovata plexus, including *B. quadrata* Plummer and *B. ovata* d'Orbigny (Speijer, 1994, p.110, Pl.1, Fig.10).As these species are often flattened by compression, further discrimination is often impossible.
Chilostomelloides eocaenica Cushman (Aubert and Berggren, 1976, p. 427, Pl. 7, Fig. 11).
Cibicidoides abudurbensis (Nakkady) (Speijer, 1994, p.54, Pl.4, Fig.6).
Cibicidoides pseudoacutus (Nakkady) (Speijer, 1994, p.54, Pl.7, Fig.6; p.158, Pl.4, Fig.2).
Cibicidoides cf. *hyphalus* (Fisher) (Speijer, 1994, p.54, Pl.5, Fig.2: biconvex, Fig.3: planoconvex).
Cibicidoides cf. *pseudoperlucidus* (Bykova) (Speijer, 1994, p.114, Pl.2, Fig.2; p.158, Pl.6, Fig.1).
Cibicidoides cf. *succedens* = cf. *Cibicidoides succedens* (Brotzen). This species from the type species in having a more flattened and planoconvex morphology (Speijer, 1994, p. 158, Pl. 6, Fig. 2).
Cibicidoides sp. 1 (Speijer, 1994, p.54, Pl.6, Figs.5-7).

Cibicidoides suzakensis (Bykova) (Speijer, 1994, p.54, Pl.5, Fig.1).
Coryphostoma midwayensis (Cushman) (Aubert and Berggren, 1976, p.420, Pl.4, Fig.10a-c).
Eponides elevatus (Plummer)(Aubert and Berggren, 1976, p. 425, Pl. 7, Fig. 2a-c).
Gaudryina pyramidata Cushman (Speijer, 1994, p.44, Pl.4, Fig.1).
Gavelinella beccariiformis (White) (Speijer, 1994, p.62, Pl.10, Fig.4; p.168, Pl.1, Fig.4).
Gyroidinoides aequilateralis (Plummer) (Kellough, 1965, p.118, Pl.13, Fig.2).
Gyroidinoides girardanus (Reuss) (Speijer, 1994, p.118, Pl.3, Fig.3; p.166, Pl.8, Fig.9).
Gyroidinoides octocameratus (Cushman and Hanna) (Speijer, 1994, p.62, Pl.4, Fig.4).
Gyroidinoides subangulatus (Plummer) (Aubert and Berggren, 1976, p.429, Pl.8, Fig.8a-c).
Gyroidinoides sp. 1 (Speijer, 1994, p.62, Pl.9, Fig.6).
Karreria fallax Rhezak (Luger, 1985, p.113, Pl.9, Fig.11,12).
Loxostomoides applinae (Plummer) (Speijer, 1994, p.109, Pl.1, Fig.11; p.148, Pl.8, Figs.1, 2).
Nonionella ovata Brotzen (Aubert and Berggren, 1976, p.428, Pl.8, Fig.2).
Oridorsalis plummerae (Cushman) (Speijer, 1994, p.58, Pl.6, Fig.8; p.116, Pl.4, Figs.5-7; p.162, Pl.5, Fig.9).
Osangularia plummerae Brotzen (Speijer, 1994, p.56, Pl.7, Fig.5; p.160, Pl.4, Fig.1).
Pseudouvigerina plummerae Cushman (Speijer, 1994, p. 48, Pl. 4, Fig. 2).
Pseudouvigerina sp. 1 (Speijer, 1994, p. 50, Pl. 9, Fig. 1).
Pulsiphonina prima (Plummer) (Speijer, 1994, p.52, Pl.10, Fig.1).
Quadrimorphina allomorphinoides (Reuss) (Luger, 1985, p.109, Pl.7, Fig.16).
Siphogenerinoides eleganta (Plummer) (Speijer, 1994, p.110, Pl.1, Fig.6).
Spiroplectinella dentata (Alth) (Aubert and Berggren, 1976, p.408, Pl.1, Fig.5).
Spiroplectinella esnaensis (LeRoy) (Speijer, 1994, p.147, Pl.3, Fig.1).*Spiroplectinella knebeli* LeRoy is included in this morphotype (Luger, 1985, p. 76, Pl. 3, Fig. 2).
Spiroplectinella cf. *plummerae* = cf. *Spiroplectinella plummerae* (Cushman) (Speijer, 1994, p.147. Pl.9, Fig.1).
Sporobulimina eocena Bykova (Aubert and Berggren, 1976, p.419, Pl.4, Fig.9a-c).
Valvulineria scrobiculata (Schwager) (Speijer, 1994, p.112, Pl.4, Figs.1-3).
Valvulineria(?) *insueta* Cushman and Bermúdez (Speijer, 1994, p.112, Pl.3, Fig.4).

Selected late Miocene species

Ammonia beccarii (Linnaeus): *Nautilus beccarii* Linnaeus, 1758, p. 710, Pl. 1, figs. 1a-c; *Rotalia beccarii* (Linnaeus), Cushman, 1931, p. 58, Pl. 12, figs. 1-7; *Ammonia beccarii* (Linnaeus), Loeblich and Tappan, 1964, p. C607, Pl. 479, figs. 2, 3.
Anomalinoides flintii (Cushman): *Anomalina ammonoides* Flint, 1899 (not Reuss), p. 335, Pl. 78, fig. 4; *Anomalina flintii* Cushman, 1931, p. 108, Pl. 18, fig. 5a-c.
Anomalinoides alazanensis (Nuttall): *Anomalina alazanensis* Nuttall, 1932, p. 31, Pl 8, figs. 5-7.
Anomalinoides grosserugosus (Gümbel): *Truncatulina grosserugosa* Gümbel, 1868, p. 660, Pl. 2, figs. 10a, b; *Anomalina grosserugosa* (Gümbel), Brady, 1884, p. 673, Pl. 94, figs. 4, 5; *Cibicides grosserugosus* (Gümbel), Verhoeve, 1971, p. 59, Pl. 10, fig. 3.
Anomalinoides helicinus (Costa): *Nonionina helicina* Costa, 1855, p. 123, Pl. 1, figs. 18a-c; *Anomalina helicina* (Costa), Christodolou, 1960, p. 89, Pl. 8, figs. 5a-c.
Asterigerina planorbis d'Orbigny, 1846, p. 205, Pl. 11, figs. 1-3; Marks, 1951, p. 66, Pl. 8, fig. 1a-c.

Astrononion italicum Cushman and Edwards, 1937, p. 35, Pl. 3, figs. 19, 20.

Astrononion stelligerum (d'Orbigny): *Nonionina stelligera* d'Orbigny, 1839, p. 128, Pl. 3, figs. 1, 2; *Astrononion stelligerum* (d'Orbigny), Cushman and Edwards, 1937, p. 31, Pl. 3, fig. 7; Barker, 1960, p. 224, Pl. 109, figs. 3, 4.

Bigenerina nodosaria d'Orbigny, 1826, p. 261, Pl. 11, figs. 9-12; Brady, 1884, p. 369, Pl. 44, figs. 14-18; Longinelli, 1956, p. 103, Pl. 12, fig. 1.

Bolivina alata (Seguenza): *Vulvulina alata* Seguenza, 1862, p. 115, Pl. 2, fig. 5; *Bolivina alata* (Seguenza), Cushman, 1937b, p. 106, Pl. 13, figs. 3-11.

Bolivina sp. cf. *B. antiqua* d'Orbigny, 1846, p. 240, Pl. 14, fig. 11-13; Cushman, 1937b, p. 77, Pl. 9, fig. 15, 16.

Bolivina arta (Mcfadyen): *Bolivina arta* Macfadyen, 1930, p. 58, Pl. 4, figs. 21a, b.

Bolivina dilatata Reuss, 1850, p. 381, Pl. 48, figs. 15a, b, c; Macfadyen, 1930, p. 57, Pl. 2, fig.1; Cushman, 1937b, p. 78, Pl. 9, fig. 17-20.

Bolivina hebes Macfadyen, 1930, p. 59, Pl. 2, figs. 5a-c; Cushman, 1937b, p. 82, Pl. 9, figs. 27-29.

Bolivina plicatella Cushman, 1930c, p. 46, Pl. 8, figs. 10a, b; Cushman, 1937b, p. 89, Pl. 11, figs. 3, 4.

Bolivina plicatella Cushman, 1930c, var. *mera* Cushman and Ponton, 1932, p. 82, Pl. 12, figs. 4a, b.

Bolivina plicatella var. *pseudoplicata*: *Bolivina* cf. *B. pseudo-plicata* Heron-Allen and Earland, 1930, p. 81, Pl. 3, figs. 36-40.

Bolivina punctata d'Orbigny, 1839a, p. 63, Pl. 8, figs. 10-12.

Bolivina reticulata Hantken, 1875, p. 65, Pl. 15, figs. 6a, b; Cushman, 1937b, p. 50, Pl. 6, figs. 24-27.

Bolivina scalprata Schwager var. *miocenica* Macfadyen, 1930, p. 61, Pl. 4, figs. 22a, b; *Bolivinoides miocenicus* Gianotti, 1953, p. 38, Pl. 5, figs. 10-13.

Bolivina spathulata (Williamson): *Textularia variabilis* Williamson var. *spathulata* Williamson, 1858, p. 76, Pl. 6, figs. 164, 165; *Bolivina spathulata* (Williamson), Barker, 1960, p. 106, Pl. 52, fig. 20, 21.

Bolivina tortuosa Brady, 1881, p. 57; Brady, 1884, pp. 420-1, Pl. 52, figs. 31-34.

Bulimina aculeata d'Orbigny, 1826, p. 269, mod. 7; Brady, 1884, p. 406, Pl. 51, fig. 7-9; Fornasini, 1902, p. 153, fig. 4.

Bulimina costata d'Orbigny, 1826, p. 269; fig. in Fornasini, 1901, p. 174, Pl. 1; Cushman and Parker, 1938, p. 54, Pl. 9, figs. 1, 2.

Bulimina elegans d'Orbigny, 1826, p. 270, mod. No. 9; Parker, Jones and Brady, 1865, p. 20, Pl. 2, fig. 64; Brady, 1884, pp. 298-9, Pl. 50, figs. 1-4.

Bulimina elongata d'Orbigny, 1846, p. 187, Pl. 11, figs. 19, 20; Cushman and Parker, 1937, p. 49, Pl. 7, figs. 1-3.

Bulimina elongata d'Orbigny var. *lappa*, Cushman and Parker, 1937, p. 51, Pl. 7, fig. 8.

Bulimina elongata d'Orbigny var. *subulata* Cushman and Parker, 1937, p. 51, Pl. 7, figs. 6, 7; *Bulimina aculeata* d'Orbigny var. *minima* Tedeschi and Zanmatti, 1957.

Bulimina inflata Seguenza, 1862, p. 109, Pl. 1, fig. 10; Brady, 1884, pp. 406-7, Pl. 51, figs. 10-13.

Bulimina elongata d'Orbigny var. *lappa* Cushman and Parker, 1937, p. 51, Pl. 7, fig. 8.

Bulimina inflata Seguenza var. *mexicana* Cushman, 1922, p. 95, Pl. 21, fig. 2.

Bulimina striata d'Orbigny, 1826, p. 269; fig. in Fornasini, 1902, p. 372, Pl. 1.

Bulimina tenera Reuss, 1867, p. 94, Pl. 4, figs. 11, 12.

Cancris auricula (Fichtel and Moll): *Nautilus auricula* Fichtel and Moll, 1798, p. 108, 110, Pl. 20, figs. a-c (var. a), figs. d-f (var. b); *Cancris auricula* (Fichtel and Moll), Murray, 1971, p. 136, 137, Pl. 57, figs. 1-7.

Cassidulina carinata (d'Orbigny) Silvestri: *Cassidulina laevigata* d'Orbigny var. *carinata* Silvestri, 1896, p. 104, Pl. 2, fig. 10; Barker, 1960, p. 110, Pl. 54, figs. 2, 3.

Cassidulina crassa d'Orbigny, 1839a, p. 56, Pl. 7, figs. 18-20; Barker, 1960, p. 112, Pl. 54, figs. 4, 5.

Cassidulina laevigata d'Orbigny, 1826, p. 282, Pl. 15, figs. 4, 5; Cushman, 1922a, p. 122, Pl. 24, fig. 4; Dieci, 1959, p. 84, Pl. 7, fig. 7.

Cassidulina sp. cf. *C. laevigata* d'Orbigny, 1826.

Cassidulinoides bradyi (Norman): *Cassidulina bradyi* Norman, 1881, in Brady, 1884, p. 431, Pl. 54, fig. 6-9; *Cassidulinoides bradyi* (Norman), Barker, 1960, p. 112, Pl. 54, fig. 6-9.

Chilostomella oolina Schwager, 1878, p. 527, Pl. 1, fig. 16; Barker, 1960, p. 114, Pl. 55, figs. 12-14, 17, 18.

Chilostomella ovoidea Reuss, 1850, p. 380, Pl. 48, figs. 12a-e; Brady, 1884, p. 436, Pl. 55, figs. 12-14, 17, 18 (not figs. 15, 16, 21-23).

Cibicides bradyi (Trauth): *Truncatulina bradyi* Trauth, 1918, p. 235; *Cibicides bradyi* (Trauth), Barker, 1960, Pl. 95, fig. 5; Pflum and Frerichs, 1976, Pl. 3, figs. 6, 7.

Cibicides dutemplei (d'Orbigny): *Rotalina dutemplei* d'Orbigny, 1846; *Cibicides dutemplei* (d'Orbigny), Batjes, 1958, p. 157, Pl. 8, fig. 9; *Heterolepa dutemplei*, Loeblich and Tappan, 1964, p. C759, Pl. 623, figs. 3a-c; Verhoeve, 1971, p. 108, Pl. 5, figs. 18a-c.

Cibicides italicus Di Napoli Alliata, 1952, p. 3, figs. 1-7.

Cibicides kullenbergi (Parker): *Cibicidoides kullenbergi* Parker, 1953, p. 49, Pl. 11, figs. 7, 8; Wright, 1978, p. 713, Pl. 4, figs. 5-7.

Cibicides lobatulus (Walker and Jacob): *Nautilus lobatulus* Walker and Jacob, 1798, in Kanmacher, p. 642, Pl. 14, fig. 36; *Cibicides lobatulus* (Walker and Jacob), Longinelli, 1956, p. 182, Pl. 6, fig. 12; Hageman, 1979, p. 91, Pl. 3, figs. 6a, b, Pl. 4, figs. 1a, b.

Cibicides pachyderma (Rhezak): *Truncatulina pachiderma* Rhezak, 1886, p. 87, Pl. 1, fig. 5; *Cibicides floridanus* (Cushman), Longinelli, 1956, p. 184, Pl. 6, fig. 14; *Cibicides pachydermis* (Rhezak), Wright, 1978, p. 713, Pl. 3, figs. 19, 20.

Cibicides pseudoungerianus (Cushman): *Truncatulina pseudoungeriana* Cushman, 1922a, p. 97, Pl. 20, fig. 9; *Cibicides pseudoungeriana* Cushman, 1931, p. 123, Pl. 22, fig. 3-7; *Cibicides pseudoungerianus* Cushman, Longinelli, 1956, p. 183, Pl. 6, figs. 9a, b.

Cibicides refulgens De Montfort, 1808, p. 123, Pl. on p. 122; *Truncatulina refulgens* (De Montfort), Brady, 1884, p. 659, Pl. 92, figs. 7-9; *Cibicides refulgens* De Montfort, Loeblich and Tappan, 1964, p. C688, Pl. 554, fig. 1a-c.

Cibicides robertsonianus (Brady): *Truncatulina robertsonianus* Brady, 1881, p. 65; Brady, 1884, p. 664, Pl. 95, fig. 4.

Cibicides tenellus (Reuss): *Truncatulina tenella* Reuss, 1865, p. 477, Pl. 5, fig. 8; *Cibicides tenellus* (Reuss), Batjes, 1958, p. 151, Pl. 9, figs. 3, 4.

Cibicides ungerianus (d'Orbigny): *Rotalina ungeriana* d'Orbigny, 1846, p. 157, Pl. 8, figs. 16-18; *Cibicides ungerianus* (d'Orbigny), Marks, 1951, p. 73, Pl. 8, figs. 2a, b.

Cibicides wuellerstorfi (Schwager): *Anomalina wuellerstorfi* Schwager, 1866; *Planulina wuellerstorfi* (Schwager) Phleger, Parker and Peirson, 1953.

Discorbis advena Cushman: *Discorbina rosacea* Brady (partim), 1884, p. 644, Pl. 87, fig. 1; *Discorbis* *rosacea* Cushman, 1922, p. 40; Cushman, 1931, p. 13, Pl. 2, figs. 8a-c.

Discorbis araucana (d'Orbigny): *Rosalina araucana* d'Orbigny, 1839a, p. 44, Pl. 6, figs. 16-18; *Discorbina araucana* (d'Orbigny), Brady, 1884, p. 645, Pl. 86, figs. 10, 11.

Dorothia gibbosa d'Orbigny, 1826, p. 262, mod. no. 28; *Dorothia gibbosa* (d'Orbigny), Longinelli, 1956, p. 101, Pl. 1, figs. 2-4.

Eggerella bradyi (Cushman): *Verneuilina bradyi* Cushman, 1911, p. 54, Pl. 87, fig. 3; Cushman, 1933, p.120, Pl. 12, fig. 5.

Elphidium aculeatum (Silvestri, 1901): *Polystomella macella* (Fichtel and Moll) var. *aculeata* Silvestri, 1901, p. 45.

Elphidium advenum (Cushman): *Polystomella advena* Cushman, 1922a, p. 56, Pl. 9, figs. 11, 12; *Elphidium advenum* (Cushman), Cushman, 1930b, p. 25, Pl. 10, figs. 1, 2; Barker, 1960, p. 226, Pl. 110, fig. 1.

Elphidium crispum (Linnaeus): *Nautilus crispus* Linnaeus, 1758, p. 709, Pl. 19, figs. a-d; *Elphidium crispum* (Linnaeus), Cushman, 1939, p. 50, Pl. 13, figs. 17-21.

Elphidium fichtellianum (d'Orbigny): *Polystomella fichtelliana* d'Orbigny 1846, p. 125, Pl. 6, figs. 7, 8; *Elphidium fichtellianum* (d'Orbigny), Cushman, 1939, p. 42, Pl. 11, fig. 12.

Elphidium macellum (Fichtel and Moll): *Nautilus macellus* Fichtel and Moll, 1798, p. 66, Pl. 10, figs. h-k; *Elphidium macellum* (Fichtel and Moll), Cushman, 1939, p. 51, Pl. 14, figs. 1-3.

Elpidium poeyanum (d'Orbigny): *Polystomella poeyana* d'Orbigny, 1839b, p. 55, Pl. 6, figs. 25, 26; *Elphidium poeyanum* (d'Orbigny), Cushman, 1929b, p. 54, Pl. 14, figs. 25, 26.

Globocassidulina oblonga (Reuss): *Cassidulina oblonga* Reuss, 1850, p. 376, Pl. 48, figs. 5, 6; *Globocassidulina oblonga* (Reuss), Loeblich and Tappan, 1964, p. C738, Pl. 604, figs. 7a, b.

Globocassidulina subglobosa (Brady): *Cassidulina subglobosa* Brady, 1881, p. 60, fig. in Brady, 1884, p. 430, Pl. 54, fig. 17; Barker, 1960, p. 112, Pl. 54, fig. 17.

Gyroidina soldanii d'Orbigny var. *altiformis* R.E. and K.C. Stewart, p. 67, Pl. 9, fig.2.

Gyroidina longispira Tedeschi and Zanmatti, 1957, p. 253, Pl. 7, figs. a-c.

Gyroidina orbicularis d'Orbigny, 1826, p. 278, mod. 13; Parker, Jones and Brady, 1865, Pl. 3, fig. 85; Loeblich and Tappan, 1964, p.C750, Pl. 614, figs. 5, 6.

Gyroidina parva Cushman & Renz, 1941, p. 23, Pl. 4, fig. 2.

Gyroidina soldanii (d'Orbigny): *Rotalina soldanii* d'Orbigny, 1846, p. 155, Pl. 8, figs. 10-12; *Gyroidina soldanii* (d'Orbigny), Cushman, 1929a, p. 38, Pl. 8, figs. 3-8; Longinelli, 1956, Pl. 14, figs. 16a, b.

Hanzawaia boueana (d'Orbigny): *Truncatulina boueana* d'Orbigny, 1846, p. 169, Pl. 9, figs. 24-26; *Cibicides boueanus* (d'Orbigny), Marks, 1951, p. 72, Pl. 8, fig. 9; *Hanzawaia boueana* (d'Orbigny), Batjes, 1958, p. 154, Pl. 8, fig. 5.

Hoeglundina elegans (d'Orbigny): *Rotalia (Turbulina) elegans* d'Orbigny, 1826, p. 276, no. 54; *Hoeglundina elegans* (d'Orbigny), Christodolou, 1960, p. 115, Pl. 9, figs. 5, 6.

Karreriella bradyi (Cushman): *Gaudryina pupoides* (not d'Orbigny, 1840), Brady, 1884, p. 378, Pl. 46, figs. 1-4; *Gaudryina bradyi,* Cushman, 1911, p. 67, Pl. 2, figs. 107a-c; *Karreriella bradyi* (Cusman), Dieci, 1959, p. 21, Pl. 1, fig. 15.

Martinottiella communus (d'Orbigny): *Clavulina communis* d'Orbigny, 1826, p. 102, no. 4; d'Orbigny, 1846, p.196, Pl. 12, figs. 1, 2; *Martinotiella communis* (d'Orbigny), Dieci, 1959, p. 23, Pl. 1, fig. 18.

Melonis barleeanum (Williamson): *Nonionina barleeana* Williamson, 1858, p. 32, Pl. 3, figs, 68, 69.

Neoeponides schreibersii (d'Orbigny, 1846): *Rotalia schreibersii* d'Orbigny, 1846, p. 154, Pl. 8, figs. 4-6;

Eponides schreibersii (d'Orbigny), Barker, 1960, p. 236, Pl. 115, fig. 1a-c.

Nonion pompilioides (Fichtel and Moll): *Nautilus pompilioides* Fichtel and Moll, 1798, p. 31, Pl. 2, figs. a-c; *Nonion pompilioides* (Fichtel and Moll), Cushman, 1930b, p. 4, Pl. 1, figs. 7-11; *Melonis pompilioides* (Fichtel and Moll), Murray, 1971, p. 199, Pl. 84, figs. 1-7.

Oridorsalis stellatus (Silvestri): *Truncatulina tenera*? Brady, var. *stellata* Silvestri, 1898, p. 297, Pl. 6, figs. 9a-c; *Oridorsalis stellatus* (Silvestri), Brolsma, 1978, Pl. 3, Fig. 2.

Patellina corrugata Williamson, 1858, p. 48, Pl. 3, figs. 86- 89; Cushman, 1931, p. 11, Pl. 2, figs. 6, 7.

Planorbulina mediterranensis d'Orbigny, 1826, p. 280, Pl. 14, figs. 4-6; Von Daniels, 1970, p. 89, Pl. 8, fig. 4.

Planulina ariminensis d'Orbigny, 1826, p. 280, Pl. 14, figs. 1-3; Loeblich and Tappan, 1964, p. C686, Pl. 552, fig. 1, Pl. 553.

Pleurostomella alternans Schwager, 1866, p. 238, Pl. 6, figs. 79, 80; McFadyen, 1930, p. 63, Pl. 1, figs. 25a, b; Christodolou, 1960, p. 57, Pl. 7, figs. 30, 31.

Pullenia bulloides (d'Orbigny): *Nonionina bulloides* d'Orbigny, 1846, p. 107, Pl. 5, figs. 9, 10; *Pullenia bulloides* (d'Orbigny), Dieci, 1959, p. 87, Pl. 7, fig. 16; Christodolou, 1960, p. 56, Pl. 2, figs, 11, 12.

Pullenia quinqueloba (Reuss): *Nonionina quinqueloba* Reuss, 1851, p. 71, Pl. 5, fig. 31; *Pullenia quinqueloba* (Reuss), Brady, 1884, p. 617, Pl. 84, figs. 14, 15; Marks, 1951, p. 69, Pl. 7, fig. 19.

Quinqueloculina seminula (Linnaeus): *Serpulina seminulum* Linnaeus, 1758, p. 786; *Quinqueloculina seminula* (Linnaeus), Brady, 1884, p. 157, Pl. 5, fig. 6; Loeblich & Tappan, 1964, p. C458, Pl. 349, fig. 1.

Reussella spinulosa (Reuss): *Verneuilina spinulosa* Reuss, 1850, p. 374, Pl. 47, figs. 12a-c; *Reussella spinulosa* (Reuss), Loeblich and Tappan, 1964, p. C563, Pl. 445, figs. 3-5.

Rosalina globularis d'Orbigny, 1826, p. 271, Pl. 13, figs. 1-4; Loeblich and Tappan, 1964, p. C584, Pl. 459, fig. 1; Murray, 1971, p. 135, Pl. 56, figs. 1-6.

Sigmoilopsis schlumbergeri (Silvestri): *Sigmoilina schlumbergeri* Silvestri, 1904, p. 267; Loeblich and Tappan, 1964, p. C466, Pl. 353, figs. 2a-c.

Siphonina planoconvexa (Silvestri): *Truncatulina reticulata* (Czjzek) var. *planoconvexa* Silvestri, 1898, p. 300, Pl. 6, figs. 12a-c; *Siphonina planoconvexa* (Silvestri), Dieci, 1959, p. 81, Pl. 7, fig. 1.

Siphonina reticulata (Czjzek): *Rotalina reticulata* Czjzek, 1848, p. 145, Pl. 13, figs. 7-9; *Truncatulina reticulata* (Czjzek), Brady, 1884, p. 669, Pl. 96, figs. 8a-c; *Siphonina bradyana* (Czjzek), Cushman, 1927, p. 11, Pl. 1, figs. 4a-c; *Siphonina reticulata* (Czjzek), Loeblich and Tappan, 1964, p. C591, Pl. 468, fig. 1a, b.

Siphotextularia concava (Karrer): *Plecanium concavum* Karrer, 1868, p. 129, Pl. 1, fig. 3.

Sphaeroidina bulloides d'Orbigny, 1826, p. 267, mod. 65; d'Orbigny, 1846, p. 284, Pl. 20, figs. 19, 20; Longinelli, 1956, p.77, Pl. 10, fig. 1.

Spiroplectammina deperdita (d'Orbigny): *Textularia deperdita* d'Orbigny, 1846, p. 244, Pl. 14, figs. 23-25.

Trifarina angulosa (Williamson): *Uvigerina angulosa* Williamson, 1858, p. 67, Pl. 5, fig. 140; *Angulogerina angulosa* (Williamson), Barker, 1960, p. 154, Pl. 74, figs. 15, 16.

Uvigerina bononiensis Fornasini, 1888, p. 48, Pl. 3, fig. 12; Cushman & Todd, 1941, p. 74, Pl. 18, fig. 1; Pl. 19, figs. 14-16; *Hopkinsina bononiensis* (Fornasini), Marks, 1951, p. 62, 63, Pl. 7, fig. 8.

Uvigerina cylindrica cylindrica (d'Orbigny): *Clavulina cylindrica* d'Orbigny, 1826, p. 268; Fornasini, 1897, pp. 13-14; *Rectuvigerina cylindrica* Salvatorini, 1966, p. 664, Pl. 2, figs. 1-5; *Uvigerina cylindrica cylindrica* Thomas, p. 150, Pl. 1, figs. 1a-c, Pl. 5, figs. 3, 5.

Uvigerina cylindrica gaudryinoides Lipparini, 1932: *Uvigerina tenuistriata* Reuss var. *gaudryinoides* Lipparini, 1932, p. 65, Pl. 3, figs. 7, 8, *Uvigerina cylindrica gaudryinoides* Lipparini, Thomas, 1980, p. 150-151, Pl.1, figs. 2a-c, Pl. 4, figs. 5, 6, Pl. 5, figs. 2, 4, 7.

Uvigerina peregrina Cushman, 1923, p. 166, Pl. 42, fig. 7-10.

Uvigerina proboscidea Schwager, 1866, p. 250, Pl. 7, fig. 96.

Uvigerina pygmaea d'Orbigny, 1826, p. 269, Pl. 12, fig. 8,9, mod. no. 67; d'Orbigny, 1846, p. 190, Pl. 11, fig. 25, 26.

Uvigerina rutila Cushman and Todd, 1941, p. 78, Pl. 20, figs. 16-22.

Uvigerina striatissima Perconig, 1955, p. 187, Pl. 3, figs. 1-4.

Valvulineria complanata (d'Orbigny): *Rosalina complanata* d'Orbigny, 1846, p. 175, Pl. 10, figs. 13-15; *Discorbina bradyana* Fornasini, 1900, p. 393, Pl. 43, fig. 1; *Valvulineria bradyana* (Fornasini), Longinelli, 1956, p. 168, Pl. 24, figs. 3a, b.

Vulvulina pennatula (Batsch): *Nautilus (Orthoceras) pennatula* Batsch, 1791, Pl. 4, figs. 13a-d; *Vulvulina pennatula* (Batsch), Dieci, 1959, p. 18, Pl. 1, fig. 8a.

References

Barker, R.W., 1960, Taxonomic notes on the species figured by H.B. Brady in his Report on the Foraminifera dredged by the H.M.S. Challenger during the years 1873 - 1876. Soc. Econ. Pal. And Mineral., Spec. Publ., 9, Tulsa, Oklahoma.

Batjes, D.A.J., 1958, Foraminifera of the Oligocene of Belgium, Mém. Inst. Roy. Sci. Belg., Vol. 143, 188 pp., Brussels.

Batsch, A. I. G. C., 1791, Sechs Kupfertafeln mit Conchiliën de Seesandes, gezeignet und gestochen von A.J.G.K. Batsch: 6 Pl., Jena.

Brady, H.B., 1881, Notes on some of the reticularian Rhizopoda of the Challenger Expedition, Pt. 3, Quart. J. Micr. Sci., vol. 21, London.

Brady, H.B., 1884, Report on the Foraminifera dredged by H.M.S. Challenger, during the years 1873-1876, In: Report on the Scientific Results of the Voyage of H.M.S. Challenger during the years 1873-1876. Zoölogy, Vol. 9, 814 pp., London.

Brolsma, M.J., 1978, Quantitative foraminiferal analysis and environmental interpretation of the Pliocene and topmost Miocene on the south coast of Sicily, Utrecht Micropaleont. Bull., 18, 159 pp.

Christodolou, G., 1960, Geologische und mikropaläontologische Untersuchungen auf der Insel Karpathos (Dodekanesos), Paläontographica, Abt. A, Bd. 115 , 143 pp., 16 Tafeln, 23 Abb., Stuttgart.

Costa, O.G., 1855, Foraminiferi fossili della marne Torziari di Messina, R. Accad. Sci. Napoli, Vol. 2.

Cushman, J.A., 1911, A monograph of the Foraminifera of the North Pacific Ocean, Pt. 2: *Textulariidae*, U.S. Nat. Mus. Bull., Vol. 71, 108 pp., Washington D.C.

Cushman, J.A., 1922a, The Foraminifera of the Atlantic Ocean, Pt. 3: *Textulariidae*, U.S. Nat. Hist. Mus. Bull., 104, 143 pp., Washington D.C.

Cushman, J.A., 1922b, Shallow-water Foraminifera of the Tortugas region, Carnegie Inst.

Washington, Publ. No. 311 (Dept. Mar. Biol. Pap., Vol. 17), p. 1-85.

Cushman, J.A., 1927, Proc. U.S. Nat.Mus., Vol. 72, No. 2716, art. 20 Sret n.i. L&T, kan qua telling

Cushman, J.A., 1929a, The Foraminifera of the Atlantic Ocean, Pt. 6: Miliolidae, Ophtalmidiidae and Fisherinidae, U.S. Nat. Mus. Bull., 104., Washington D.C.

Cushman, J.A., 1929b, U.S. Geol. Surv. Prof. Paper, 191

Cushman, J.A., 1930a, On Uvigerina pigmea d'Orbigny, Contr. Cushman Lab. Foram. Res., Vol. 6, pt. 3, no. 94

Cushman, J.A., 1930b, The Foraminifera of the Atlantic Ocean, Pt. 7: Nonionidae, Camerinidae, Peneroplidae and Alveolinidae, U.S. Nat. Mus. Bull., no. 104., Washington D.C.

Cushman, J.A., 1930c, The foraminifera of the Choctawhatchee Formation of Florida, Florida State Geol. Surv. Bull., 4, Tallahasse, Florida.

Cushman, J.A., 1931, The Foraminifera of the Atlantic Ocean, Pt. 8: Rotaliidae, Amphisteginidae, Calcarinidae, Cymbaloporettidae, Globorotaliidae, Anomalinidae, Planorbulinidae, Rupertiidae, and Homotremidae, U.S. Nat. Mus. Bull., Vol. 104, Washington D.C.

Cushman, J.A., 1933, Foraminifera, their classification and economic use, Cushman Lab. Foram. Res., Spec. Publ. No. 4, 349 pp.

Cushman, J.A., 1937a, A monograph of the Foraminiferal family Valvulinidae, Cushman Lab. Foram. Res., Spec. Publ., 8, 210 pp.

Cushman, J.A., 1937B, A monograph of the Foraminiferal family Virgulininae of the foraminiferal family Buliminidae, Cushman Lab. Foram. Res., Spec. Publ., 9, 228 pp.

Cushman, J.A., 1939, A monograph of the Foraminiferal family Nonionidae, U.S. Geol. Survey, Prof. Paper, 191, 100 pp.

Cushman J.A. and Ponton, G.M., 1932, The foraminifera of the upper, middle and part of the lower Miocene of Florida, Florida State Geol. Surv. Bull., 9, Tallahasse, Florida.

Cushman, J.A. and Edwards, P.G., 1937, Astrononion, a new genus of the Foraminifera, and its species, Contr. Cushman Lab. Foram. Res., Vol. 13, pt. 1, p. 29-36.

Cushman, J.A. and Parker, F.L., 1937A, Contr. Cushman Lab. Foram. Res., Vol. 14, Pt. 3, Sharon, Mass.

Cushman, J.A. and Parker, F.L., 1937b, Notes on some European Eocene species of Bulimina and Buliminella, Contr. Cushman Lab. Foram. Res., Vol. 13, Pt. 2, p. 46-54.

Cushman, J.A. and Renz, H.H., 1941, New Oligocene - Miocene Foraminifera from Venezuela, Contr. Cushman Lab. Foram. Res., Vol. 17, no. 1, p. 1-27.

Cushman, J.A. and Todd, R., 1941, Notes on the species of Uvigerina and Angulogerina described from the Pliocene and Pleistocene, Contr. Cushman Lab. Foram. Res., Vol. 17, Pt. 3.

Czjzek, J., 1848, Beitrag zur Kenntniss der fossilen Foraminiferen des Wiener Beckens, Haidinger's Naturwiss. Abh., Vol. 2, Pt. 1, p. 137-150.

De Montfort, D., 1808, Conchyliologie systématique et classification methodique des coquilles, Vol. 1.

Dieci, G, 1959, I foraminiferi Tortoniani di Montegibbio e Castelvetro, Paleont. Ital., Vol. 54, 113 pp.

Di Napoli Alliata, E., 1952, Nuove specie di Foraminiferi nel Pliocene e nel Pleistocene della zona di Castel-l'Arquato (Piacenza), Riv. Ital. Paleont. Strat., vol. 58, no. 3, p. 95-109.

d'Orbigny, A.D., 1826, Tableau méthodique de la classe des Céphalopodes, Ann. Sci. Nat. Paris, série 1, Vol. 7, p. 245-315 (fide Loeblich and Tappan, 1964).

d'Orbigny, A.D., 1839A, Voyage dans l'Amérique méridionale - Foraminifères, Vol. 5, Pt. 5, 86 pp., 9 Pl., Pitois-Levrault et C^{e} (Paris), V. Levrault (Strasbourg).

d'Orbigny, A.D., 1839B, Foraminifères, in: R. de la Sagra, Histoire physique, politique et naturelle de l'île de Cuba, atlas, 12 Pl.

d'Orbigny, A.D., 1846, Foraminifères fossiles du Bassin Tertiaire de Vienne (Autriche), 312 pp., 21 Pl., Gide et Comp^{e} , Paris.

Ellis, B.F. and Messina, A.R., 1940, Catalogue of Foraminifera, Am. Mus. Nat. Hist. (supplements post-1940).

Fichtel, L. von and Moll, J.P.C. von, 1798, Testacea Microscopica alia que minuta ex generibus Argonauta et Nautilus, ad natura pictura et descripta (Mikroskopsche und andere kleine Schaltiere aus den geschlechtern Argonaute und Schiffer), Camesina, Wien.

Flint, J.M., 1899, Recent Foraminifera, A descriptive catalogue of specimens dredged by the U.S. Fish Commission Steamer Albatross, U.S. Nat. Mus., Ann. Rep. (1897), p. 249-349. Cibicides

Fornasini, C., 1888, Tavola paleo-protistografica, Boll. Soc. Geol. Ital., Vol. 7, fasc. 1.

Fornasini, C., 1897, La "*Clavulina cylindrica*" di A.D. d'Orbigny, Riv. It. Pal. Strat., Vol. 3, Pt. 5.

Fornasini, C., 1900, R. Accad. Sci. Ist. Bologna, ser. 5, Vol. 8

Fornasini, C., 1901, Boll. Soc. Geol. Ital., vol. 20

Fornasini, C., 1902, Contributo alla conoscenza de le Bulimine Adriatiche, Mem. R. Accad. Sci. Ist., Bologna, ser. 5, Vol. 9.

Gianotti, A., 1953, Microfauna delle serie Tortoniano del Rio Mazzapiedi Castellania (Tortona-Allessandria), Riv. Ital. Pal. Strat., Mem., Vol. 6, pp. 167-308.

Gümbel, C.W.,1868, Beiträge zur Foraminiferenfauna der nordalpinen Eocängebilde, K. Bayer. Akad. Wiss. Abh., Cl. II, Vol. 10, Pt. 2, p. 581-730.

Hageman, J., 1979, Benthic foraminiferal associations from Plio-Pleistocene open bay to lagoonal sediments of the western Peloponnesus (Greece), UMB 20, 171 pp.

Hantken, M. von, 1875, Die Fauna der Clavulina Szabói Schichten, Teil 1, Foraniniferen, Magy. Kir. Földt int. évkönyve, (Mitt. Jahrb. K. Ung. Geol. Anst.) Vol. 4.

Heron-Allen, E. and Earland, A., 1930, The foraminifera of the Plymouth district, Pt. 1, J. Roy. Micr. Soc., London. (B plic ps-pl)

Karrer, F., 1868, Die miozene Foraminiferenfauna von Kostej im Banat, K. Acad. Wiss. Wien, Math.-Nat. C1., Sitzungber., Vol. 58, Pt. 1, p. 121-193.

Lamarck, J.B., 1804, Suite des mémoires sur les fossiles des environs de Paris, Ann. Mus. Hist. Nat., Vol. 5, Paris.

Linnaeus, C., 1758, Systema naturae per regna tria naturae, secundum classes, ordines, genera, species, cum characteribus, differentiis, synonymis, locis, Ed. 10, Vol. 1, 824 pp., G. Engelman (Lipsiae) (fide Loeblich and Tappan, 1964).

Lipparini, T., 1932, Foraminiferi delle "Marne Azurre" a Orbitolites e Hydrobia del MioceneSuperiore presso Bologna, Anali del Mus. Geol. Di Bologna, Vol. 7, p. 55-74.

Loeblich, A.R. and Tappan, H., 1964, Sarcodina, chiefly "Thecamoebians" and Foraminifera, Vol. 1, 2, In: R.C. Moore, Ed., Treatise on invertebrate paleontology, pt. C, Protista 2, The Geol. Soc. of Am. and the Univ. of Kansas Press.

Longinelli, A., 1956, Foraminifera del Calabriano e Piacenziano di Rosignano marittimo e della Val di Cecina, Paleontogr. Ital., nov. ser., Vol. 19, 116 pp.

Macfadyen, W.A., 1930, Miocene Foraminifera from the clysmic area of Egypt and Sinaï Egypt, Geol. Surv., Cairo.

Marks, P., 1951, A revision of the smaller Foraminifera from the Vienna Basin, Contr. Cushman Found. Foram. Res., Vol. 2, Pt. 2.

Murray, J.W., 1971, An atlas of British Recent Foraminiferids, Heinemann Educ. Books Ltd., London.

Norman, A.M., 1881, A list of the post-Tertiary foraminifera of the North-east of Ireland, Quart. J. Micr. Soc., London, new ser., Vol. 21.

Nuttall, W.L.F., 1932, Lower Oligocene Foraminifera from Mexico, J. Paleont., Vol. 4, p. 3-35.

Parker, F.L., 1958, Swedish Deep Sea Exped., vol. 7

Parker, W.K., Jones, T.R. and Brady, H.B., 1865, On the nomenclature of the Foraminifera. Pt. 12: The species enumerated by d'Orbigny in the "Annales des Sciences Naturelles", Vol. 7, 1826, Ann. & Mag. Nat. Hist., ser. 3, Vol. 16, p. 15-41.

Perconig, E., 1955, Boll. Ital. Serv. Geol., Vol. 77.

Pflum, C.E. and Frerichs, W.E., 1976. Gulf of Mexico deep-water foraminifers. Cushman Found. Foram. Res., Spec. Publ., 14.

Phleger, F.P., Parker, F.L. and Peirson, J.F., 1953, North Atlantic Foraminifera, Rep. Swedish Deep Sea Exped., Vol. VII, Sediment cores from the North Atlantic Ocean, Mar. For. Lab., Scripps Inst. Ocean., California.

Reuss, A.E., 1850, Neue Foraminiferen aus den Schichten des österreichischen Tertiärbeckens, Denkschr. K. Akad. Wiss. Wien, Math.-Nat. Cl., Vol. 1, p. 365-390.

Reuss, A.E., 1851, Über die fossilen Foraminiferen und Entomostraceen des Septarientonen der Umgegend von Berlin, Deutsch. Geol. Gesellsch. Zeitschr., Vol. 3, p. 49-91.

Reuss, 1865, Sitz. Ber. K. Akad. Wien, Vol. 50

Rhezak, A., 1886, Die Foraminiferenfauna der Neogen Formation der Umgebung von Mähr-Ostrau. Naturf. Ver. Brünn, Band 24.

Salvatorini, G., 1966, Alcune nuove specie de foraminiferi del Miocene superiore della Toscana Marittima, Atti Soc. Tosc. Sci. Nat., Mem., Ser. A, Vol. 73, pp. 659-672.

Schwager, C., 1866, Fossile Foraminiferen von Kar-Nicobar, Novara Exp., 1857-1859, Geol. Theil, Vol. 2, p. 187-268.

Schwager, C., 1878, Nota su alcuni foraminiferi nuovi del tuffo di Stretto preso Girgenti, Boll. Uff. Geol. (R. Com. Geol. Ital.), Vol. 9, Roma.

Seguenza, G., 1862, Prime recerche intorno ai Rizopodi fossili delle argile Pleistoceniche dei dintorni di Catania, Accad.Gioenia Sci. Nat. Catania, ser. 2, vol. 18, Atti, Catania.

Silvestri, A., 1896, Foraminiferi Pliocenici della Provincia di Siena, Pt. 1, Mem. Accad. Pont. Nuovi Lincei, Vol. 12.

Silvestri, A., 1898, Foraminiferi Pliocenici della Provincia di Siena, Pt. 2, Mem. Accad. Pont. Nuovi Lincei, Vol. 15, p. 155-381.

Silvestri, A., 1901, Atti. R. Acad. Sci. Lett. Acireale, Vol. 10.

Silvestri, A., 1904, Ricerche strutturali su alcune forme dei trubi di Bonfornello (Palermo), Mem. Accad. Pont. Rom. Nuovi Lincei, Vol. 22, Rome.

Stewart, R.E. and Stewart, K.C., 1930, Post-Miocene foraminifera from the Ventura Quadrangle, Ventura County, California, J. Paleont., Vol. 4, no. 1.

Tedeschi and Zanmatti, 1957, Riv. Ital. Pal. Strat., vol. 63(4)

Thomas, E., 1980, Details of Uvigerina development in the Cretan Mio-Pliocene, Utrecht Micropaleont. Bull., 23, 167 pp.

Trauth, F., 1918, Das Eozänvorkommen bei Radstadt im Pongau und seine Beziehungen zu den gleichalterigen Ablagerungen beu Kirchberg am Wechsel und Wimpassing am Leithagebirge, Denkschr. K. Akad. Wissensch. Wien, Math. -Nat. Cl., Vol. 95, p. 171-278.

Verhoeve, D., 1971, Benthonic foraminifera of the Neogene Asteri Dhramia and Francocastello Formations from western Crete (Greece), Kon. Ul. Dep. Aardwet., Leuven.

Von Daniels, 1970, Göttinger Abh. Geol. Pal., 8

Walker, G. and Jacob, E., 1798, Adams' essays on the microscope, In: F. Kanmacher, London, edition 2.

Williamson, W.C., 1858, On the Recent Foraminifera of Great Britain, Ray Soc., London.

Wright, R., 1978, Neogene benthic foraminifers from DSDP leg 42A, Mediterranean Sea. Init. Rep. DSDP, Vol. 42, pt. 1, Washington D.C.

PLATES

Plate 1

Figure 1	*Cibicides lobatulus*, Moroccan composite, sample AEB 209
Figure 2	*Cibicides ungerianus*, Moroccan composite, sample AEB 209
Figure 3	*Cibicides pseudoungerianus*, Moroccan composite, sample OAK 111
Figure 4	*Cibicides kullenbergi*, Monte Gibliscemi, sample Jt 14.495

Scale bars 100 µm

Plate 1

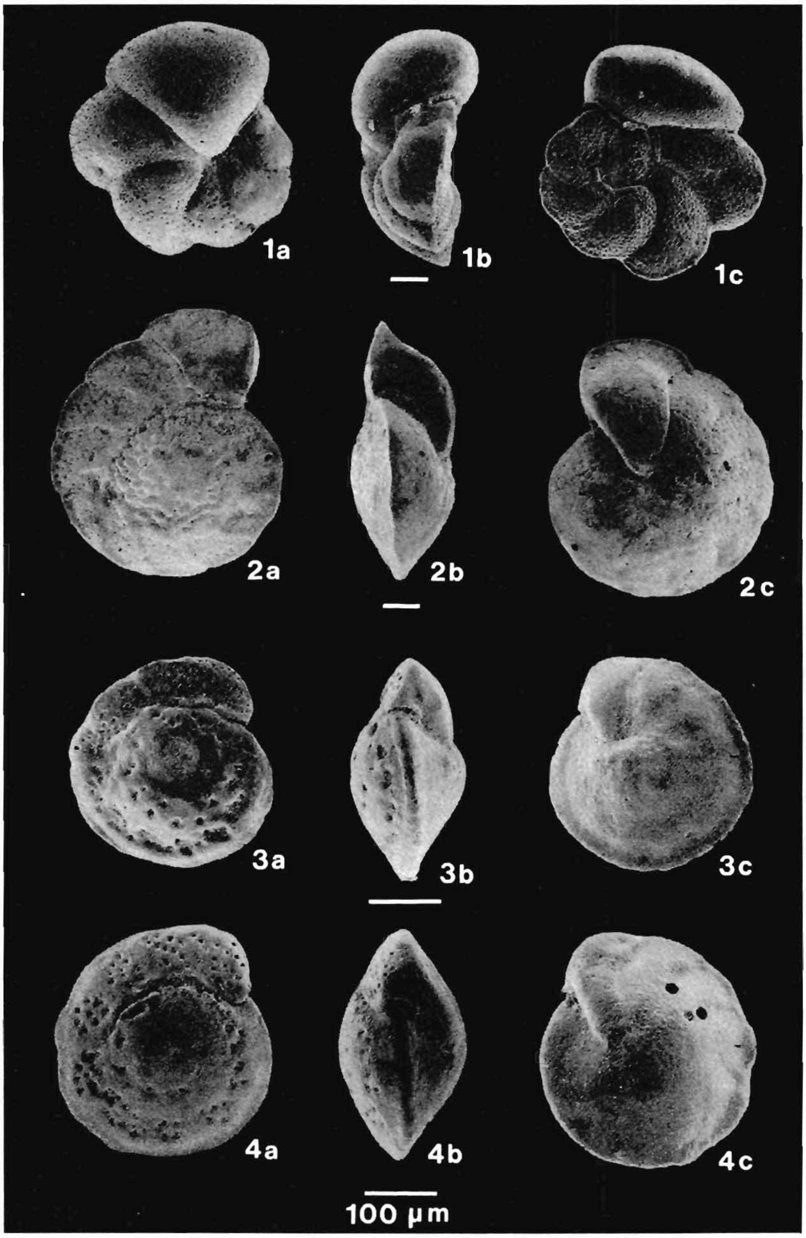

Plate 2

Figure 1	*Cibicides pachyderma*, Moroccan composite, sample AEB 271
Figure 2	*Cibicides dutemplei*, Moroccan composite, sample AEB 240
Figure 3	*Cibicides wuellerstorfi*, Monte del Casino, sample Jt 17.976

Plate 2

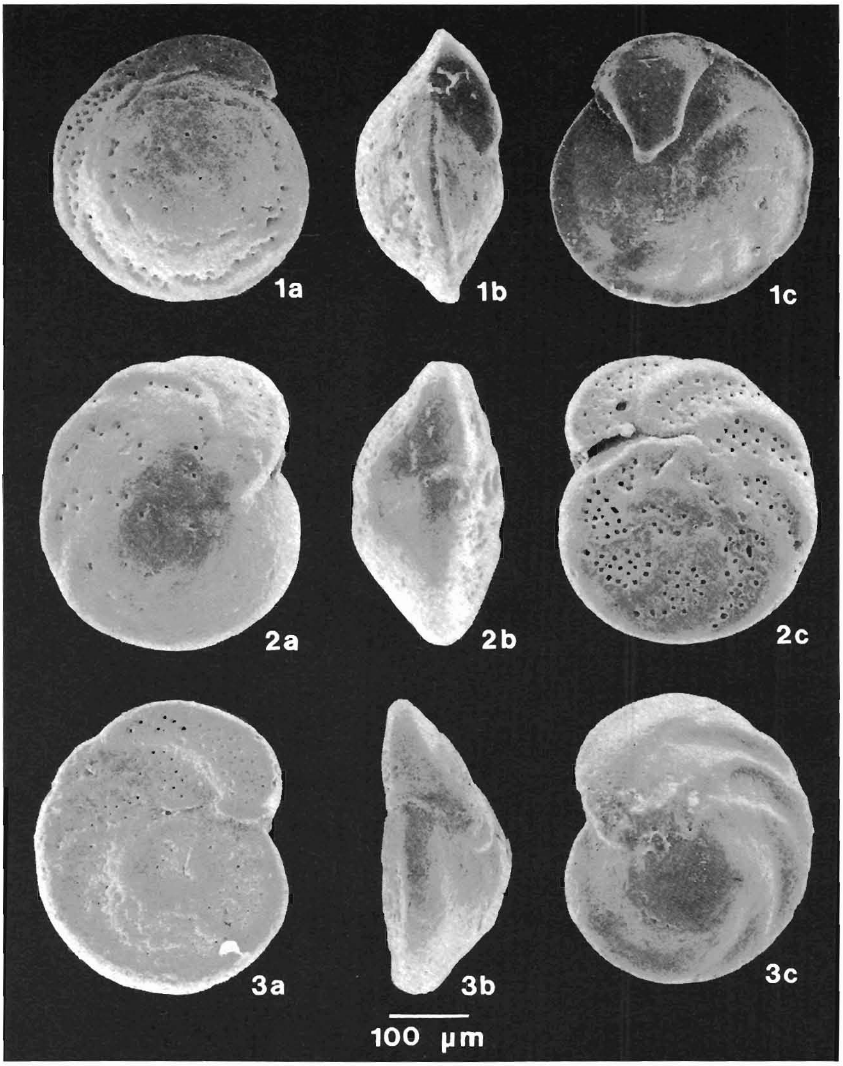

Plate 3

Figure 1	*Cibicidoides bradyi*, Monte Gibliscemi, sample Jt 14.325
Figure 2	*Cibicidoides italicus*, Monte Gibliscemi, sample Jt 14.445
Figure 3	*Cibicidoides robertsonianus*, Monte Gibliscemi, sample Jt 14.406

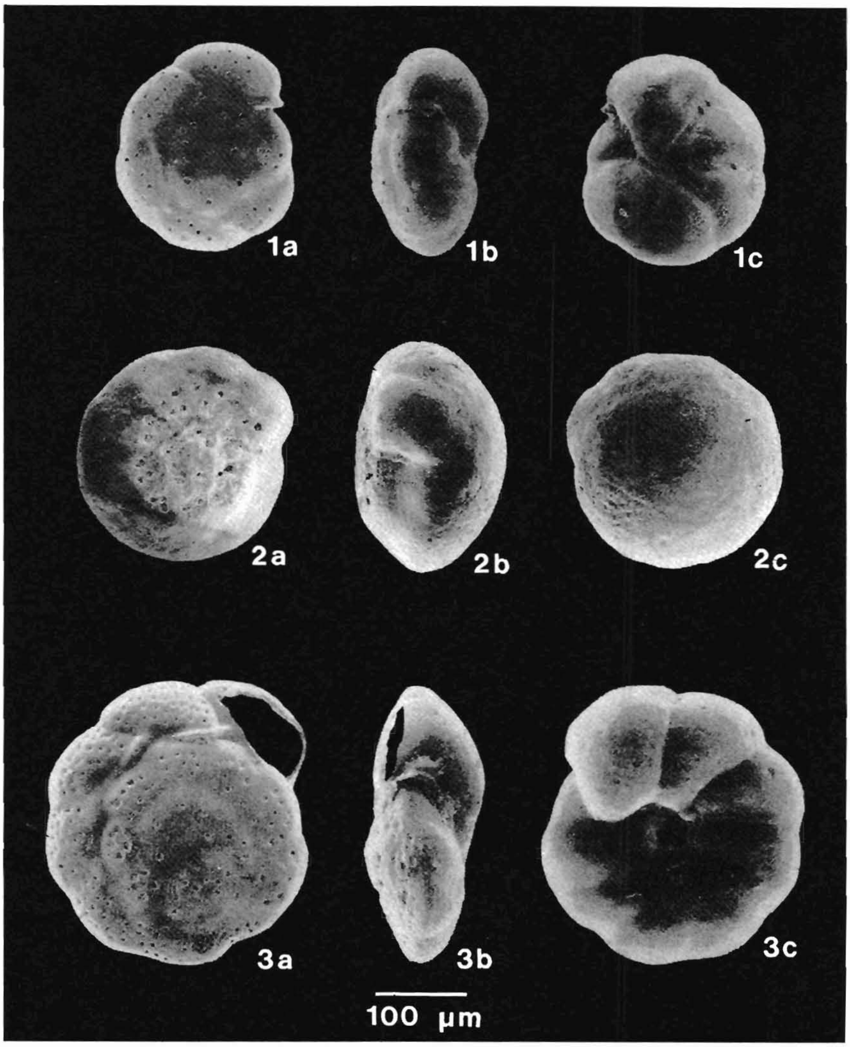
1a
1b
1c
2a
2b
2c
3a
3b
3c
100 µm

Plate 4

Figure 1	*Gyroidina orbicularis*, Moroccan composite, sample AEB 286
Figure 2	*Gyroidina soldanii*, Faneromeni, sample Gr 5808
Figure 3	*Gyroidinoides neosoldanii*, Moroccan composite, sample AEB 286
Figure 4	*Gyroidina altiformis*, Monte del Casino, sample Jt 17.991

Scale bars 100 µm

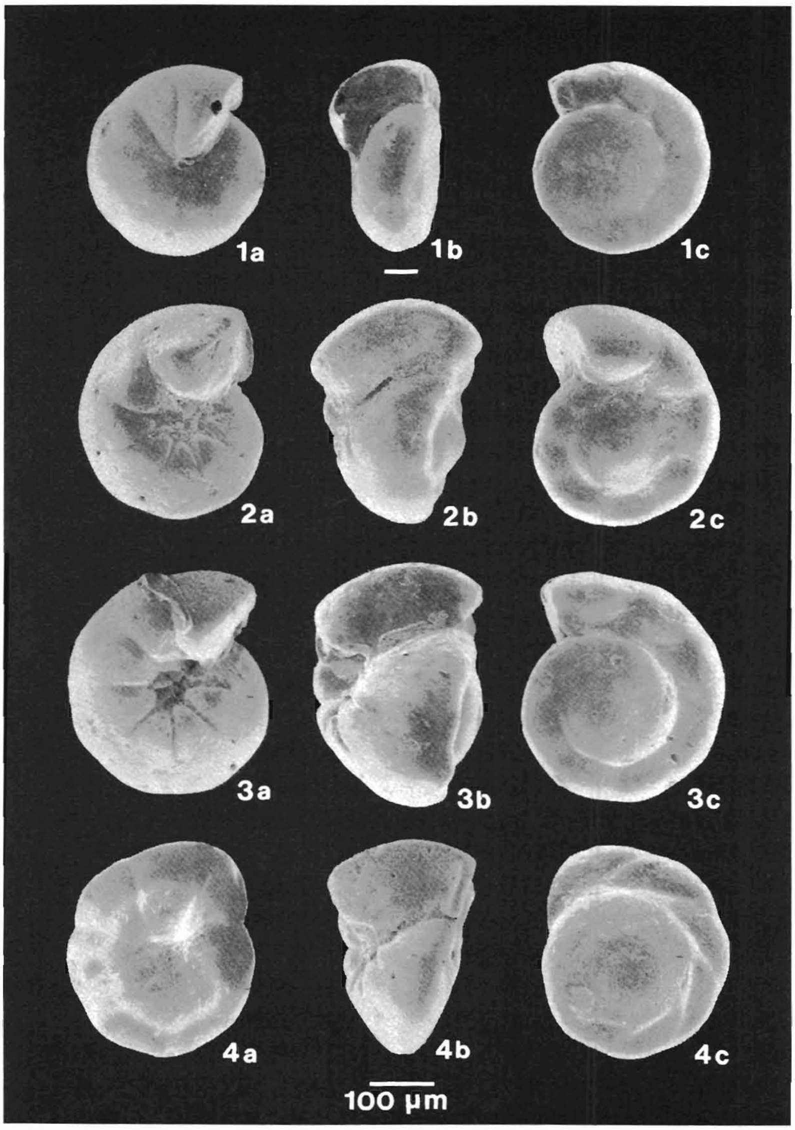
1a
1b
1c
2a
2b
2c
3a
3b
3c
4a
4b
4c
100 µm

Plate 5

Figure 1	*Gyroidina parva*, Moroccan composite, sample AEB 240
Figure 2	*Quinqueloculina* sp., Monte del Casino, sample Jt 17.925
Figure 3	*Quinqueloculina* sp., Monte del Casino, sample Jt 17.937
Figure 4	*Vulvulina pennatula*, Monte del Casino, sample Jt 17.931
Figure 5	*Eggerella bradyi*, Monte Gibliscemi, sample Jt 14.395
Figure 6	*Spiroplectammina carinata*, Faneromeni, sample Gr 5815
Figure 7	*Karreriella bradyi*, Monte del Casino, sample Jt 18.158
Figure 8	*Bigenerina nodosaria*, Moroccan composite, sample AEB 240
Figure 9	*Clavulina* sp., Monte del Casino, sample Jt 18.213

Scale bars 100 µm

Plate 5

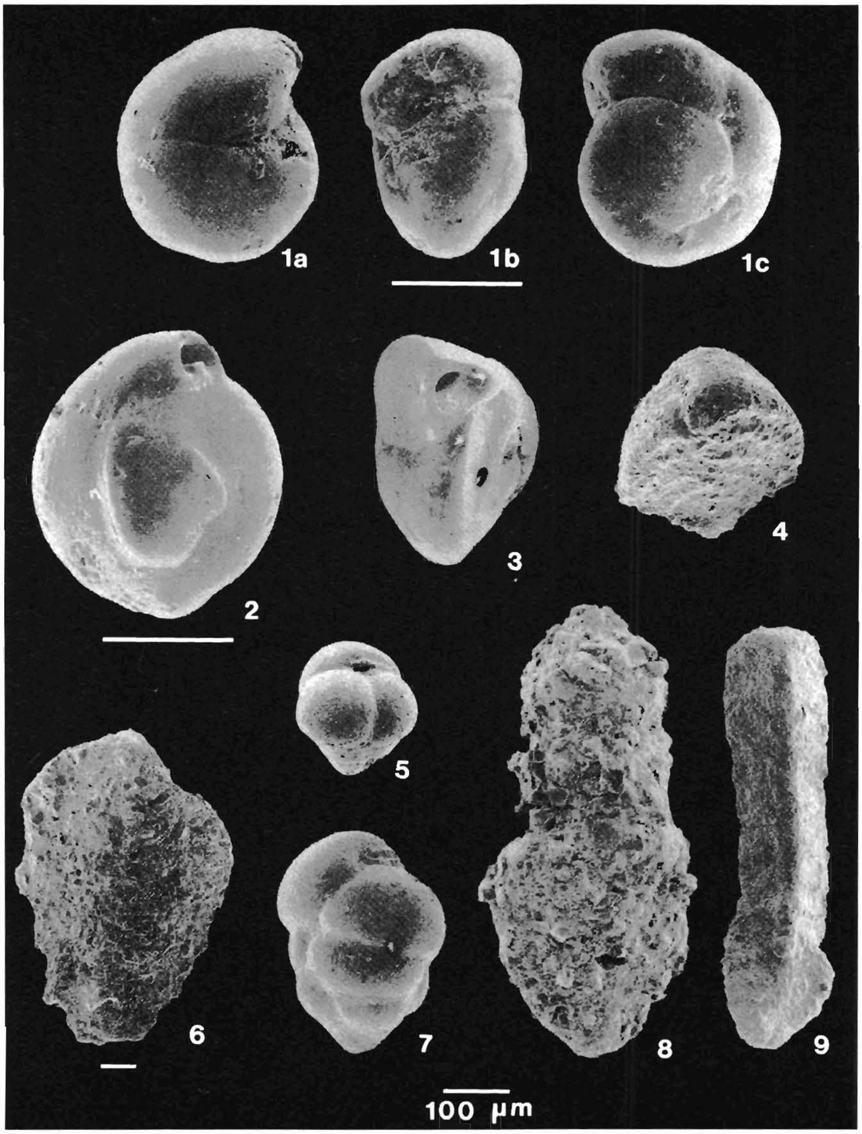

Plate 6

Figure 1	*Oridorsalis* sp., Monte Gibliscemi, sample Jt 14.465
Figure 2	*Oridorsalis stellatus*, Monte Gibliscemi, sample Jt 14.445
Figure 3	*Siphonina reticulata*, Monte Gibliscemi, sample Jt 14.195
Figure 4	*Siphonina planoconvexa*, Faneromeni, sample Gr 5810

Scale bars 100 µm

Plate 6

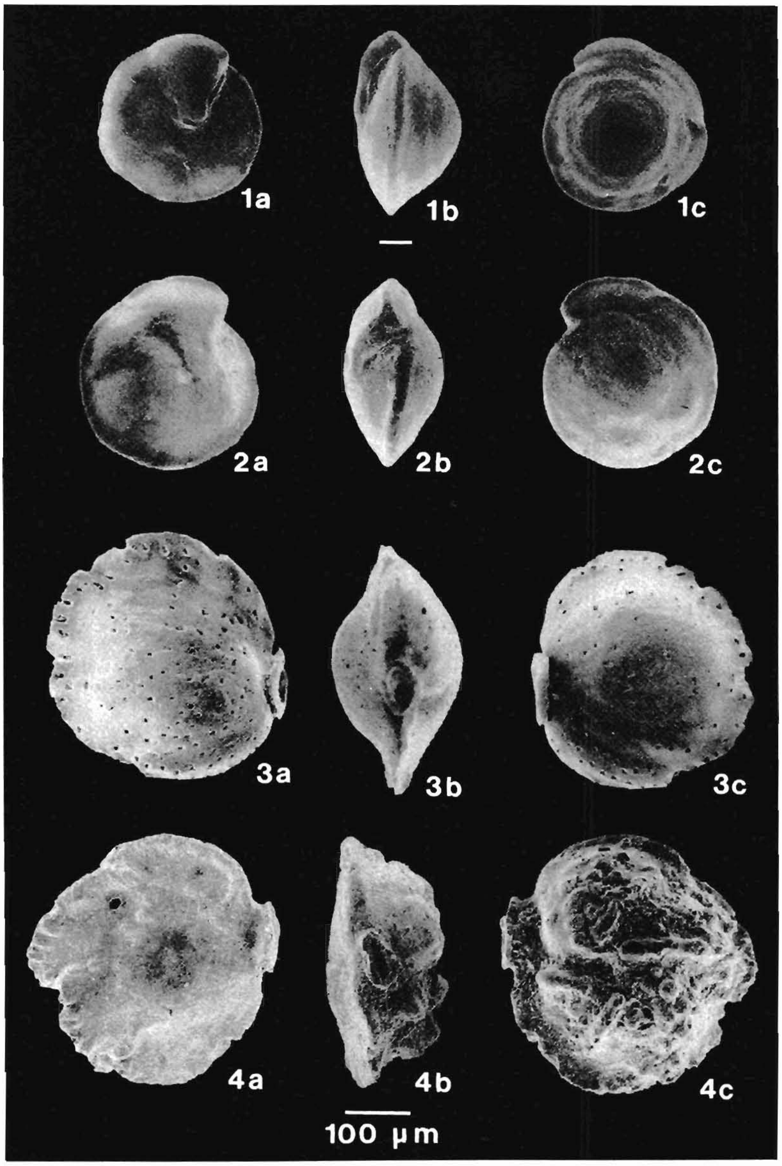

Plate 7

Figure 1	*Pullenia quinqueloba*, Monte Gibliscemi, sample Jt 14.465
Figure 2	*Pullenia bulloides*, Moroccan composite, sample OAK 111
Figure 3	*Svratkina perlata*, Faneromeni, sample Gr 5836
Figure 4	*Planulina ariminensis*, Moroccan composite, sample AEB 240
Figure 5	*Anomalinoides helicinus*, Faneromeni, sample Gr 5808

Scale bars 100 μm

Plate 7

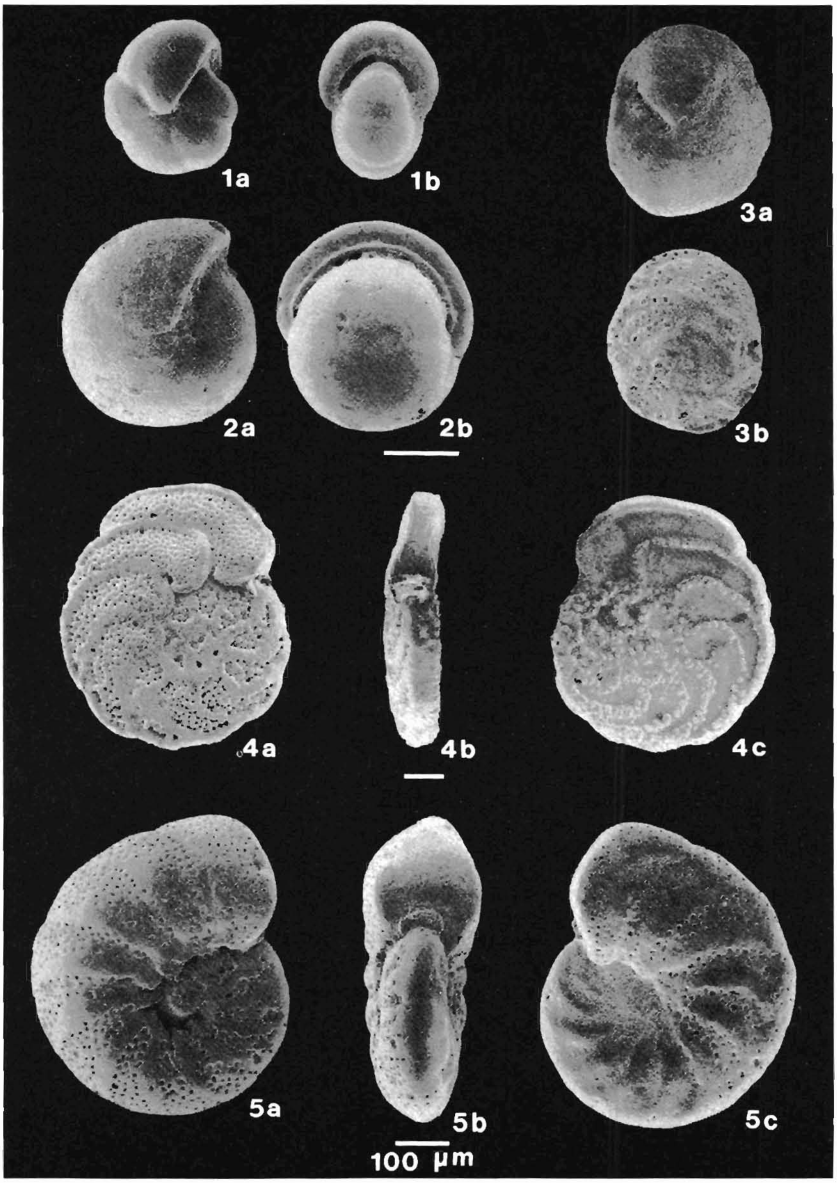

Plate 8

Figure 1	*Melonis barleeanus*, Monte del Casino, sample Jt 18.000
Figure 2	*Astrononion stelligerum*, Monte del Casino, sample Jt 17.782
Figure 3	*Hanzawaia boueana*, Monte Gibliscemi, sample Jt 14.625
Figure 4	*Cancris oblongus*, Monte Gibliscemi, sample Jt 14.175
Figure 5	*Rosalina globularis*, Moroccan composite, sample AEB 240
Figure 6	*Elphidium poeyanum*, Faneromeni, sample Gr 5810
Figure 7	*Elphidium complanatum*, Faneromeni, sample Gr 5810
Figure 8	*Elphidium fichtellianum*, Faneromeni, sample Gr 5716

Scale bars 100 µm

Plate 8

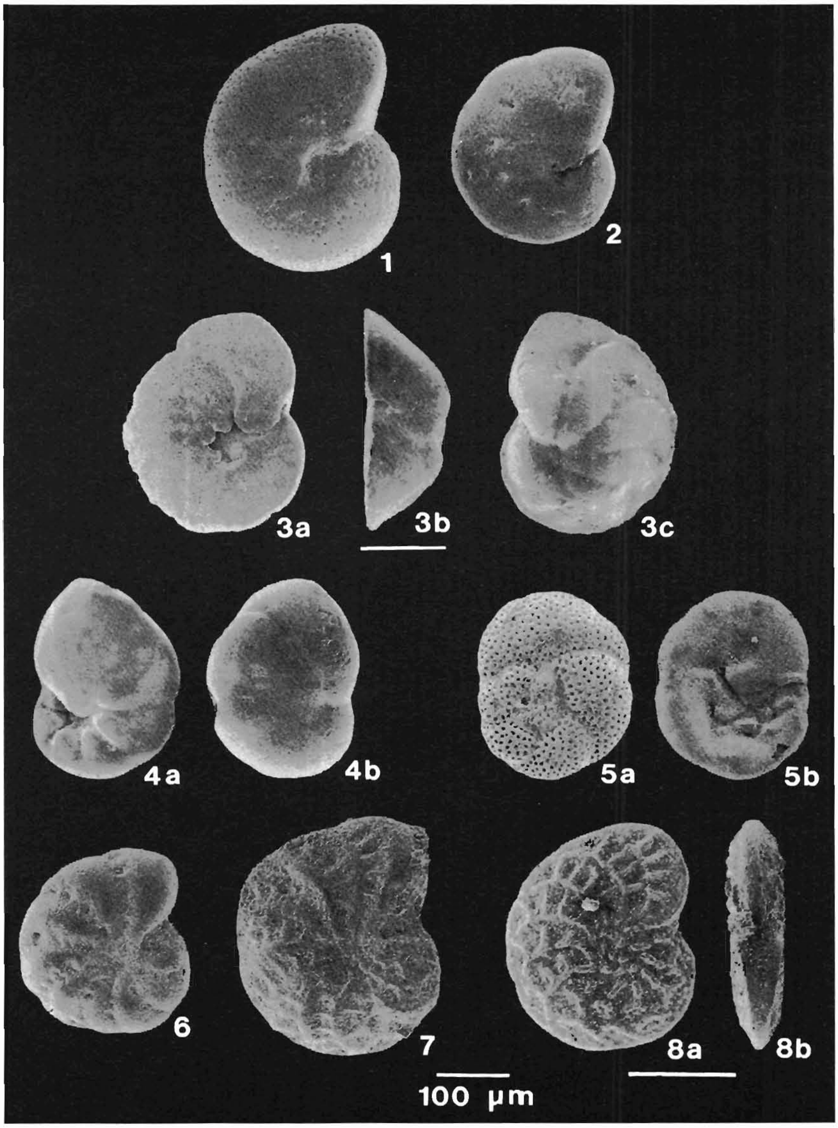

Plate 9

Figure 1	*Bulimina costata,* Moroccan composite, sample AEB 240
Figure 2	*Bulimina aculeata*, Monte del Casino, sample Jt 17.832
Figure 3	*Bulimina subulata,* var. *Lappa*, Moroccan composite, sample OAK 104
Figure 4	*Bulimina subulata*, Moroccan composite, sample OAK 104
Figure 5	*Bulimina elegans*, Monte del Casino, sample Jt 17.797
Figure 6	*Pleurostomella alternans*, Monte del Casino, sample Jt 18.019
Figure 7	*Globobulimina* sp., Monte Gibliscemi, sample Jt 14.175
Figure 8	*Chilostomella ovoidea*, Monte del Casino, sample Jt 18.034
Figure 9	*Ehrenbergina pacifica*, Monte del Casino, sample Jt 17.795
Figure 10	*Cassidulinoides bradyi,* Moroccan composite, sample AEB 240
Figure 11	*Cassidulina* cf. *C. laevigata*, Faneromeni, sample Gr 5808
Figure 12	*Globocassidulina subglobosa*, Moroccan composite, sample AEB 256

Plate 9

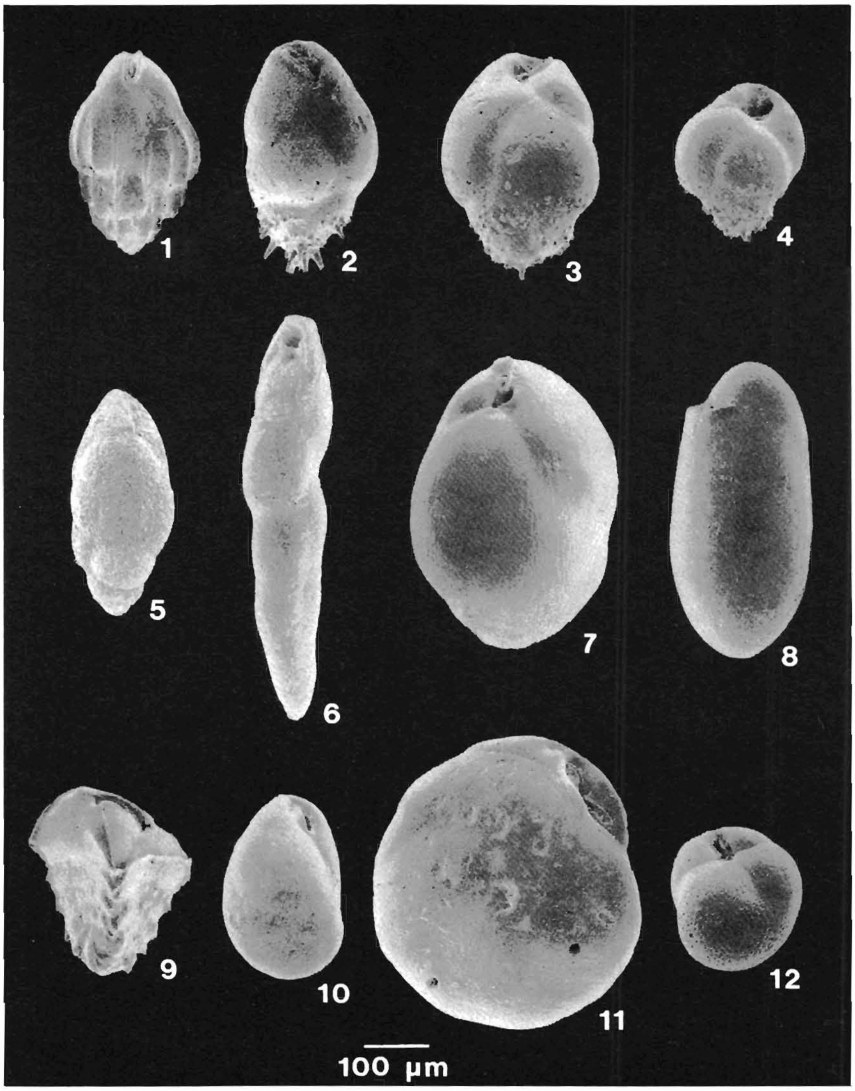

Plate 10

Figure 1	*Bolivina spathulata*, Faneromeni, sample Gr 5836
Figure 2	*Bolivina dilatata*, Monte del Casino, sample Jt 17.817
Figure 3	*Bolivina hebes*, Moroccan composite, sample AEB 229
Figure 4	*Bolivina scalprata miocenica*, Monte del Casino, sample 18.000
Figure 5	*Bolivina scalprata miocenica*, Faneromeni, sample Gr 5810
Figure 6	*Bolivina reticulata,* Monte del Casino, sample Jt 18.125
Figure 7	*Bolivina reticulata*, Faneromeni, sample Gr 5857
Figure 8	*Bolivina plicatella* var. *pseudoplicata*, Faneromeni, sample Gr 5815
Figure 9	*Bolivina plicatella* var. *mera*, Faneromeni, sample Gr 5808
Figure 10	*Bolivina tortuosa*, Moroccan composite, sample AEB 194

Plate 10

Plate 11

Figure 1	*Uvigerina peregrina*, Moroccan composite, sample AEB 183
Figure 2	*Uvigerina peregrina*, Moroccan composite, sample AEB 240
Figure 3	*Uvigerina pygmea*, Moroccan composite, sample AEB 286
Figure 4	*Uvigerina proboscidea*, Monte del Casino, sample Jt 18.000
Figure 5	*Uvigerina* sp.1, Moroccan composite, sample OAK 077
Figure 6	*Uvigerina* sp.1, Moroccan composite, sample OAK 077
Figure 7	*Uvigerina striatissima*, Faneromeni, sample Gr 5810
Figure 8	*Uvigerina rutila*, Moroccan composite, sample AEB 271
Figure 9	*Uvigerina cylindrica cylindrica*, Monte del Casino, sample Jt 17.802
Figure 10	*Uvigerina cylindrica gaudryinoides*, Monte del Casino, sample Jt 17.835
Figure 11	*Trifarina angulosa angulosa*, Moroccan composite, sample AEB 240
Figure 12	*Trifarina angulosa pauperata*, Moroccan composite, sample AEB 183

Plate 11

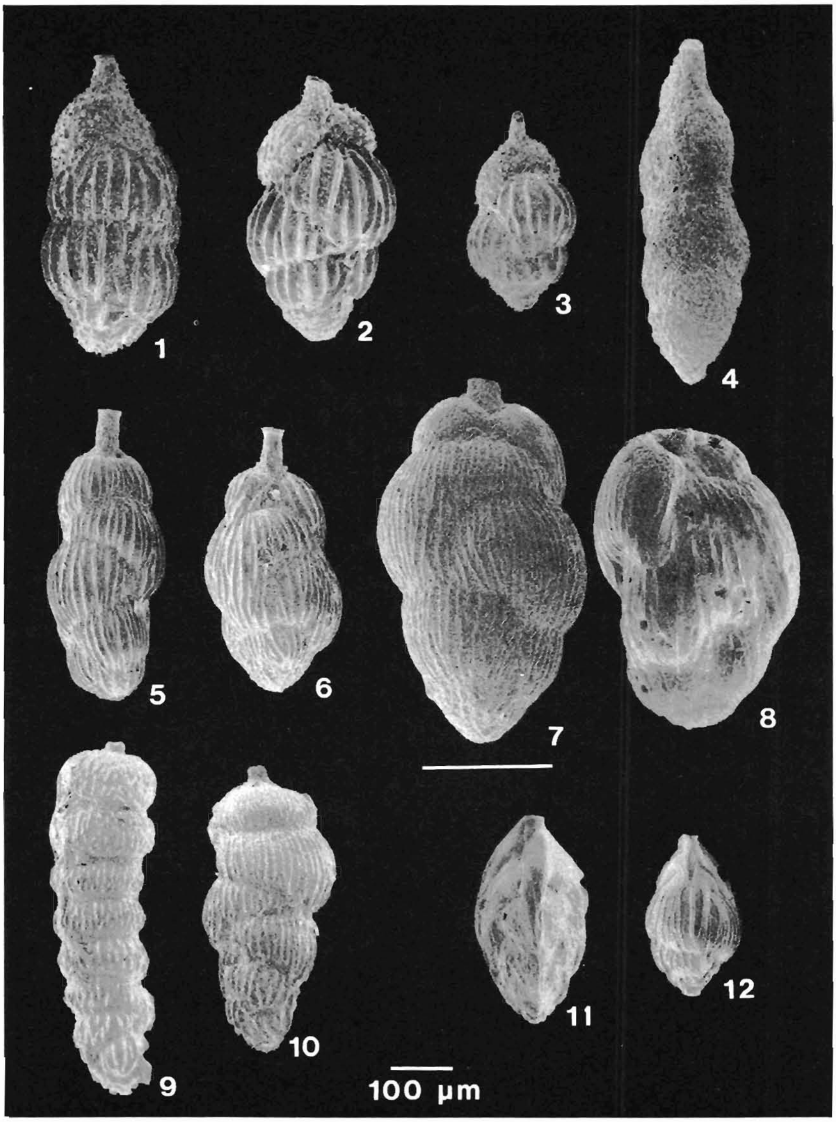

Samenvatting (Summary in Dutch)

Om het nu volgende ook voor minder ingewijden begrijpelijk te maken, volgt eerst een korte verklaring van enkele regelmatig terugkerende begrippen; daarna volgt bij * de eigenlijke samenvatting. In de eerste plaats, foraminiferen: dit zijn eencellige organismen met een gemiddelde grootte van 100 micron. Ze leven drijvend in de bovenste waterlagen (planktonisch) of op en in de zeebodem (benthonisch). Een aantal soorten foraminiferen bouwt harde schelpjes. Het organisme zelf sterft en vergaat, maar onder gunstige omstandigheden kunnen de schaaltjes in geologische afzettingen, aangeduid als sedimenten, bewaard blijven.

Sedimentpakketten zijn opgebouwd uit lagen, of strata; geologie is van oorsprong een beschrijvende wetenschap, die deze strata beschreef met de volgorde waarin ze waren afgezet: de stratigrafie. In een vroeg stadium werd onderkend dat bij het bepalen van de volgorde van afzetting fossielen uiterst nuttige hulpmiddelen kunnen zijn. Pas later groeide het inzicht dat fossielen ook belangrijke informatie kunnen verschaffen over de omstandigheden waarin die sedimenten zijn afgezet, bijvoorbeeld klimaat en waterdiepte. De afzetting van sedimentpakketten gebeurt in de regel in een depressie in het aardoppervlak. In veel gevallen ontstaan deze depressies naar aanleiding van tektoniek: differentiële vertikale bewegingen in de aardkorst, waarbij de hoger gelegen delen eroderen of afslijten. Het afvalmateriaal wordt in depressies (sedimentbekkens) gedeponeerd, die soms op land, maar veelal in zee liggen. Tektoniek is in veel gevallen gerelateerd aan de relatieve bewegingen van aardschollen, of aardplaten, ten opzichte van elkaar. Zo zijn in de loop van de laatste 65 miljoen jaar, het Cenozoicum, de platen met daarop Eurazië en Afrika naar elkaar toe bewogen. Wanneer door dit soort plaatconvergente bewegingen ruimtegebrek onstaat, wordt de aardkorst omhoog geduwd en onstaan gebergteketens, in dit geval de Alpen. In het front van gebergteketens ligt dan een voordiep, een forse depressie in de aardkorst waarin zich veel sediment verzamelt.

* Onderzoek aan foraminiferen begon in de 17e eeuw, sinds de uitvinding van de microscoop, en bestond in eerste instantie uit beschrijving en classificatie. Al veel eerder was onderkend dat mariene fossielen informatie kunnen geven over het relatieve verloop van de geologische tijd: ze vormden en vormen de basis van de stratigrafie. Benthonische foraminiferen (Phylum Foraminifera) hebben zich ontwikkeld vanaf het Cambrium als onderdeel van het mariene ecosysteem. Sindsdien zijn ze aanwezig in bijna alle mariene milieus. Door hun wijdverspreide voorkomen en hun grote aantallen behoren ze tot de meest bruikbare fossielen om biotische veranderingen te onderzoeken die in het verleden hebben plaatsgevonden. In de afgelopen eeuw is het inzicht gegroeid dat benthonische foraminiferen minder geschikt zijn voor stratigrafische doeleinden dan

bijvoorbeeld planktonische foraminiferen, maar veel informatie geven over processen en gebeurtenissen die zich in het verleden in zee hebben afgespeeld. Van deze kennis, die nog lang niet volledig is, wordt gebruik gemaakt bij het reconstrueren van scherpe veranderingen (biotische crises) in het mariene milieu.

De geologische geschiedenis zoals verteld door fossielen, is per definitie fragmentarisch: veel is bewaard gebleven, maar veel is ook verloren gegaan door verval en diagenese. Dit geldt evenzeer voor benthonische foraminiferen. De ecologische samenhang tussen soorten is bijvoorbeeld vaak onherkenbaar. Hiervoor moeten we te rade gaan bij de gestaag groeiende kennis die beschikbaar komt over nu levende equivalenten van de foraminiferen, die we willen bestuderen. Op hun beurt geven de huidige faunas geen informatie over de tijd die gemoeid is met processen die het milieu beinvloeden en hun effecten op de ontwikkeling en evolutie van benthonische leefgemeenschappen. Voor informatie hierover vallen we terug op fossiele faunas en precieze dateringen, die bepaald worden met gecombineerde technieken, waaronder bio- en magnetostratigrafie. In het Middellandse Zeegebied, waar sinds het midden-Mioceen de afzetting van sapropelen gestuurd wordt door astronomische processen, blijkt cyclostratigrafie een uiterst nauwkeurige dateringsmethode te zijn.

Grote biotische crises markeren het begin en einde van belangrijke perioden in de geologische geschiedenis. Dit heeft te maken met het feit dat de relatieve tijdschaal in eerste instantie is opgezet met gebruikmaking van grote cesuren in de historie van de aarde. Het begin van het Cenozoicum, 65 miljoen jaar geleden, is gedefinieerd op basis van de biotische crisis op de grens van Krijt naar Paleogeen, die mariene en terrestrische biota verregaand heeft beïnvloed. Dat inslag van een asteroïde heeft plaatsgevonden, is inmiddels geen punt van discussie meer. Het is echter nog altijd de vraag, of de inslag uiteindelijk de enige oorzaak was van de extincties in die periode. Onderzoek hiernaar duurt nog voort.

In het Cenozoicum hebben zich meerdere biotische crises voorgedaan, die zowel op wereldwijde als op meer lokale schaal effect hadden. In dit proefschrift worden zes belangrijke fasen van verandering, die optraden in het aardse milieu gedurende het Cenozoicum, meer of minder uitgebreid beschreven. Een aantal hiervan traden meer geleidelijk op, andere worden gekarakteriseerd door – vanuit geologisch oogpunt – zeer snelle en ingrijpende veranderingen. Elk van deze perioden heeft sporen nagelaten in leefgemeenschappen van benthonische foraminiferen, die het onderwerp zijn van dit proefschrift.

Tijdens het Cenozoicum heeft de paleogeografische evolutie van het Mediterrane gebied de ontwikkeling van benthonische faunas verregaand beïnvloed. In de loop van het Cenozoicum versmalde de oude Tethys, in het Paleoceen een brede equatoriale corridor, onder invloed van de convergentie van de Euraziatische en de Afrikaanse platen. Het gebied werd opgebroken in kleinere bekkens waartussen de connecties verloren gingen. Het deels afgesloten

Middellandse Zeebekken is daar één van. Tien miljoen jaar na de Krijt/Paleogeengrens werd de Paleoceen/Eoceengrens gekenmerkt door een plotseling en wereldwijd uitsterven van (onder andere) groepen van benthonische foraminiferen. In de loop van het Eoceen en tijdens de overgang naar het Oligoceen werden de benthonische ecosystemen beïnvloed door meer geleidelijke processen, die evenwel grote en blijvende veranderingen in gang zetten in benthonische faunas. Op een meer regionale schaal leidde de afsluiting van de Tethys naar het oosten gedurende het midden-Mioceen tot effecten op het paleomilieu. Waarschijnlijk als gevolg daarvan ontstonden in het huidige Mediterrane bekken sapropelitische sedimenten en ontwikkelden zich benthonische faunas die gekarakteriseerd werden door endemische vormen. In het laat-Mioceen leidden plaatconvergentie en lokale tektoniek tot verdere restrictie van het Middellandse Zeebekken en vervolgens tot de afzetting van grote hoeveelheden evaporieten in zeer korte tijd (tussen 5.96 en 5.33 Ma): dit wordt de zoutcrisis van het Messinien genoemd.

Het onderwerp van dit proefschrift is de paleoecologische analyse van Cenozoische benthonische foraminiferen. Al het bestudeerde fossiele materiaal is afkomstig uit het Tethysgebied, om precies te zijn, uit het gebied dat zich ontwikkelde tot het Middellandse Zeegebied in de loop van het Cenozoicum. Hoofdstuk 2 beschrijft het herstel van het benthonische ecosysteem na de Krijt/Paleogeengrens en de daaropvolgende ontwikkeling naar de Paleoceen/ Eoceengrens, zoals gereconstrueerd is uit sedimenten van de El Kef sectie in Tunesie. Deze sectie representeert de zuidelijke marge van de Tethys, zoals die in het Paleoceen bestond. De Krijt/Paleogeengrens en de Paleoceen/Eoceengrens zijn twee perioden waarin ecosystemen onder druk stonden. In beide perioden waren de effecten wereldwijd, maar aard en oorzaak waren verschillend. Waar een meteorietinslag waarschijnlijk mede de crisis op de Krijt/Paleogeengrens veroorzaakte, werd de crisis op de Paleoceen/Eoceengrens gekenmerkt door wereldwijde stijging van de temperatuur. Beide crises speelden zich in korte tijd af, misschien zelfs in een tempo dat vergelijkbaar is met het effect van veranderingen die veroorzaakt worden door menselijke interactie met het milieu.

Tussen het Paleoceen enerzijds, en de gebeurtenissen die in de hoofdstukken 3 t/m 7 besproken worden, gaapt een kloof van meer dan 45 miljoen jaar. In die tijd veranderde de configuratie van het gebied ingrijpend en ontstond er een bekken dat de vorm begon aan te nemen van de huidige Middellandse Zee. De genoemde hoofdstukken beschrijven gebeurtenissen in het laat-Mioceen in het Mediterrane gebied, die uiteindelijk leidden tot de zoutcrisis van het Messinien en afzetting van evaporieten. De zoutcrisis trad lokaal op, maar de effecten kunnen in een groter geografisch gebied hun sporen hebben nagelaten, alleen al vanwege de hoeveelheid zout die aan de oceanen onttrokken moet zijn. De zoutcrisis werd waarschijnlijk mede veroorzaakt door plaatconvergentie en daarmee samen-hangende tektoniek, waardoor het Mediterrane bekken van de omringende oceanen werd geïsoleerd. De ontwikkeling van laat-Miocene faunas voorafgaand aan en volgend op de zoutcrisis is de laatste decennia onderwerp geweest van onderzoek, en inmiddels krijgt men meer inzicht in processen die een rol gespeeld hebben in die periode in het Mediterrane gebied. Voor dit proefschrift zijn laat-Miocene secties bestudeerd, sommige in meer detail dan andere, die op verschillende waterdieptes zijn afgezet, en er is gepoogd trends en gebeurtenissen te reconstrueren die het ontstaan van de zoutcrisis mede veroorzaakten.

Gedetailleerde reconstructies van in betrekkelijk diep water afgezette secties zijn het onderwerp van de hoofdstukken 3 en 4. In hoofdstuk 3 wordt de Monte del Casino sectie beschreven en wordt een vergelijking gemaakt met geselecteerde gegevens van de Metochia sectie. De Monte del Casino sectie (8.15–6.3 Ma, noord-Italie) is afgezet op voordiep-sedimenten, die zijn gerelateerd aan opbouw van de Apennijnen. Er zijn effecten van zowel regionale gebeurtenissen, als van lokale opheffing. Die effecten konden onderscheiden worden op basis van de respons van benthonische foraminiferen. Er werden aanwijzingen gevonden dat de ontwikkeling naar de zoutcrisis van het Messinien al 7.16 miljoen jaar geleden begonnen is: meer dan een miljoen jaar voor de afzetting van de evaporieten

Hoofdstuk 4 beschrijft de Metochia sectie die een periode van drie miljoen jaar representeert (9.7–6.7 Ma) van benthonische ontwikkeling in het oostelijk Mediterrane gebied. De sectie ligt op Gavdos, juist ten zuiden van Kreta en net als in de Monte del Casino sectie compliceren tektonische bewegingen het beeld enigszins. Ook hier vinden we aanwijzingen voor een vroegtijdige aanzet tot de zoutcrisis, mogelijk zelfs eerder dan 7.16 Ma, en een relatie met vertikale bewegingen in de aardkorst bij de westelijke corridors naar de Atlantische Oceaan.

Onderzoek aan moderne foraminiferenfaunas heeft veel bijgedragen aan een beter begrip van benthonische ecosystemen en hun reactie op verstoringen van het milieu. Deze kennis is toepasbaar op fossiele milieus. Kortgeleden werd, op basis van microhabitatpatronen van recente faunas, een proxy ontwikkeld om beluchting van bodemwater in het geologisch verleden te reconstrueren. Hoofdstuk 5 beschrijft een eerste poging om deze proxy te valideren in een fossiele situatie. Hierbij werd de inmiddels goed beschreven Monte del Casino sectie als uitgangspunt gebruikt. Een belangrijke vraagstelling was, of Recente microhabitat-patronen bruikbaar zijn als analogen voor fossiele, en of dit realistische reconstructies oplevert. De resultaten zijn veelbelovend, en bieden daarnaast de gelegenheid om de aan deze reconstructies gerelateerde problemen scherper te definieren.

In hoofdstuk 6 wordt de zuurstofproxy toegepast op vijf secties, die op verschillende dieptes zijn afgezet, en is een reconstructie gemaakt van de water-circulatie in het centrale en oostelijke deel van het Mediterrane bekken. Doel was, na te gaan of deze toepassing van de proxy zou resulteren een realistisch beeld dat niet in tegenspraak is met eerder geformuleerde ideeën. Voorts was de vraag of het circulatiepatroon theoretisch geleid kan hebben tot afzetting van evaporieten. In overweging nemende dat van de huidige circulatie in het Mediterrane bekken nog niet alles bekend is, kon deze reconstructie niet al te gedetailleerd zijn. De eerste resultaten lijken aan te sluiten bij de theoretische verwachtingen.

In hoofdstuk 7 wordt een beschrijvend model gepresenteerd van de in de Miocene secties aangetroffen benthonische foraminiferenfaunas en hun ontwikkeling in het laat-Mioceen. Het model is gebaseerd op gegevens die verzameld zijn gedurende dit onderzoek en op informatie uit de literatuur. Faunas afkomstig uit vijf Mediterrane secties en een sectie aan de grens met de Atlantische Oceaan worden besproken en vergeleken. Hierbij blijkt dat faunas uit verschillende milieus anders reageren op de ontwikkelingen in het laat-Mioceen.

In hoofdstuk 8 worden de uiteenlopende tijdssegmenten, Paleoceen en laat-Mioceen, samengebracht in de vorm van een synthese, die de tussenliggende periode aanstipt, en wordt de respons van Paleocene en laat-Miocene faunas op verstoringen van het mariene milieu vergeleken. We concluderen dat een verschuiving is opgetreden in de structuur van leefgemeenschappen van benthonische foraminiferen over een periode van ~50 miljoen jaar en dat oorzaken van deze verandering mogelijk eerder gezocht moeten worden in perioden van geleidelijke transities dan in kortdurende biotische crises.

Tenslotte worden taxonomische notities gepresenteerd over geselecteerde benthonische foraminiferen die in het monstermateriaal zijn aangetroffen. Voor foto's van Paleocene soorten, die goed zijn gedocumenteerd, wordt verwezen naar eerdere publicaties. Van Miocene soorten zijn platen bijgevoegd. Een aantal van deze soorten zijn onderwerp van voortdurende taxonomische discussie, en door middel van deze afbeeldingen willen we duidelijk maken wat de in dit onderzoek gehanteerde taxonomische concepten zijn, daar dit belangrijk is in het licht van de paleomilieu-reconstructies die hier gepresenteerd worden.

Een belangrijke conclusie van dit onderzoek is dat benthonische foraminiferen veel hoogwaardige informatie kunnen geven over fossiele milieus en de veranderingen die daarin opgetreden zijn. Het inzicht in de struktuur van leefgemeenschappen breidt zich nog steeds uit en zal bijdragen aan hun waarde voor de reconstructie van het geologisch verleden. Daarnaast vinden we aanwijzingen voor het feit dat geleidelijke transities, die zich over miljoenen jaren uitstrekken, waarschijnlijk even belangrijk zijn, of misschien belangrijker, voor de evolutie van benthonische leefgemeenschappen als kortdurende ecologische crises.

Dankwoord (Acknowledgements)

Ik wil graag iedereen bedanken die betrokken is geweest bij het werk aan dit proefschrift. In de eerste plaats ben ik veel dank verschuldigd aan mijn promotoren, Professor Bert van der Zwaan en Professor Johan Meulenkamp, die me in staat stelden om dit onderzoek te doen en die elk op hun eigen, specifieke manier hebben bijgedragen aan de afronding van dit proefschrift. Bert van der Zwaan leverde een onuitputtelijke stroom ideeën en creativiteit. Johan Meulenkamp bood me de ruimte die nodig was om ervaring in wetenschappelijk onderzoek op te doen. Beiden plaatsten mijn onderzoek in een breder kader en waren te allen tijde bereid om hun omvangrijke kennis met me te delen.

Met Maryke den Dulk, Natasja Jannink, Ivo Duijnstee en Sander Ernst deelde ik de laatste jaren een kamer. Ondanks de wat krappe behuizing was de werksfeer altijd goed, en was iedereen bereid een helpende hand te reiken in tijden van stress. Het verschil in karakters in de kleine ruimte leidde soms tot problemen, die steeds met veel humor werden opgelost. Aan discussies betreffende benthosecologie werd in veel gevallen door iedereen deelgenomen, wat de uitwisseling van een grote hoeveelheid informatie met zich mee bracht.

Ook de andere collega's (waarvan sommige ex-) droegen bij aan de prettige werksfeer, hetzij door hun interesse en waar nodig, opbeurende woorden, hetzij door middel van discussies en praktische hulp: Hayfaa Abdul Aziz, Marloes van Hoeve, Albert Oost, Jan van Dam, Jan-Berend Stuut, Albert van der Meulen, René Fraaye, Jelmer Cleveringa, Max van Heijst, Maarten Prins, Charon Duermeyer, George Postma, Poppe de Boer, Hans de Bruin, Lucas Lourens, Johan ten Veen, Joris Steenbrink, Gert-Jan Reichart. Michiel van der Meulen bedank ik speciaal voor zijn onverstoorbare pragmatisme en zijn hulp bij computerproblemen.

Veel van mijn monstermateriaal was reeds verzameld door Frits Hilgen, Wout Krijgsman en Luc Lourens. De keren dat ik met Frits en Wout in Italië het veld in ben geweest voor dit onderzoek, heb ik van hen veel kunnen leren; dit oversteeg het monsteren zelf. Ze hebben zich bij deze gelegenheden tevens laten kennen als ware heren.

Tijdens veldwerk in Italië heb ik een aantal enthousiaste collega's ontmoet, die me zeer gastvrij hebben onthaald – thanks to Roberta Calieri and Mauro Casadei, with whom I stayed, and to Claudia Terzi, Stefania Ferretti and "Scanna"!

Ook aan andere niet-Nederlandse collega's heb ik veel te danken. Many thanks to Marit-Solveig Seidenkrantz for the pleasant and efficient cooperation, and the hospitality when I was in Aarhus. Special thanks are due to Elena Turco, for a good talk with a cigaret. Kati Baldi, maybe we have time now to compare Tethyan and Paratethyan faunas?

Gerrit van 't Veld en Geert Ittmann wil ik bedanken voor het wassen, opzoeken, administreren, kortom, het managen van monstermateriaal. Doorke van den Akker, Alexander Okx en Marc Rauhé hebben een groot aantal monsters gepikt. Marjan Reith, Paul Anten, Arnold van Dijk en Helen de Waard hebben materiaal bewerkt en geochemische analyses gedaan. Wil den Hartog heeft de foto's gemaakt en bewerkt, en Tom van Hinte heeft voor me getekend in Autocad, toen ik zelf nog niet goed uit de voeten kon met tekenprogramma's. Ank Pouw en Marnella van der Tol waren altijd

bereid me bij te staan bij problemen van meer administratieve aard. De uiterst vriendelijke mensen van de bibliotheek hebben me steeds opnieuw wegwijs gemaakt bij het zoeken naar publicaties: Lidy Jansen, Agaath van Rhee, Jan Jansen, Marcel Stelling, Willem van Hattem en Frans Verdaasdonk, bedankt! Het ijzeren geheugen van Jan heeft meermalen z'n waarde bewezen.

Bijzonder goede herinneringen heb ik aan veldwerken in Spanje, de Pyreneeën en Griekenland. Daar heb ik ook de mensen beter leren kennen die ertoe hebben bijgedragen dat ik het paleontologische pad ben ingeslagen. Henko de Stigter speurde onvermoeibaar strata af op zoek naar fossielen. Jan-Willem Zachariasse bracht me het vermogen bij om kalk van kalk te onderscheiden. Frans Jorissen wist al wat mijn toekomstige werkkring zou worden, toen ik tijdens het zoeken naar orchideeën in de Pyreneeën beweerde dat ik forams saai vond. Frits Hilgen leerde me sedimentaire cycli monsteren (met vooruitziende blik?). Bert van der Zwaan wist, staande voor een ontsluiting, zulke levendige beelden op te roepen van paleomilieus, dat ik ze letterlijk voor me zag. Met Rob Speijer ben ik niet het veld in geweest, maar hij hij heeft er wel toe bijgedragen dat ik besloot verder te gaan in de benthos-paleoecologie, toen hij mijn afstudeerscriptie begeleidde.

Met Bert van der Zwaan heb ik later, tot mijn grote genoegen, menige vrijdagmiddag mogen discussieren over 'het vak', evolutie en meer of minder gerelateerde onderwerpen. Zijn brede belangstelling waarborgde altijd een onderwerp van gesprek. Ik prijs zijn geduld, dat ik zwaar op de proef heb gesteld, onder andere door regelmatig te beweren "het komt wel goed", als we beiden wisten dat het halen van een deadline kantje-boord ging worden. Het is goed gekomen, niet in de laatste plaats dankzij zijn strakke regie.

Mijn familie, vrienden en Ries bedank ik voor hun belanstelling en steun, en hun begrip voor het feit dat dit promotie-onderzoek niet altijd op werkdagen tussen 9 en 5 werd uitgevoerd.

I would like to thank the members of the dissertation committee: Dr. W.A. Berggren, Prof. Dr. S.A. Iaccarino, Prof. Dr. C.G. Langereis, Prof. Dr. H. Visscher, and Prof. Dr. Th.E. Wong, for thourough reading of the manuscript and for valuable suggestions.

Curriculum Vitae

De auteur van dit proefschrift werd geboren op 3 september 1956 in Amsterdam. Na het behalen van het Atheneum-B diploma in 1975 en het diploma verpleegkundige A in 1979 werd in diverse functies in de gezondheidszorg gewerkt. In 1988 werd de studie Geologie begonnen aan de Faculteit Aardwetenschappen van de Universiteit Utrecht. De propedeuse werd afgerond in 1990 en het doctoraal in 1994. Tijdens een aanstelling van 1994 tot 1999 als assistent in opleiding (AIO) aan dezelfde universiteit werd het onderzoek verricht waarover in dit proefschrift wordt gerapporteerd.